Group invariant solutions for a pre-existing fracture driven by a non-Newtonian fluid in permeable and impermeable rock

ADEWUNMI GIDEON FAREO

A thesis submitted to the Faculty of Science, University of the Witwatersrand, Johannesburg, South Africa, in fulfilment of the requirements for the degree of Doctor of Philosophy

Abstract

The aim of the thesis is to derive group invariant, exact, approximate analytical and numerical solutions for a two-dimensional laminar, non-Newtonian pre-existing hydraulic fracture propagating in impermeable and permeable elastic media. The fracture is driven by the injection of an incompressible, viscous non-Newtonian fluid of power law rheology in which the fluid viscosity depends on the magnitude of the shear rate and on the power law index $n > 0$. By the application of lubrication theory, a nonlinear diffusion equation relating the half-width of the fracture to the fluid pressure is obtained.

When the interface is permeable the nonlinear diffusion equation has a leak-off velocity sink term. The half-width of the fracture and the net fluid pressure are linearly related through the PKN approximation. A condition, in the form of a first order partial differential equation for the leak-off velocity, is obtained for the nonlinear diffusion equation to have Lie point symmetries. The general form of the leak-off velocity is derived. Using the Lie point symmetries the problem is reduced to a boundary value problem for a second order ordinary differential equation. The leak-off velocity is further specified by assuming that it is proportional to the fracture half-width. Only fluid injection at the fracture entry is considered. This is the case of practical importance in industry.

Two exact analytical solutions are derived. In the first solution there is no fluid injection at the fracture entry while in the second solution the fluid velocity averaged over the width of the fracture is constant along the length of the fracture. For other working conditions at the fracture entry the problem is solved numerically by transforming the boundary value problem to a pair of initial value problems. The numerical solution is matched to the asymptotic solution at the fracture tip. Since the fracture is thin the fluid velocity averaged over the width

of the fracture is considered. For the two analytical solutions the ratio of the averaged fluid velocity to the velocity of the fracture tip varies linearly along the fracture. For other working conditions the variation is approximately linear. Using this observation approximate analytical solutions are derived for the fracture half-width. The approximate analytical solutions are compared with the numerical solutions and found to be accurate over a wide range of values of the power-law index n and leak-off parameter β.

The conservation laws for the nonlinear diffusion equation are investigated. When there is fluid leak-off conservation laws of two kinds are found which depend in which component of the conserved vector the leak-off term is included. For a Newtonian fluid two conservation laws of each kind are found. For a non-Newtonian fluid the second conservation law does not exist. The behaviour of the solutions for shear thinning, Newtonian and shear thickening fluids are qualitatively similar. The characteristic time depends on the properties of the fluid which gives quantitative differences in the solution for shear thinning, Newtonian and shear thickening fluids.

Declaration

I declare that this dissertation is my own unaided work. It is being submitted for the degree of Doctor of Philosophy at the University of the Witwatersrand, Johannesburg. It has not been submitted before for any degree or examination at any other university.

Fareo Adewunmi Gideon

January 23, 2013

Dedication

To the Almighty God, the giver of life.

To my mother, Olanrewaju Fareo, whose toil has brought me thus far.

Acknowledgement

First, I would like to thank my supervisor, Professor David Paul Mason, for his thorough supervision, academic and moral support throughout the period in which this research was carried out and the thesis written up. Your encouragement and confidence in me has enabled me to carry on.

I am thankful to Professor Ebrahim Momoniat, Head of the School of Computational and Applied Mathematics, for his firm support and advice and to Professor F.M. Mahomed who helped me with the understanding of Symmetry Methods for Differential Equations. To the entire DECMA group, I say thank you for the constructive comments during seminars and workshops which have enabled me to become a better researcher.

My appreciation also goes to my family members who have constantly called to encourage me and remind me that I am always in their prayers. Specifically, many thanks to my uncle, Bayo Seweje, and my sisters, Ifedayo Akinsolu and Iyabo Akinsolu and to my mum, Mrs Olanrewaju Fareo for their encouragement, moral support and prayers.

I must acknowledge my friends Catherine Ogunmefun, Onyekwelu Okeke, Dennis Ikpe, Doomnull Attah, Adeyemi Oladiran, Ayandibu Olabode, Uno Okon, Ayokunle Osuntunyi amongst others for the cheerful and happy times that kept me going. To Pumeza Qaba I say thank you for always being there as my best friend and great companion.

Finally I am grateful to the University of the Witwatersrand for the Postgraduate Merit Awards and to the School of Computational and Applied Mathematics for the initial grant without which I would not have been able to start my doctoral studies.

I also acknowledge the African Institute for Mathematical Sciences and the German Academic Exchange Service for a DAAD Postgraduate Scholarship.

Contents

Chapter 1

Introduction

1.1 Introduction

Hydraulic fracturing is a process by which fractures in rock are propagated by the injection of ultra high pressure viscous fluid into the fracture. This technique is a core technology in petroleum production and in the fast growing areas of the extraction of gas and the generation of geothermal energy. It is also a cornerstone of innovative new methods in mining. It occurs naturally in the formation of intrusive dykes and sills in the earth's crust [1]. Hydraulic fracturing is generated by viscous incompressible fluid injection into the fracture under a sufficiently high pressure, such that the tensile strength of the rock or the fracture toughness and the far-field compressive stress are overcome. The fracture then evolves in the direction perpendicular to the far-field compressive stress.

Modelling the hydraulic fracture process has been an active area of research over the past sixty years and it has attracted numerous contributions [2, 3, 4, 5, 6, 7, 8, 9]. A major research effort has been the development of numerical algorithms used to predict the propagation of hydraulic fractures in the complex and variable geological conditions under which oil extracting operations take place[10]. Despite the significant progress made, the numerical simulation of fluid driven fractures remains a particularly challenging computational problem [11, 12]. The challenges encountered are discussed briefly in [13]. Due to the complexity of the hydraulic fracture process which is shown in Figure 1.1.1, theoretical analysis of the problem through

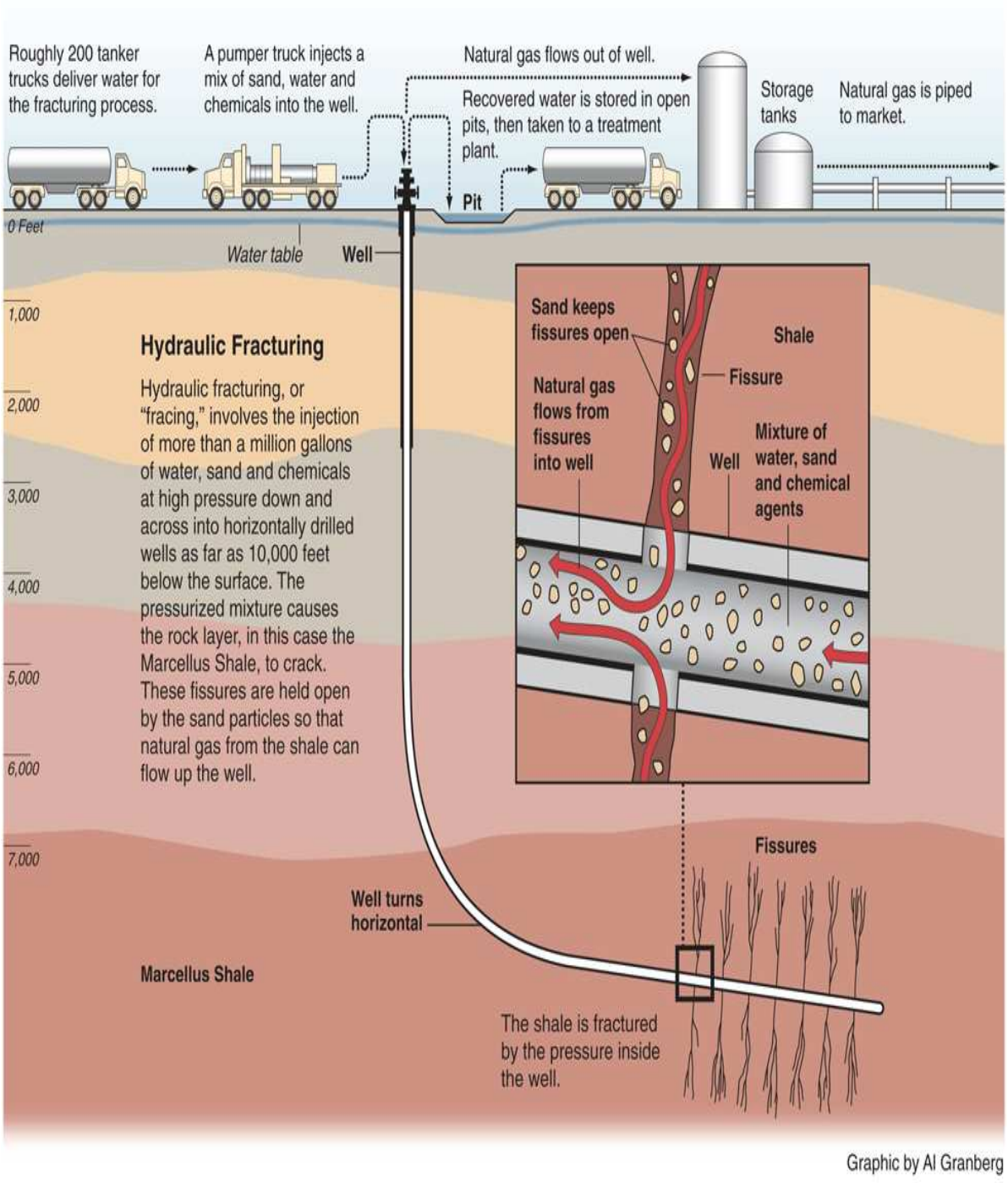

Figure 1.1.1: An overview of Hydraulic Fracturing. Retrieved 28 Nov, 2011, from ProPublicaWeb http://www.ProPublica.org/special/hydraulic-fracturing-national. Reproduced with permission from Pro Publica inc.

idealized or simplified fracture geometry models has made a significant contribution. These models which serve as fracture prototypes for analysing the influence of the problem parameters give insights into the hydraulic fracture process. One of the first fracture geometry models is called the PKN model [4, 6]. The model assumes that the fracture length is much greater than the fracture width, that its width slowly varies along the length of the fracture and that the fracture evolves under plane strain within any vertical cross-section perpendicular to the length of the fracture. The model proposes an elasticity equation in which the net fluid pressure in the fracture is linearly proportional to the width of the fracture. The proportionality constant depends on the material properties of the rock. In this thesis, I consider a two-dimensional fracture driven by ultra high pressure fluid and propagating under plane strain conditions in a homogenous permeable rock. The deformation of the rock is modelled using the PKN formulation and the fluid flow in the fracture is modelled using the lubrication equations. Because the PKN model is used the width of the fracture satisfies a nonlinear diffusion equation.

Fitt et al [14] were the first to apply the powerful method of symmetry analysis of differential equations to hydraulic fracturing. They solved the problem of a two-dimensional hydraulic fracture with the PKN model and for a fracture with non-zero initial length. Fareo and Mason [15] extended the work of Fitt et al to include permeable rock with fluid leak-off into the rock formation. Fitt et al [14] and Fareo and Mason [15] considered the special case in which the fracturing fluid is Newtonian.

A new feature of this thesis is that the fracturing fluid is non-Newtonian. A two-dimensional fracture with non-zero initial length driven by an incompressible, non-Newtonian fluid of power-law rheology will be considered. The fluid flow in the fracture is considered laminar and with negligible inertia. The extension to non-Newtonian fluids is motivated by the recogniton that most fluids used in hydraulic fracture operations display non-Newtonian behaviour. They can be modelled as power-law fluids [16, 17].

1.2 Objectives and outline of the thesis

In this thesis, the objective is to study the problem of a two-dimensional fracture driven by a power-law fluid in both permeable and impermeable rock. The PKN model, which assumes

a linear relationship between the excess fluid pressure in the fracture and the fracture half-width will be used. The mathematical method employed for solving the mathematical models derived in this thesis is Lie group analysis which avails us with systematic techniques for obtaining exact analytical solutions. Numerical methods are used on the nonlinear ordinary differential equations derived in this thesis when further reduction is not possible due to insufficient symmetries.

In Chapter 2, a brief discussion is made on Newtonian and non-Newtonian fluids and their classification. The various constitutive models characterizing these fluids are briefly outlined and the shortcomings of some of these constitutive models are reviewed. Eact time, such shortcomings pave the way for a more robust constitutive model.

In Chapter 3, we give a concise introduction to Lie group analysis of differential equation. We focus on the theory of the Lie point symmetry method for the reduction of differential equations, which is used in this thesis. Finally, we discuss the application of invariance criterion in the formulation of a boundary value problem as a pair of initial value problems.

In Chapter 4, we study the problem of modelling a two-dimensional power-law fluid-driven fracture in impermeable rock. The chapter begins with the derivation of the two-dimensional thin film equations in dimensionless form. Introducing dimensionless quantities allows the simplification of the Navier-Stokes and continuity equations for a thin fracture. With the aid of boundary conditions, the evolution equation describing the half-width of the fracture is derived. Lie group analysis is used to reduce the evolution equation, which is a nonlinear partial differential equation, to a nonlinear ordinary differential equation. Fitt et al [14] were the first to use this approach. Numerical solutions of the nonlinear ordinary differential equations are also investigated. A new feature is the investigation of the streamlines and the fluid velocity averaged across the fracture. This leads to an approximate solution for the fracture profile which is accurate even for a shear thinning fluid with small values for the power-law exponent.

Chapter 5 considers the problem of modelling a two-dimensional power-law fluid-driven fracture in permeable rock. The velocity of the flow in the fracture is taken to be the width-averaged fluid velocity. The thin film equations derived in Chapter 5 are similar to those derived in Chapter 4. The main difference is the leak-off velocity which is introduced in the

evolution equation through the boundary condition at the fluid-rock interface. Exact analytical solutions and numerical solutions are obtained and analysed. The average fluid velocity in the fracture is investigated.

In Chapter 6, conservation laws for a power-law fluid-driven fracture are considered using three different approaches, the direct method, the characteristic method and the partial Noether approach. The generation of new conserved vectors from known conserved vectors is considered. The association of a Lie point symmetry with a conserved vector is investigated to determine the physical significance of the conservation law. A new feature of the leak-off velocity as a term in the partial differential equation is the existence two kinds of conservation law depending on which component of the conserved vector the leak-off velocity is included. Finally, conclusions are summarised in Chapter 7.

Chapter 2

Non-Newtonian fluids and their constitutive models

2.1 Introduction

This chapter reviews the literature on non-Newtonian fluids and the various constitutive models characterizing their behaviour which are applicable to the study of fluid-driven fracturing of rock. We first recall the very basic and widely accepted definitions of such terms as a fluid and viscosity. The definitions provide a valuable insight into the very essence of the non-Newtonian characteristics of certain fluids.

A fluid is a substance that deforms continously under the application of a shear stress, while viscosity is the immediate resistance produced by the fluid to such a rate of deformation. For certain fluids, the rate of deformation that they experience has no effect on their viscosity. Such fluids are called Newtonian fluids and the relationship between the shear stress, τ, applied on them and the deformation rate, ϵ, is described as [18, 19]

$$\tau = \mu\epsilon, \tag{2.1.1}$$

where μ, called the dynamic viscosity, is constant. Examples of fluids that fall into this category include water, air, certain motor oils, honey, gasoline, kerosene and most mineral oils. The Newtonian fluid is the basis for classical fluid mechanics. On the other hand, some fluids have a viscosity which changes as they are being deformed. This class of fluids is called

non-Newtonian fluids. The relationship between the shear stress and shear deformation rate for such fluids cannot be described by the simple relation in equation (2.1.1), since μ, their dynamic viscosity, depends on the magnitude of the rate of shear. It can also depend on time for some materials that behave in different ways depending on how long the stress is applied for.

Non-Newtonian fluids arise in virtually every environment around us. They are encountered in the chemical and plastic industry as polymeric fluids [19]. Paints, quicksand, slurries, drilling mud, lubricants, nylon, and colloids all exhibit non-Newtonian behaviour. They are found in our homes, for example, a mix of cornstarch and water, melted chocolate, eggwhites, tomato ketchup, toothpaste, body paste, mayonaise, and gelatine; in the human body, for example, mucus, whole blood (composed of plasma, red and white blood cells, platelets); and they occur naturally as molten magma and mud slurries. Unfortunately, due to the diverse manner in which these non-Newtonian fluids respond to shear deformation rate, there is not a single model that can describe the behaviour of all non-Newtonian fluids. As a result, much theory has been developed and non-Newtonian fluids can be classified into different categories depending on how the shear stress is related to the shear rate. Many models have been proposed for the constitutive relationship between the shear stress and the shear rate for non-Newtonian fluids. The aim in this chapter is to act as a guide through some of the developments and to elaborate on how and where the models can be used, as well as the shortcomings of some of the models. A brief discussion on a molecular scale is first given on how the macroscopic flow of fluid and flow deformation rate are related to the configuration and motion of the individual molecules, and how, in turn, the viscous resistance is related to the intermolecular and interparticle forces in the fluid.

2.2 Microstructure and macroscopic fluid phenomena

Flow or deformation involves the relative motion of adjacent elements of the material. As a consequence such processes are sensitive to interatomic, intermolecular and interparticle forces. The macroscopic behaviour displayed by most non-Newtonian fluids is primarily a reflection of an underlying microstructure. For example, a variety of non-Newtonian fluids

are colloidal suspensions. These fluids are Newtonian solvents such as water containing a dispersion phase of small particles, ranging in size from 1 nanometer (10^{-9}m) to 1 micrometer (10^{-6}m). Table (2.2.1) displays some important types of colloidal systems [20]. Interparticle forces, which are attributed to the aggregate interactions between individual molecules, electrostatic forces, effect of the intervening solvent medium, are all factors ensuring the stability of such colloidal dispersions and that the particles do not settle out by gravity. For these colloidal suspensions, the microstructure that develops is from particle-particle or particle-solvent interactions which are often of electrostatic or chemical origin. In the case of polymeric fluids, the microstucture is their molecular chemical composition and structure [19].

Disperse systems	Disperse phase	Disperse medium
Milk, butter, mayonnaise, pharmaceutical creams, asphalt	Liquid	Liquid
Clay slurries, toothpaste, muds, polymer latices	Solid	Liquid
Blood	Corpuscles	Serum
Fog, mist, tobacco smoke,aerosol sprays	Liquid	Gas
Inorganic colloids (gold, silver iodide, sulphur metallic hydroxides), paints	Solid	Liquid
Jellies, glue	Macromolecules	Solvent

Table 2.2.1: Some typical colloidal systems.

The deviation from the Newtonian fluid behaviour given by equation (2.1.1) occurs when we do not have a linear relationship between the shear stress, τ, and the shear rate, ϵ or when the $\tau - \epsilon$ graph does not pass through the origin. As shown in Figure (2.2.1), non-Newtonian fluids can be classified into the following three categories [21]:

- Fluids for which the value of the shear stress, τ, depend on the current value of the shear rate, ϵ. These fluids are variously known as purely viscous, inelastic, time-independent

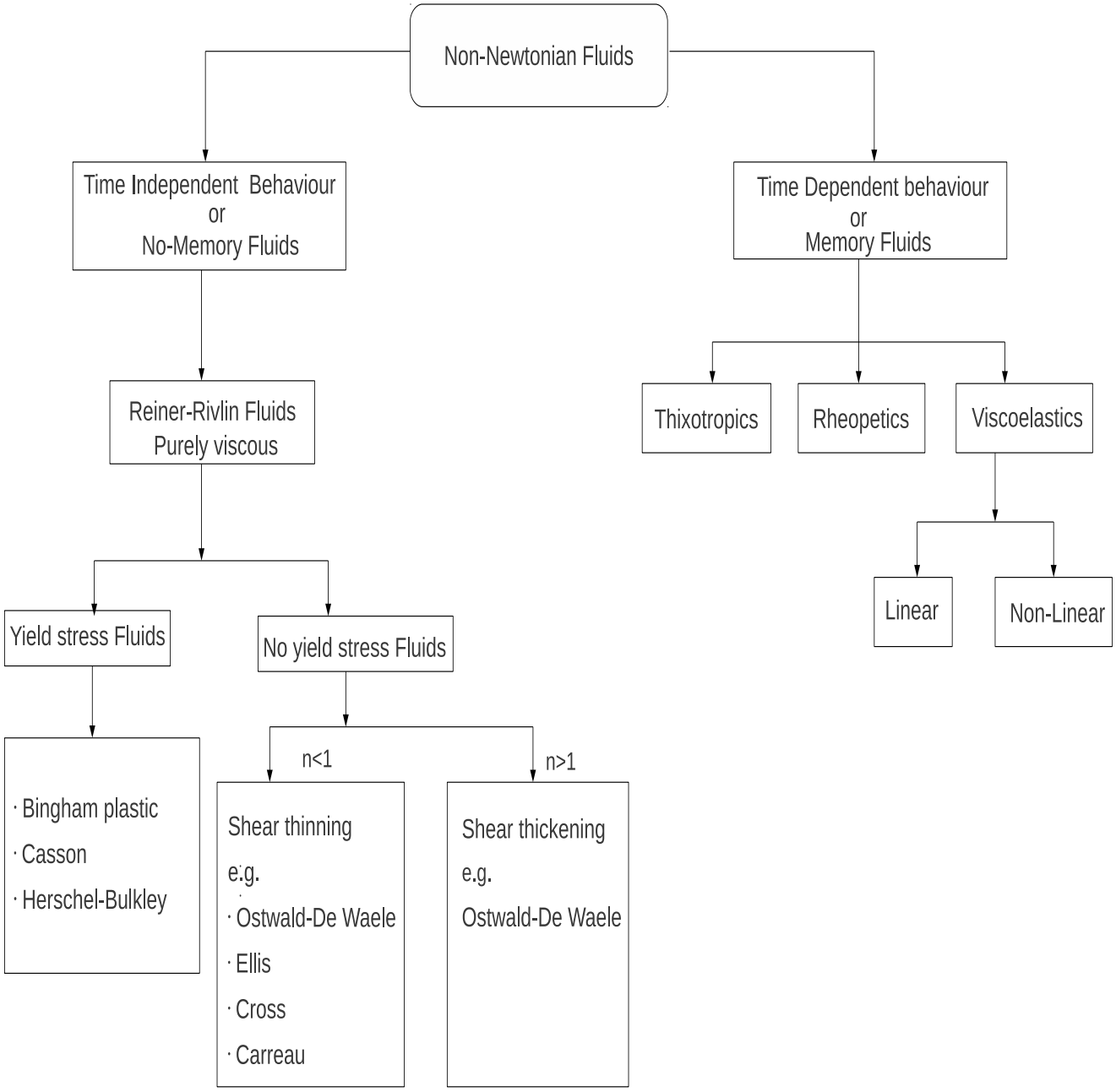

Figure 2.2.1: Classification of non-Newtonian fluids.

or generalized Newtonian fluids,

- Fluids for which the shear stress, τ, depends on the shear rate ϵ, as well as on the kinematic history and the duration of shear, t. These are known as time-dependent or memory fluids,

- Fluids that exhibit both a blend of viscous fluid behaviour and of elastic solid-like behaviour. These are called visco-elastic fluids or elastico-viscous fluids.

The above classification is quite arbitrary since most fluids often display a combination of two or all of these properties. We will now discuss each of these classifications in turn and also present the constitutive equations characterizing them.

2.3 Constitutive equations for purely viscous fluids

By a purely viscous fluid, we mean a fluid for which the stress at any given material point and time is a function of the velocity gradient evaluated at the point and time of interest. This class of fluid has no memory and hence does not depend on time since the fluid response is characterized solely by motion at the present time. They are sometimes referred to as "generalized Newtonian fluids" [19] and are described by the empirical relation

$$\tau = \eta\epsilon \tag{2.3.1}$$

where η is a function of the magnitude of the rate of shear or by

$$\epsilon = \frac{\tau}{\eta} \tag{2.3.2}$$

where η is a function of the shear stress.

Depending upon the form of equation (2.3.1) or (2.3.2), there are three possible behaviours that these fluids display:

- Shear thinning of pseudoplastic behaviour,

- Viscoplastic behaviour with or without shear thinning

- Shear thickening or dilatant behaviour

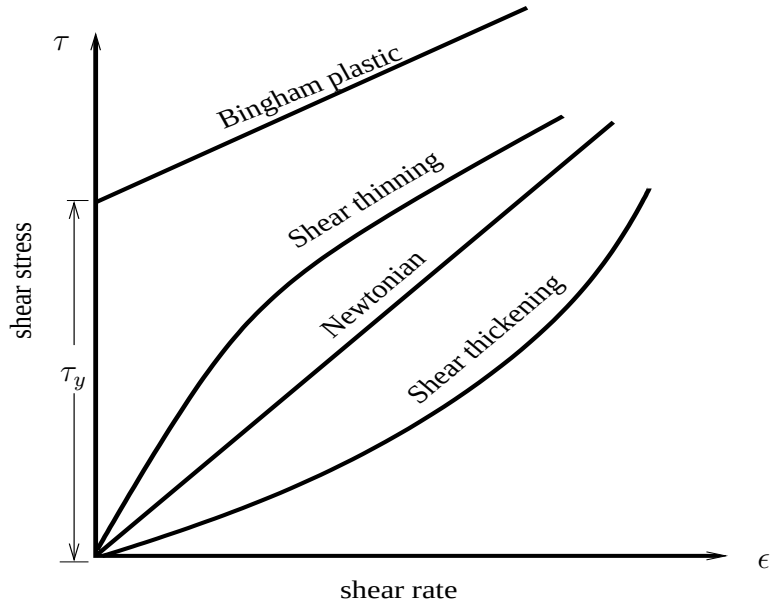

Figure 2.3.1

In Figure (2.3.1), the qualitative behaviour of these three categories of fluids is shown. The curve having a straight line through the origin represents a Newtonian fluid.

2.3.1 Shear thinning fluids

These are the most widely encountered time-independent non-Newtonian fluids in engineering practice. Most of the fracturing fluids used in the mining and petroleum industry are shear thinning [22]. These fluids have viscosity which gradually decreases with increasing shear rate. According to [19, 21], almost all polymer solutions and melts that exhibit a shear rate dependent viscosity are shear thinning. However, at low and high shear rates, most shear thinning polymer solutions and melts have limiting viscosity that remains constant in some range of shear rate and they are said to display Newtonian behaviour. This is observable in Figures (2.3.1) and (2.3.2). The limiting viscosity of shear thinning fluids at low shear rate is called zero-shear viscosity, denoted by η_0 while that at high shear rate is called infinite-shear viscosity, denoted by η_∞. Thus, the viscosity of shear thinning fluids decreases from η_0 to η_∞ with increasing shear rate and is therefore bounded below by η_∞ and above by η_0.

In mathematically representing the shear thinning behaviour of fluids, many mathematical

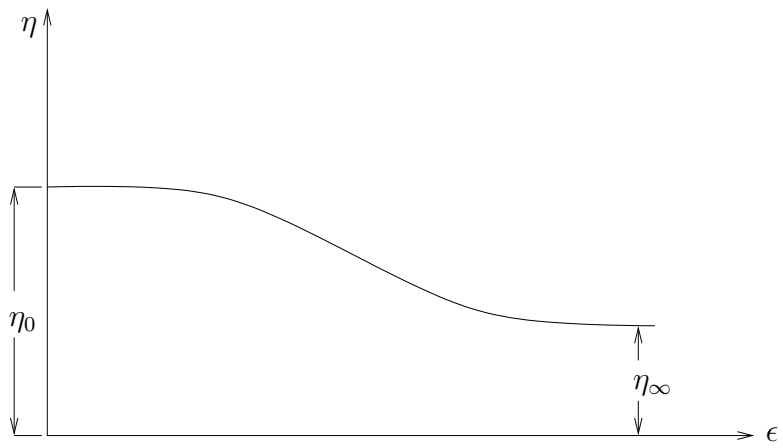

Figure 2.3.2

models of varying complexity and forms have been reported in the literature. Some of these are attempts at curve fitting of the experimental data to give an empirical relationship for the shear stress - shear rate curves or the viscosity - shear rate curve, while others have some theoretical basis in statistical mechanics [23]. An extensive listing of viscosity models can be found in several textbooks [19, 23]. Some of the widely used viscosity models for shear thinning fluids are now discussed.

(i) The power-law model of Ostwald and De Waele

The standard power-law model with two parameters k and n expresses viscosity as a function of shear rate by the relation

$$\eta = k\,|\epsilon|^{n-1}\,, \tag{2.3.3}$$

where k is the consistency coefficient and n is the power-law exponent. The parameters k and n are temperature dependent. For $0 < n < 1$, $\frac{d\eta}{d\epsilon} < 0$ which means that η decreases with increasing shear rate. For $n > 1$, $\frac{d\eta}{d\epsilon} > 0$ which means that η increases with increasing shear rate. The case $n = 1$ represents Newtonian behaviour. The power-law model (2.3.3) is a relatively simple equation which models to a reasonable approximation those features of shear thinning fluid viscosity which are important over an interval of shear rate. It is this simplicity that makes the power-law model the most well-known and widely-used empirical formula in engineering work [19]. However, this model has its weaknesses and shorcomings. As seen in Figure (2.3.1) and (2.3.2), one of these weaknesses lies in the fact that the power-law model

is incapable of predicting the lower and upper Newtonian plateau in the limits $\epsilon \to \infty$ and $\epsilon \to 0$. It therefore applies to a limited range of shear rates and the values of the parameters k and n will depend only on the range of shear rates considered. More on the shorcomings can be found in [19, 21].

In order to rectify and overcome some of the shortcomings of the power-law model in describing shear thinning fluid behaviour, the price of additional empirical constants is paid. Cross [24] and Carreau [25] presented empirical formulations which take into account the viscosity of shear thinning fluids in the limits $\epsilon \to \infty$ and $\epsilon \to 0$, while the Ellis model [26, 27, 28] takes into account the fluid viscosity of shear thinning fluids in the limit $\epsilon \to 0$.

(ii) The Cross model

The cross model is typically written in terms of four parameters

$$\eta = \eta_\infty + \frac{\eta_0 - \eta_\infty}{1 + k\epsilon^n}, \tag{2.3.4}$$

where η_0 and η_∞ are the zero-shear-rate and infinite-shear-rate viscosities respectively and k and n are as defined in the power-law equation (2.3.3). For $0 < n < 1$, (2.3.4) describes shear thinning fluid behaviour. In the limit $\epsilon \to 0$, $\eta = \eta_0$ and for $\epsilon \to \infty$, $\eta = \eta_\infty$. Therefore the Cross model correctly predicts the lower and the upper limiting viscosities. The Newtonian limit is fully recovered when $k = 0$.

(iii) The Carreau-Yasuda model

The Carreau-Yasuda model, comprising five parameters is given as

$$\eta = \eta_\infty + (\eta_0 - \eta_\infty)\left(1 + (\lambda\epsilon)^a\right)^{\frac{n-1}{a}}. \tag{2.3.5}$$

The parameters η_0 and η_∞ are as defined in the Cross model, λ is a time constant, n is the power law exponent and a is a dimensionless parameter that describes the transition region between the zero-shear-rate region and the power-law region. When $a = 2$, (2.3.5) reduces to the Carreau model with four parameters

$$\eta = \eta_\infty + (\eta_0 - \eta_\infty)\left(1 + (\lambda\epsilon)^2\right)^{\frac{n-1}{2}}. \tag{2.3.6}$$

(iv) The Ellis model

The Ellis model takes the form (2.3.2) and the viscosity, expressed in terms of shear stress is given as

$$\frac{1}{\eta} = \frac{1}{\eta_0}\left(1 + \left|\frac{\tau}{\tau_{\frac{1}{2}}}\right|^{\alpha-1}\right), \tag{2.3.7}$$

where η_0 is the viscosity at zero shear and $\tau_{\frac{1}{2}}$ is the value of the shear stress at which the fluid viscosity, η, drops to $\eta_0/2$. At a very low value of shear stress, (and hence shear rate), Newtonian behaviour with viscosity η_0 is approached. As the shear stress, τ, becomes large with respect to $\tau_{\frac{1}{2}}$, such that $\tau/\tau_{\frac{1}{2}} >> 1$, we have $\eta = \eta_0\tau_{\frac{1}{2}}/\tau^{\alpha-1}$ and substituting into (2.3.3) gives

$$\tau = \tau_{\frac{1}{2}}^{\left(1-\frac{1}{\alpha}\right)}\eta_0^{\frac{1}{\alpha}}\epsilon^{\frac{1}{\alpha}},$$

which is a power-law model with $k = \tau_{\frac{1}{2}}^{\left(1-\frac{1}{\alpha}\right)}\eta_0^{\frac{1}{\alpha}}$ and $n = 1/\alpha$. The Ellis model does not predict the upper Newtonian regime, the viscosity at infinite shear rate.

2.3.2 Viscoplastic fluids

Non-Newtonian fluids include those that will not flow or deform except if acted on by some finite threshold stress called yield stress. These fluids are called yield-stress fluids. Yield stress is that stress below which the substance behaves like an elastic solid and above which the substance behaves like a liquid with a plastic viscosity η_p. The simplest yield-stress material is called the Bingham plastic fluid which obeys the constitutive relation

$$\begin{aligned} &\tau = \tau_y + \eta_p\epsilon, \quad && |\tau| > |\tau_y| \\ &\epsilon = 0, && |\tau| < |\tau_y|\,. \end{aligned} \tag{2.3.8}$$

Model (2.3.8) describes the Newtonian behaviour of viscoplastic fluids for $|\tau| > |\tau_y|$. Fluids exhibiting Bingham plastic behaviour include highly concentrated suspensions of solid particles [29]. Viscoplastic materials exhibiting shear thinning behaviour are referred to as Herschel-Bulkley materials [29] and are described by the Herschel-Bulkley model

$$\begin{aligned} &\tau = \tau_y + k\epsilon^n, \quad && |\tau| > |\tau_y| \\ &\epsilon = 0, && |\tau| < |\tau_y|\,. \end{aligned} \tag{2.3.9}$$

Another model which has its origin in blood modelling, but has been widely found useful for modelling some other viscoplastic substances is the Casson model given as

$$\begin{aligned} \sqrt{\tau} &= \sqrt{\tau_y} + \sqrt{\eta_p \left|\epsilon\right|}, \quad && \left|\tau\right| > \left|\tau_y\right| \\ \epsilon &= 0, && \left|\tau\right| < \left|\tau_y\right|. \end{aligned} \tag{2.3.10}$$

Despite these fascinating models describing viscoplastic fluid behaviour, it is worth observing that Barnes et al [30, 31] have challenged the existence of the yield stress. They argued that "yield stress is a mere idealisation, and that given accurate measurements, no yield stress exists". They continued in their arguement by stating that "with the aid of new generation rheometers, accurate measurements at low enough shear rates which nullifies the yield stress theory can be made".

2.3.3 Shear thickening fluids

Shear thickening fluids are also called dilatant fluids. They have the property that their viscosity increases with increasing shear rate. Examples of fluid exhibiting shear thickening are concentrated suspensions of china clay, titanium dioxide and a mix of corn starch and water [19, 21]. Of the time-independent fluids, dilatant fluids have generated very little attention since most fluids do not display dilatant behaviour. The flow behaviour of shear thickening fluids is described by the power law model of equation (2.3.3) where $n > 1$.

2.4 Constitutive equations for time dependent fluids

This class of fluids have viscosities that depend not only on the rate of shear, but also on the time for which the fluid has been subjected to shearing. Their internal structures undergo rearrangements during deformations at a rate quite slow to maintain equilibrium configurations. This results in the shear stress changing with the duration of shear. Time dependent fluids can be classified into two kinds: Thixotropic fluid and Rheopetic fluids.

2.4.1 Thixotropic fluids

These fluids exhibit behaviour called thixotropy and have viscosities which decrease with time of shearing when sheared at a constant rate. Examples include clay suspension, emulsions, drilling fluids, protein solutions, certain paints, inks and coating greases [29, 32]. A detailed literature review and models describing thixotropic behaviour is found in [32].

2.4.2 Rheopetic fluids

The behaviour exhibited by these fluids is called rheopexy, and it is the opposite of thixotropy. Rheopetic fluids are fluids whose viscosities increase with time of shearing when sheared at a constant rate. Examples include bentonite solutions, colloidal suspension of vanadium pentoxide at moderate shear rates and coal-water slurries [21, 29].

Much effort has been invested in the development of constitutive relations describing thixotropic behaviour, stemming from its wide and frequent occurrence in industrial processes [32, 33]. However, many of the models used to describe thixotropy involve alterations of the existing constitutive equations-the generalized Newtonian fluid model, Herschel-Bulkley model, Bingham model, in such a way as to incorporate time dependence into the fluid viscosity and yield stress.

2.4.3 Viscoelastic fluids

Viscoelastic fluids are fluids having both viscous and elastic properties. These fluids, when deformed and upon removal of the stress causing deformation have the ability to recover and regain their original shape in an elastic manner. Polymeric fluids are dominant among the different classes of fluids exhibiting viscoelasticity [29] and they are indeed sometimes refered to as viscoelastic fluids [19]. Some non-polymeric materials exhibiting viscoelasticity are gels, soap solutions, emulsions, synovial fluids and foams [21].

An important effect of viscoelasticity is that shear flows give rise to normal stresses which act in the direction normal to that of shear. The effects of these normal stresses are manifested in physical phenomena such as rod climbimg (Weissenberg effect), die swell and tubeless

syphon [19, 34]. Viscoelastic fluids can be classified into two kinds depending on their displacement behaviour in response to applied stress. They are linear viscoelastic fluids-with a very small displacement gradient response and nonlinear viscoelastic fluids- with large displacement gradients response. A thorough coverage of mathematical models describing linear and nonlinear viscoelastic fluids is found in [19, 21, 34].

A class of fluid called the Rivlin-Ericksen fluid of order two, which is a member of a general category of fluids called fluids of differential type or informally as Rivlin-Ericksen fluids [35] can describe the normal stress effects encountered in phenomena like die swell and the Weissenberg effect. It is described by the constitutive equation

$$T = -pI + \mu A_1 + \alpha_1 A_2 + \alpha A_1^2 \tag{2.4.1}$$

where μ, α_1 and α are material constants, μ being the viscosity. The tensors A_1, which is twice the rate of strain tensor and A_2 are the Rivlin-Ericksen tensors defined by

$$A_1 = \nabla V + \nabla V^T, \tag{2.4.2}$$

$$A_2 = \frac{dA_1}{dt} + A_1 \nabla V + \nabla V^T A_1. \tag{2.4.3}$$

A detailed account of the characteristics of second - grade fluids is well documented in [35].

2.5 Conclusions

In this chapter, a review of non-Newtonian fluids and the various constitutive models characterizing them has been made. The power-law constitutive model, which is the model used in the remainder of this thesis has been discussed. The advantages that the power-law model has over the other constitutive models for non-Newtonian fluids have been highlighted. The shortcomings of the model have also been discussed.

Chapter 3

Mathematical preliminaries

3.1 Introduction

In Chapter 2, we described non-Newtonian fluids by their constitutive models. The equations derived using these models are often highly nonlinear and difficult to solve analytically. Numerical computations have been used in an attempt at obtaining solutions to these nonlinear equations. Without underestimating the importance of numerically solving these equations for the problem under investigation, analytical solutions remain more profound because they help us see how variables are related to one another as well as understanding the effect of parameters that are present in the differential equation and boundary conditions.

There are many problems in non-Newtonian and Newtonian fluid mechanics where closed form solutions are not easily obtainable by the standard methods of integration due to the nonlinearity of the differential equations encountered in these problems. An approach developed by the 19th century Norwegian mathematician, Sophus Lie (1842-1899) enables exact analytical solutions to linear and nonlinear differential equations to be derived in a systematic manner. We begin this chapter by outlining the essential features of Lie's classical approach to solving partial differential equations. A non-classical approach to solving differential equations, which is a generalisation of Lie's method for finding group invariant solutions, was proposed by Bluman and Cole in [36]. In Section 3.2, we discuss the theory of Lie group analysis of partial differential equations, an approach implemented in this thesis to reduce a

second order partial differential equation to a second order nonlinear ordinary differential equation. Finally in Section 3.3, we describe briefly a method to transform a boundary value problem into a pair of initial value problems, an approach we will use in this research to derive numerical solutions.

3.2 Lie's classical symmetry method for partial differential equations

We will briefly describe the theory of Lie group analysis of partial differential equations which is required in this thesis.

For simplicity and without loss of generality, consider the kth-order ($k \geq 1$) partial differential equation in one dependent variable u and n independent variables $x = (x^1, x^2, \ldots, x^n)$:

$$F(x, u, u_{(1)}, \ldots, u_{(k)}) = 0, \tag{3.2.1}$$

where $u_{(1)}$, $u_{(2)}$ up to $u_{(k)}$ are the collection of all distinct first-, second- up to kth-order partial derivatives with respect to the independent variables:

$$u_{(1)} = \{\frac{\partial u}{\partial x^i}\},\ u_{(2)} = \{\frac{\partial^2 u}{\partial x^i \partial x^j}\}, \ldots, u_{(k)} = \{\frac{\partial^k u}{\partial x^{i_1}, \ldots, \partial x^{i_k}}\}$$

with $1 \leq i, j, i_1, \ldots, i_k \leq n$.

By a classical symmetry group of (3.2.1), we mean a continous group of invertible point transformations in a plane that depends on the group parameter $a \epsilon R$,

$$\begin{aligned} \bar{x}^i &= f^i(x, u, a), \quad i = 1, \ldots, n \\ \bar{u} &= g(x, u, a), \end{aligned} \tag{3.2.2}$$

which acts on the space of independent and dependent variables, leaving equation (3.2.1) form invariant and converting any classical solution of (3.2.1) into another classical solution of (3.2.1). The transformations (3.2.2) satisfy all four properties of a group which are closure, inverse, identity and associativity and are said to form a one-parameter symmetry group.

The solutions of (3.2.1) which are invariant under (3.2.2) are called group invariant solutions, and are found by solving a differential equation which has fewer independent variables

than (3.2.1). The transformations (3.2.2) which leave (3.2.1) invariant provide symmetries which are used in the reduction of the number of independent variables in (3.2.1). The procedure leading to the derivation of the symmetries used in the reduction process is now outlined. We first note that for a sufficiently small, the finite transformations (3.2.2) can be expanded in a Taylor series about $a = 0$ to obtain the infinitesimal transformation

$$\begin{aligned} \bar{x}^i &= x^i + a\xi^i(x,u), \quad i = 1,\ldots,n \\ \bar{u} &= u + a\eta(x,u), \end{aligned} \tag{3.2.3}$$

where

$$f^i(x,u,0) = x^i,\ g(x,u,0) = u,\ \xi^i(x,u) = \left.\frac{\partial f^i(x,u,a)}{\partial a}\right|_{a=0},\ \eta(x,u) = \left.\frac{\partial g(x,u,a)}{\partial a}\right|_{a=0}.$$

To recover the one parameter finite group of transformations (3.2.2) from the infinitesimal transformations, we solve the Lie equations

$$\xi^i(\bar{x},\bar{u}) = \frac{d\bar{x}^i}{da}, \quad \eta(\bar{x},\bar{u}) = \frac{d\bar{u}}{da}, \tag{3.2.4}$$

subject to the initial conditions

$$\left.\bar{x}^i\right|_{a=0} = x^i, \quad \left.\bar{u}\right|_{a=0} = u, \tag{3.2.5}$$

where $\bar{x} = (\bar{x}^1,\ldots,\bar{x}^n)$. The infinitesimal transformation (3.2.3) can be conveniently represented by the linear differential operator

$$X = \xi^1(x,u)\frac{\partial}{\partial x^1} + \xi^2(x,u)\frac{\partial}{\partial x^2} + \ldots + \xi^n(x,u)\frac{\partial}{\partial x^n} + \eta(x,u)\frac{\partial}{\partial u}, \tag{3.2.6}$$

called the symbol of the infinitesimal transformation. Equation (3.2.6) is also referred to as the infinitesimal operator or Lie symmetry generator.

The infinitesimal point transformation (3.2.3) can be extended to include the partial derivatives of the dependent variable u. Since the point transformation (3.2.3) form a one-parameter group, their extension to the partial derivatives of u of any order is also a one-parameter group and is called an extended point transformation group.

3.2.1 Lie point symmetries of differential equations

The partial differential equation (3.2.1) is solved by deriving their group invariant solution. The first step towards obtaining a group invariant solution involves the derivation of the Lie point symmetry generators of (3.2.1).

The Lie point symmetry generators

$$X = \xi^1(x,u)\frac{\partial}{\partial x^1} + \xi^2(x,u)\frac{\partial}{\partial x^2} + \ldots + \xi^n(x,u)\frac{\partial}{\partial x^n} + \eta(x,u)\frac{\partial}{\partial u} \tag{3.2.7}$$

of equation (3.2.1) are derived by solving the determining equation

$$X^{[k]}F(x,u,u_{(1)},\ldots,u_{(k)})\Big|_{F=0} = 0, \tag{3.2.8}$$

for $\xi^1(x,u)$, $\xi^2(x,u)$, ..., $\xi^n(x,u)$ and $\eta(x,u)$, where $X^{[k]}$, called the kth prolongation of X, is given by

$$X^{[k]} = X + \sum_{i=1}^{n}\zeta_{x^i}\frac{\partial}{\partial u_{x^i}} + \sum_{i=1}^{n}\sum_{j=1}^{n}\zeta_{x^ix^j}\frac{\partial}{\partial u_{x^ix^j}} + \ldots + \sum_{i_1=1}^{n}\ldots\sum_{i_k=1}^{n}\zeta_{x^{i_1}\ldots x^{i_k}}\frac{\partial}{\partial u_{x^{i_1}\ldots x^{i_k}}}, \tag{3.2.9}$$

for $i \leq j$ and $i_1 \leq i_2 \leq \ldots \leq i_k$, where

$$\begin{aligned}
\zeta_{x^i} &= D_{x^i}(\eta) - \sum_{l=1}^{n} u_{x^l}D_{x^i}(\xi^l),\\
\zeta_{x^ix^j} &= D_{x^j}(\zeta_{x^i}) - \sum_{l=1}^{n} u_{x^ix^l}D_{x^j}(\xi^l),\\
&\vdots\\
\zeta_{x^{i_1}\ldots x^{i_k}} &= D_{x^{i_k}}(\zeta_{x^{i_1}\ldots x^{i_{k-1}}}) - \sum_{l=1}^{n} u_{x^lx^{i_1}\ldots x^{i_{k-1}}}D_{x^{i_k}}(\xi^l).
\end{aligned} \tag{3.2.10}$$

The total derivatives with respect to the independent variable x^i in (3.2.10) is

$$D_i = D_{x^i} = \frac{\partial}{\partial x^i} + u_{x^i}\frac{\partial}{\partial u} + \sum_{l=1}^{n} u_{x^lx^i}\frac{\partial}{\partial u_{x^l}} + \ldots. \tag{3.2.11}$$

The unknown functions $\xi^1(x^1,\ldots,x^n,u)$, $\xi^2(x^1,\ldots,x^n,u)$, ..., $\xi^n(x^1,\ldots,x^n,u)$ and $\eta(x^1,\ldots,x^n,u)$ in the Lie point symmetry do not depend on the derivatives of u. The derivatives of u in the determining equation (3.2.8) are independent. Hence, the coefficients of the powers and products of the partial derivatives of u in the determining equation (3.2.8) must each be zero.

The determining equation is then separated according to the powers and products of the partial derivatives of u and the coefficient of each power and product of derivatives set to zero. One then obtains an overdetermined system of linear homogenous partial differential equations for the $n+1$ coefficient functions ξ^i and η. Solving this overdetermined system of equations produces expressions for the ξ^i and η. These solutions contain a finite number of arbitrary constants and may contain undetermined functions of the variables . Setting all the constants and undetermined functions to zero except one in turn, we obtain all the Lie point symmetry generators admitted by the differential equation. If the partial differential equation (3.2.1) contains an arbitrary function of some of the independent variables x^1, x^2, ..., x^n, a partial differential equation for the arbitrary function, which must be satisfied for the Lie point symmetries to exist, is obtained.

3.2.2 Group invariant solutions

The symmetries obtained are of the form

$$X_i = \xi_i^1(x,u)\frac{\partial}{\partial x^1} + \xi_i^2(x,u)\frac{\partial}{\partial x^2} + \ldots + \xi_i^n(x,u)\frac{\partial}{\partial x^n} + \eta_i(x,u)\frac{\partial}{\partial u} \tag{3.2.12}$$

for $i = 1, 2, \ldots r$, where r is the number of admitted Lie point symmetries. Since a constant multiple of a Lie point symmetry is also a Lie point symmetry, any linear combination of Lie point symmetries is also a Lie point symmetry. Denoting this linear combination by X_c, we obtain

$$X_c = c_1X_1 + c_2X_2 + c_3X_3 + \ldots + c_rX_r, \tag{3.2.13}$$

where c_i, $i = 1, 2, \ldots r$, are constants.

The group invariant solution, $u = \psi(x^1, x^2, \ldots, x^n)$, of the nonlinear partial differential equation (3.2.1) is obtained by solving the first order quasilinear partial differential equation for ψ,

$$X_c\left(u - \psi(x^1, x^2, \ldots, x^n)\right)\Big|_{u=\psi(x^1,x^2,\ldots,x^n)} = 0. \tag{3.2.14}$$

The group invariant solution is then substituted back into equation (3.2.1). One then obtains a partial differential equation in $n-1$ independent variables. The number of independent

variables is thus reduced by one. This technique when repeated may eventually reduce the partial differential equation to an ordinary differential equation in one independent variable.

3.3 Formulation of a boundary value problem as a pair of initial value problems

In solving numerically a two-point linear or nonlinear boundary value problem several techniques have been developed. These techniques involve iterative methods such as the shooting method, finite difference methods, integral methods, and non-iterative methods such as the method of superposition, method of adjoint operators, invariant embedding and the method of transforming the boundary value problem to a pair of initial value problems.

The method of transformation is employed to solve the boundary value problems encountered in this research. The applicability of this method hinges on invariance principles and it involves the formulation of the boundary value problem as a pair of initial value problems. This method proves useful for a class of differential equations or systems of differential equations that are invariant under certain groups of homogenous linear transformations. This invariance condition then ensures the convertibility of the boundary value problem into two initial value problems. The first initial value problem is solved to obtain an initial condition for the second initial value problem. The solution of the second initial value problem is the solution of the original boundary value problem. Numerical techniques like the Runge-Kutta method can be used to solve the initial value problems if exact solutions cannot be obtained.

The method was used to solve the Blasius boundary value problem over a semi-infinite domain for steady two-dimensional flow of an incompressible fluid past a flat plate placed edgewise to the stream [37]. Several extensions of the method have been made. The connection of the method to group theory was first discovered by Klamkin [37]. He extended the idea to a broader class of ordinary differential equations and systems of differential equations invariant under a linear transformation, with boundary conditions specified at the origin and at infinity. The boundary condition at the origin was homogenous. The extensions to boundary value problems over a finite domain, with boundary conditions specified at both ends, and to

some equations that are not invariant under the linear group, but are invariant under the spiral group, was made by Tsung Yen Na [38, 39]. The homogeneity condition at the initial point was later replaced by a mix condition by Klamkin [40]. Further information on this method is given in [41, 42].

3.4 Conclusions

In this chapter, we have discussed the theory of the mathematical methods that will be used to solve the mathematical models derived in this thesis. They are powerful methods which can be applied to nonlinear problems.

Chapter 4

Modelling two dimensional power-law fluid driven fracture in impermeable rock

This chapter considers a two-dimensional PKN fracture model for impermeable rock. A review of hydraulic fracture modelling has been given by Mendelsohn [43]. The fracture model under consideration is driven by non-Newtonian fluid of power-law rheology.

4.1 Derivation of the thin fluid film equations

In this section, we will derive the two-dimensional thin film equations for the flow of the injected power-law incompressible fluid in the fracture. Consider a two-dimensional fluid-driven fracture propagating in an isotropic, homogenous, impermeable and linearly elastic medium. The medium is characterized by its Youngs' modulus E and Poisson ratio ν. The two-dimensional model was first developed by Khristianovic and Zheltov [2]. The nomenclature and coordinate system used are illustrated in Figure 4.1.1.

The fluid flow which is laminar is independent of y and obeys the two-dimensional momentum balance equation and conservation of mass equation for an incompressible fluid,

$$\rho\left(\frac{\partial \underline{v}}{\partial t} + (\underline{v}\cdot\underline{\nabla})\underline{v}\right) = \underline{\nabla}\cdot\underline{\underline{S}} + \underline{F}, \quad \underline{\nabla}\cdot\underline{v} = 0, \tag{4.1.1}$$

where $\underline{v} = (v_x(x,z,t), 0, v_z(x,z,t))$ denotes the fluid velocity, ρ, the density of the fluid which is a constant, $\underline{F}$, the body force per unit mass and $\underline{\underline{S}}$, the Cauchy stress tensor, which

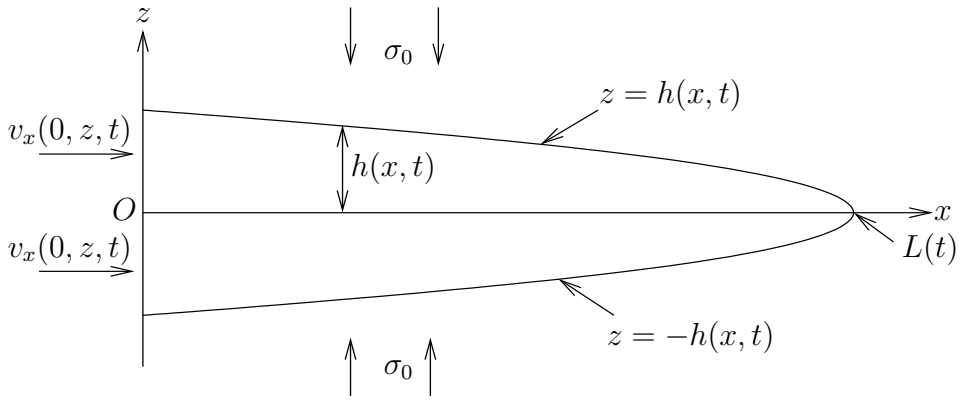

Figure 4.1.1: A hydraulic fracture propagating in an elastic impermeable medium. The coordinate direction y points into the page and σ_0 is the far field compressive stress.

can be decomposed into the isotropic part and the trace-free deviatoric part as follows:

$$S_{ij} = -p\delta_{ij} + \tau_{ij}, \quad \tau_{ii} = 0. \tag{4.1.2}$$

We consider the constitutive rheological relation for an incompressible power-law fluid of the form

$$\tau_{ij} = K\,|\epsilon|^{n-1}\,\epsilon_{ij}, \tag{4.1.3}$$

where the parameter K (with units of Pa.s^n) is called the consistency index and n (dimensionless) is the power-law exponent, also called the fluid behaviour index. In (4.1.3), $|\epsilon|$, the magnitude of the rate of shear, is defined by

$$|\epsilon| = \sqrt{\frac{1}{2}\sum_i \sum_j \epsilon_{ij}\epsilon_{ij}} = \sqrt{\frac{1}{2}\,(\mathrm{tr}\,\epsilon^2)}. \tag{4.1.4}$$

By definition,

$$\epsilon = \nabla\underline{v} + \nabla\underline{v}^T,$$

is the first Rivlin-Ericksen tensor where $\nabla\underline{v}$ is an outer product defined by

$$\nabla\underline{v} = \begin{pmatrix} \frac{\partial}{\partial x} \\ 0 \\ \frac{\partial}{\partial z} \end{pmatrix} \Big(v_x, 0, v_z \Big). \tag{4.1.5}$$

Also

$$\epsilon = \begin{bmatrix} 2\frac{\partial v_x}{\partial x} & 0 & \frac{\partial v_z}{\partial x} + \frac{\partial v_x}{\partial z} \\ 0 & 0 & 0 \\ \frac{\partial v_x}{\partial z} + \frac{\partial v_z}{\partial x} & 0 & 2\frac{\partial v_z}{\partial z} \end{bmatrix} \tag{4.1.6}$$

and

$$\epsilon^2 = \begin{bmatrix} 4\left(\frac{\partial v_x}{\partial x}\right)^2 + \left(\frac{\partial v_z}{\partial x} + \frac{\partial v_x}{\partial z}\right)^2 & 0 & 2\left(\frac{\partial v_x}{\partial x} + \frac{\partial v_z}{\partial z}\right)\left(\frac{\partial v_x}{\partial z} + \frac{\partial v_z}{\partial x}\right) \\ 0 & 0 & 0 \\ 2\left(\frac{\partial v_x}{\partial x} + \frac{\partial v_z}{\partial z}\right)\left(\frac{\partial v_x}{\partial z} + \frac{\partial v_z}{\partial x}\right) & 0 & \left(\frac{\partial v_z}{\partial x} + \frac{\partial v_x}{\partial z}\right)^2 + 4\left(\frac{\partial v_z}{\partial z}\right)^2 \end{bmatrix}. \tag{4.1.7}$$

But since the fluid is incompressible, from (4.1.1)

$$\frac{\partial v_x}{\partial x} + \frac{\partial v_z}{\partial z} = 0 \tag{4.1.8}$$

and therefore the tensor ϵ^2 is diagonal. Hence

$$\sqrt{\frac{1}{2}\left(\operatorname{tr}\epsilon^2\right)} = \sqrt{2\left(\frac{\partial v_x}{\partial x}\right)^2 + 2\left(\frac{\partial v_z}{\partial z}\right)^2 + \left(\frac{\partial v_x}{\partial z} + \frac{\partial v_z}{\partial x}\right)^2}. \tag{4.1.9}$$

Using (4.1.4) and (4.1.9), equation (4.1.3) becomes

$$\tau_{ij} = K\left(2\left(\frac{\partial v_x}{\partial x}\right)^2 + 2\left(\frac{\partial v_z}{\partial z}\right)^2 + \left(\frac{\partial v_x}{\partial z} + \frac{\partial v_z}{\partial x}\right)^2\right)^{\frac{n-1}{2}} \epsilon_{ij}. \tag{4.1.10}$$

The body force $\underline{F}$ due to gravity is neglected. The momentum balance equation in (4.1.1) is, in component form,

$$\rho\left(\frac{\partial v_x}{\partial t} + v_x\frac{\partial v_x}{\partial x} + v_z\frac{\partial v_x}{\partial z}\right) = -\frac{\partial p}{\partial x} + \frac{\partial}{\partial x}\left(K\Pi^{n-1}2\frac{\partial v_x}{\partial x}\right) + \frac{\partial}{\partial z}\left(K\Pi^{n-1}\left(\frac{\partial v_z}{\partial x} + \frac{\partial v_x}{\partial z}\right)\right), \tag{4.1.11}$$

$$\rho\left(\frac{\partial v_z}{\partial t} + v_x\frac{\partial v_z}{\partial x} + v_z\frac{\partial v_z}{\partial z}\right) = -\frac{\partial p}{\partial z} + \frac{\partial}{\partial x}\left(K\Pi^{n-1}\left(\frac{\partial v_z}{\partial x} + \frac{\partial v_x}{\partial z}\right)\right) + \frac{\partial}{\partial z}\left(K\Pi^{n-1}2\frac{\partial v_z}{\partial z}\right), \tag{4.1.12}$$

and the conservation of mass equation in (4.1.1) is given by (4.1.8). In (4.1.11) and (4.1.12),

$$\Pi = \left[2\left(\left(\frac{\partial v_x}{\partial x}\right)^2 + \left(\frac{\partial v_z}{\partial z}\right)^2\right) + \left(\frac{\partial v_z}{\partial x} + \frac{\partial v_x}{\partial z}\right)^2\right]^{\frac{1}{2}}. \tag{4.1.13}$$

For a Newtonian fluid $K\Pi^{n-1}$ reduces to the viscosity μ. We can therefore regard $K\Pi^{n-1}$ as an effective viscosity.

The fluid is incompressible and there is no leak-off into the rock mass. Hence, per unit length in the $y-$direction:

$$\begin{pmatrix} \text{rate of change of the total} \\ \text{volume of the fracture} \end{pmatrix} = \begin{pmatrix} \text{rate of flow of fluid into the fracture} \\ \text{at the fracture entry} \end{pmatrix}. \quad (4.1.14)$$

Let $V(t)$ denote the total volume of the fracture per unit length in the $y-$direction. Then

$$V(t) = 2\int_0^{L(t)} h(x,t)\,\mathrm{d}x, \quad (4.1.15)$$

where $L(t)$ is the length of the fracture at time t. Denote by $Q(x,t)$ the total volume flux of fluid in the $x-$direction along the fracture. Then

$$Q(x,t) = 2\int_0^{h(x,t)} v_x(x,z,t)\,\mathrm{d}z \quad (4.1.16)$$

and the balance law (4.1.14) becomes

$$\frac{dV}{dt} = Q(0,t) = 2\int_0^{h(0,t)} v_x(0,z,t)\,\mathrm{d}z. \quad (4.1.17)$$

In order to simplify (4.1.11) and (4.1.12) for a thin fracture we introduce the dimensionless variables of lubrication theory [18]. Since the length of the fracture is much greater than its width, two length scales are used, $L_0 = L(0)$, the initial fracture length and $H = h(0,0)$, the initial fracture half-width at the fracture entry. Let U be a typical fluid speed in the fracture in the $x-$direction which will be specified later. Therefore, from the continuity equation (4.1.8), the typical fluid speed in the fracture in the $z-$direction is UH/L_0. Then

$$K\Pi^{n-1} = O\left(K\left(\frac{U}{H}\right)^{n-1}\right) \quad (4.1.18)$$

and we define

$$\mu_e = K\left(\frac{U}{H}\right)^{n-1}, \quad (4.1.19)$$

where μ_e is the order of magnitude of the effective viscosity, $K\Pi^{n-1}$, of the power-law fluid in the fracture. For the power-law fluid in the fracture the Reynolds number Re is defined by

$$Re = \frac{\rho U L_0}{\mu_e} = \frac{\rho U^{2-n} L_0 H^{n-1}}{K}. \quad (4.1.20)$$

We will make the thin film approximation of lubrication theory [18] which is

$$\frac{H}{L} << 1, \quad Re\left(\frac{H}{L}\right)^2 << 1. \tag{4.1.21}$$

The characteristic fluid pressure, P, of the power-law fluid in the fracture is derived by balancing the pressure gradient along the fracture with the viscous stress. Consider the $x-$ component of the momentum balance equation (4.1.11) which, replacing the terms by their order of magnitude, is

$$\rho\frac{U^2}{L_0} \sim -\frac{P}{L_0} + \mu_e\frac{U}{L_0^2} + \mu_e\left(\frac{U}{L_0^2} + \frac{U}{H^2}\right). \tag{4.1.22}$$

By the lubrication approximation the viscous terms can be approximated by $\mu_e U/H^2$ and (4.1.22) becomes

$$\rho\frac{U^2}{L_0} \sim -\frac{P}{L_0} + \mu_e\frac{U}{H^2}. \tag{4.1.23}$$

The inertia term in (4.1.23) is neglected since by the lubrication approximation

$$\frac{\text{inertia term}}{\text{viscous term}} = \frac{\frac{\rho U^2}{L_0}}{\mu_e\frac{U}{H^2}} = Re\left(\frac{H}{L_0}\right)^2 << 1. \tag{4.1.24}$$

Equation (4.1.23) therefore reduces to

$$P = \frac{UL_0\mu_e}{H^2} = \frac{U^n L_0 K}{H^{n+1}}, \tag{4.1.25}$$

which is the characteristic fluid pressure.

The dimensionless variables are defined by

$$\begin{aligned} &\overline{t} = \frac{Ut}{L_0},\ \overline{x} = \frac{x}{L_0},\ \overline{z} = \frac{z}{H},\ \overline{v}_x = \frac{v_x}{U},\ \overline{v}_z = \frac{v_z L_0}{UH}, \\ &\overline{p} = \frac{pH^2}{UL_0\mu_e} = \frac{pH^{n+1}}{KL_0U^n},\ \bar{h} = \frac{h}{H},\ \bar{L}(t) = \frac{L(t)}{L_0},\ \bar{V}(t) = \frac{V(t)}{HL_0}. \end{aligned} \tag{4.1.26}$$

With these scalings, (4.1.11), (4.1.12) and (4.1.8) become

$$\begin{aligned} Re\left(\frac{H}{L_0}\right)^2\left(\frac{\partial\overline{v}_x}{\partial\overline{t}} + \overline{v}_x\frac{\partial\overline{v}_x}{\partial\overline{x}} + \overline{v}_z\frac{\partial\overline{v}_x}{\partial\overline{z}}\right) = &-\frac{\partial\overline{p}}{\partial\overline{x}} + 2\left(\frac{H}{L_0}\right)^2\frac{\partial}{\partial\bar{x}}\left(\bar{\Pi}^{n-1}\frac{\partial\overline{v}_x}{\partial\overline{x}}\right) \\ &+ \frac{\partial}{\partial\bar{z}}\left(\bar{\Pi}^{n-1}\left(\left(\frac{H}{L_0}\right)^2\frac{\partial\bar{v}_z}{\partial\bar{x}} + \frac{\partial\overline{v}_x}{\partial\overline{z}}\right)\right), \end{aligned} \tag{4.1.27}$$

$$Re\left(\frac{H}{L_0}\right)^4\left(\frac{\partial\overline{v}_z}{\partial\overline{t}}+\overline{v}_x\frac{\partial\overline{v}_z}{\partial\overline{x}}+\overline{v}_z\frac{\partial\overline{v}_z}{\partial\overline{z}}\right)=-\frac{\partial\overline{p}}{\partial\overline{z}}+\left(\frac{H}{L_0}\right)^2\frac{\partial}{\partial\bar{x}}\left(\bar{\Pi}^{n-1}\left(\left(\frac{H}{L_0}\right)^2\frac{\partial\overline{v}_z}{\partial\overline{x}}+\frac{\partial\overline{v}_x}{\partial\overline{z}}\right)\right)$$
$$+2\left(\frac{H}{L_0}\right)^2\frac{\partial}{\partial\bar{z}}\left(\bar{\Pi}^{n-1}\frac{\partial\bar{v_z}}{\partial\bar{z}}\right), \tag{4.1.28}$$

$$\frac{\partial\overline{v}_x}{\partial\overline{x}}+\frac{\partial\overline{v}_z}{\partial\overline{z}}=0, \tag{4.1.29}$$

where

$$\bar{\Pi}=\left[2\left(\frac{H}{L_0}\right)^2\left(\left(\frac{\partial\bar{v_x}}{\partial\bar{x}}\right)^2+\left(\frac{\partial\bar{v_z}}{\partial\bar{z}}\right)^2\right)+\left(\left(\frac{H}{L_0}\right)^2\frac{\partial\bar{v_z}}{\partial\bar{x}}+\frac{\partial\bar{v_x}}{\partial\bar{z}}\right)^2\right]^{\frac{1}{2}}$$

and the Reynolds number Re is as defined in (4.1.20). We impose the thin film approximation of lubrication theory given in (4.1.21). Expressed in dimensionless variables and by dropping the overhead bars the momentum balance and conservation of mass equations reduce to

$$\frac{\partial p}{\partial x}=\frac{\partial}{\partial z}\left(\left|\frac{\partial v_x}{\partial z}\right|^{n-1}\frac{\partial v_x}{\partial z}\right), \tag{4.1.30}$$

$$\frac{\partial p}{\partial z}=0, \tag{4.1.31}$$

$$\frac{\partial v_x}{\partial x}+\frac{\partial v_z}{\partial z}=0. \tag{4.1.32}$$

The fluid flows through a two-dimensional fracture channel which is symmetrical about the $x-$axis. We will consider the upper half of the fracture and only fluid injection into the fracture. We assume that there is no backflow in the fracture. Then $v_x(x,z,t)$ has a maximum value at $z=0$ and decreases to zero at $z=h(x,t)$ because of the no-slip boundary condition at the fluid-rock interface. Thus in the upper half of the fracture

$$\frac{\partial v_x}{\partial z}<0, \quad 0\le z<h(x,t) \tag{4.1.33}$$

and (4.1.30) can be written as

$$\frac{\partial p}{\partial x}=\frac{\partial}{\partial z}\left(\left(-\frac{\partial v_x}{\partial z}\right)^{n-1}\frac{\partial v_x}{\partial z}\right). \tag{4.1.34}$$

4.2 Initial and boundary conditions

Consider now the boundary conditions. Away from the fracture tip, $x = L(t)$, the width of the fracture varies slowly along its length and the tangential and normal components of the fluid velocity at the fluid-rock interface are approximately $v_x(x, h(x,t), t)$ and $v_z(x, h(x,t), t)$. The boundary conditions at the solid boundary $z = h(x,t)$ of the fracture are the no-slip condition for a viscous fluid and no fluid leak-off because the rock is impermeable and no cavity formation:

$$z = h(x,t): \qquad v_x(x, h(x,t), t) = 0, \tag{4.2.1}$$

$$z = h(x,t): \qquad v_z(x, h(x,t), t) = \left.\frac{Dh}{Dt}\right|_{z=h(x,t)} = \frac{\partial h}{\partial t}. \tag{4.2.2}$$

The above boundary conditions are applicable under the thin fluid film approximation [44]. From symmetry of the two-dimensional fracture about the $x-$axis, $v_z(x,z,t)$ vanishes on the $x-$axis and $v_x(x,z,t)$ attains a maximum value on the $x-$axis. Thus

$$z = 0: \quad v_z(x,0,t) = 0, \quad \frac{\partial v_x}{\partial z}(x,0,t) = 0. \tag{4.2.3}$$

At the fracture tip, $x = L(t)$, the width of the fracture vanishes:

$$h(L(t), t) = 0. \tag{4.2.4}$$

The initial conditions are

$$t = 0: \qquad L(0) = 1, \qquad h(0,0) = 1. \tag{4.2.5}$$

We impose the conditions $L(0) = 1$ and $h(0,0) = 1$ because the characteristic length in the $x-$direction is the initial length of the fracture and the characteristic length in the $z-$direction is the initial half-width at the fracture entry. A pre-existing fracture exists in the rock mass:

$$t = 0: \qquad h(0,x) = h_0(x), \qquad h_0(0) = 1, \qquad 0 \le x \le L(t). \tag{4.2.6}$$

The initial fracture profile $h_0(x)$ and hence the initial volume V_0 cannot be specified arbitrarily. They are determined from the group invariant solution.

The partial differential equation for $h(x,t)$ is obtained from the boundary condition (4.2.2). From (4.1.31), $p = p(x,t)$. Integrating (4.1.34) once with respect to z and imposing the second boundary condition in (4.2.3) gives

$$\left(-\frac{\partial v_x}{\partial z}\right)^n = -z\frac{\partial p}{\partial x}(x,t), \quad 0 \le z \le h(x,t). \tag{4.2.7}$$

Thus

$$\frac{\partial p}{\partial x}(x,t) \le 0, \quad 0 \le x \le L(t). \tag{4.2.8}$$

Integrating (4.2.7) with respect to z and imposing the no slip boundary condition (4.2.1) yields

$$v_x(x,z,t) = \frac{n}{(n+1)}\left(\frac{-\partial p}{\partial x}\right)^{\frac{1}{n}}\left(h^{\frac{n+1}{n}}(x,t) - z^{\frac{n+1}{n}}\right), \quad 0 \le z \le h(x,t). \tag{4.2.9}$$

In order to obtain $v_z(x,h,t)$, we integrate (4.1.32) with respect to z from $z = 0$ to $z = h(x,t)$ and use the first boundary condition in (4.2.3) and the formula for differentiation under the integral sign [45] with boundary condition (4.2.1). This gives

$$v_z(x,h,t) = -\frac{\partial}{\partial x}\int_0^{h(x,t)} v_x(x,z,t)\,\mathrm{d}z. \tag{4.2.10}$$

Using (4.2.10), the boundary condition (4.2.2) at the interface $z = h(x,t)$ becomes

$$\frac{\partial h}{\partial t} + \frac{\partial}{\partial x}\int_0^{h(x,t)} v_x(x,z,t)\,\mathrm{d}z = 0. \tag{4.2.11}$$

Substituting (4.2.9) into (4.2.11) yields the nonlinear relation between $h(x,t)$ and $p(x,t)$

$$\frac{\partial h}{\partial t} + \frac{n}{(2n+1)}\frac{\partial}{\partial x}\left(h^{\frac{2n+1}{n}}\left(-\frac{\partial p}{\partial x}\right)^{\frac{1}{n}}\right) = 0. \tag{4.2.12}$$

On substituting (4.2.9) into the total volume flux of fluid in the $x-$direction, $Q(x,t)$, given by (4.1.16), we obtain

$$Q(x,t) = \frac{2n}{(2n+1)}\left(-\frac{\partial p}{\partial x}(x,t)\right)^{\frac{1}{n}} h^{\frac{2n+1}{n}}(x,t). \tag{4.2.13}$$

The balance law for fluid volume, (4.1.17), becomes

$$\frac{dV}{dt} = \frac{2n}{(2n+1)}\left(-\frac{\partial p}{\partial x}(0,t)\right)^{\frac{1}{n}} h^{\frac{2n+1}{n}}(0,t). \tag{4.2.14}$$

The total flux $Q(x,t)$ given by (4.2.13) must vanish at the fracture tip $x = L(t)$ which gives the condition

$$h^{\frac{2n+1}{n}}(L(t),t)\left(-\frac{\partial p}{\partial x}(L(t),t)\right)^{\frac{1}{n}} = 0. \tag{4.2.15}$$

In order to close the system of equations and boundary conditions a relation between the internal fluid pressure $p(x,t)$ and the half-width $h(x,t)$ is required. We will use the PKN theory [4, 6, 46, 47] for which, in the original dimensional variables,

$$p(x,t) - \sigma_0 = \Lambda h(x,t), \tag{4.2.16}$$

where $p(x,t)$ is the internal fluid pressure, σ_0 is the far field compressive stress perpendicular to the fracture and [4]

$$\Lambda = \frac{E}{(1-\nu^2)B}. \tag{4.2.17}$$

The constant Λ is calculated from the material properties of the rock mass. In (4.2.17), E and ν are the Young's modulus and Poisson ratio of the rock and B is the breadth of the fracture in the $y-$direction. In the framework of the PKN model, it is assumed that: (1) the fracture length is much greater than its half-width and (2) that the half-width of the fracture varies only slightly along its length, with maximum variation occurring near the tip. Therefore in planes normal to the direction of propagation of the fracture, a state of plane strain holds and the stress states in any two cross-sections perpendicular to the direction of fracture propagation are independent. There has been renewed interest in the PKN model. Adachi and Peirce [46] have shown that the PKN approximation is applicable in an outer expansion region away from the fracture tip. The PKN model has been re-examined recently by Kovalyshen and Detournay [47] using new approaches for moving boundary problems.

The characteristic velocity U has still to be specified. We choose U by balancing the pressure gradient $\frac{\partial p}{\partial x}$ with $\Lambda\frac{\partial h}{\partial x}$. This gives the alternative expression for the characteristic pressure,

$$P = \Lambda H, \tag{4.2.18}$$

and using (4.1.25) for P we obtain

$$U = \left(\frac{\Lambda H^{n+2}}{L_0 K}\right)^{\frac{1}{n}} = \left(\frac{E H^{n+2}}{(1-\nu^2)B L_0 K}\right)^{\frac{1}{n}}. \tag{4.2.19}$$

When the far field compressive stress σ_0 is scaled by P and expressed in dimensionless form, (4.2.16) becomes

$$p = \sigma_0 + h(x,t). \tag{4.2.20}$$

The dimensionless time in (4.1.26) is rescaled by defining

$$t^* = \frac{n}{(2n+1)}t. \tag{4.2.21}$$

Equation (4.2.12) becomes the nonlinear diffusion equation for $h(x,t^*)$,

$$\frac{\partial h}{\partial t^*} + \frac{\partial}{\partial x}\left(h^{\frac{2n+1}{n}}\left(-\frac{\partial h}{\partial x}\right)^{\frac{1}{n}}\right) = 0. \tag{4.2.22}$$

The balance law for fluid volume (4.2.14) and the boundary condition (4.2.4) become

$$\frac{dV}{dt^*} = 2\left(-\frac{\partial h}{\partial x}(0,t^*)\right)^{\frac{1}{n}} h^{\frac{2n+1}{n}}(0,t^*), \tag{4.2.23}$$

$$h(L(t^*),t^*) = 0. \tag{4.2.24}$$

Condition (4.2.15) becomes

$$h^{\frac{2n+1}{n}}(L(t^*),t^*)\left(-\frac{\partial h}{\partial x}(L(t^*),t^*)\right)^{\frac{1}{n}} = 0. \tag{4.2.25}$$

The problem is to solve the nonlinear diffusion equation (4.2.22) for the fracture half-width $h(x,t^*)$ subject to the boundary conditions (4.2.23) and (4.2.24). The solution obtained must satisfy condition (4.2.25) that the flux of fluid vanishes at the fracture tip.

The fluid velocity and the flux (4.1.16) are rescaled according to

$$v_x^* = \frac{(2n+1)}{n}v_x, \qquad v_z^* = \frac{(2n+1)}{n}v_z, \qquad Q^* = \frac{(2n+1)}{n}Q. \tag{4.2.26}$$

Equation (4.2.9) for v_x becomes

$$v_x^*(x,z,t^*) = \left(\frac{2n+1}{n+1}\right)\left(\frac{-\partial h}{\partial x}\right)^{\frac{1}{n}}\left(h^{\frac{n+1}{n}}(x,t^*) - z^{\frac{n+1}{n}}\right). \tag{4.2.27}$$

The time t is scaled by the characteristic time T defined by

$$T = \frac{(2n+1)}{n}\frac{L_0}{U} = \frac{(2n+1)}{n}\left(\frac{(1-\nu^2)\,BKL_0^{n+1})}{EH^{n+2}}\right)^{\frac{1}{n}} \tag{4.2.28}$$

and is highly dependent on the power-law exponent n. It can be used when comparing the evolution of the fracture for different working conditions at the fracture entry with the same value of n. It cannot be used to compare the same working conditions for different n; the results would then have to be expressed in terms of the unscaled time t.

The time t^* will be used in the remainder of the chapter but to keep the notation simple the star on the time and on the fluid variables will be suppressed, it being understood that the scaled time is used unless otherwise stated.

4.3 Lie point symmetry generators and general properties of the group invariant solution

The group invariant solution of the partial differential equation (4.2.22) is the solution left invariant under a continous symmetry group. The Lie point symmetry generators

$$X = \xi^1(t,x,h)\frac{\partial}{\partial t} + \xi^2(t,x,h)\frac{\partial}{\partial x} + \eta(t,x,h)\frac{\partial}{\partial h} \tag{4.3.1}$$

of equation (4.2.22) are derived by solving for ξ^1, ξ^2 and η the determining equation [42, 48]

$$X^{[2]}F\Big|_{F=0} = 0, \tag{4.3.2}$$

where

$$F(h,h_t,h_x,h_{xx}) = h_t + \frac{(2n+1)}{n}h^{\frac{n+1}{n}}(-h_x)^{\frac{n+1}{n}} - \frac{1}{n}h^{\frac{2n+1}{n}}(-h_x)^{\frac{1-n}{n}}h_{xx} \tag{4.3.3}$$

and subscripts denote partial differentiation. The second prolongation $X^{[2]}$ of X is

$$X^{[2]} = X + \zeta_1\frac{\partial}{\partial h_t} + \zeta_2\frac{\partial}{\partial h_x} + \zeta_{11}\frac{\partial}{\partial h_{tt}} + \zeta_{12}\frac{\partial}{\partial h_{tx}} + \zeta_{22}\frac{\partial}{\partial h_{xx}}, \tag{4.3.4}$$

where

$$\zeta_i = D_i(\eta) - h_k D_i(\xi^k), \qquad i = 1,2, \tag{4.3.5}$$

$$\zeta_{ij} = D_j(\zeta_i) - h_{ik}D_j(\xi^k), \qquad i,j = 1,2, \tag{4.3.6}$$

with summation over the repeated index k from 1 to 2 and

$$D_1 = D_t = \frac{\partial}{\partial t} + h_t\frac{\partial}{\partial h} + h_{tt}\frac{\partial}{\partial h_t} + h_{xt}\frac{\partial}{\partial h_x} + \dots\ , \tag{4.3.7}$$

$$D_2 = D_x = \frac{\partial}{\partial x} + h_x\frac{\partial}{\partial h} + h_{tx}\frac{\partial}{\partial h_t} + h_{xx}\frac{\partial}{\partial h_x} + \dots .\ . \tag{4.3.8}$$

Since $F = F(h, h_t, h_x, h_{xx})$ only ζ_1, ζ_2 and ζ_{22} have to be calculated. The partial derivative h_t, which occurs in ζ_1, ζ_2 and ζ_{22} as well as in (4.2.22), is eliminated from (4.3.2) by evaluating (4.3.2) on $F = 0$. It is found that for $0 < n < \infty$,

$$\begin{aligned} X &= (c_1 + c_2 t)\frac{\partial}{\partial t} + (c_4 + c_3 x)\frac{\partial}{\partial x} + \frac{1}{(n+2)}\left((n+1)c_3 - nc_2\right) h\frac{\partial}{\partial h}, \\ &= c_1 X_1 + c_2 X_2 + c_3 X_3 + c_4 X_4, \end{aligned} \tag{4.3.9}$$

where c_1, c_2, c_3 and c_4 are arbitrary constants and

$$\begin{aligned} X_1 &= \frac{\partial}{\partial t}, & X_2 &= t\frac{\partial}{\partial t} - \left(\frac{n}{n+2}\right) h\frac{\partial}{\partial h}, \\ X_3 &= x\frac{\partial}{\partial x} + \left(\frac{n+1}{n+2}\right) h\frac{\partial}{\partial h}, & X_4 &= \frac{\partial}{\partial x}. \end{aligned} \tag{4.3.10}$$

The values $n = 1$ for a Newtonian fluid and $n = \frac{1}{2}$ had to be treated separately but the final result is given by (4.3.9). Equation (4.3.9) for $n = 1$ agrees with the Lie point symmetry derived for a Newtonian fluid fracture [15]. Only the ratio of the constants c_1 to c_4 can be determined because a Lie point symmetry is not changed by a constant factor. The complete derivation of the Lie point symmetries of equation (4.2.22) is presented in Appendix A.

Now, $h = \Phi(x, t)$ is a group invariant solution of (4.2.22) provided

$$X\left(h - \Phi(x,t)\right)\Big|_{h=\Phi} = 0, \tag{4.3.11}$$

that is, provided

$$(c_1 + c_2 t)\frac{\partial \Phi}{\partial t} + (c_4 + c_3 x)\frac{\partial \Phi}{\partial x} = \frac{1}{n+2}\left((n+1)c_3 - nc_2\right)\Phi. \tag{4.3.12}$$

The system of first order differential equations of the characteristic curves of (4.3.12) are

$$\frac{dt}{c_1 + c_2 t} = \frac{dx}{c_4 + c_3 x} = \frac{(n+2)\, d\Phi}{\left((n+1)\, c_3 - nc_2\right)\Phi}. \tag{4.3.13}$$

It is equivalently rewritten as

$$\frac{dt}{c_1 + c_2 t} = \frac{dx}{c_4 + c_3 x}\ , \qquad \frac{dt}{c_1 + c_2 t} = \frac{(n+2)\, d\Phi}{\left((n+1)\, c_3 - nc_2\right)\Phi}. \tag{4.3.14}$$

On integrating each of the differential equations in (4.3.14), one arrives at the following two first integrals:

$$\Gamma_1 = \frac{c_4 + c_3 x}{(c_1 + c_2 t)^{\frac{c_3}{c_2}}}\ , \qquad \Gamma_2 = \frac{\Phi}{(c_1 + c_2 t)^{\left(\frac{n+1}{n+2}\right)\frac{c_3}{c_2} - \frac{n}{n+2}}}. \tag{4.3.15}$$

The general form of the solution of the quasi-linear partial differential equation (4.3.12) is

$$\Gamma_2 = f(\Gamma_1), \tag{4.3.16}$$

where f is an arbitrary function. Hence

$$\Phi(x,t) = (c_1 + c_2 t)^{\left(\frac{n+1}{n+2}\right)\frac{c_3}{c_2} - \frac{n}{n+2}} f(\xi), \tag{4.3.17}$$

where

$$\xi = \frac{c_4 + c_3 x}{(c_1 + c_2 t)^{\frac{c_3}{c_2}}}. \tag{4.3.18}$$

Since $\Phi(x,t) = h$, it follows that

$$h(x,t) = (c_1 + c_2 t)^{\left(\frac{n+1}{n+2}\right)\frac{c_3}{c_2} - \frac{n}{n+2}} f(\xi), \tag{4.3.19}$$

where $f(\xi)$ is an arbitrary function of ξ. Equation (4.3.19) will now be used to reduce the partial differential equation (4.2.22) to an ordinary differential equation.

Consider the partial differential equation (4.2.22). Substituting (4.3.19) into (4.2.22) reduces (4.2.22) to the second order nonlinear ordinary differential equation

$$c_3^{\frac{1}{n}} \frac{d}{d\xi}\left[f^{2+\frac{1}{n}} \left(-\frac{df}{d\xi} \right)^{\frac{1}{n}} \right] - \frac{d}{d\xi}(\xi f) - \frac{n}{(n+2)} \left(\frac{c_2}{c_3} - \frac{(2n+3)}{n} \right) f(\xi) = 0. \tag{4.3.20}$$

Equation (4.3.20) does not depend on c_4. We therefore take $c_4 = 0$ to give $\xi = 0$ when $x = 0$. From the boundary condition (4.2.24)

$$f(w) = 0 \quad \text{where} \quad w(t) = \frac{c_3 L(t)}{(c_1 + c_2 t)^{\frac{c_3}{c_2}}}. \tag{4.3.21}$$

Differentiate (4.3.21) with respect to t. Then

$$\frac{df}{dw}\frac{dw}{dt} = 0 \tag{4.3.22}$$

and therefore, assuming that $f(w)$ is not constant, it follows that $w(t)$ is constant. Since $L(0) = 1$ we obtain

$$L(t) = \left(1 + \frac{c_2}{c_1} t \right)^{\frac{c_3}{c_2}}. \tag{4.3.23}$$

For sufficiently large time, $L(t)$ becomes approximately the power law at^b, where $a = \frac{c_2}{c_1}^{\frac{c_3}{c_2}}$ and $b = \frac{c_3}{c_2}$.

The total volume of the fracture per unit length in the $y-$ direction, $V(t)$, is given by (4.1.15). Rewriting (4.1.15) using (4.3.19) and (4.3.23) gives

$$V(t) = \frac{2}{c_3}(c_1 + c_2 t)^{\left(\frac{2n+3}{n+2}\right)\frac{c_3}{c_2} - \frac{n}{n+2}} \int_0^{c_3 c_1^{-\frac{c_3}{c_2}}} f(\xi)\,\mathrm{d}\xi, \tag{4.3.24}$$

which may be rewritten as

$$V(t) = V_0 \left(1 + \frac{c_2}{c_1} t\right)^{\left(\frac{2n+3}{n+2}\right)\frac{c_3}{c_2} - \frac{n}{n+2}}, \tag{4.3.25}$$

where V_0, the initial volume of the fracture, is

$$V_0 = \frac{2}{c_3} c_1^{\left(\frac{2n+3}{n+2}\right)\frac{c_3}{c_2} - \frac{n}{n+2}} \int_0^{c_3 c_1^{-\frac{c_3}{c_2}}} f(\xi)\,\mathrm{d}\xi. \tag{4.3.26}$$

The balance law for total volume is given by (4.2.23). Substituting (4.3.24) into (4.2.23) and rewriting the right hand side of (4.2.23) using (4.3.19), puts the balance law in the form

$$c_3^{\frac{1}{n}} f(0)^{2+\frac{1}{n}} \left(-\frac{df}{d\xi}(0)\right)^{\frac{1}{n}} = \frac{n}{(n+2)} \left(\frac{2n+3}{n} - \frac{c_2}{c_3}\right) \int_0^{c_3 c_1^{-\frac{c_3}{c_2}}} f(\xi)\,\mathrm{d}\xi. \tag{4.3.27}$$

Finally, condition (4.2.25) that the fluid flux vanish at the fracture tip becomes

$$f^{\frac{2n+1}{n}} \left(c_3 c_1^{-\frac{c_3}{c_2}}\right) \left(-\frac{df}{d\xi}\left(c_3 c_1^{-\frac{c_3}{c_2}}\right)\right)^{\frac{1}{n}} = 0. \tag{4.3.28}$$

We make the change of variables

$$u = \frac{x}{L(t)}, \quad \xi = c_3 c_1^{-\frac{c_3}{c_2}} u, \quad f(\xi) = c_3^{\frac{n}{n+2}} c_1^{-\left(\frac{n+1}{n+2}\right)\frac{c_3}{c_2}} F(u), \tag{4.3.29}$$

where $0 \le u \le 1$ and define

$$c = \frac{c_3}{c_2}, \qquad V_c = 2\int_0^1 F(u)\,\mathrm{d}u. \tag{4.3.30}$$

The ratio $\frac{c_3}{c_1}$ is obtained from (4.3.26) which gives

$$\frac{c_3}{c_1} = \left(\frac{V_0}{V_c}\right)^{\frac{n+2}{n}} \tag{4.3.31}$$

and therefore

$$\frac{c_2}{c_1} = \frac{c_2}{c_3}\frac{c_3}{c_1} = \frac{1}{c}\left(\frac{V_0}{V_c}\right)^{\frac{n+2}{n}}. \tag{4.3.32}$$

The quantities n and c are specified. The problem is to solve the ordinary differential equation

$$\frac{d}{du}\left[F^{2+\frac{1}{n}}\left(-\frac{dF}{du}\right)^{\frac{1}{n}}\right]-\frac{d}{du}\left(uF\right)-\frac{n}{n+2}\left[\frac{1}{c}-\frac{(2n+3)}{n}\right]F=0, \tag{4.3.33}$$

subject to the boundary conditions

$$F(1)=0, \tag{4.3.34}$$

$$\left(F(0)\right)^{2+\frac{1}{n}}\left(-\frac{dF}{du}(0)\right)^{\frac{1}{n}}=\frac{n}{n+2}\left(\frac{2n+3}{n}-\frac{1}{c}\right)\int_0^1 F(u)\,\mathrm{d}u. \tag{4.3.35}$$

Once $F(u)$ has been calculated, $V(t)$, $L(t)$ and $h(x,t)$ are obtained from (4.3.25), (4.3.23) and (4.3.19) which take the form

$$V(t)=\ V_0\left[1+\frac{1}{c}\left(\frac{V_0}{V_c}\right)^{\frac{n+2}{n}}t\right]^{\left(\frac{2n+3}{n+2}\right)c-\frac{n}{n+2}}, \tag{4.3.36}$$

$$L(t)=\left[1+\frac{1}{c}\left(\frac{V_0}{V_c}\right)^{\frac{n+2}{n}}t\right]^{c}, \tag{4.3.37}$$

$$h(x,t)=\frac{V_0}{V_c}\left[1+\frac{1}{c}\left(\frac{V_0}{V_c}\right)^{\frac{n+2}{n}}t\right]^{\left(\frac{n+1}{n+2}\right)c-\frac{n}{n+2}}F(u), \tag{4.3.38}$$

and the fluid pressure is given by

$$p(x,t)=\sigma_0+h(x,t). \tag{4.3.39}$$

Since H, the characteristic distance in the z-direction, is the initial half-width at the entry to the fracture, $h(0,0)=1$ and therefore from (4.3.38)

$$\frac{V_0}{V_c}=\frac{1}{F(0)}. \tag{4.3.40}$$

Hence using (4.3.30)

$$V_0=\frac{2}{F(0)}\int_0^1 F(u)\,\mathrm{d}u. \tag{4.3.41}$$

The initial half-width at the fracture entry, H, and the initial length of the fracture, L_0, are specified. However, the initial volume of the fracture, V_0, in the group invariant solution cannot be specified. It is determined from (4.3.41). The ratio $\frac{V_0}{V_c}$ which occurs in (4.3.36)

to (4.3.39) is given simply by (4.3.40). The solutions (4.3.36) to (4.3.38) for $V(t)$, $L(t)$ and $h(x,t)$ can be written entirely in terms of $F(u)$ as follows:

$$V(t) = V_0 \left[1 + \frac{t}{cF(0)^{\frac{n+2}{n}}}\right]^{\left(\frac{2n+3}{n+2}\right)c - \frac{n}{n+2}}, \tag{4.3.42}$$

$$L(t) = \left[1 + \frac{t}{cF(0)^{\frac{n+2}{n}}}\right]^{c}, \tag{4.3.43}$$

$$h(x,t) = \left[1 + \frac{t}{cF(0)^{\frac{n+2}{n}}}\right]^{\left(\frac{n+1}{n+2}\right)c - \frac{n}{n+2}} \frac{F(u)}{F(0)}, \tag{4.3.44}$$

where V_0 is given by (4.3.41).

The solution for $F(u)$ must satisfy condition (4.3.28) that the flux of fluid vanish at the fracture tip, $u = 1$:

$$(F(1))^{2+\frac{1}{n}} \left(-\frac{dF}{du}(1)\right)^{\frac{1}{n}} = 0. \tag{4.3.45}$$

The value of c is determined from the operating conditions at the entrance to the fracture. A range of operating conditions with the corresponding values of c, which depend on n, are presented in Table 4.3.1. The results in Table 4.3.1 are readily derived by considering the exponents in (4.3.42) to (4.3.44) for $V(t)$, $L(t)$, $h(x,t)$ and equation (4.3.39) for $p(x,t)$. From (4.3.43), for large values of time, $L(t)$ grows approximately like t^c. Except for the case $c = 1$, c is an increasing function of n. The way c increases as n increases from $0 < n < 1$ for shear thinning fluids, to $n = 1$ for a Newtonian fluid, to $n > 1$ for shear thickening fluids, is shown in Fig 4.3.1. The evolution of the fracture has stronger dependence on the working conditions for shear thinning than shear thickening fluids. Except when the volume of the fracture remains constant, for shear thickening fluids c rapidly approaches unity as n increases and for large values of n the evolution of the fracture does not depend strongly on the working conditions at the fracture entry. The curves in Figure 4.3.1 do not intersect and therefore the relative effect of the working conditions on the evolution of the fracture does not depend on n.

A general asymptotic result can be derived which holds for all values of c and all $n > 0$. We look for an asymptotic solution of (4.3.33) of the form $F(u) \sim A\,(1-u)^p$ as $u \to 1$.

Operating conditions	$c(n)$	Values of $c(n)$				
		$n=0$	$n=0.5$	$n=1$	$n=2$	$n=\infty$
Length of fracture is constant	0	0	0	0	0	0
Total volume of fluid in fracture is constant	$\frac{n}{2n+3}$	0	0.125	0.2	0.286	0.5
Pressure at fracture entry is constant	$\frac{n}{n+1}$	0	0.333	0.5	0.667	1
Rate of change of the total volume of the fracture is constant. Equivalently, rate of fluid injection at the fracture entry is constant	$\frac{2(n+1)}{2n+3}$	0.66	0.75	0.8	0.857	1
Speed of propagation of the fracture is constant	1	1	1	1	1	1

Table 4.3.1: Physical significance of values of c.

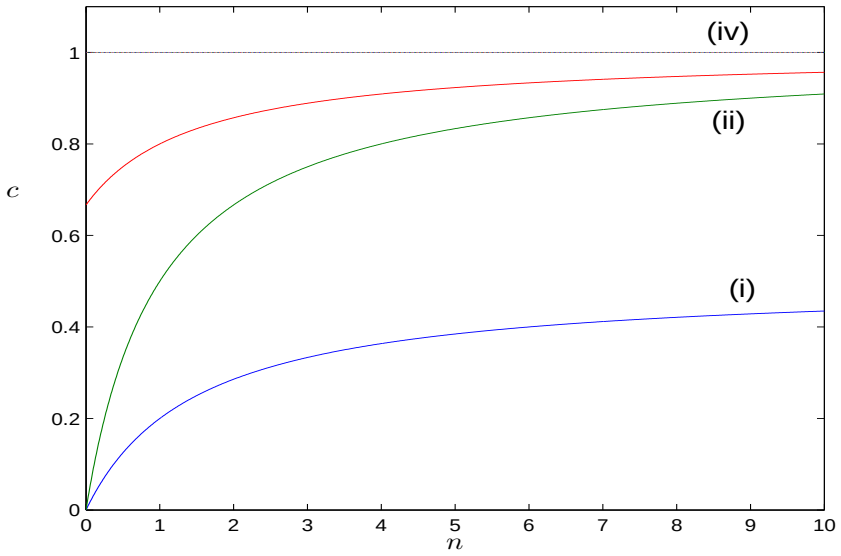

Figure 4.3.1: Variation of the exponent c with n for (i) $c=\frac{n}{2n+3}$, (ii) $c=\frac{n}{n+1}$, (iii) $c=\frac{2(n+1)}{2n+3}$ and (iv) $c=1$.

When this form is substituted into (4.3.33), we obtain

$$A^{\frac{2n+2}{n}} p^{\frac{1}{n}} \left(\frac{2p\,(n+1)-1}{n} \right) (1-u)^{\frac{(2p-1)(n+1)}{n}} - Ap\,(1-u)^{p-1} + \left[(p+1) - \frac{n}{n+2} \left(\frac{2n+3}{n} - \frac{1}{c} \right) \right] A\,(1-u)^{p} \sim 0, \quad (4.3.46)$$

as $u \to 1$. The dominant terms balance each other in (4.3.46) provided

$$\frac{(2p-1)(n+1)}{n} = p-1, \quad (4.3.47)$$

which implies that $p = \frac{1}{n+2}$. Substituting this expression for p into (4.3.46) yields

$$A^{\frac{2n+2}{n}} \left(\frac{1}{n+2} \right)^{\frac{n+1}{n}} (1-u)^{-\left(\frac{n+1}{n+2}\right)} - \frac{A}{n+2} (1-u)^{-\left(\frac{n+1}{n+2}\right)} + \left(\frac{n}{n+2} \right) A \left(\frac{1}{c} - 1 \right) (1-u)^{\frac{1}{n+2}} \sim 0, \quad (4.3.48)$$

as $u \to 1$, and therefore

$$A^{\frac{2n+2}{n}} \left(\frac{1}{n+2} \right)^{\frac{n+1}{n}} - \frac{A}{n+2} + \left(\frac{n}{n+2} \right) A \left(\frac{1}{c} - 1 \right) (1-u) \sim 0 \quad (4.3.49)$$

as $u \to 1$. Hence, setting $u = 1$ in (4.3.49), we obtain

$$A = (n+2)^{\frac{1}{n+2}}. \quad (4.3.50)$$

Thus, the asymptotic solution of (4.3.33) as $u \to 1$, which is true for all values of c and $n > 0$ is

$$F(u) \sim (n+2)^{\frac{1}{n+2}} (1-u)^{\frac{1}{n+2}} \quad \text{as} \quad u \to 1. \quad (4.3.51)$$

This result is used in Section 4.5 when deriving the numerical solution by a shooting method. Using (4.3.51) it can be shown that

$$F(u)^{2+\frac{1}{n}} \left(-\frac{dF}{du}(u) \right)^{\frac{1}{n}} = (n+2)^{\frac{1}{n+2}} (1-u)^{\frac{1}{n+2}} = F(u) \to 0 \quad \text{as} \quad u \to 1. \quad (4.3.52)$$

Condition (4.3.45) that the flux of fluid vanish at the fracture tip, $u = 1$, is therefore satisfied for all $n > 0$. The lubrication approximation, however, breaks down at the fracture tip. For

$$\frac{dF}{du} \sim -\left[(n+2)(1-u) \right]^{-\left(\frac{n+1}{n+2}\right)} \quad \text{as} \quad u \to 1 \quad (4.3.53)$$

and hence from (4.3.38)

$$\frac{\partial h}{\partial x} \to -\infty \quad \text{as} \quad x \to L(t). \tag{4.3.54}$$

The condition $\frac{H}{L_0} << 1$ is therefore no longer satisfied near the tip. Also, the boundary conditions (4.2.1) and (4.2.2) are no longer a good approximation because v_x is not approximately tangential and v_z is not approximately normal to the interface near $x = L(t)$.

4.4 Exact analytical solutions

There are two special cases for which exact analytical solutions can be derived. The first case is when

$$c = \frac{n}{2n+3}. \tag{4.4.1}$$

Equation (4.3.33) reduces to

$$\frac{d}{du}\left[F^{2+\frac{1}{n}}\left(-\frac{dF}{du}\right)^{\frac{1}{n}}\right] - \frac{d}{du}\left(uF\right) = 0, \tag{4.4.2}$$

subject to the boundary conditions

$$F(1) = 0, \tag{4.4.3}$$

$$\frac{dF}{du}(0) = 0. \tag{4.4.4}$$

The differential equation (4.4.2) can be integrated and its solution subject to the boundary conditions (4.4.3) and (4.4.4) is

$$F(u) = \left(\frac{n+2}{n+1}\right)^{\frac{1}{n+2}} \left(1 - u^{n+1}\right)^{\frac{1}{n+2}}. \tag{4.4.5}$$

Since from (4.4.5),

$$F(u)^{\frac{2n+1}{n}}\left(-\frac{dF}{du}\right)^{\frac{1}{n}} = uF(u), \tag{4.4.6}$$

we can again verify that the zero flux condition (4.3.45) at the tip, $u = 1$, is satisfied. From (4.4.6) we see that the flux also vanishes at the fracture entrance, $u = 0$. Equations (4.3.42) to

(4.3.44) give

$$V(t) = V_0 = 2\int_0^1 \left(1-u^{n+1}\right)^{\frac{1}{n+2}}\,\mathrm{d}u, \tag{4.4.7}$$

$$L(t) = \left[1 + \frac{(2n+3)}{n}\left(\frac{n+1}{n+2}\right)^{\frac{1}{n}} t\right]^{\frac{n}{2n+3}}, \tag{4.4.8}$$

$$h(x,t) = \frac{1}{L(t)}\left[1-u^{n+1}\right]^{\frac{1}{n+2}}. \tag{4.4.9}$$

From (4.4.7) we see that the physical significance of this special solution is that the total volume of the fracture remains constant. The influx of fluid at the fracture entry vanishes but the length of the fracture increases as the fracture evolves. The half-width decreases to keep the total volume of the fracture constant. In Figure 4.4.1 the evolution of the half-width of the fracture for various values of the power-law index, n, is shown.

The second analytical solution is obtained by looking for a solution of (4.3.33) of the form

$$F(u) = A(1-u)^p, \tag{4.4.10}$$

where A and p are constants. Substituting (4.4.10) into (4.3.33), we obtain

$$A^{\frac{2n+2}{n}} p^{\frac{1}{n}} \left(\frac{2p\,(n+1)-1}{n}\right)(1-u)^{\frac{(2p-1)(n+1)}{n}} - Ap\,(1-u)^{p-1} + \left[(p+1) - \frac{n}{n+2}\left(\frac{2n+3}{n} - \frac{1}{c}\right)\right] A\,(1-u)^p = 0. \tag{4.4.11}$$

Equation (4.4.11) will be satisfied provided

$$A^{\frac{2n+2}{n}} p^{\frac{1}{n}} \left(\frac{2p\,(n+1)-1}{n}\right)(1-u)^{\frac{(2p-1)(n+1)}{n}} - Ap\,(1-u)^{p-1} = 0 \tag{4.4.12}$$

and

$$p + 1 - \frac{n}{n+2}\left(\frac{2n+3}{n} - \frac{1}{c}\right) = 0. \tag{4.4.13}$$

Equating the powers of $(1-u)$ in (4.4.12) yields $p = \frac{1}{n+2}$, and when this expression for p is substituted into (4.4.12) and (4.4.13), we obtain

$$A = (n+2)^{\frac{1}{n+2}} \tag{4.4.14}$$

and

$$c = 1. \tag{4.4.15}$$

(i)

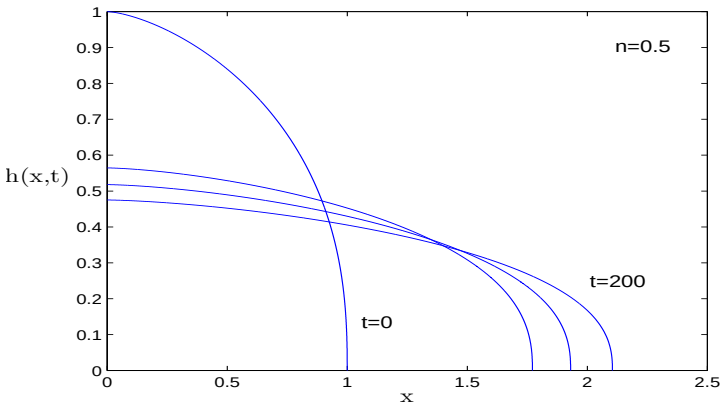

(ii)

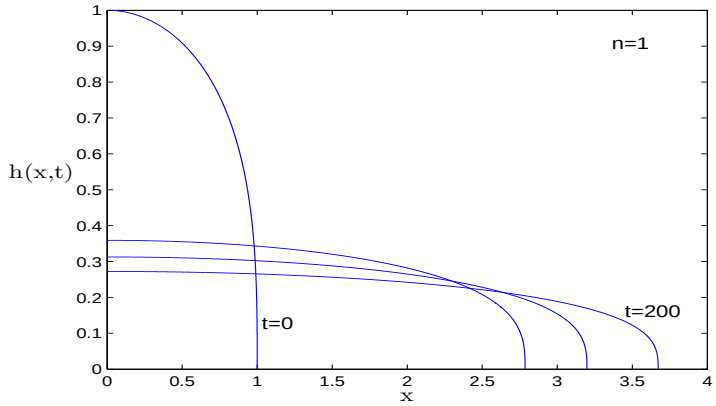

(iii)

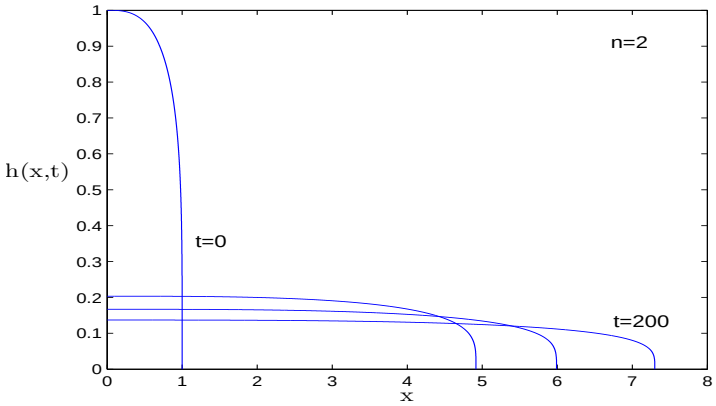

Figure 4.4.1: Fracture propagating with constant volume. Fracture half-width $h(x,t)$ given by (4.4.9) plotted against x at times $t = 0, 50, 100, 200$ for (i) a shear thinning fluid with $n = \frac{1}{2}$, (ii) Newtonian fluid for which $n = 1$ and (iii) shear thickening fluid with $n = 2$. The time t is scaled according to (4.2.28).

Hence, the solution to (4.3.33) of the form (4.4.10) is

$$F(u) = (n+2)^{\frac{1}{n+2}} (1-u)^{\frac{1}{n+2}} \tag{4.4.16}$$

provided $c = 1$. The boundary condition (4.3.34) is also satisfied. With $F(u)$ given by (4.4.16) it can be shown that

$$F(u)^{2+\frac{1}{n}} \left(-\frac{dF}{du}\right)^{\frac{1}{n}} = F(u). \tag{4.4.17}$$

Using these results it can be checked that the boundary condition (4.3.35) is satisfied. It follows also that the flux condition (4.3.45) is satisfied. Equations (4.3.42) to (4.3.44) give

$$V(t) = 2\left(\frac{n+2}{n+3}\right)\left[1 + (n+2)^{-\frac{1}{n}} t\right]^{\frac{n+3}{n+2}}, \tag{4.4.18}$$

$$L(t) = 1 + (n+2)^{-\frac{1}{n}} t\,, \tag{4.4.19}$$

$$h(x,t) = L(t)^{\frac{1}{n+2}} (1-u)^{\frac{1}{n+2}}\,. \tag{4.4.20}$$

The special feature of this exact solution is that the speed of propagation of the fracture, $\frac{dL}{dt}$, is constant. In Figure 4.4.2, the evolution of the half-width for a range of values of the exponent n is shown.

The exact analytical solutions will be investigated further in Section 4.6. They are useful for checking the accuracy of numerical methods.

4.5 Numerical solution

In general the differential equation (4.3.33) cannot be integrated completely analytically because it admits only one Lie point symmetry generator,

$$X = (n+2)u\frac{\partial}{\partial u} + (n+1)F\frac{\partial}{\partial F}. \tag{4.5.1}$$

It is therefore integrated numerically. The transformation generated by (4.5.1) is used to transform the boundary value problem, (4.3.33) to (4.3.35), into a pair of initial value problems as was done for a Newtonian fluid by Fitt et al. [14] for a hydraulic fracture in impermeable rock and by Fareo and Mason [15] for a hydraulic fracture in permeable rock.

(i)

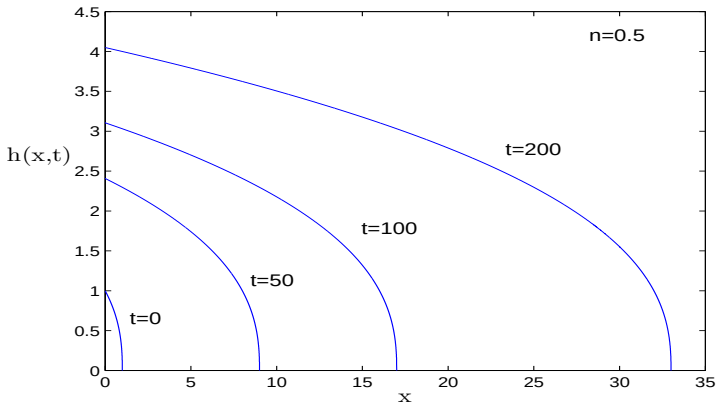

(ii)

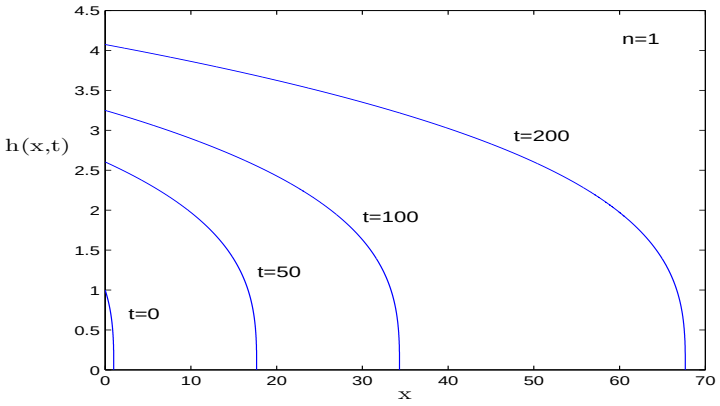

(iii)

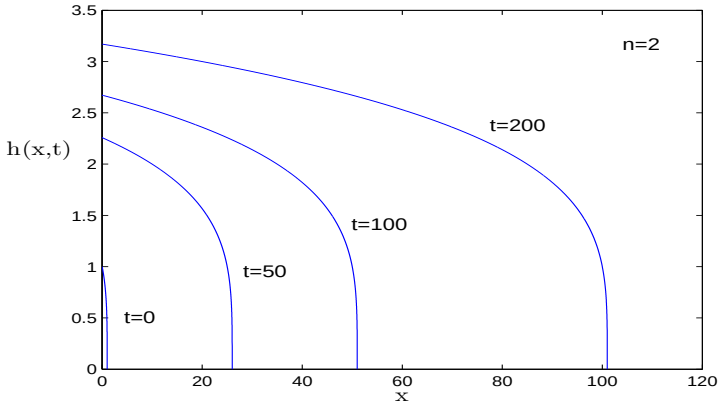

Figure 4.4.2: Fracture propagating with constant speed. Fracture half-width $h(x,t)$ given by (4.4.20) plotted against x at times $t = 0, 50, 100, 200$ for (i) a shear thinning fluid with $n = \frac{1}{2}$, (ii) Newtonian fluid for which $n = 1$ and (iii) shear thickening fluid with $n = 2$. The time t is scaled according to (4.2.28).

Using Lie's equations [42] it can be verified that the Lie point symmetry (4.5.1) generates the scaling transformation

$$\bar{u} = \lambda u, \qquad \bar{F}(\bar{u}) = \lambda^{\frac{n+1}{n+2}} F(u), \tag{4.5.2}$$

where λ is a parameter. The transformation (4.5.2) leaves the form of the differential equation (4.3.33) invariant. We choose $\bar{F}(0) = 1$ and therefore

$$F(0) = \lambda^{-\left(\frac{n+1}{n+2}\right)}. \tag{4.5.3}$$

The parameter λ is determined from the condition $\bar{F}(\lambda) = 0$ which is derived from the boundary condition (4.3.34).

The boundary value problem, (4.3.33) to (4.3.35), is transformed to the following pair of initial value problems:

Initial Value Problem I

$$\frac{d}{d\bar{u}}\left[\bar{F}^{2+\frac{1}{n}}\left(-\frac{d\bar{F}}{d\bar{u}}\right)^{\frac{1}{n}}\right] - \frac{d}{d\bar{u}}\left(\bar{u}\bar{F}\right) - \frac{n}{n+2}\left[\frac{1}{c} - \frac{2n+3}{n}\right]\bar{F} = 0, \tag{4.5.4}$$

$$\bar{F}(0) = 1, \tag{4.5.5}$$

$$\left(-\frac{d\bar{F}}{d\bar{u}}(0)\right)^{\frac{1}{n}} = \frac{n}{n+2}\left(\frac{2n+3}{n} - \frac{1}{c}\right)\int_0^{\lambda} \bar{F}(\bar{u})\,\mathrm{d}\bar{u}, \tag{4.5.6}$$

where $0 \leq \overline{u} \leq \lambda$ and λ satisfies

$$\bar{F}(\lambda) = 0. \tag{4.5.7}$$

Initial Value Problem II

$$\frac{d}{du}\left[F^{2+\frac{1}{n}}\left(-\frac{dF}{du}\right)^{\frac{1}{n}}\right] - \frac{d}{du}\left(uF\right) - \frac{n}{n+2}\left[\frac{1}{c} - \frac{2n+3}{n}\right]F = 0, \tag{4.5.8}$$

$$F(0) = \lambda^{-\left(\frac{n+1}{n+2}\right)}, \tag{4.5.9}$$

$$\frac{dF}{du}(0) = \lambda^{\frac{1}{n+2}}\frac{d\bar{F}}{d\bar{u}}(0), \tag{4.5.10}$$

where $0 \leq u \leq 1$ and the parameter λ and $\frac{d\bar{F}}{d\bar{u}}(0)$ are obtained from Problem I.

Problem I is used only to calculate λ and $\frac{d\bar{F}}{d\bar{u}}(0)$. The solution of Problem II gives the required function $F(u)$. The remainder of the solution is obtained from (4.3.36) to (4.3.39).

For the special case (4.4.1),

$$\bar{F}(\bar{u}) = \left(\frac{n+2}{n+1}\right)^{\frac{1}{n+2}} \left[\frac{n+1}{n+2} - \bar{u}^{n+1}\right]^{\frac{1}{n+2}}, \quad \lambda = \left(\frac{n+1}{n+2}\right)^{\frac{1}{n+1}}, \quad \frac{d\bar{F}}{d\bar{u}}(0) = 0, \quad (4.5.11)$$

while for the special case $c = 1$,

$$\bar{F}(\bar{u}) = (n+2)^{\frac{1}{(n+1)(n+2)}} \left[\lambda - \bar{u}\right]^{\frac{1}{n+2}}, \quad \lambda = (n+2)^{-\frac{1}{(n+1)}}, \quad \frac{d\bar{F}}{d\bar{u}}(0) = -\lambda^n. \quad (4.5.12)$$

Problem I is not a pure initial value problem because λ in the initial condition (4.5.6) is obtained from the boundary condition (4.5.7). Problems I and II were solved numerically using the IVP solver ODE45 of Matlab which is a variable step-size embedded Runge-Kutta scheme.

Problem I was transformed to the coupled system of first order differential equations

$$\frac{d\bar{F}}{d\bar{u}} = -\bar{y}, \quad (4.5.13)$$

$$\frac{d\bar{y}}{d\bar{u}} = \frac{n}{\bar{F}^{\frac{2n+1}{n}} (\bar{y})^{\frac{1}{n}-1}} \left[\frac{(2n+1)}{n} \left(\bar{F}\bar{y}\right)^{1+\frac{1}{n}} - \bar{u}\bar{y} + \frac{n}{(n+2)} \left(\frac{1}{c} - \frac{(n+1)}{n}\right) \bar{F}\right], \quad (4.5.14)$$

subject to the initial and boundary conditions

$$\overline{F}(0) = 1, \quad \bar{y}(0) = \bar{A}, \quad \bar{F}(\lambda) = 0, \quad (4.5.15)$$

where $\bar{A}$ is to be determined. The right hand side of (4.5.14) has a singularity at $\bar{u} = \lambda$ because $\bar{F}(\lambda) = 0$. The difficulty was overcome with the aid of the asymptotic solution of $\bar{F}(\bar{u})$ as $\bar{u} \to \lambda$. The method was used in numerical solutions by Acton et al.[49] of viscous gravity currents and by Fareo and Mason[15] of hydraulic fracturing of permeable rock by a Newtonian fluid. The asymptotic solution of (4.5.4) as $\bar{u} \to \lambda$ may be obtained from the asymptotic solution (4.3.51) using the scaling transformation (4.5.2):

$$\bar{F}(\bar{u}) \sim \lambda^{\frac{n}{n+2}} (n+2)^{\frac{1}{n+2}} (\lambda - \bar{u})^{\frac{1}{n+2}} \quad \text{as} \quad \bar{u} \to \lambda, \quad (4.5.16)$$

and therefore

$$\bar{y}(\bar{u}) \sim \lambda^{\frac{n}{n+2}} (n+2)^{-\left(\frac{n+1}{n+2}\right)} (\lambda - \bar{u})^{-\left(\frac{n+1}{n+2}\right)} \quad \text{as} \quad \bar{u} \to \lambda, \quad (4.5.17)$$

$$\frac{d\bar{y}}{d\bar{u}} \sim (n+1)\, \lambda^{\frac{n}{n+2}} (n+2)^{-\left(\frac{2n+3}{n+2}\right)} (\lambda - \bar{u})^{-\left(\frac{2n+3}{n+2}\right)} \quad \text{as} \quad \bar{u} \to \lambda. \quad (4.5.18)$$

The degree of the singularity in $\frac{d\bar{y}}{d\bar{u}}$ at $\bar{u} = \lambda$ increases monotonically as n increases and it is therefore more singular for shear thickening fluids than for shear thinning fluids; for n =

0, 1 and ∞, $\frac{d\bar{y}}{d\bar{u}}$ behaves like $(\lambda-\bar{u})^{-\frac{3}{2}}$, $(\lambda-\bar{u})^{-\frac{5}{3}}$ and $(\lambda-\bar{u})^{-2}$ respectively, as $\bar{u}\to\lambda$. Backward integration was commenced at an $\epsilon-$neighbourhood of the point $\bar{u}=\lambda$ with the asymptotic representation (4.5.17) and (4.5.18) as initial conditions. In order to obtain a rapid convergence of the solution $\bar{F}(\bar{u})$, iteration based on the bisection algorithm was used until the condition $\bar{F}(0)=1$ was met. The bisection algorithm was then used again on Problem I, starting the integration with $\bar{y}(0)$ obtained from the initial iteration until $\bar{A}$ converged to

$$\bar{A}=\left[\frac{n}{(n+2)}\left(\frac{2n+3}{n}-\frac{1}{c}\right)\int_0^{\lambda}\bar{F}(\bar{u})\,\mathrm{d}\bar{u}\right]^n. \tag{4.5.19}$$

Problem II was then solved. The differential equation (4.5.8) was transformed to the same coupled first order system, (4.5.13) and (4.5.14), but without the overhead bars. The initial conditions are

$$F(0)=\lambda^{-\left(\frac{n+1}{n+2}\right)},\qquad y(0)=\lambda^{\frac{1}{n+2}}\bar{y}(0), \tag{4.5.20}$$

where λ and $\bar{y}(0)$ are obtained from the solution of Problem I. The solution for $F(u)$ is the required solution of the boundary value problem (4.3.33) to (4.3.35).

The two exact analytical solutions, (4.4.5) and (4.4.16), were used to test the accuracy of the numerical method. In the Initial Value Problem I the order of the singularity in $\frac{d\bar{y}}{d\bar{u}}$ at $\bar{u}=\lambda$ increased with n. We therefore choose $n=2$ to test the accuracy of the numerical method. In Figure 4.5.1 the numerical solution for $L(t)$ is compared with the analytical solutions (4.4.8) and (4.4.19). The graphs for the numerical and analytical solutions overlap. Since the two analytical solutions are extreme cases we conclude that the numerical method is reliable.

In Figure 4.5.2 the fracture length $L(t)$ given by (4.3.43) is plotted against t with a range of working conditions as outlined in Table 4.3.1 for a shear thinning fluid ($n=\frac{1}{2}$), a Newtonian fluid ($n=1$) and a shear thickening fluid ($n=2$). The ordering of the curves remains invariant in the three diagrams which shows that the relative effectiveness of the different working conditions is the same for shear thinning, Newtonian and shear thickening fluids. For the four cases considered $L(t)$ grows most slowly for the fracture propagating with constant volume and most rapidly for the fracture propagating with constant speed. Keeping the rate of fluid injection constant at the fracture entry grows the length of the fracture faster than keeping the pressure constant at the fracture entry.

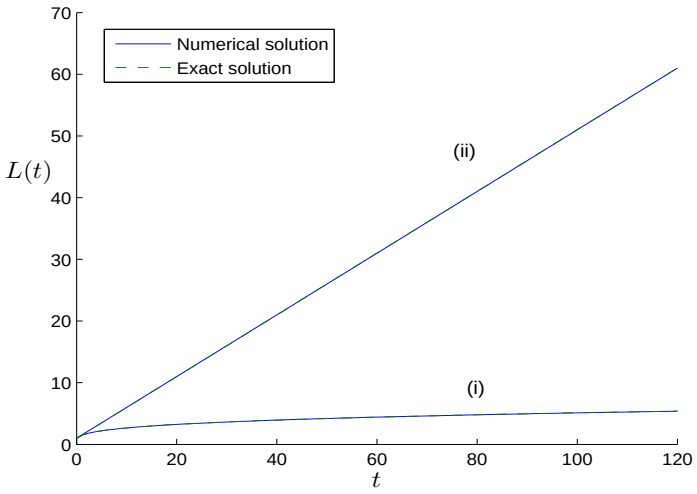

Figure 4.5.1: Comparison of the numerical solution (——) with exact solutions (- - - - -) for $L(t)$ with $n = 2$: (i) numerical solution and exact solution (4.4.8) for a fracture with constant volume, (ii) numerical solution and exact solution (4.4.19) for a fracture propagating with constant speed.

From (4.3.44), the half-width at the fracture entry, $h(0,t)$, decreases, is constant , increases with time depending on whether

$$c < \frac{n}{n+1}, \quad c = \frac{n}{n+1}, \quad c > \frac{n}{n+1}. \tag{4.5.21}$$

In Figure 4.3.1, the curve (ii) defined by

$$c = \frac{n}{n+1} \tag{4.5.22}$$

divides the (n,c) plane into two parts. Below the curve, $h(0,t)$ decreases with time while above it, $h(0,t)$ increases with time. On the curve, $h(0,t)$ is constant. The physical significance of the curve (4.5.22) is that the pressure is constant at the fracture entry which follows from the PKN approximation (4.2.16). When the rate of fluid injection into the fracture is constant $h(0,t)$ will increase and the half-width of the fracture will increase while if the fluid pressure at the fracture entry is constant $h(0,t)$ will remain constant. When fluid injection stops the fracture will continue to evolve but with constant volume and $h(0,t)$ will decrease. For this reason propants such as sand and glass beads are added to the fracturing fluid and transported along the length of the fracture. The propants are trapped in the fracture and resist

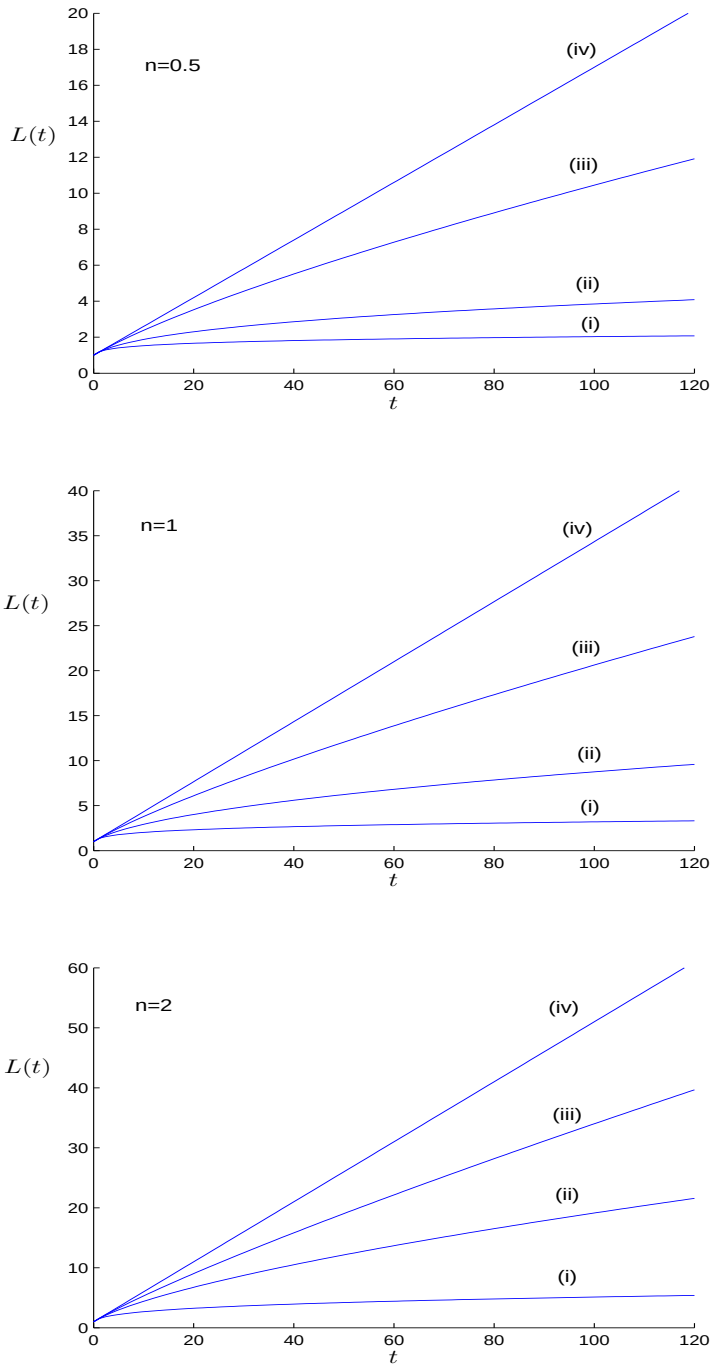

Figure 4.5.2: Fracture length $L(t)$ plotted against t for a range of working conditions at the fracture entry: (i) total volume of the fracture is constant, (ii) pressure at the fracture entry is constant, (iii) rate of fluid injection into fracture is constant, (iv) speed of propagation of the fracture is constant. The corresponding values of c for each value of n are given in Table 4.3.1. The time t is scaled according to (4.2.28).

the relaxation of the half-width after injection of fracturing fluid has been halted. These are ilustrated in Figure 4.5.3 where $h(x,t)$ is plotted against x for a range of values of time for a shear thinning fluid with $n = \frac{1}{2}$. Propants will also be required if the working conditions at the fracture entry are such that $c < \frac{n}{n+1}$ for then the fracture half-width decreases as fluid is injected into the fracture. When the total volume of the fracture remains constant we see that initially the half-width decreases rapidly and the length increases rapidly, consistent with Figure 4.4.1 for $L(t)$. For larger values of time the rate of decrease of the half-width and the rate of increase of the length is much smaller.

From (4.2.8), which is a consequence of the assumption that there is no fluid extraction from the fracture and the PKN approximation,

$$\frac{\partial h}{\partial x} < 0, \quad 0 \le x \le L(t). \tag{4.5.23}$$

Figure 4.5.3 clearly shows that (4.5.23) is satisfied. It shows that (4.3.54) is also satisfied and therefore that the lubrication approximation (4.1.21) breaks down at the fracture tip. When comparing hydraulic fracturing using shear thinning, Newtonian and shear thickening fluids it is essential to consider the same working conditions at the fracture entry. Consider the important case in which the rate of fluid injection into the fracture is constant. Expressed in terms of the dimensional time t and using the characteristic time (4.2.28), the length of the fracture (4.3.43) becomes

$$L(t) = \left[1 + \frac{n(2n+3)}{2(n+1)(2n+1)} \left(\frac{EH^{n+2}}{(1-\nu^2)\, BK(n) L_0^{n+1} F(0)^{n+2}} \right)^{\frac{1}{n}} t \right]^{\frac{2(n+1)}{2n+3}}. \tag{4.5.24}$$

For large values of time we have approximately

$$L(t) \propto t^{\frac{2(n+1)}{2n+3}}. \tag{4.5.25}$$

The exponent of t in (4.5.25) is an increasing function of n. For example, for n=0.5, 1 and 2, $L(t)$ grows at a rate approximately proportional to $t^{\frac{3}{4}}$, $t^{\frac{4}{5}}$ and $t^{\frac{6}{7}}$, respectively. For small values of time the rate of growth of $L(t)$ depends critically on the physical properties of the fracturing fluid through $K(n)$ and $F(0)$ and on the surrounding rock mass through E and ν. To make a reliable estimate of $L(t)$ accurate values of the physical parameters need to be given.

(i)

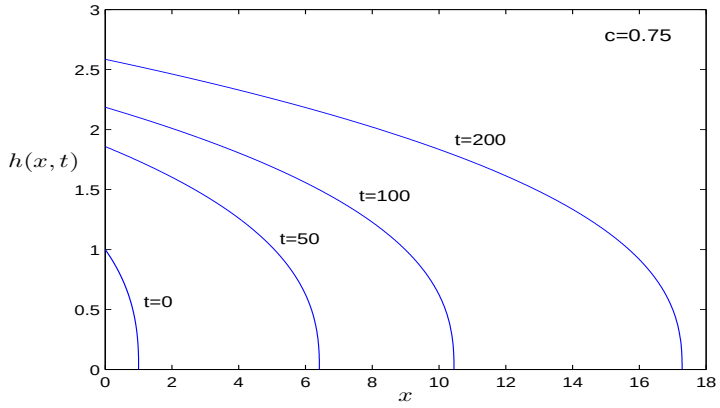

(ii)

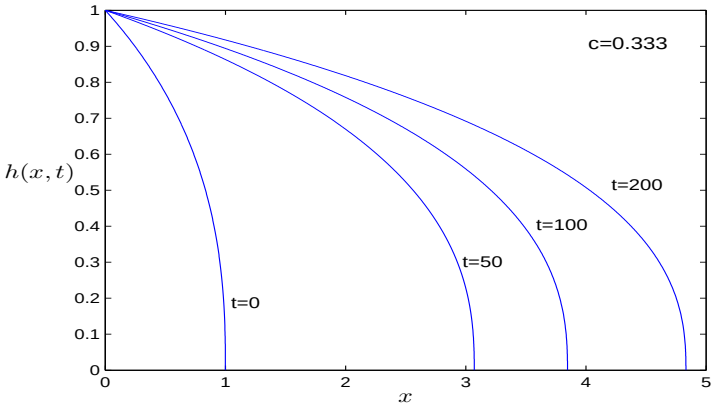

(iii)

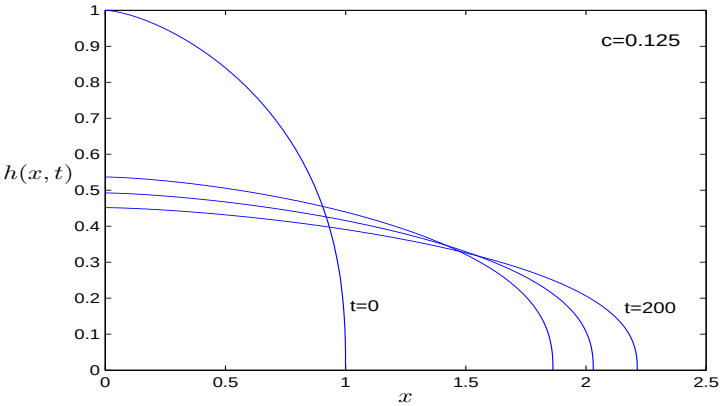

Figure 4.5.3: Fracture half-width $h(x,t)$ given by (4.3.44) plotted against x for a shear thinning fluid with $n = \frac{1}{2}$: (i) rate of fluid injection into the fracture is constant ($c = 0.75$), (ii) pressure at the fracture entry is constant $(c = 0.333)$, (iii) total volume of the fracture is constant $(c = 0.125)$. The time t is scaled according to (4.2.28).

4.6 Streamlines and average fluid velocity

The fluid velocity vector is tangent to the streamlines at each point in the fluid at any instant. The stream function $\psi(x,z,t)$ which is constant along a streamline satisfies

$$v_x(x,z,t)=\frac{\partial\psi}{\partial z},\quad v_z(x,z,t)=-\frac{\partial\psi}{\partial x}. \tag{4.6.1}$$

The velocity component $v_x(x,z,t)$ is given by (4.2.27). The component $v_z(x,z,t)$ is obtained by integrating the continuity equation (4.1.8) with respect to z from $z=0$ to $h(x,t)$ and imposing the symmetry condition $v_z(x,0,t)=0$. We obtain

$$\begin{aligned} v_z(x,z,t)=&\frac{1}{(n+1)}\left(-\frac{\partial h}{\partial x}\right)^{\frac{1}{n}-1}\frac{\partial^2 h}{\partial x^2}\left[\frac{(2n+1)}{n}zh^{1+\frac{1}{n}}(x,t)-z^{2+\frac{1}{n}}\right]\\ &+\frac{(2n+1)}{n}\left(-\frac{\partial h}{\partial x}\right)^{1+\frac{1}{n}}h^{\frac{1}{n}}(x,t)z. \end{aligned} \tag{4.6.2}$$

It is readily verified that the compatibility condition

$$\frac{\partial^2\psi}{\partial x\partial z}=\frac{\partial^2\psi}{\partial z\partial x} \tag{4.6.3}$$

is satisfied. The solution of system (4.6.1) for $\psi(x,z,t)$ is

$$\psi(x,z,t)=\frac{n}{(n+1)}\left(-\frac{\partial h}{\partial x}\right)^{\frac{1}{n}}\left[\frac{(2n+1)}{n}zh^{1+\frac{1}{n}}(x,t)-z^{2+\frac{1}{n}}\right]+f(t), \tag{4.6.4}$$

where $f(t)$ is an arbitrary function of time. The streamlines at time t are the curves

$$\psi(x,z,t)=k, \tag{4.6.5}$$

where k is a constant parameter. By using (4.3.44) for $h(x,t)$ and (4.3.43) for $L(t)$, equation (4.6.5) can be written as

$$A(u)z^{2+\frac{1}{n}}-B(u,t)z=C(t), \tag{4.6.6}$$

where

$$A(u)=\left(-\frac{dF}{du}\right)^{\frac{1}{n}},\quad B(u,t)=\frac{(2n+1)}{n}\left[L(t)^{\frac{1}{n}}\frac{dL}{dt}\right]^{\frac{n+1}{n+2}}F(u)^{1+\frac{1}{n}}\left(-\frac{dF}{du}\right)^{\frac{1}{n}} \tag{4.6.7}$$

and $C(t)$ is an arbitrary function of t. For a Newtonian fluid, $n{=}1$ and (4.6.6) reduces to a cubic equation for z.

In Figure 4.6.1 the streamlines are drawn at time $t=1$ for constant rate of fluid injection into the fracture with $n=0.5$, $n=1$ and $n=2$. The fluid flow is approximately parallel to the axis of the fracture for most of the cross-section but near the fluid-rock interface the streamlines curve to become perpendicular to the interface in order to satisfy the no-slip boundary condition. Since $\operatorname{div} \underline{v} = 0$ the perpendicular distance between neighbouring streamlines decreases in regions of high velocity and increases in regions of low velocity. The streamlines move apart near the fluid-rock interface indicating a region of lower velocity at the fracture boundary consistent with no leak-off into the surrounding rock.

Consider now the fluid velocity on the axis of the fracture. From (4.2.27)

$$v_x(x,0,t) = \left(\frac{2n+1}{n+1}\right)\left(-\frac{\partial h}{\partial x}\right)^{\frac{1}{n}} h^{1+\frac{1}{n}}(x,t). \tag{4.6.8}$$

But using (4.3.44) for $h(x,t)$ and (4.3.43) for $L(t)$, it can be verified that

$$h^{1+\frac{1}{n}}(x,t)\left(-\frac{\partial h}{\partial x}\right)^{\frac{1}{n}} = F(u)^{\frac{n+1}{n}}\left(-\frac{dF}{du}\right)^{\frac{1}{n}}\frac{dL}{dt} \tag{4.6.9}$$

and therefore

$$v_x(x,0,t) = \left(\frac{2n+1}{n+1}\right)F(u)^{\frac{n+1}{n}}\left(-\frac{dF}{du}\right)^{\frac{1}{n}}\frac{dL}{dt}. \tag{4.6.10}$$

Consider the fluid velocity on the axis at the fracture tip. Using the asymptotic solution (4.3.51), it can be shown that

$$F(u)^{\frac{n+1}{n}}\left(-\frac{dF}{du}\right)^{\frac{1}{n}} \to 1, \quad \text{as} \quad u \to 1 \tag{4.6.11}$$

and therefore

$$v_x(L(t),0,t) = \left(\frac{2n+1}{n+1}\right)\frac{dL}{dt}. \tag{4.6.12}$$

The factor $(2n+1)\,/\,(n+1)$ increases steadily with n. It takes the value 1 for $n=0$, 3/2 for $n=1$ and tends to 2 as n tends to infinity. In this model the fluid velocity at the fracture tip exceeds the speed of propagation of the fracture tip.

To investigate this result further consider the average fluid velocity across the fracture defined by

$$\bar{v}_x(x,t) = \frac{1}{h(x,t)}\int_0^{h(x,t)} v_x(x,z,t)\,\mathrm{d}z. \tag{4.6.13}$$

(i)

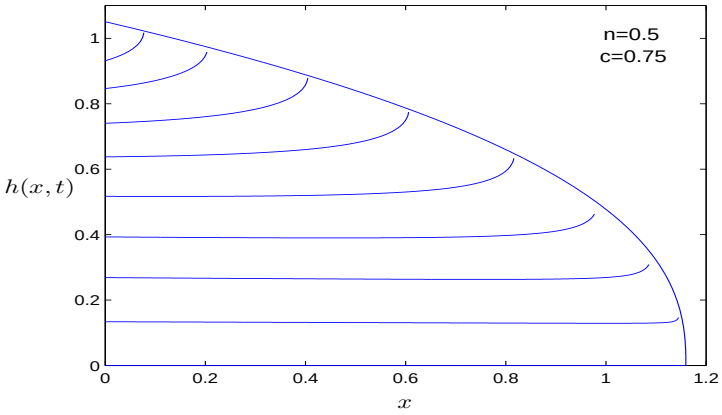

(ii)

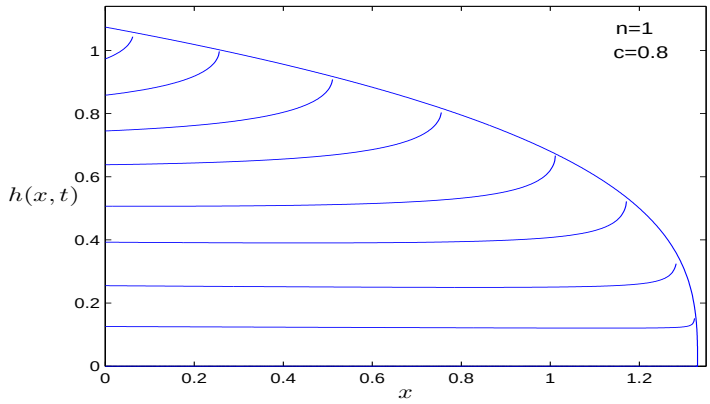

(iii)

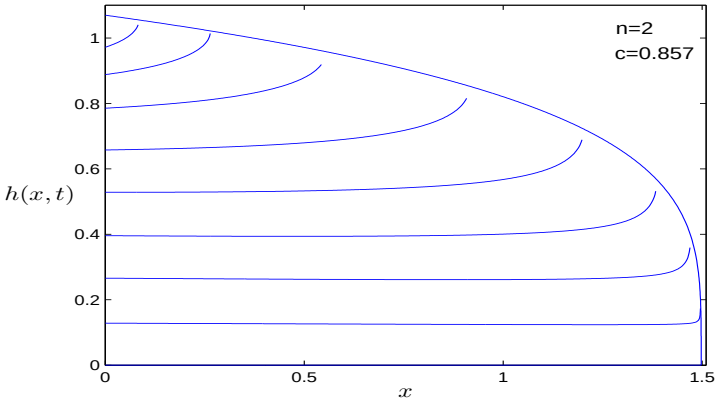

Figure 4.6.1: Streamlines in the fracture at time $t = 1$ for constant rate of fluid injection into the fracture: (i) shear thinning fluid with $n = 0.5$ ($c = 0.75$), (ii) Newtonian fluid with $n = 1$ ($c = 0.8$), (iii) shear thickening fluid with $n = 2$ ($c = 0.857$). The direction of flow is from left to right.

Using (4.2.27) it can be verified that

$$\bar{v}_x(x,t) = h^{\frac{n+1}{n}}(x,t)\left(-\frac{\partial h}{\partial x}\right)^{\frac{1}{n}} \tag{4.6.14}$$

and therefore from (4.6.8),

$$\bar{v}_x(x,t) = \left(\frac{n+1}{2n+1}\right) v_x(x,0,t). \tag{4.6.15}$$

Hence with (4.6.12), at the fracture tip

$$\bar{v}_x(L(t),t) = \frac{dL}{dt} \tag{4.6.16}$$

and the average velocity of the fluid across the fracture tends to the velocity of the fracture tip as x tends to $L(t)$. Since the fracture is thin it is more practical to work with the average fluid velocity at each value of x than with the fluid velocity at each value of x and z. The significance of the average fluid velocity can be seen by considering the total flux of fluid along the fracture defined in (4.2.26). It can be expressed in terms of the average fluid velocity as

$$Q(x,t) = 2h(x,t)\bar{v}_x(x,t). \tag{4.6.17}$$

The velocity of propagation of the flux is therefore $\bar{v}_x(x,t)$ and since (4.6.16) is satisfied there is no fluid lag in the fracture.

We now investigate the way $\bar{v}_x(x,t)$ varies with x along the fracture for $0 \leq x \leq L(t)$ or equivalently, $0 \leq u \leq 1$. From (4.6.9) and (4.6.14)

$$\bar{v}_x(x,t) = F(u)^{\frac{n+1}{n}}\left(-\frac{dF}{du}\right)^{\frac{1}{n}}\frac{dL}{dt}, \quad 0 \leq u \leq 1. \tag{4.6.18}$$

When the total volume of the fracture remains constant, $F(u)$ is given by (4.4.5) and

$$F(u)^{\frac{n+1}{n}}\left(-\frac{dF}{du}\right)^{\frac{1}{n}} = u. \tag{4.6.19}$$

Thus

$$\bar{v}_x(x,t) = u\frac{dL}{dt}, \quad 0 \leq u \leq 1. \tag{4.6.20}$$

We see from (4.6.20) that the average fluid velocity vanishes at the fracture entry. To maintain

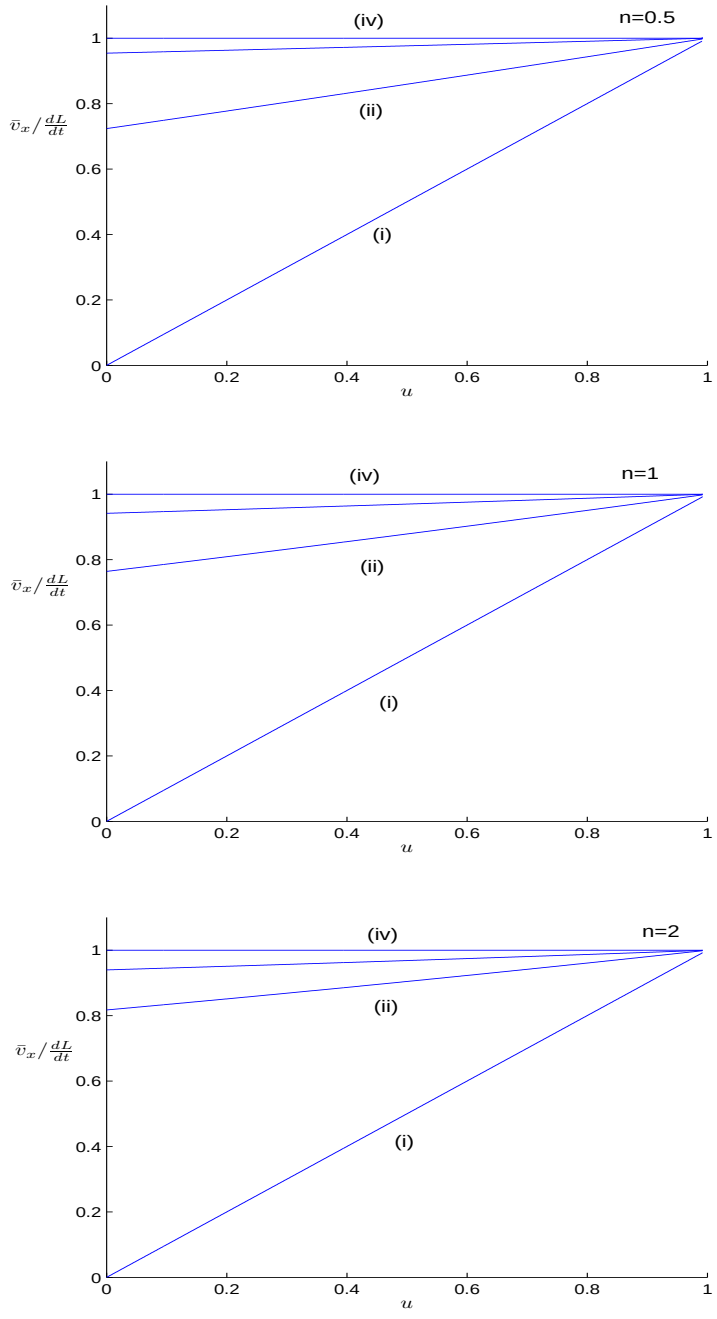

Figure 4.6.2: Velocity ratio $\bar{v}_x/\frac{dL}{dt}$ plotted against $u = x/L(t)$ for $n = 0.5, 1, 2$ and for a range of working conditions at the fracture entry: (i) total volume of the fracture is constant, (ii) fluid pressure constant at fracture entry, (iii) rate of fluid injection is constant, (iv) speed of propagation of the fracture is constant.

constant volume there can be no net input of fluid at the fracture entry. When the rate of propagation of the fracture is constant, $F(u)$ is given by (4.4.16). Hence

$$F(u)^{\frac{n+1}{n}} \left(-\frac{dF}{du}\right)^{\frac{1}{n}} = 1 \tag{4.6.21}$$

and from (4.6.18)

$$\bar{v}_x(x,t) = \frac{dL}{dt}. \tag{4.6.22}$$

From (4.6.22) we see that the average fluid velocity is constant along the whole length of the fracture and equals the constant rate of propagation of the fracture. The velocity ratio

$$\frac{\bar{v}_x(x,t)}{dL/dt} = F(u)^{\frac{n+1}{n}} \left(-\frac{dF}{du}\right)^{\frac{1}{n}} \tag{4.6.23}$$

is independent of t and depends only on n and the working conditions, c. In Figure 4.6.2, the velocity ratio is compared for the same value of n with different working conditions at the fracture entry. For the three cases considered, n=0.5, 1 and 2, the curves are bounded below by the straight line for a fracture evolving with constant volume and above by the horizontal line for a fracture propagating with constant speed. The ordering of the curves according to working conditions at the fracture entry is the same for shear thinning, Newtonian and shear thickening fluids. Except when the speed of propagation of the fracture is constant, the average fluid velocity increases steadily along the fracture and attains its maximum value at the fracture tip which equals the velocity of propagation of the fracture.

4.7 Approximate analytical solution

In Figure 4.6.2 the graphs for the two limiting cases, the constant volume fracture and the fracture propagating with constant speed, are straight lines. We see that the curves between the two limiting graphs are approximately straight lines. Denote the point of intersection of the curve on the velocity ratio axis as (0,A) where A depends on n and on the working condition c. Then the gradient of the straight line joining the points (0,A) and (1,1) is 1-A. When the pressure is constant at the fracture entry and $n = 0.5$ then $A = 0.724$ and $1 - A = 0.276$. The gradient of the numerical curve joining (0,A) and (1,1) varies from 0.266 to 0.285 with

a maximum departure from $1 - A$ of 3.113%. We approximate the curve joining the points (0,A) and $(1, 1)$ by a straight line as shown in Figure 4.7.1. Then from (4.6.23),

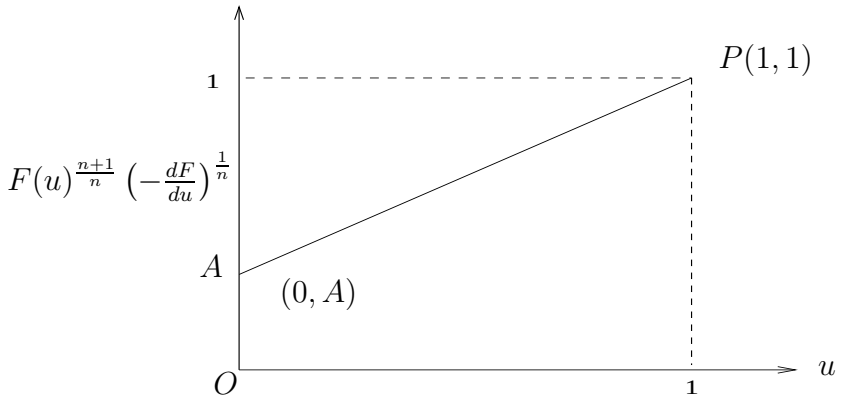

Figure 4.7.1: The straight line joining the points $(0, A)$ and $(1, 1)$ which approximates the curve joining the points.

$$F(u)^{\frac{n+1}{n}}\left(-\frac{dF(u)}{du}\right)^{\frac{1}{n}} = (1-A)u + A. \tag{4.7.1}$$

The analytical solution for $A = 1$ is known and given by (4.4.16). We therefore consider $A \neq 1$ although later we will investigate the limit $A \to 1$ in the solution. We solve the first order ordinary differential equation (4.7.1) for $F(u)$, subject to the boundary condition $F(1) = 0$, to obtain

$$F(u) = \left[\frac{n+2}{(n+1)(1-A)}\right]^{\frac{1}{n+2}}\left[1 - \left[A + (1-A)\,u\right]^{n+1}\right]^{\frac{1}{n+2}}. \tag{4.7.2}$$

For a specific value of n and working condition c the numerical value of A can be used. In order to obtain a general expression for A which is approximately valid for a range of values of n and c, consider the second boundary condition (4.3.35) which is

$$(F(0))^{2+\frac{1}{n}}\left(-\frac{dF}{du}(0)\right)^{\frac{1}{n}} = \frac{n}{n+2}\left(\frac{2n+3}{n} - \frac{1}{c}\right)\int_0^1 F(u)\,\mathrm{d}u. \tag{4.7.3}$$

When (4.7.2) is substituted into (4.7.3), the left hand side of (4.7.3) gives

$$F(0)^{\frac{2n+1}{n}}\left(-\frac{dF}{du}(0)\right)^{\frac{1}{n}} = A\left(\frac{(n+2)}{(n+1)(1-A)}\right)^{\frac{1}{n+2}}\left[1 - A^{n+1}\right]^{\frac{1}{n+2}}. \tag{4.7.4}$$

The integral on the right hand side of (4.7.3) is evaluated by expanding in powers of $u(1-A)$:

$$\begin{aligned}\int_0^1 F(u)\,\mathrm{d}u &= \left[\frac{n+2}{(n+1)\,(1-A)}\right]^{\frac{1}{n+2}} \int_0^1 \left[1-\left[A+(1-A)\,u\right]^{n+1}\right]^{\frac{1}{n+2}}\,\mathrm{d}u \\ &= \left[\frac{n+2}{(n+1)\,(1-A)}\right]^{\frac{1}{n+2}} \int_0^1 \Bigg[1-A^{n+1}\left(1+\frac{(n+1)(1-A)}{A}u\right. \\ &\quad \left.+\frac{n(n+1)(1-A)^2}{2!A^2}u^2+\frac{n(n-1)(n+1)(1-A)^3}{3!A^3}u^3+\ldots\ldots\right)\Bigg]^{\frac{1}{n+2}}\,\mathrm{d}u. \quad (4.7.5)\end{aligned}$$

For working conditions of interest, A lies in the range $0.75 \le A \le 1$. Retaining only terms that are first order in $(1-A)$, we make the approximation

$$\left[1-\left[A+(1-A)\,u\right]^{n+1}\right]^{\frac{1}{n+2}} \simeq \left[\left(1-A^{n+1}\right)-A^n(n+1)(1-A)u\right]^{\frac{1}{n+2}} \quad (4.7.6)$$

so that (4.7.5) becomes

$$\int_0^1 F(u)\,\mathrm{d}u \simeq \left[\frac{n+2}{(n+1)\,(1-A)}\right]^{\frac{1}{n+2}} \left(1-A^{n+1}\right) \int_0^1 \left[1-\frac{A^n(n+1)(1-A)}{(1-A^{n+1})}u\right]^{\frac{1}{n+2}}\mathrm{d}u. \quad (4.7.7)$$

In the integrand in (4.7.7) we make the approximation $A=1$ and use

$$\lim_{A\to 1}\frac{A^n(1-A)}{1-A^{n+1}} = \frac{1}{n+1}. \quad (4.7.8)$$

Hence (4.7.7) becomes approximately

$$\int_0^1 F(u)\,\mathrm{d}u = \left(\frac{n+2}{n+3}\right)\left[\frac{n+2}{(n+1)(1-A)}\right]^{\frac{1}{n+2}}\left[1-A^{n+1}\right]^{\frac{1}{n+2}}. \quad (4.7.9)$$

From (4.7.4) and (4.7.9), the boundary condition (4.7.3) yields the approximate value

$$A = \frac{n}{(n+3)}\left[\frac{2n+3}{n}-\frac{1}{c}\right]. \quad (4.7.10)$$

Due to the truncation of $\mathcal{O}(((1-A)u)^2)$ in (4.7.5), the integral in (4.7.9) is slightly over-overestimated.

Finally we check that (4.7.2) and (4.7.10) approximately satisfy the differential equation (4.3.33). Substituting (4.7.2) into (4.3.33) and after simplification, we have

$$A = \frac{n\left[\dfrac{2n+3}{n}-\dfrac{1}{c}\right]}{(n+2)+\dfrac{(n+1)\left[A+(1-A)u\right]^n}{\left[1-(A+(1-A)u)^{n+1}\right]}-\dfrac{(n+1)\left[A+(1-A)u\right]^{n+1}}{\left[1-(A+(1-A)u)^{n+1}\right]}}. \quad (4.7.11)$$

The denominator in (4.7.11) can be further simplified so that the expression for A becomes

$$A = \frac{n}{(2n+3) - (n+1)\lambda(u;A)} \left[\frac{2n+3}{n} - \frac{1}{c} \right], \tag{4.7.12}$$

where

$$\lambda(u;A) = \frac{1 - [A + (1-A)\,u]^n}{1 - [A + (1-A)\,u]^{n+1}}. \tag{4.7.13}$$

The function $\lambda(u;A)$ must be approximated by a constant value which could depend on n. In the same way as when considering the second boundary condition, we evaluate $\lambda(u;A)$ at $A = 1$:

$$\lim_{A \to 1} \lambda(u;A) = \frac{n}{n+1}. \tag{4.7.14}$$

With (4.7.14), equation (4.7.12) agrees with (4.7.10).

We now verify that (4.7.2) for $F(u)$ reduces to the asymptotic solution (4.3.51) as $u \to 1$. The approximate solution (4.7.2) can be written in the form

$$F(u) = \left[\frac{n+2}{(n+1)\,(1-A)} \right]^{\frac{1}{n+2}} \left[1 - [1 - (1-A)\,(1-u)]^{n+1} \right]^{\frac{1}{n+2}}. \tag{4.7.15}$$

Now,

$$[1 - (1-A)\,(1-u)]^{n+1} = 1 - (n+1)(1-A)(1-u) + \mathcal{O}\left((1-A)(1-u)\right)^2 \text{ as } u \to 1. \tag{4.7.16}$$

Substituting (4.7.16) into (4.7.15) yields

$$F(u) \sim (n+2)^{\frac{1}{n+2}}\,(1-u)^{\frac{1}{n+2}} \text{ as } u \to 1. \tag{4.7.17}$$

Hence the approximate solution tends to the asymptotic solution (4.3.51) as $u \to 1$.

As $A \to 0$, (4.7.2) reduces to (4.4.5) and (4.7.10) gives condition (4.4.1) for a fracture evolving with constant volume. It can be verified that as $A \to 1$, (4.7.2) reduces to the exact solution (4.4.16) and when $A = 1$, (4.7.10) gives $c = 1$. The approximate solution given by (4.7.2) and (4.7.10) should be useful for small values of n close to $n = 0$ where the numerical solution may have difficulty in converging. Taking the limit $n \to 0$ in (4.7.2) gives formally

$$F(u) = \sqrt{2}\,(1-u)^{\frac{1}{2}}. \tag{4.7.18}$$

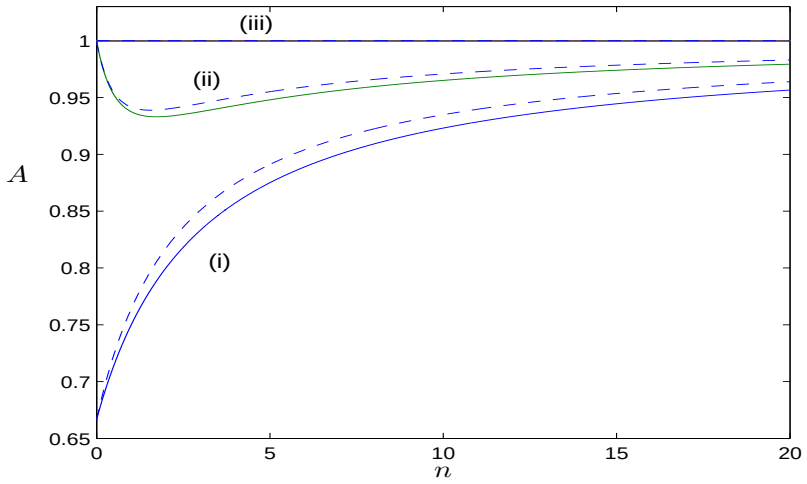

Figure 4.7.2: Velocity ratio at fracture entry, A, plotted against n for a range of working conditions at the fracture entry: (——) approximate solution (4.7.10), (- - - - -) numerical solution. (i) Pressure is constant, (ii) rate of fluid injection is constant , (iii) speed of propagation of the fracture is constant.

The solution of the fracture problem, of course, is not valid in the limit $n \to 0$ because the power $1/n$ is introduced in equation (4.2.9) leading to the exponent $1/n$ in the characteristic time (4.2.28).

To check the accuracy of the approximation for A let A_1 and A_2 be the approximate values given by (4.7.10) when, at the fracture entry, the pressure is constant and the rate of fluid injection is constant, respectively. Then, using c from Table 4.3.1,

$$A_1 = \frac{n+2}{n+3}, \quad A_2 = \frac{(n+2)(2n+3)}{2(n+1)(n+3)}. \tag{4.7.19}$$

The minimum values of A_1 and A_2 occur at $n = 0$ and $n = \sqrt{3}$, respectively and

$$\frac{2}{3} \leq A_1 \leq 1, \quad 0.933 \leq A_2 \leq 1. \tag{4.7.20}$$

The approximate solutions (4.7.19) for A_1 and A_2 are compared with the numerical solutions in Figure 4.7.2. When the pressure is constant at the fracture entry, A steadily increases with n but interestingly when the rate of fluid injection is constant, A first decreases from unity as n increases, reaches a minimum value which occurs for a shear thickening fluid before starting to increase and returning to $A = 1$ as $n \to \infty$. For the numerical solution the minimum values

for A_2 occur for $n = 1.557$ which gives an error of about 11% in the approximate values. The numerical values for the minima of A_1 and A_2 are 0.667 and 0.939 which gives an error of less than 1% in the approximate values. Since the minimum value for A_1 occurs for $n = 0$, which cannot be achieved numerically, extrapolation was carried out to obtain the minimum value for A_1. From Figure 4.7.2 we see that the error in A increases as n increases. It is least accurate when the pressure at the fracture entry is constant because the approximation $A = 1$ was used in the derivation of (4.7.10).

Operating conditions at fracture entry	n=0.1	n=0.25	n=0.5	n=0.75	n=1	n=2
Pressure constant $c = \frac{n}{n+1}$ $A = \frac{n+2}{n+3}$	$A = 0.677$ $A_N = 0.679$ $\%E = 0.360$	$A = 0.692$ $A_N = 0.697$ $\%E = 0.795$	$A = 0.714$ $A_N = 0.723$ $\%E = 1.303$	$A = 0.733$ $A_N = 0.745$ $\%E = 1.629$	$A = 0.750$ $A_N = 0.764$ $\%E = 1.838$	$A = 0.800$ $A_N = 0.817$ $\%E = 2.122$
Rate of fluid injection constant $c = \frac{2(n+1)}{2n+3}$ $A = \frac{(n+2)(2n+3)}{2(n+1)(n+3)}$	$A = 0.985$ $A_N = 0.985$ $\%E = 0.012$	$A = 0.969$ $A_N = 0.969$ $\%E = 0.068$	$A = 0.952$ $A_N = 0.954$ $\%E = 0.194$	$A = 0.942$ $A_N = 0.945$ $\%E = 0.318$	$A = 0.937$ $A_N = 0.941$ $\%E = 0.427$	$A = 0.933$ $A_N = 0.939$ $\%E = 0.682$

Table 4.7.1: Comparison of the numerical value A_N with the analytical value A.

In Figures 4.7.3 and 4.7.4 the approximate and numerical solutions for $h(x,t)$ are compared. Two modes of working at the fracture entry are considered. When the pressure at the fracture entry is constant, the expressions for A and c are given in Table 4.7.1 and the approximate solution, using (4.3.44) is

$$h(x,t) = \frac{F(u)}{F(0)}, \tag{4.7.21}$$

where

$$F(u) = \left[\frac{(n+2)(n+3)}{(n+1)}\right]^{\frac{1}{n+2}} \left[1 - \left(\frac{n+2}{n+3}\right)^{n+1} \left(1 + \frac{u}{(n+2)}\right)^{n+1}\right]^{\frac{1}{n+2}} \tag{4.7.22}$$

and

$$x = uL(t) = u\left[1 + \frac{(n+1)}{nF(0)^{\frac{n+2}{n}}}t\right]^{\frac{n}{n+1}}, \qquad 0 \le u \le 1. \tag{4.7.23}$$

When the rate of fluid injection into the fracture is constant the approximate solution is

$$h(x,t) = \left[1 + \frac{(2n+3)}{2(n+1)F(0)^{\frac{n+2}{n}}}\ t\right]^{\frac{1}{2n+3}} \frac{F(u)}{F(0)}, \tag{4.7.24}$$

where

$$F(u) = \left[\frac{2(n+2)(n+3)}{n}\right]^{\frac{1}{n+2}} \left[1 - \left(\frac{(n+2)(2n+3)}{2(n+1)(n+3)}\right)^{n+1} \times \left(1 + \frac{n}{(n+2)(2n+3)}\ u\right)^{n+1}\right]^{\frac{1}{n+2}} \tag{4.7.25}$$

and

$$x = uL(t) = u\left[1 + \frac{(2n+3)}{2(n+1)F(0)^{\frac{n+2}{n}}}\,t\right]^{\frac{2(n+1)}{2n+3}}, \qquad 0 \le u \le 1. \tag{4.7.26}$$

Both approximate solutions slightly overestimate the width and length of the fracture. They are useful approximations to $h(x,t)$ for shear thinning, Newtonian and shear thickening fluids over a large range of time. The approximate solution may be particularly useful for shear thinning fluids for which numerical solutions can sometimes be difficult to obtain as n approaches zero.

(i)

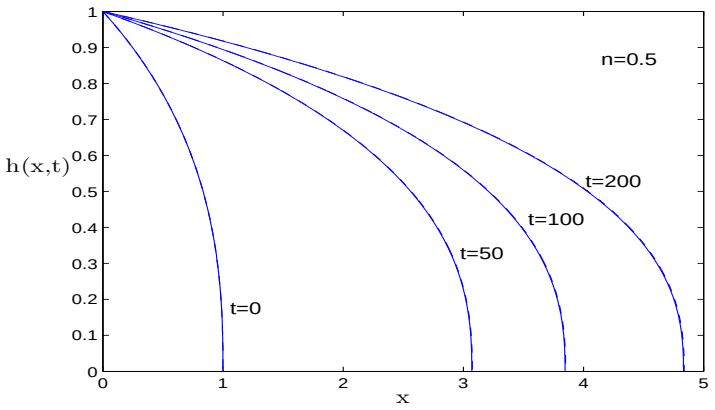

(ii)

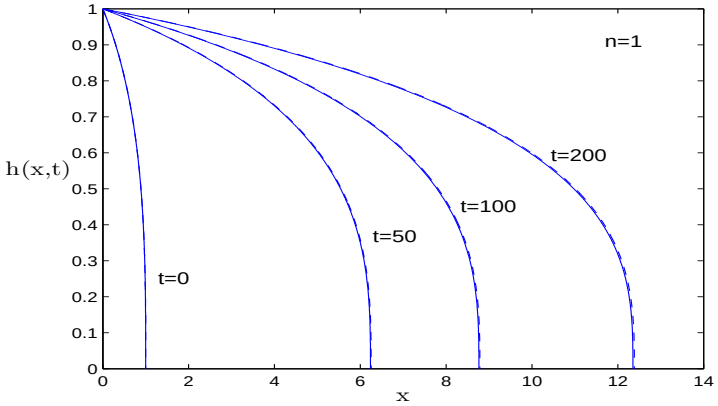

(iii)

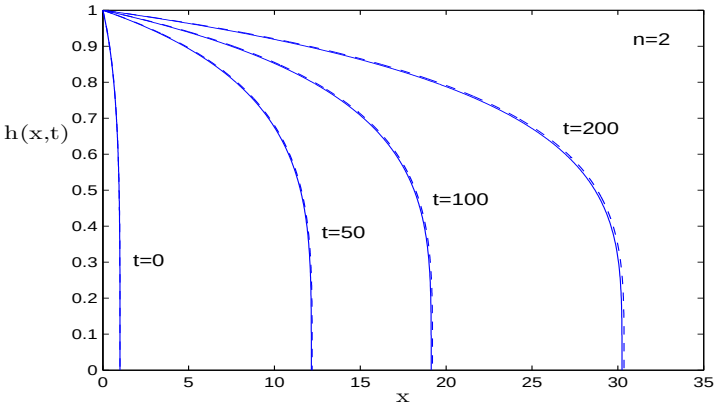

Figure 4.7.3: Comparison of the approximate solution (- - - - -) with the numerical solution (——) for $h(x,t)$ when pressure is constant at the fracture entry for $n = 0.5$, $n = 1$ and $n = 2$.

(i)

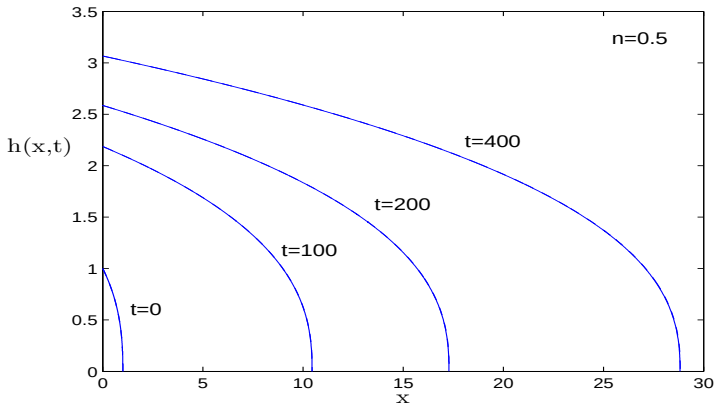

(ii)

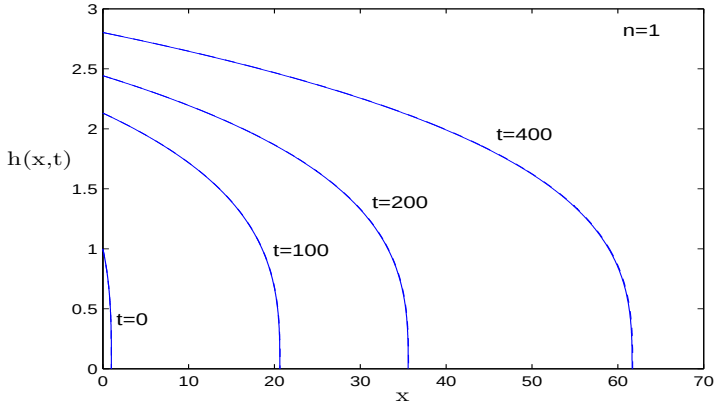

(iii)

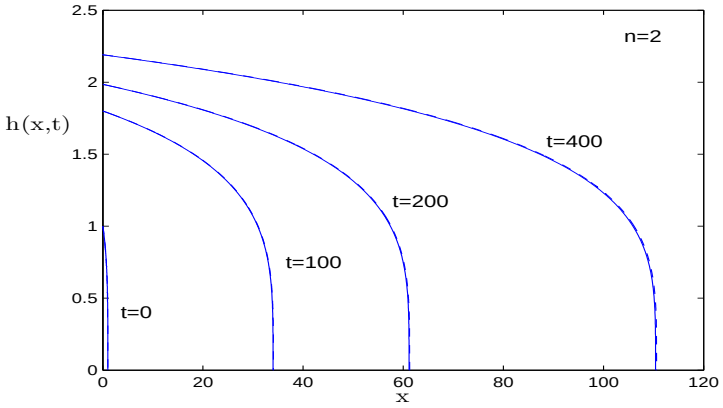

Figure 4.7.4: Comparison of the approximate solution (- - - - -) with the numerical solution (——) for $h(x,t)$ when the rate of fluid injection is constant for $n = 0.5$, $n = 1$ and $n = 2$.

4.8 Conclusions

In this chapter, we have considered a two-dimensional pre-existing fracture propagating in impermeable rock. The propagation is induced when fracturing fluid of power-law rheology, under high pressure, is injected into the two-dimensional fracture. The fluid flow in the fracture is governed by momentum balance equation which was simplified using lubrication theory. The ratio of the half-width to the length of the fracture must be sufficiently small that the lubrication approximation (4.1.21) is satisfied. With the aid of boundary conditions a diffusion equation which describes the evolution of the half-width of the fracture was derived. The physical mechanism for the propagation of the fracture in the rock is therefore diffusion.

Using Lie symmetry analysis, the diffusion equation was reduced to a nonlinear second order ordinary differential equation. The boundary condition could also be expressed in terms of the transformed variables. The problem contained one parameter c which is determined by the working conditions at the fracture entry. The Lie point symmetry which generated the solution is of the form

$$X = \left(\frac{c_1}{c_2} + t\right)\frac{\partial}{\partial t} + cx\frac{\partial}{\partial x} + \frac{1}{(n+2)}\left[(n+1)c - n\right]h\frac{\partial}{\partial h}, \tag{4.8.1}$$

where

$$\frac{c_1}{c_2} = cF(0)^{\frac{n+2}{n}}. \tag{4.8.2}$$

It is not a scaling symmetry since $c_1 \neq 0$ and this is because the initial length of the fracture is non-zero. The simpler methods described by Dresner [50] of using a scaling transformation to derive a similarity solution could therefore not be applied and the full theory of Lie point symmetries is required.

Initial value problems are easier to solve numerically than boundary value problems. The transformation of the boundary value problem into a pair of initial value problems, together with the application of the asymptotic solution at the fracture tip, gave satisfactory numerical results. When compared with the two analytical solutions they were found to be very accurate.

In the literature the main emphasis has been on the growth and shape of the hydraulic fracture and comparatively little work has been done on the velocity of the fluid in the fracture. The streamlines obtained were as expected but that the fluid velocity at the fracture tip exceeds

the tip velocity was unexpected. The mean fluid velocity averaged over the width of the fracture equals the velocity at the fracture tip and it can be concluded that in a thin fracture the mean velocity is more physically significant and the velocity to consider. It was unexpected that the mean velocity would increase approximately linearly along the fracture and exactly linearly when the total volume of the fracture is constant. In the case for which the speed of propagation of the fracture is constant, the mean velocity is constant along the fracture. The approximation based on this observation gave a mathematically simple analytical result for the half-width which was very accurate and may be useful especially for shear thinning fluids for values of n close to $n = 0$.

The results depend on the PKN approximation in which the fluid pressure is linearly related to the half-width of the fracture. The PKN approximation closed the system of equations and leads to the definition of a characteristic velocity along the fracture. It is the simplest physical approximation that can be made. It can be expected that the results obtained will be modified in more physically realistic models especially near the fracture tip.

Chapter 5

Modelling two dimensional power-law fluid driven fracture in permeable rock

5.1 Introduction

In Chapter 4 we considered the problem of modelling a two-dimensional power-law fluid-driven fracture in impermeable rock. We saw that the concept of an average fluid velocity field in the $x-$direction is relevant to the problem of fluid-flow in a thin fracture. This is because for a thin fracture, quantities such as fluid pressure and velocity vary only slightly in the direction normal to the direction of flow. This is a consequence of the half-width of the fracture being much less than its length.

In this Chapter, the problem of a two-dimensional fluid-driven fracture in permeable rock is considered. We begin by outlining the dimensionless equations of the thin film approximation of the equations of motion for the flow of a non-Newtonian fluid in a two-dimensional fracture. These equations form a system of partial differential equations and were used in the derivation of the evolution equation for the fracture half-width in impermeable rock in Chapter 4. The assumptions made in the problem are the same to those stated in Chapter 4 except that the surrounding rock mass is permeable. The assumptions are that the fracturing fluid is incompressible, non-Newtonian and of power-law rheology and that the fluid flow in the fracture is laminar. Also, it is assumed that the rock is a linearly elastic material which assumes

small displacement gradients and, as shown in Figure 5.2.1, the fracture which is one-sided propagates in the positive $x-$direction.

5.2 Mathematical model

The distinguishing feature of this Chapter is that the interface between the fluid and the rock is permeable and that fracturing fluid leaks off at the fluid/rock interface in the direction of the unit vector $\underline{n}$, normal to the fluid/rock interface, with velocity $v_l(x,t)$ relative to the interface. The hydraulic fracture is illustrated in Figure 5.2.1.

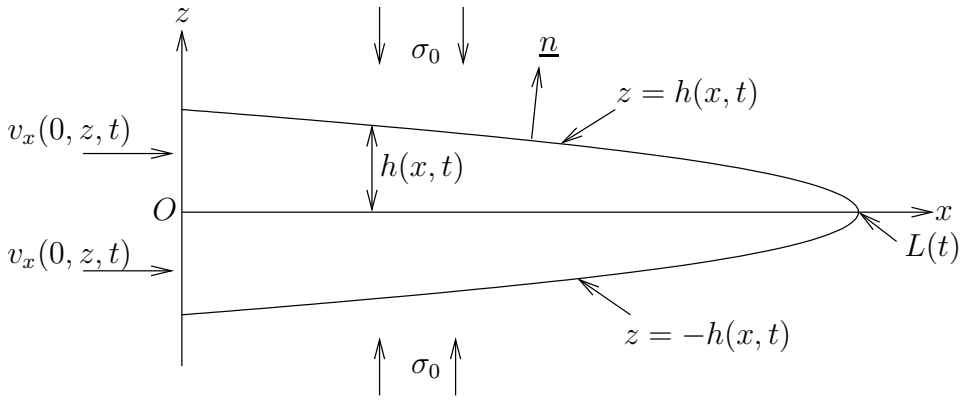

Figure 5.2.1: A hydraulic fracture propagating in an elastic permeable medium. The coordinate direction y points into the page and σ_0 is the far field compressive stress.

The fluid flow is symmetrical about the $x-$axis. As in Chapter 4 we will consider the upper half of the fracture and only fluid injection into the fracture. The no-slip boundary condition still applies at the fluid-rock interface and therefore $v_x(x,z,t)$ decreases from a maximum value at $z=0$ to zero at $z=h(x,t)$. Thus in the upper half of the fracture

$$\frac{\partial v_x}{\partial z}(x,z,t) < 0, \qquad 0 \leq z \leq h(x,t).$$

The two-dimensional momentum balance and continuity equations in dimensionless form

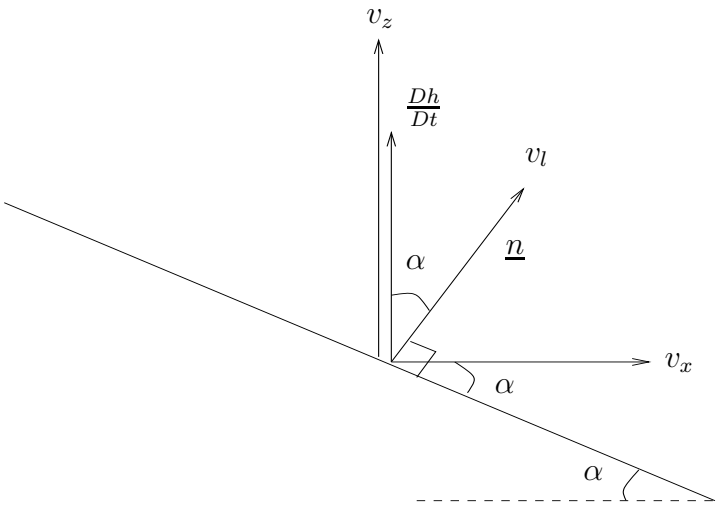

Figure 5.2.2: Tangent plane at a point on the surface, $z = h(x,t)$.

were derived in Chapter 4 for $0 \leq z \leq h(x,t)$ and are given by

$$\frac{\partial p}{\partial x} = \frac{\partial}{\partial z}\left(\left(-\frac{\partial v_x}{\partial z}\right)^{n-1}\frac{\partial v_x}{\partial z}\right), \tag{5.2.1}$$

$$\frac{\partial p}{\partial z} = 0, \tag{5.2.2}$$

$$\frac{\partial v_x}{\partial x} + \frac{\partial v_z}{\partial z} = 0. \tag{5.2.3}$$

The boundary conditions for integrating (5.2.1) to (5.2.3) are obtained from the analysis based on Figure 5.2.2.

From Figure 5.2.2, we obtain the following boundary conditions at $z = h(x,t)$.

No slip condition:

Tangential component of the fluid velocity at the boundary equals the tangential component of the velocity of the boundary:

$$z = h(x,t): \qquad v_x(x,h,t)\cos\alpha - v_z(x,h,t)\sin\alpha = -\frac{Dh}{Dt}\sin\alpha, \tag{5.2.4}$$

where $\frac{D}{Dt}$ denotes the material time derivative.

Leak-off condition:

Normal component of the fluid velocity at the boundary equals the normal component of the velocity of the boundary + normal component of the velocity of fluid relative to the

boundary:

$$z = h(x,t): \qquad v_x(x,h,t)\sin\alpha + v_z(x,h,t)\cos\alpha = \frac{Dh}{Dt}\cos\alpha + v_l(x,t), \tag{5.2.5}$$

where $v_l = \underline{v}.\underline{n}\big|_{z=h(x,t)}$.

Now

$$\tan\alpha = -\frac{\partial h}{\partial x} = \mathcal{O}\left(\frac{H}{L}\right) \tag{5.2.6}$$

and in the thin film approximation $\frac{H}{L} << 1$. Thus α is small and

$$\tan\alpha = \mathcal{O}(\alpha) = \mathcal{O}\left(\frac{H}{L}\right), \quad \sin\alpha = \mathcal{O}(\alpha) = \mathcal{O}\left(\frac{H}{L}\right), \quad \cos\alpha = \mathcal{O}(1) \tag{5.2.7}$$

and the boundary conditions (5.2.4) and (5.2.5) reduce to the following conditions.

No-slip condition:

$$z = h(x,t): \qquad v_x(x,h,t) = 0, \tag{5.2.8}$$

Leak-off condition:

$$z = h(x,t): \qquad v_z(x,h,t) = \frac{Dh}{Dt} + v_l(x,t), \tag{5.2.9}$$

The thin film approximation $\frac{H}{L} << 1$ is a good approximation except near the tip of the fracture. The boundary conditions (5.2.8) to (5.2.9) will therefore be valid except near the fracture tip where the thin film approximation breaks down. Equations (5.2.8) and (5.2.9) are expressed in dimensionless form. The leak-off velocity v_l has been made dimensionless by division by the characteristic velocity in the z-direction $\frac{H}{L}U$. By expanding the material time derivative, (5.2.9) becomes

$$\begin{aligned} v_z(x,h,t) &= \frac{\partial h}{\partial t} + v_x(x,h,t)\frac{\partial h}{\partial x} + v_l(x,t) \\ &= \frac{\partial h}{\partial t} + v_l(x,t), \end{aligned} \tag{5.2.10}$$

since $v_x(x,h,t) = 0$ from the no slip boundary condition (5.2.8). From the symmetry of the fracture,

$$v_z(x,0,t) = 0, \quad \frac{\partial v_x}{\partial z}(x,0,t) = 0, \tag{5.2.11}$$

and at the tip of the fracture, $x = L(t)$,

$$h(L(t),t) = 0. \tag{5.2.12}$$

The initial conditions are

$$t = 0 : \qquad L(0) = 1, \qquad h(0,0) = 1. \tag{5.2.13}$$

A pre-existing fracture exists in the rock mass:

$$t = 0 : \qquad h(0,x) = h_0(x), \quad h_0(0) = 1 \qquad 0 \le x \le L(t). \tag{5.2.14}$$

The initial volume V_0 and the initial fracture profile $h_0(x)$ cannot be specified arbitrarily. They are determined from the group invariant solution.

We make the PKN approximation in which the fluid pressure is linearly related to the half-width of the fracture. Expressed in dimensionless form the PKN approximation is given by (4.2.20):

$$p = \sigma_0 + h(x,t), \tag{5.2.15}$$

where σ_0 is the far field compressive stress.

Integrating (5.2.3) over the upper half of the fracture, and using boundary conditions (5.2.8), (5.2.10) and (5.2.11), the continuity equation expressed in terms of $\bar{v}_x(x,t)$, the $x-$component of the fluid velocity averaged over the upper half of the fracture, is

$$\frac{\partial h}{\partial t} + \frac{\partial}{\partial x}\left(h\bar{v}_x\right) + v_l = 0, \tag{5.2.16}$$

where

$$\bar{v}_x(x,t) = \frac{1}{h}\int_0^h v_x(x,z,t)\,\mathrm{d}z. \tag{5.2.17}$$

The $x-$component of the fluid velocity, obtained by integrating (5.2.1), and using the PKN approximation, is given by (4.2.27):

$$v_x(x,z,t) = \left(\frac{2n+1}{n+1}\right)\left(\frac{-\partial h}{\partial x}\right)^{\frac{1}{n}}\left(h^{\frac{n+1}{n}}(x,t) - z^{\frac{n+1}{n}}\right), \quad 0 \le z \le h(x,t). \tag{5.2.18}$$

When (5.2.18) is substituted into (5.2.17), the average fluid velocity becomes

$$\bar{v}_x(x,t) = \left(-\frac{\partial h}{\partial x}\right)^{\frac{1}{n}} h^{\frac{n+1}{n}}. \tag{5.2.19}$$

Substituting (5.2.19) into (5.2.16) yields

$$\frac{\partial h}{\partial t} + \frac{\partial}{\partial x}\left[\left(-\frac{\partial h}{\partial x}\right)^{\frac{1}{n}} h^{\frac{2n+1}{n}}\right] + v_l = 0. \tag{5.2.20}$$

Equation (5.2.20) is a nonlinear diffusion equation for $h(x,t)$ and differs from (4.2.22) by the leak-off term $v_l(x,t)$.

The total volume flux of fluid in the $x-$direction along the fracture, $Q_1(x,t)$, is

$$Q_1(x,t) = 2\int_0^{h(x,t)} v_x(x,z,t)\mathrm{d}z = 2h(x,t)\bar{v}_x(x,t) = 2h^{\frac{2n+1}{n}}\left(-\frac{\partial h}{\partial x}\right)^{\frac{1}{n}}. \tag{5.2.21}$$

At the fracture tip

$$Q_1(L(t),t) = 2h^{\frac{2n+1}{n}}\left(-\frac{\partial h}{\partial x}\right)^{\frac{1}{n}}\Bigg|_{x=L(t)}. \tag{5.2.22}$$

Because there is fluid leak-off into the rock mass the total volume flux may not vanish at the fracture tip. It may depend on the model used for fluid leak-off.

Consider now the volume balance equation. The fluid is incompressible and there is leak-off into the rock mass. Hence, per unit length in the $y-$direction:

$$\begin{pmatrix}\text{rate of change of the total}\\ \text{volume of the fracture}\end{pmatrix} = \begin{pmatrix}\text{rate of flow of fluid into the}\\ \text{fracture at the fracture entry}\end{pmatrix} - \begin{pmatrix}\text{rate of flow of leaked-off}\\ \text{fluid at the fluid-rock interface}\end{pmatrix}. \tag{5.2.23}$$

That is,

$$\frac{dV}{dt} = Q_1 - Q_2, \tag{5.2.24}$$

where

$$V(t) = 2\int_0^{L(t)} h(x,t)\,\mathrm{d}x, \tag{5.2.25}$$

$$Q_1(0,t) = 2\int_0^{h(0,t)} v_x(0,z,t)\,\mathrm{d}z = 2h(0,t)\bar{v}_x(0,t), \tag{5.2.26}$$

and

$$Q_2(t) = 2\int_0^{L(t)} v_l(x,t)\,\mathrm{d}x. \tag{5.2.27}$$

When (5.2.19), evaluated at $x = 0$, is substituted into (5.2.26), the balance law (5.2.24) becomes

$$\frac{dV}{dt} = 2\left(-\frac{\partial h}{\partial x}(0,t)\right)^{\frac{1}{n}} h^{\frac{2n+1}{n}}(0,t) - 2\int_0^{L(t)} v_l(x,t)\,\mathrm{d}x. \tag{5.2.28}$$

The leak-off velocity $v_l(x,t)$ is not prescribed at the start of the analysis. It is partly determined from the condition that the partial differential equation (5.2.20) admits Lie point symmetries. The remaining freedom in the functional form of $v_l(x,t)$ is then determined in the modelling process.

The problem is to solve the nonlinear diffusion equation (5.2.20) for the fracture half-width $h(x,t)$ subject to the boundary condition, (5.2.12), at the fracture tip and the balance law for fluid volume, (5.2.28), at the entry to the fracture and the initial conditions (5.2.13). The leak-off velocity is obtained as the solution progresses.

5.3 Group invariant solution

Following the procedure outlined in Appendix A, it can be verified that for $0 < n < \infty$, the Lie point symmetry generator of (5.2.20) is of the form

$$\begin{aligned} X &= (c_1 + c_2 t)\frac{\partial}{\partial t} + (c_4 + c_3 x)\frac{\partial}{\partial x} + \frac{1}{(n+2)}\left((n+1)c_3 - nc_2\right) h\frac{\partial}{\partial h}, \\ &= c_1 X_1 + c_2 X_2 + c_3 X_3 + c_4 X_4, \end{aligned} \tag{5.3.1}$$

where c_1, c_2, c_3 and c_4 are arbitrary constants and

$$X_1 = \frac{\partial}{\partial t}, \qquad X_2 = t\frac{\partial}{\partial t} - \left(\frac{n}{n+2}\right) h\frac{\partial}{\partial h},$$

$$X_3 = x\frac{\partial}{\partial x} + \left(\frac{n+1}{n+2}\right) h\frac{\partial}{\partial h}, \qquad X_4 = \frac{\partial}{\partial x},$$

provided that the leak-off velocity $v_l(x,t)$ satisfies the first order quasi-linear partial differential equation

$$(c_1 + c_2 t)\,\frac{\partial v_l}{\partial t} + (c_4 + c_3 x)\,\frac{\partial v_l}{\partial x} = \left(\frac{n+1}{n+2}\right)(c_3 - 2c_2)\, v_l. \tag{5.3.2}$$

The values $n=1$ and $n=1/2$ had to be treated separately in the derivation of the Lie symmetries but the general result obtained in (5.3.1) to (5.3.2) is true for all values of the power-law exponent n.

Now, $h = \Phi(x,t)$ is a group invariant solution of (5.2.20) provided

$$X\left(h - \Phi(x,t)\right)\Big|_{h=\Phi} = 0, \tag{5.3.3}$$

that is, provided

$$(c_1 + c_2 t)\frac{\partial \Phi}{\partial t} + (c_4 + c_3 x)\frac{\partial \Phi}{\partial x} = \frac{1}{n+2}\left((n+1)c_3 - nc_2\right)\Phi. \tag{5.3.4}$$

Equation (5.3.4) was solved in Section 4.3 and the general solution that was obtained is

$$h(x,t) = (c_1 + c_2 t)^{\left(\frac{n+1}{n+2}\right)\frac{c_3}{c_2} - \frac{n}{n+2}} f(\xi), \qquad \xi = \frac{c_4 + c_3 x}{(c_1 + c_2 t)^{\frac{c_3}{c_2}}}, \tag{5.3.5}$$

where $f(\xi)$ is an arbitrary function of ξ.

Consider now the fluid leak-off velocity $v_l(x,t)$. For (5.3.5) to be a group invariant solution of (5.2.20), the leak-off velocity v_l has to satisfy (5.3.2). The differential equations of the characteristic curves of (5.3.2) are

$$\frac{dt}{c_1 + c_2 t} = \frac{dx}{c_4 + c_3 x} = \frac{dv_l}{\left(\frac{n+1}{n+2}\right)(c_3 - 2c_2)\, v_l}, \tag{5.3.6}$$

which is equivalently written as

$$\frac{dt}{c_1 + c_2 t} = \frac{dx}{c_4 + c_3 x}\ , \qquad \frac{dt}{c_1 + c_2 t} = \frac{dv_l}{\left(\frac{n+1}{n+2}\right)(c_3 - 2c_2)\, v_l}. \tag{5.3.7}$$

We integrate each of the two differential equations in (5.3.7) to obtain the two first integrals

$$I_1 = \frac{c_4 + c_3 x}{(c_1 + c_2 t)^{\frac{c_3}{c_2}}}, \quad I_2 = \frac{v_l}{(c_1 + c_2 t)^{\left(\frac{n+1}{n+2}\right)\left(\frac{c_3}{c_2} - 2\right)}}. \tag{5.3.8}$$

The general solution is therefore of the form

$$v_l = (c_1 + c_2 t)^{\left(\frac{n+1}{n+2}\right)\left(\frac{c_3}{c_2} - 2\right)} g(\xi), \tag{5.3.9}$$

where $g(\xi)$ is an arbitrary function of ξ.

The problem will now be expressed in terms of the similarity variable ξ and the functions $f(\xi)$ and $g(\xi)$. Substituting (5.3.5) and (5.3.9) for $h(x,t)$ and $v_l(x,t)$ into (5.2.20) reduces the partial differential equation to the second order nonlinear ordinary differential equation

$$c_3^{\frac{1}{n}} \frac{d}{d\xi}\left[f(\xi)^{\frac{2n+1}{n}} \left(-\frac{df}{d\xi}\right)^{\frac{1}{n}} \right] - \frac{d}{d\xi}(\xi f) - \frac{n}{n+2}\left[\frac{c_2}{c_3} - \frac{2n+3}{n}\right] f + \frac{1}{c_3} g(\xi) = 0. \tag{5.3.10}$$

Since (5.3.10) does not depend on c_4, we choose $c_4 = 0$ so that $\xi = 0$ when $x = 0$.

From (5.3.5) and (5.2.12), the boundary conditions become

$$f(s) = 0 \quad \text{where} \quad s(t) = \frac{c_3 L(t)}{(c_1 + c_2 t)^{\frac{c_3}{c_2}}}, \tag{5.3.11}$$

so that

$$\frac{df}{ds}\frac{ds}{dt} = 0, \qquad t \geq 0. \tag{5.3.12}$$

Assuming that $f(s)$ is not constant, it follows that $s(t)$ is constant. Since $L(0) = 1$ we obtain

$$L(t) = \left(1 + \frac{c_2}{c_1}t\right)^{\frac{c_3}{c_2}}. \tag{5.3.13}$$

Equation (5.3.13) has the same form as (4.3.23) but $\frac{c_2}{c_1}$ will be different due to leak-off. When (5.3.13) is substituted into (5.3.11), the boundary condition (5.3.11) becomes

$$f(c_3 c_1^{-\frac{c_3}{c_2}}) = 0. \tag{5.3.14}$$

Consider next the balance law (5.2.28). Substituting (5.3.5) and (5.3.9) for $h(x,t)$ and $v_l(x,t)$ into (5.2.28) and using (5.3.13) for $L(t)$ puts (5.2.28) in the form

$$\frac{dV}{dt} = (c_1 + c_2 t)^{\left(\frac{2n+3}{n+2}\frac{c_3}{c_2} - \frac{2(n+1)}{n+2}\right)} \left[2c_3^{\frac{1}{n}} f(0)^{\frac{2n+1}{n}} \left(-\frac{df(0)}{d\xi}\right)^{\frac{1}{n}} - \frac{2}{c_3}\int_0^{c_3 c_1^{-\frac{c_3}{c_2}}} g(\xi)\,\mathrm{d}\xi\right]. \tag{5.3.15}$$

The total volume of the fracture per unit length in the $y-$direction is derived in (4.3.24) and is

$$V(t) = \frac{2}{c_3}(c_1 + c_2 t)^{\left(\frac{2n+3}{n+2}\right)\frac{c_3}{c_2} - \frac{n}{n+2}} \int_0^{c_3 c_1^{-\frac{c_3}{c_2}}} f(\xi)\,\mathrm{d}\xi, \tag{5.3.16}$$

Differentiating (5.3.16) with respect to t and putting the resulting expression on the left hand side of (5.3.15) yields, after simplification

$$c_3^{\frac{1}{n}} f(0)^{\frac{2n+1}{n}} \left(-\frac{df}{d\xi}(0)\right)^{\frac{1}{n}} = \left(\frac{n}{n+2}\right)\left[\frac{2n+3}{n} - \frac{c_2}{c_3}\right]\int_0^{c_3 c_1^{-\frac{c_3}{c_2}}} f(\xi)\,\mathrm{d}\xi + \frac{1}{c_3}\int_0^{c_3 c_1^{-\frac{c_3}{c_2}}} g(\xi)\,\mathrm{d}\xi. \tag{5.3.17}$$

In order to simplify these equations, we make the change of variables:

$$\xi = c_3 c_1^{-\frac{c_3}{c_2}} u, \quad f(\xi) = c_3^{\frac{n}{n+2}} c_1^{-\left(\frac{n+1}{n+2}\right)\frac{c_3}{c_2}} F(u), \quad g(\xi) = c_3^{2\left(\frac{n+1}{n+2}\right)} c_1^{-\left(\frac{n+1}{n+2}\right)\frac{c_3}{c_2}} G(u), \tag{5.3.18}$$

where $u = \frac{x}{L(t)}$, such that $0 \leq u \leq 1$. Also, as in Chapter 4, let $c = \frac{c_3}{c_2}$. Expressed in terms of the similarity variables $F(u)$ and $G(u)$, and using (4.3.30) and (4.3.32), the problem is therefore to solve the ordinary differential equation

$$\frac{d}{du}\left[F(u)^{\frac{2n+1}{n}}\left(-\frac{dF}{du}\right)^{\frac{1}{n}}\right] - \frac{d}{du}(uF) + \frac{n}{n+2}\left[\frac{2n+3}{n} - \frac{1}{c}\right]F(u) + G(u) = 0, \tag{5.3.19}$$

subject to the boundary conditions

$$F(1) = 0, \tag{5.3.20}$$

$$F(0)^{\frac{2n+1}{n}} \left(-\frac{dF}{du}(0)\right)^{\frac{1}{n}} = \frac{n}{n+2}\left[\frac{2n+3}{n} - \frac{1}{c}\right]\int_0^1 F(u)\mathrm{d}u + \int_0^1 G(u)\mathrm{d}u. \tag{5.3.21}$$

Using (4.3.30) to (4.3.32), the expressions for $V(t)$, $L(t)$, $h(x,t)$ and $v_l(x,t)$ are obtained from (5.3.16), (5.3.13), (5.3.5) and (5.3.9) and are of the form

$$V(t) = V_0\left[1 + \frac{1}{c}\left(\frac{V_0}{V_c}\right)^{\frac{n+2}{n}} t\right]^{\left(\frac{2n+3}{n+2}\right)c - \frac{n}{n+2}}, \tag{5.3.22}$$

$$L(t) = \left[1 + \frac{1}{c}\left(\frac{V_0}{V_c}\right)^{\frac{n+2}{n}} t\right]^{c}, \tag{5.3.23}$$

$$h(x,t) = \frac{V_0}{V_c}\left[1 + \frac{1}{c}\left(\frac{V_0}{V_c}\right)^{\frac{n+2}{n}} t\right]^{\left(\frac{n+1}{n+2}\right)c - \frac{n}{n+2}} F(u), \tag{5.3.24}$$

$$v_l(x,t) = \left(\frac{V_0}{V_c}\right)^{2\left(\frac{n+1}{n}\right)}\left[1 + \frac{1}{c}\left(\frac{V_0}{V_c}\right)^{\frac{n+2}{n}} t\right]^{\left(\frac{n+1}{n+2}\right)c - 2\left(\frac{n+1}{n+2}\right)} G(u), \tag{5.3.25}$$

and the dimensionless fluid pressure from (5.2.15) is given by

$$p(x,t) = \sigma_0 + h(x,t). \tag{5.3.26}$$

Since the characteristic distance H is the initial half-width, $h(0,0) = 1$, equations (5.3.22) to (5.3.25) written in terms of $F(u)$, become

$$V(t) = V_0\left[1 + \frac{t}{cF(0)^{\frac{n+2}{n}}}\right]^{\left(\frac{2n+3}{n+2}\right)c - \frac{n}{n+2}}, \tag{5.3.27}$$

$$L(t) = \left[1 + \frac{t}{cF(0)^{\frac{n+2}{n}}}\right]^{c}, \tag{5.3.28}$$

$$h(x,t) = \left[1 + \frac{t}{cF(0)^{\frac{n+2}{n}}}\right]^{\left(\frac{n+1}{n+2}\right)c - \frac{n}{n+2}} \frac{F(u)}{F(0)}, \tag{5.3.29}$$

$$v_l(x,t) = \frac{1}{F(0)^{2\left(\frac{n+1}{n}\right)}}\left[1 + \frac{t}{cF(0)^{\frac{n+2}{n}}}\right]^{\left(\frac{n+1}{n+2}\right)(c-2)} G(u), \tag{5.3.30}$$

where

$$V_0 = \frac{2}{F(0)}\int_0^1 F(u)\,\mathrm{d}u. \tag{5.3.31}$$

5.4 Invariant solutions when leak-off velocity is proportional to half-width of fracture

To solve the boundary value problem (5.3.19) to (5.3.21), it is required that a form of $G(u)$ is specified or a relation between $F(u)$ and $G(u)$ is known. The function $G(u)$ describes the spatial distribution of the leak-off fluid across the fluid-rock interface.

Consider now a relation between $G(u)$ and $F(u)$ which is of the form

$$G(u) = \beta F(u), \quad \beta \in \mathbb{R}. \tag{5.4.1}$$

It follows from (5.3.29) and (5.3.30) that

$$v_l(t,x) = \frac{\beta h(t,x)}{\left(F(0)^{\frac{n+2}{n}} + \frac{t}{c}\right)}. \tag{5.4.2}$$

This implies that the leak-off velocity is proportional to the half-width, $h(t,x)$, of the fracture at any time t. In most practical situations in hydraulic fracturing, $\beta \geq 0$. The case $\beta > 0$ represents fluid leak-off into the surrounding rock formation, and when $\beta = 0$, which was considered in Chapter 4, the rock mass is impermeable and no fluid leaks off into the surrounding rock formation. The leak-off velocity, $v_l(t,x)$, which is maximum at the fracture entry where $h(t,x)$ is maximum, decreases as x increases along the fracture and vanishes at the tip of the fracture, $x = L(t)$.

The problem is therefore to solve the ordinary differential equation

$$\frac{d}{du}\left[F(u)^{\frac{2n+1}{n}}\left(-\frac{dF}{du}\right)^{\frac{1}{n}}\right] - \frac{d}{du}(uF) + \left[\frac{n}{n+2}\left(\frac{2n+3}{n} - \frac{1}{c}\right) + \beta\right]F(u) = 0, \tag{5.4.3}$$

subject to the boundary conditions

$$F(1) = 0, \tag{5.4.4}$$

$$F(0)^{\frac{2n+1}{n}}\left(-\frac{dF}{du}(0)\right)^{\frac{1}{n}} = \left[\frac{n}{n+2}\left(\frac{2n+3}{n} - \frac{1}{c}\right) + \beta\right]\int_0^1 F(u)\,\mathrm{d}u. \tag{5.4.5}$$

Since we are considering no fluid extraction at the fracture entry, from (5.4.5),

$$\beta \geq -\left(\frac{2n+3}{n+2}\right) + \frac{n}{(n+2)c}, \tag{5.4.6}$$

with equality in (5.4.6) when there is no fluid injection or extraction at the fracture entry. We will consider $0 < c < \infty$ because the working conditions of practical interest are in this range.

Equation (5.3.30) for the leak-off velocity becomes

$$v_l(t,x) = \beta \frac{1}{F(0)^{\frac{n+2}{n}}} \left[1 + \frac{t}{cF(0)^{\frac{n+2}{n}}} \right]^{\left(\frac{n+1}{n+2}\right)(c-2)} \frac{F(u)}{F(0)} \tag{5.4.7}$$

and $V(t)$, $L(t)$ and $h(x,t)$ are given by (5.3.27) to (5.3.29) and $p(x,t)$ is given by (5.3.26). In form, these equations are the same as (4.3.42) to (4.3.44) and (4.3.39). Hence, the results in Table 4.3.1 for the working conditions at the fracture entry apply when $\beta \neq 0$. However, since the differential equations (4.3.33) and (5.4.3) for $F(u)$ are not the same because (5.4.3) depends on an extra parameter β, the quantitative behavior of the solutions will be different.

By looking for a solution of the form $F(u) = A\,(1-u)^s$, the asymptotic solution for $F(u)$ as $u \to 1$ which holds for all values of β and c and all $n > 0$ is derived as

$$F(u) \sim (n+2)^{\frac{1}{n+2}}\,(1-u)^{\frac{1}{n+2}} \quad \text{as} \quad u \to 1. \tag{5.4.8}$$

The asymptotic solution near the fracture tip is unaffected by the fluid leak-off since equation (5.4.8) is the same as the asymptotic solution (4.3.51) derived in Chapter 4. The numerical solution to the boundary value problem (5.4.3) subject to (5.4.4) and (5.4.5) will require the asymptotic result (5.4.8) in order to overcome the difficulty posed by the singularity of the differential equation (5.4.3) at the tip of the fracture. From (5.4.8), the fluid flux at the fracture tip therefore vanishes since

$$F(u)^{2+\frac{1}{n}} \left(-\frac{dF}{du}(u) \right)^{\frac{1}{n}} = (n+2)^{\frac{1}{n+2}}\,(1-u)^{\frac{1}{n+2}} = F(u) \to 0 \quad \text{as} \quad u \to 1. \tag{5.4.9}$$

As with a fluid-driven fracture in an impermeable rock mass treated in Chapter 4, the lubrication approximation breaks down at the fracture tip since $\partial h/\partial x \to -\infty$ as $x \to L(t)$.

The integration of the differential equation (5.4.3) subject to the boundary conditions (5.4.4) and (5.4.5) to obtain an exact analytical solution which is valid for all values of the parameters c and β and for all $n > 0$ is not feasible. However, approximate solutions which are valid for all β, c and $n > 0$ will be investigated in Section 5.7. We will now discuss the two cases that yield exact analytical solutions.

5.4.1 Exact analytical solution for zero fluid injection at the fracture entry

When

$$\frac{n}{(n+2)}\left(\frac{2n+3}{n}-\frac{1}{c}\right)+\beta=0, \tag{5.4.10}$$

or equivalently

$$c=\frac{n}{n(\beta+2)+2\beta+3}, \tag{5.4.11}$$

the differential equation (5.4.3) and the boundary conditions (5.4.4) and (5.4.5) reduce to equation (4.4.2) and boundary conditions (4.4.3) and (4.4.4). The condition (5.4.6) is satisfied with the equal sign. The physical significance of (5.4.10) is that there is no net fluid injection or extraction at the fracture entry.

The solution of the boundary value problem is given by (4.4.5):

$$F(u)=\left(\frac{n+2}{n+1}\right)^{\frac{1}{n+2}}\left(1-u^{n+1}\right)^{\frac{1}{n+2}}. \tag{5.4.12}$$

From (5.3.27) to (5.3.29), (5.3.31) and (5.4.7) the invariant solutions are

$$L(t)=\left[1+\frac{(n+2)}{n}\left(\frac{n+1}{n+2}\right)^{\frac{1}{n}}\left(\beta+\frac{2n+3}{n+2}\right)\,t\right]^{\frac{n}{(n+2)\left(\beta+\frac{2n+3}{n+2}\right)}}, \tag{5.4.13}$$

$$V(t)=\frac{V_0}{L(t)^{\beta}}, \tag{5.4.14}$$

$$h(x,t)=\frac{1}{L(t)^{\beta+1}}\left(1-u^{n+1}\right)^{\frac{1}{n+2}}, \tag{5.4.15}$$

$$v_l(x,t)=\beta\left(\frac{n+1}{n+2}\right)^{\frac{1}{n}}\frac{1}{L(t)^{\frac{(n+1)(2\beta+3)}{n}}}\left(1-u^{n+1}\right)^{\frac{1}{n+2}}, \tag{5.4.16}$$

where

$$V_0=2\int_0^1\left(1-u^{n+1}\right)^{\frac{1}{n+2}}\,\mathrm{d}u. \tag{5.4.17}$$

The flux of fluid along the fracture at time t, $Q_1(x,t)$, is proportional to the expression

$$F(u)^{\frac{2n+1}{n}}\left(-\frac{dF}{du}\right)^{\frac{1}{n}},$$

where with $F(u)$ given by (5.4.12),

$$F(u)^{\frac{2n+1}{n}}\left(-\frac{dF}{du}\right)^{\frac{1}{n}}=uF(u). \tag{5.4.18}$$

We see again that the flux of fluid into the fracture at the fracture entry is zero which is the physical property that characterises the solution. The flux of fluid at the fracture tip, $u = 1$, also vanishes since $F(1) = 0$. When $\beta = 0$, (5.4.10) reduces to condition (4.4.1) discussed in Section 4.4.

From (5.4.16), $\beta > 0$ describes leak-off and $\beta < 0$ describes inflow at the fluid-rock interface. For the present solution we see from (5.4.13) that for $\beta > 0$ the fracture length always increases even although there is leak-off at the fluid-rock interface and from (5.4.14) the total volume of the fracture $V(t)$ decreases steadily. For

$$-\left(\frac{2n+3}{n+2}\right) < \beta < 0, \tag{5.4.19}$$

the exponent and coefficient of t in (5.4.13) for $L(t)$ are positive and the fracture length will increase steadily with time such that $L(t) \to \infty$ as $t \to \infty$. For

$$\beta < -\left(\frac{2n+3}{n+2}\right), \tag{5.4.20}$$

which describes strong inflow at the fluid-rock interface, condition (5.4.6) is not satisfied for any $c > 0$ and there is net fluid extraction at the fracture entry for which the present formulation does not apply. From (5.4.14), $V(t)$ is constant when $\beta = 0$ because then there is no net inflow of fluid at the fracture entry and there is no leak-off at the fluid-rock interface. Also from (5.4.15), $h(0,t)$ is constant when $\beta = -1$. Therefore, from the PKN approximation the pressure at the fracture entry, $p(0,t)$, is a constant when $\beta = -1$ or when $c = \frac{n}{n+1}$. For $\beta > -1$, $h(0,t)$ is a decreasing function of time while for $\beta < -1$, $h(0,t)$ increases with time. The velocity of leak-off, $v_l(x,t)$, remains constant for all time when $\beta = -1.5$. In Figures 5.4.1(i)-(iii), the half-width of the fracture $h(x,t)$ given by (5.4.15) is plotted against x for the same value of β, namely $\beta = 1$, but for different values of the power-law exponent n. The time scale (4.2.28) which depends on n is used and is therefore different in the three parts of Figure 5.4.1. In all three graphs, as the half-width of the fracture decreases with time, the fracture length increases with time. The fracture length increases even although there is fluid leak-off at the fluid-rock interface and the total volume of the fracture is decreasing. This phenomenon has already been observed in Chapter 4 when there is no leak-off and the total volume of the fracture remains constant. In Figures 5.4.2(i)-(iii), the half-width $h(x,t)$

is plotted for $\beta = +1, -1$ and -1.2, keeping the power-law exponent n fixed. The time scale is the same in the three parts of Figure 5.4.2 since n is the same and therefore the evolution of the fracture half-width with time can be compared. For all three cases the fracture length continues to increase with time. The graphs show that fluid leak-off $(\beta > 0)$ decreases the rate of growth of the length of the fracture while fluid inflow at the fluid-rock interface $(\beta < 0)$ increases the rate of growth of the fracture length. The half-width decreases with time when $\beta = +1$ for which there is fluid leak-off at the fluid-rock interface. For $\beta = -1$ the half-width at the fracture entry remains constant in time. Fluid inflow into the fracture at the fluid-rock interface when $\beta = -1$ keeps the half-width at the fracture entry constant, thereby preventing it from relaxing, while the fracture length grows. When $\beta = -\frac{3}{2}$, fluid inflow at the fluid-rock interface causes the half-width to increase with time.

5.4.2 Exact analytical solution for constant average fluid velocity along the fracture

By looking for a solution of (5.4.3) of the form $F(u) = A(1-u)^p$, where A and p are positive constants, a second exact analytical solution is obtained as

$$F(u) = (n+2)^{\frac{1}{n+2}} \, (1-u)^{\frac{1}{n+2}} \, , \tag{5.4.21}$$

provided

$$c = \frac{n}{n(\beta+1)+2\beta}. \tag{5.4.22}$$

It is easily verified that (5.4.21) satisfies (5.4.4) and the integral boundary condition (5.4.5). We will see in Section 5.6 that the physical property which characterises this analytical solution is that the fluid velocity averaged across the width of the fracture is constant along the fracture and equal to the velocity of the fracture tip.

When c given by (5.4.22) is substituted into (5.4.6) it is readily verified that condition (5.4.6) for fluid injection at the fracture entry is satisfied. From (5.4.22), for $c > 0$,

$$\beta > -\frac{n}{(n+2)}. \tag{5.4.23}$$

(i)

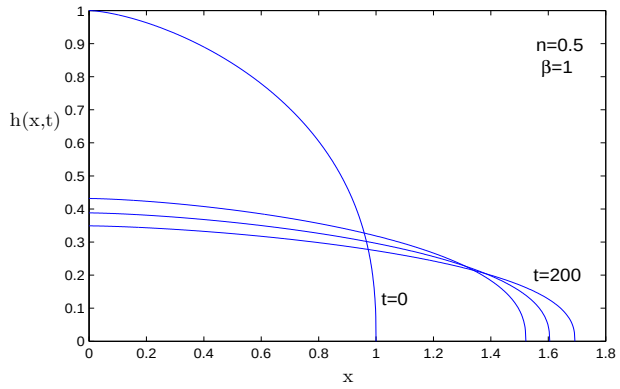

(ii)

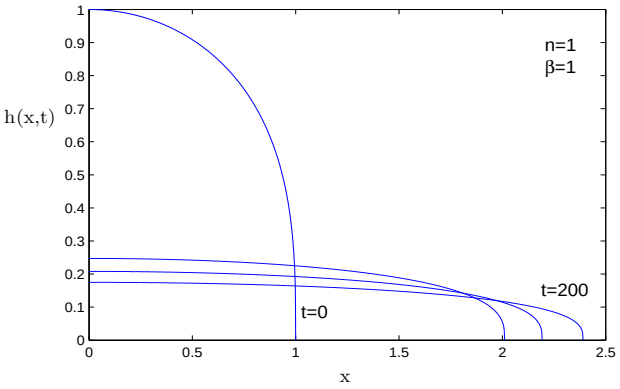

(iii)

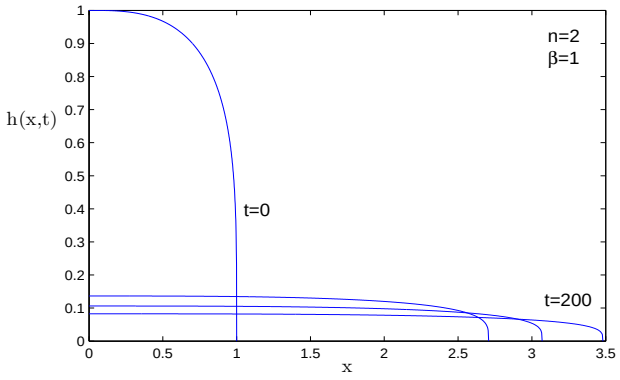

Figure 5.4.1: Flux of fluid into the fracture at the fracture entry is zero. Fracture half-width $h(x,t)$ given by (5.4.15) plotted against x at times t= 0, 50, 100, 200 for (i) Shear thinning fluid with $n = 0.5$, (ii) Newtonian fluid with $n = 1$ and (iii) Shear thickening fluid with $n = 2$. The leak-off parameter $\beta = 1$. Time is scaled by T defined by (4.2.28) which depends on n.

(i)

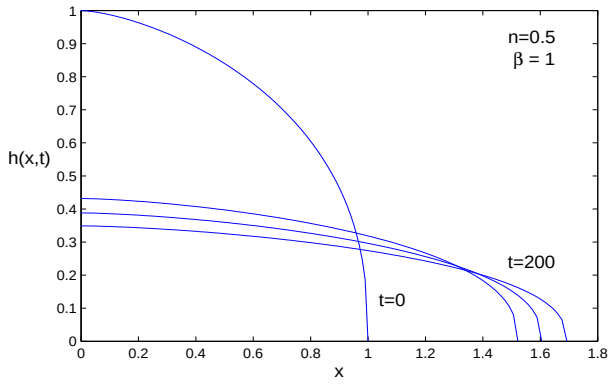

(ii)

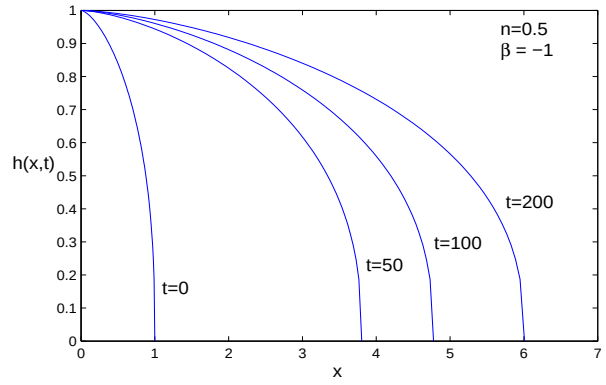

(iii)

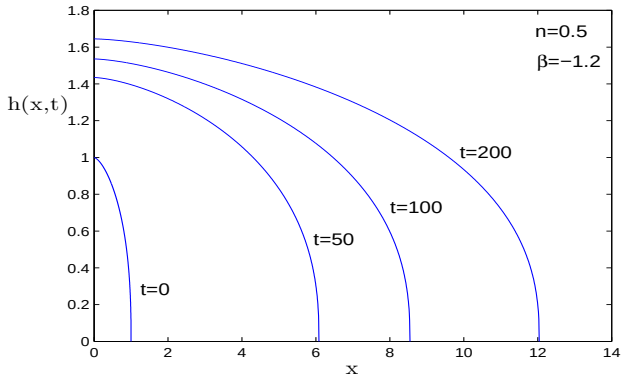

Figure 5.4.2: Flux of fluid into the fracture at the fracture entry is zero. Fracture half-width $h(x,t)$ given by (5.4.15) plotted against x at times t= 0, 50, 100, 200 for shear thinning fluid with $n = 0.5$. The leak-off parameter $\beta = +1, -1, -1.2$. Time is scaled by T defined by (4.2.28).

The flux of fluid along the fracture at time t, $Q_1(x,t)$, is proportional to, using (5.4.21),

$$F^{\frac{2n+1}{n}}(u)\left(-\frac{dF}{du}\right)^{\frac{1}{n}} = F(u). \tag{5.4.24}$$

Since $F(1) = 0$ the flux of fluid vanishes at the fracture tip, $u = 1$.

The invariant solutions (5.3.27) to (5.3.29), (5.3.31) and (5.4.7) are given by

$$L(t) = \left[1 + \frac{(n+2)^{\frac{n-1}{n}}}{n}\left(\beta + \frac{n}{n+2}\right)t\right]^{\frac{n}{(n+2)\left(\beta+\frac{n}{n+2}\right)}}, \tag{5.4.25}$$

$$V(t) = 2\left(\frac{n+2}{n+3}\right)L(t)^{\left(\frac{n+3}{n+2}\right)-\beta}, \tag{5.4.26}$$

$$h(x,t) = L(t)^{\frac{1}{n+2}-\beta}(1-u)^{\frac{1}{n+2}}, \tag{5.4.27}$$

$$v_l(x,t) = \frac{\beta}{(n+2)^{\frac{1}{n}}}L(t)^{\frac{-2(n+1)}{n}\left(\beta+\frac{n}{2(n+1)}\right)}(1-u)^{\frac{1}{n+2}}. \tag{5.4.28}$$

For $-\frac{n}{n+2} < \beta < \infty$ the length $L(t)$ of the fracture will increase with time even although there is fluid leak-off for $\beta > 0$. From (5.4.27), when $\beta = \frac{1}{n+2}$, $h(0,t)$ is constant , and hence from the PKN approximation the pressure at the fracture entry is constant. For stronger leak-off with $\beta > \frac{1}{n+2}$, $h(0,t)$ is a decreasing function of time while for weaker leak-off with $\beta < \frac{1}{n+2}$, $h(0,t)$ increases with time. The critical value, $\beta = \frac{1}{n+2}$ is a decreasing function of n. For example, when $n = 0.5, 1$ and 2, the fracture half-width at the entry, $h(0,t)$, increases with time provided $\beta < 0.4, 0.33$ and 0.25 respectively. The width of a shear thinning fluid-driven fracture will grow for values of the leak-off parameter for which the width will decrease for a shear thickening fluid-driven fracture. If the objective is to increase the width of the fracture then this particular solution illustrates that shear thinning fluids are to be preferred to drive the fracture when there is leak-off. In Figure 5.4.3 the half-width of the fracture, $h(x,t)$, given by (5.4.27) is plotted against x for a range of values of time for $\beta = 0.33$. We see from Figure 5.4.3 that for this strength of leak-off the width of the shear thinning fluid-driven fracture will increase while the width of the shear thickening fluid-driven fracture will decrease.

The fracture volume $V(t)$ is constant when $\beta = \frac{n+3}{n+2}$. For this value of β the volume flux of fluid injected at the fracture entry balances the volume flux of fluid lost due to leak-off at the fluid-rock interface. When $\beta > \frac{n+3}{n+2}$, fluid leak-off is stronger than fluid injection at the entry and the total volume $V(t)$ decreases while when $\beta < \frac{n+3}{n+2}$ the opposite is the case.

(i)

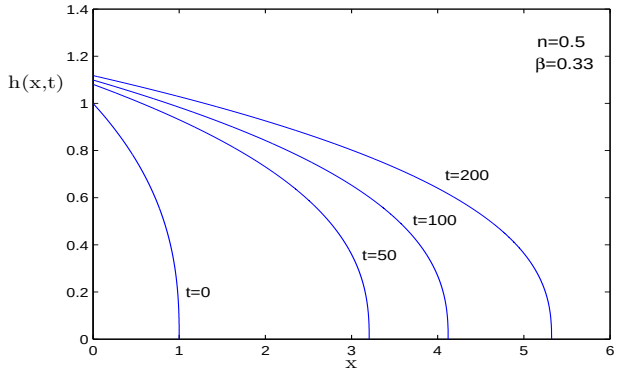

(ii)

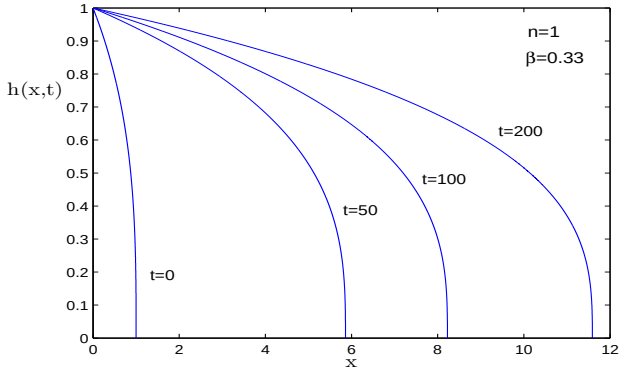

(iii)

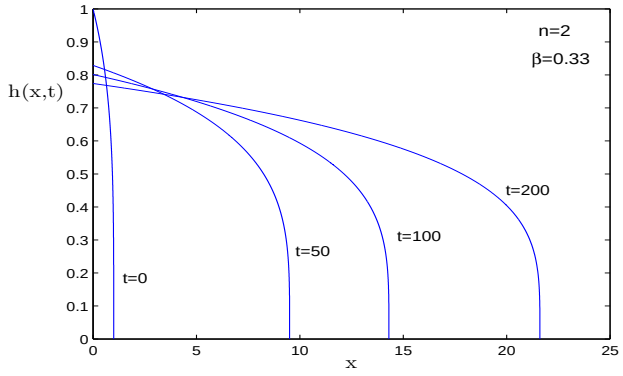

Figure 5.4.3: Average fluid velocity constant along the fracture. Fracture half-width $h(x,t)$ given by (5.4.27) plotted against x at times t= 0, 50, 100, 200 for (i) Shear thinning fluid with $n = 0.5$, (ii) Newtonian fluid with $n = 1$ and (iii) Shear thickening fluid with $n = 2$. The leak-off parameter $\beta = 0.33$. Time is scaled by T defined by (4.2.28) which depends on n.

From (5.4.25) the speed of propagation of the fracture is

$$\frac{dL}{dt} = \frac{1}{(n+2)^{\frac{1}{n}}} L(t)^{-\frac{(n+2)}{n}\beta}. \tag{5.4.29}$$

When there is no leak-off, $\beta = 0$ and $\frac{dL}{dt}$ is constant. For $\beta > 0$, $\frac{dL}{dt}$ decreases with time while for fluid inflow at the rock interface, $\beta < 0$ and $\frac{dL}{dt}$ increases with time. For the limiting case $\beta = -\frac{n}{n+2}$,

$$L(t) = \exp\left(\frac{t}{(n+2)^{\frac{1}{n}}}\right) \tag{5.4.30}$$

and the fracture length increases exponentially with time. From (5.4.26)

$$\frac{dV}{dt} = \frac{2}{(n+2)^{\frac{1}{n}}}\left(\frac{n+2}{n+2}\right)\left(\frac{n+3}{n+2} - \beta\right) L(t)^{\frac{2(n+1)}{n}\left(\frac{n}{2(n+1)(n+2)} - \beta\right)}. \tag{5.4.31}$$

The rate of change of volume of the fracture is constant when

$$\beta = \frac{n}{2(n+1)(n+2)} \tag{5.4.32}$$

and increases for values of β less than this value and decreases for values greater.

From (5.4.28) the leak-off velocity is proportional to β and is constant in time when

$$\beta = -\frac{n}{2(n+1)}. \tag{5.4.33}$$

For

$$-\frac{n}{(n+2)} < \beta < -\frac{n}{2(n+1)} \tag{5.4.34}$$

there is inflow at the fluid-rock interface and the magnitude of the inflow velocity increases as time increases. For

$$-\frac{n}{2(n+1)} < \beta < 0 \tag{5.4.35}$$

the magnitude of the inflow velocity decreases as time increases and for $\beta > 0$ the leak-off velocity decreases as time increases. The results are summarised in Table 5.4.1.

In Figures 5.4.4, 5.4.5 and 5.4.6 the working conditions and the curves in the (c, β) plane on which the two analytical solutions exist are plotted. Along the curve

$$\beta = \left(\frac{2n+3}{n+2}\right)\frac{\left[\frac{n}{2n+3} - c\right]}{c}, \tag{5.4.36}$$

derived in (5.4.10), there is no fluid injection or extraction at the fracture entry. In the region of the (c, β) plane above the curve there is fluid injection and this is the region considered in this thesis. In the region below the curve there is fluid extraction at the fracture entry. The line

$$\beta = -\left(\frac{2n+3}{n+2}\right), \tag{5.4.37}$$

is the limit of (5.4.36) as $c \to \infty$ and is the limiting value of β for which there is a solution with $c > 0$ with no fluid injection or extraction at the fracture entry. Along the curve

$$\beta = \frac{n}{n+2}\left(\frac{1-c}{c}\right), \tag{5.4.38}$$

derived from (5.4.22), the second analytical solution exists. It lies above the curve (5.4.36) in the (c, β) plane and therefore is in the region of fluid injection at the fracture entry.

Operating conditions	$\beta(n)$	Values of $\beta(n)$		
		$n = 0.5$	$n = 1$	$n = 2$
Total volume of fluid in fracture is constant	$\frac{n+3}{n+2}$	1.4	1.33	1.25
Half-width and pressure at fracture entry is constant	$\frac{1}{n+2}$	0.4	0.33	0.25
Rate of change of the total volume of the fracture is constant	$\frac{n}{2(n+1)(n+2)}$	0.066	0.0833	0.0833
Speed of propagation of the fracture is constant	0	0	0	0
Leak-off velocity is constant	$-\frac{n}{2(n+1)}$	-0.166	-0.25	-0.33

Table 5.4.1: Values of the leak-off parameter β for the second exact analytical solution for which the average fluid velocity is constant along the fracture.

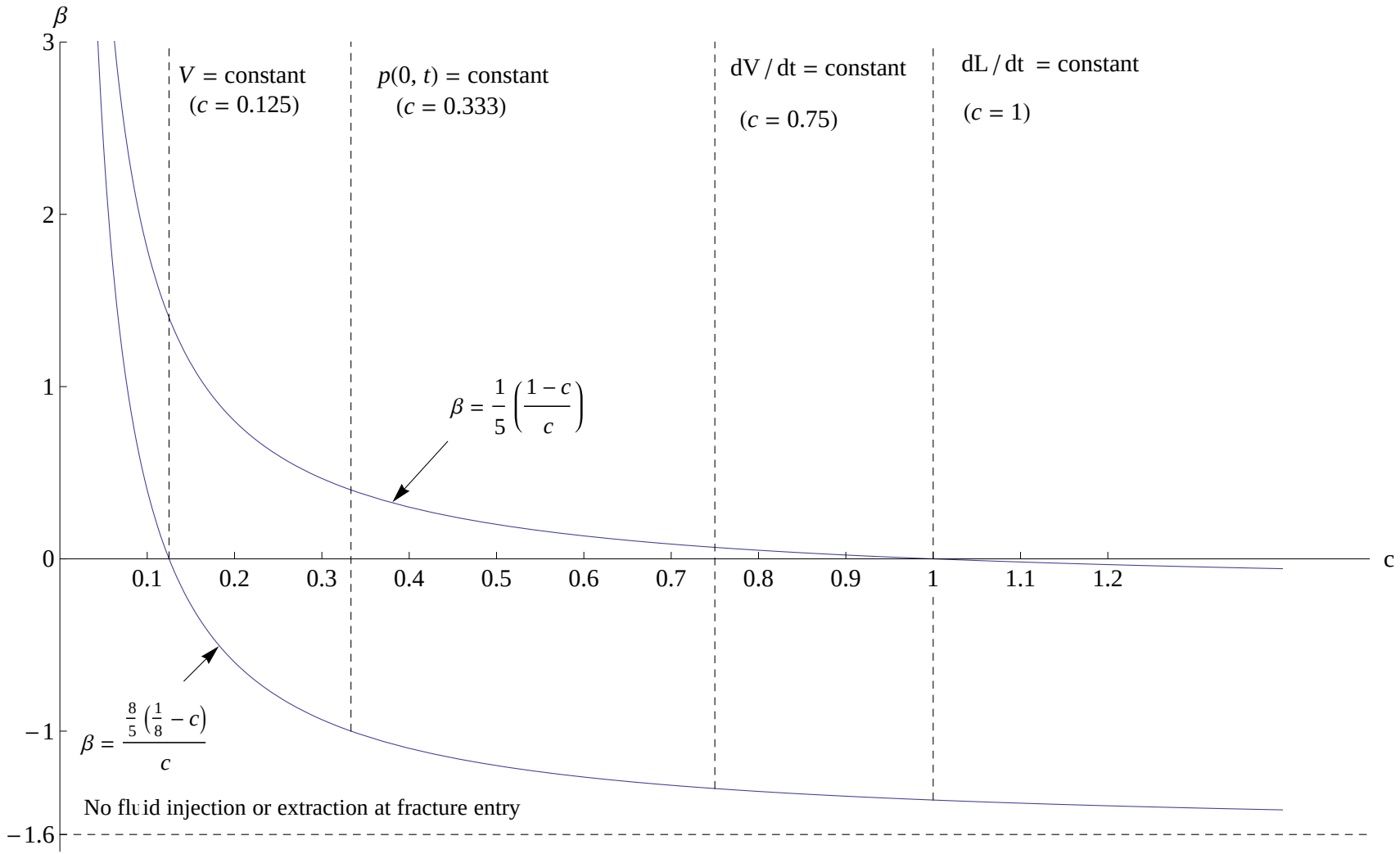

Figure 5.4.4: Curves in the (c, β) plane for the two analytical solutions for a shear thinning fluid with $n = \frac{1}{2}$.

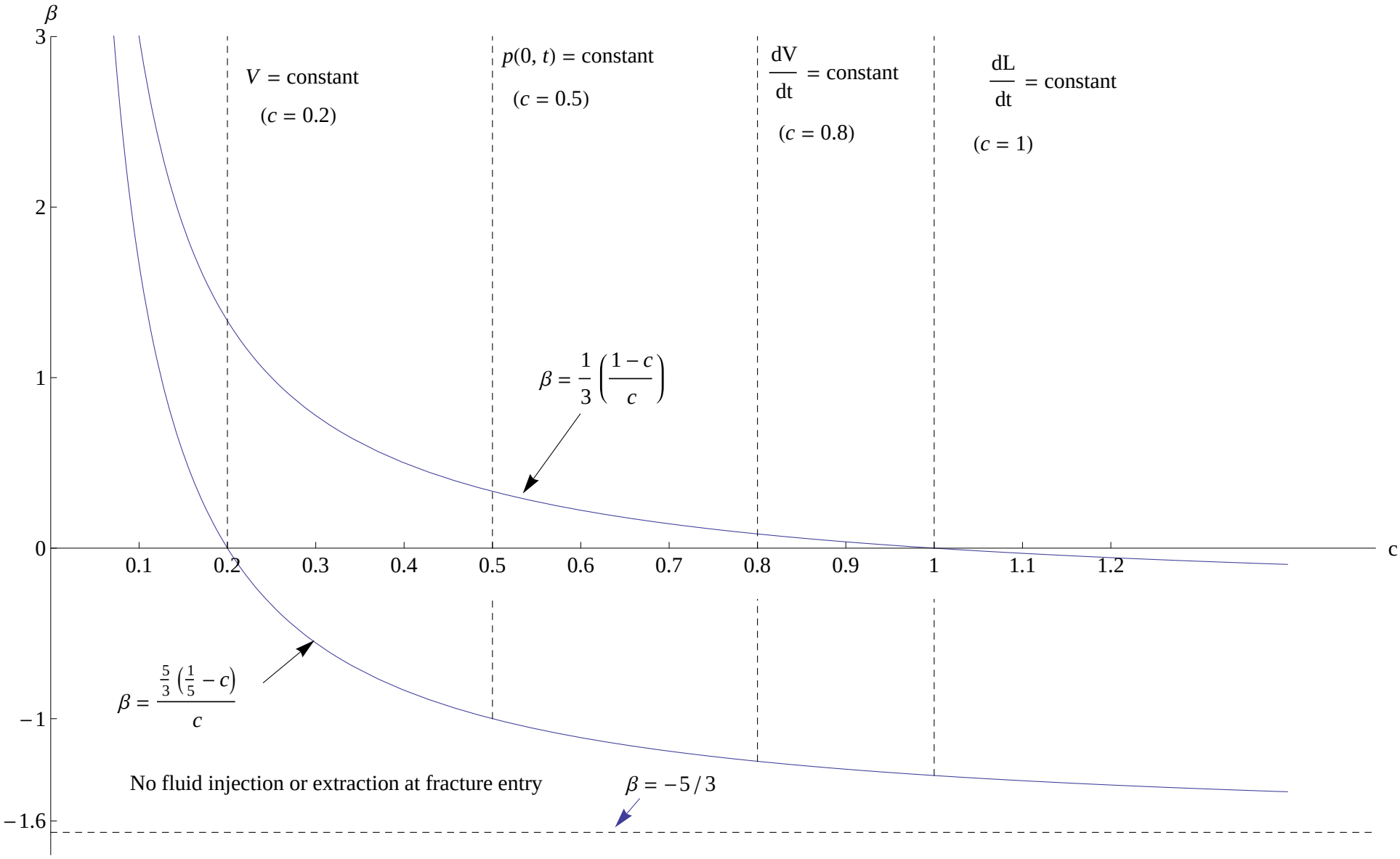

Figure 5.4.5: Curves in the (c, β) plane for the two analytical solutions for a Newtonian fluid with $n = 1$.

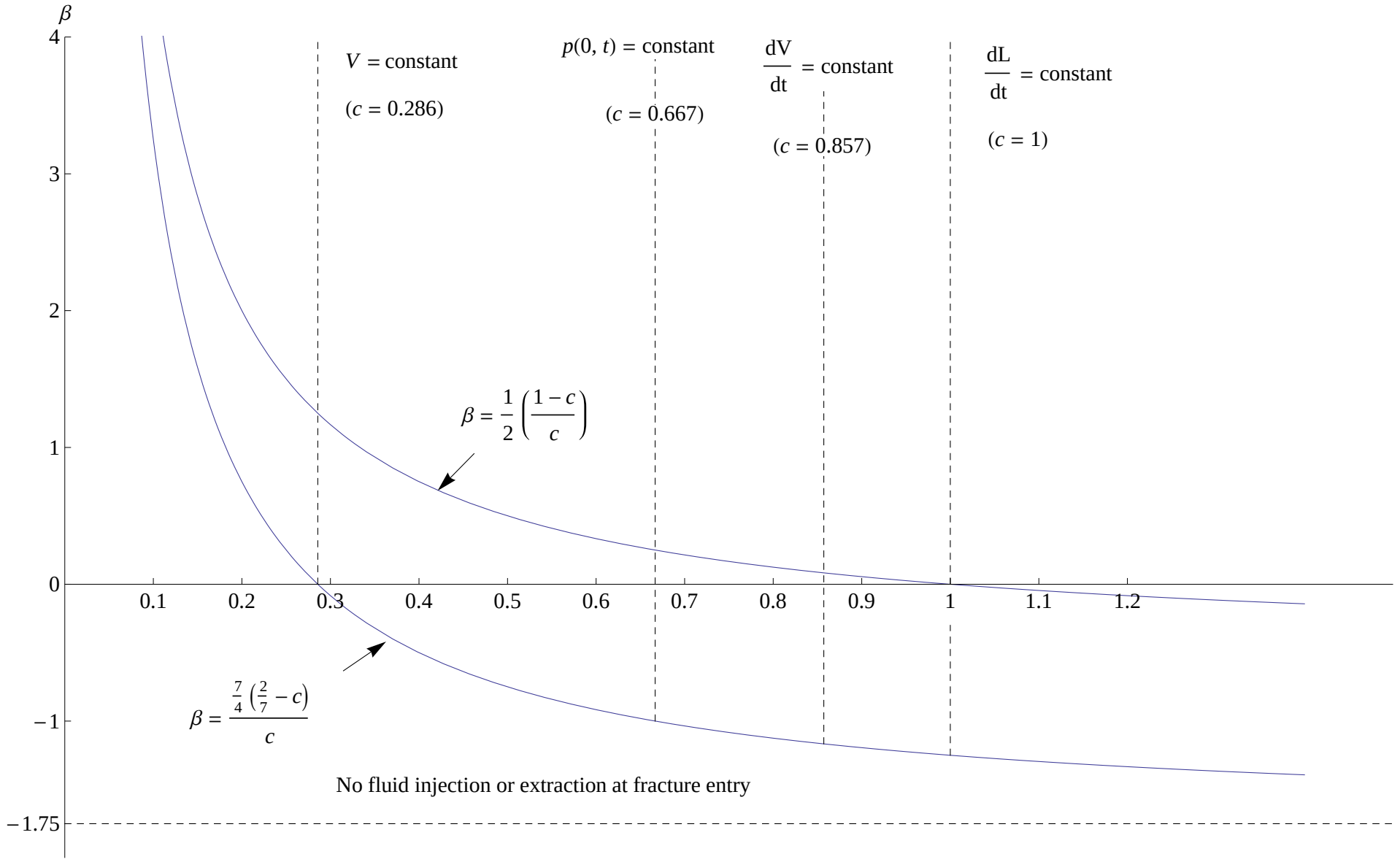

Figure 5.4.6: Curves in the (c, β) plane for the two analytical solutions for a shear thickening fluid with $n = 2$.

5.5 Numerical solution when leak-off velocity is proportional to half-width of fracture

The differential equation (5.4.3) is not in general completely integrable analytically since it admits only one Lie point symmetry generator

$$X = (n+2)\,u\frac{\partial}{\partial u} + (n+1)F\frac{\partial}{\partial F}. \tag{5.5.1}$$

It is integrated numerically in a similar way to the method described in Section 4.5 for a hydraulic fracture in impermeable rock. Using the transformation generated by (5.5.1), the boundary value problem (5.4.3) to (5.4.5) is transformed into a pair of initial value problems. The scaling transformation generated by the Lie point symmetry (5.5.1) is obtained as

$$\bar{u} = \lambda u, \qquad \bar{F}(\bar{u}) = \lambda^{\frac{n+1}{n+2}} F(u), \tag{5.5.2}$$

where λ is a parameter. We choose $\bar{F}(0) = 1$ and therefore, $F(0) = \lambda^{-\left(\frac{n+1}{n+2}\right)}$. The parameter λ is determined from the condition $\bar{F}(\lambda) = 0$, derived from the boundary condition (5.4.4).

The boundary value problem (5.4.3) to (5.4.5) is transformed to the following pair of initial value problems:

Initial Value Problem I

$$\frac{d}{d\bar{u}}\left[\bar{F}(\bar{u})^{\frac{2n+1}{n}}\left(-\frac{d\bar{F}}{d\bar{u}}\right)^{\frac{1}{n}}\right] - \frac{d}{d\bar{u}}\left(\bar{u}\bar{F}\right) + \left[\frac{n}{n+2}\left(\frac{2n+3}{n} - \frac{1}{c}\right) + \beta\right]\bar{F}(\bar{u}) = 0 \tag{5.5.3}$$

subject to the boundary condition

$$\bar{F}(0) = 1, \tag{5.5.4}$$

$$\left(-\frac{d\bar{F}(0)}{d\bar{u}}\right)^{\frac{1}{n}} = \left[\frac{n}{n+2}\left(\frac{2n+3}{n} - \frac{1}{c}\right) + \beta\right]\int_0^{\lambda}\bar{F}(\bar{u})\mathrm{d}\bar{u}, \tag{5.5.5}$$

where $0 < \bar{u} < \lambda$ and λ satisfies

$$\bar{F}(\lambda) = 0. \tag{5.5.6}$$

Initial Value Problem II

$$\frac{d}{du}\left[F(u)^{\frac{2n+1}{n}}\left(-\frac{dF}{du}\right)^{\frac{1}{n}}\right] - \frac{d}{du}\left(uF\right) + \left[\frac{n}{n+2}\left(\frac{2n+3}{n} - \frac{1}{c}\right) + \beta\right]F(u) = 0 \tag{5.5.7}$$

subject to the boundary condition

$$F(0) = \lambda^{-\left(\frac{n+1}{n+2}\right)}, \tag{5.5.8}$$

$$\frac{dF(0)}{du} = \lambda^{\frac{1}{n+2}} \frac{d\bar{F}(0)}{d\bar{u}}, \tag{5.5.9}$$

where $0 \leq u \leq 1$ and the parameter λ and $\frac{d\bar{F}}{d\bar{u}}$ are obtained from the Initial Value Problem I. Problem I is used to obtain λ and $\frac{d\bar{F}}{d\bar{u}}$. The solution $F(u)$ to Problem II is the required solution to the boundary value problem (5.4.3) to (5.4.5). For the two special cases (5.4.11) and (5.4.22), it can be verified that solutions obtained from (5.5.3) to (5.5.9) agree with those obtained in (5.4.12) and (5.4.21). Problems I and II were solved numerically using the IVP solver ODE45 of matlab. Problem I was transformed to the coupled system of first order differential equations

$$\frac{d\bar{F}}{d\bar{u}} = -\bar{y}, \tag{5.5.10}$$

$$\frac{d\bar{y}}{d\bar{u}} = \frac{n}{\bar{F}^{\frac{2n+1}{n}} (\bar{y})^{\frac{1}{n}-1}} \left[\frac{(2n+1)}{n} \left(\bar{F}\bar{y}\right)^{1+\frac{1}{n}} - \bar{u}\bar{y} + \left(\frac{n}{(n+2)} \left(\frac{1}{c} - \frac{(n+1)}{n} \right) - \beta \right) \bar{F} \right] \tag{5.5.11}$$

subject to the initial and boundary conditions

$$\overline{F}(0) = 1, \quad \bar{y}(0) = \bar{A}, \quad \bar{F}(\lambda) = 0, \tag{5.5.12}$$

where $\bar{A}$ is to be determined. Equation (5.5.11) has a singularity at the tip, $\bar{u} = \lambda$, since $\bar{F}(\lambda) = 0$. The asymptotic behaviour of $\bar{F}(\bar{u})$ near the tip, $\bar{u} = \lambda$, obtained from the asymptotic solution (5.4.8) and the scaling transformation (5.5.2),

$$\bar{F}(\bar{u}) \sim \lambda^{\frac{n}{n+2}} (n+2)^{\frac{1}{n+2}} (\lambda - \bar{u})^{\frac{1}{n+2}} \quad \text{as} \quad \bar{u} \to \lambda, \tag{5.5.13}$$

is plotted in the $\epsilon-$ neighbourhood of the tip, and is used as an initial condition for backward integration. Problem II was solved by first transforming (5.5.7) to the same coupled first order system (5.5.10) and (5.5.11), but without the overhead bars. The system is then solved subject to the initial conditions

$$F(0) = \lambda^{-\left(\frac{n+1}{n+2}\right)}, \qquad y(0) = \lambda^{\frac{1}{n+2}} \bar{y}(0), \tag{5.5.14}$$

where λ and $\bar{y}(0)$ are obtained from the solution of Problem I. The solution for $F(u)$ is the required solution of the boundary value problem (5.4.3) to (5.4.5).

In order for equation (4.2.7) to be satisfied, all solutions $h(x,t)$ must be such that $\partial h/\partial x \leq 0$ across the entire fracture. The initial fracture profile $h(x,0)$ at time $t = 0$ for any value of n, c and β is obtained from the similarity solution and is unspecified a priori. In Figure 5.5.1, $c = n = 1$ and β = -1,0, 2 and 4. It is seen that the initial profile, $h(x,0)$, varies with varying values of β, except at the fracture entry, $u = 0$, and at the fracture tip, $u = 1$, where $h(0,0) = 1$ and $h(L(0),0) = 0$. When $\beta = 4$, which represents the highest leak-off rate in

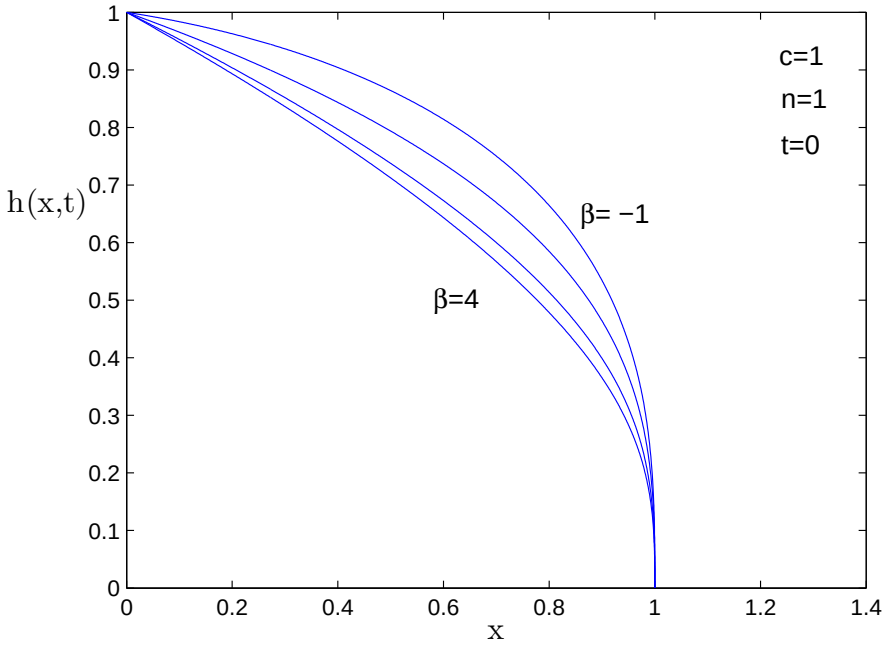

Figure 5.5.1: Initial profile of the fracture half-width, $h(x,t)$, at time $t = 0$ for $c = n = 1$ and $\beta = -1, 0, 2$ and 4.

Figure 5.5.1, the initial profile $h(x,0)$ is the thinnest and when $\beta = -1$, representing fluid injection into the fracture, the initial profile $h(x,0)$ is the widest. The effect of varying any one of the parameters n, c and β at any time, t, while keeping the remaining two parameters constant, is best understood at the points which were initially at $u = 0$ and $u = 1$ since conditions are the same for any choice of parameter at $t = 0$. Between $u = 0$ and $u = 1$, fracture profiles vary with varying choice of parameter.

In Figure 5.5.2 (i-iii), graphs of $h(x,t)$ plotted against x at time $t = 50$ for a shear thinning fluid with $n = 0.5$ are given. In each of the three parts of Figure 5.5.2, $n = 0.5$ for a shear thinning fluid while β is varied. In Figure 5.5.2 (i), the pressure at the fracture entry is constant by the PKN approximation and we see that at time $t = 50$, the fracture half-width evolves the greatest when $\beta = -1$ and the least when $\beta = 10$. The fracture half-width also evolves greatest when $\beta = -1$ and least when $\beta = 10$ in Figure 5.5.2 (ii) for which the rate of fluid injection into the fracture at the entry is constant and in Figure 5.5.2 (iii) for which the speed of propagation of the fracture is constant. Figure 5.5.3 for a Newtonian fluid ($n = 1$) and Figure 5.5.4 for a shear thickening fluid with $n = 2$ are structured in the same way as Figure 5.5.2 and the results for the dependence of the graphs on β are the same. Since n is the same in the three parts of each Figure the characteristic time T defined in (4.2.28) is the same for all graphs in that Figure and the evolution in time of the fracture can be compared in that Figure. As the parameter c increases in each of the Figures 5.5.2, 5.5.3 and 5.5.4 the rate at which both the width and length of the fracture evolve increases. The fracture half-width always evolves the least extent when $\beta = 10$, for which the leak-off is highest and evolves the greatest when $\beta = -1$, for which there is fluid inflow at the fluid-rock interface.

In order to grow the fracture the operating condition in which the speed of propagation of the fracture is constant is better than when the rate of fluid injection at the fracture entry is constant which in turn is better than when the pressure at the fracture entry is kept constant. This is satisfied for the range of leak-off considered from fluid injection at the fluid-rock interface to pure leak-off and for shear thinning, Newtonian and shear thickening fluids.

(i)

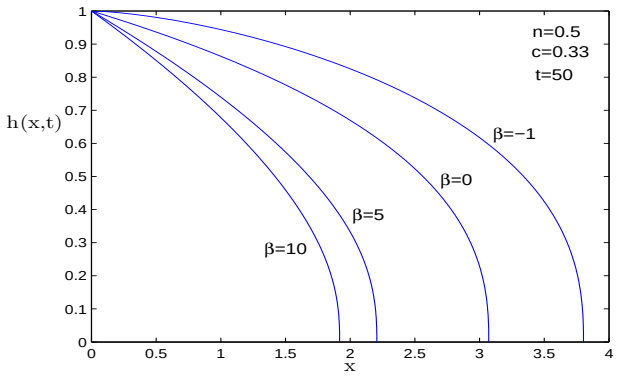

(ii)

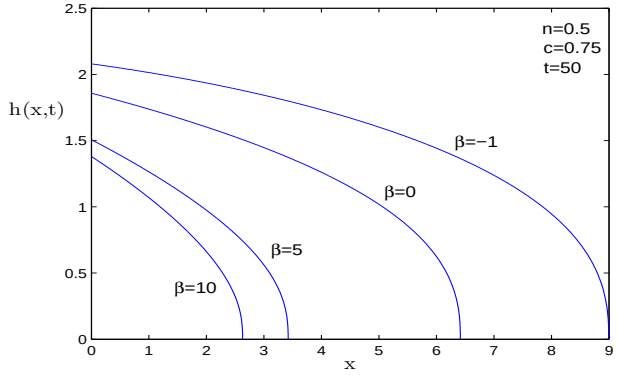

(iii)

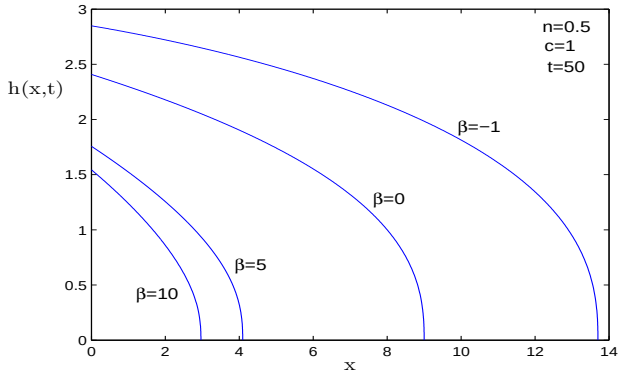

Figure 5.5.2: Numerical solution of the fracture half-width $h(x,t)$ plotted against x at time t=50 for a shear thinning fluid with $n = 0.5$ when (i) pressure at the fracture entry is constant $(c = 0.33)$, (ii) rate of fluid injection at the fracture entry is constant $(c = 0.75)$ and (iii) speed of propagation of the fracture is constant $(c = 1)$. The leak-off parameter β = -1, 0, 5, 10. Time is scaled by T defined in (4.2.28) which is the same in (i), (ii) and (iii).

(i)

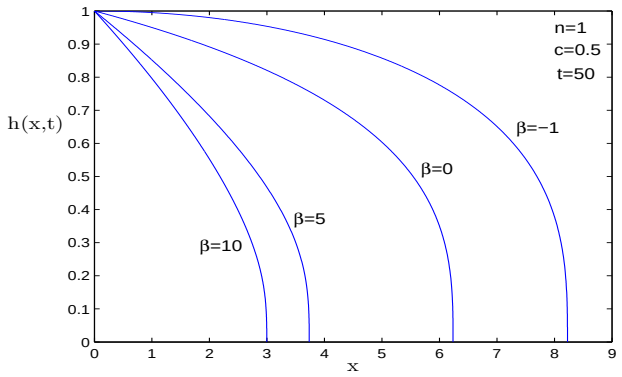

(ii)

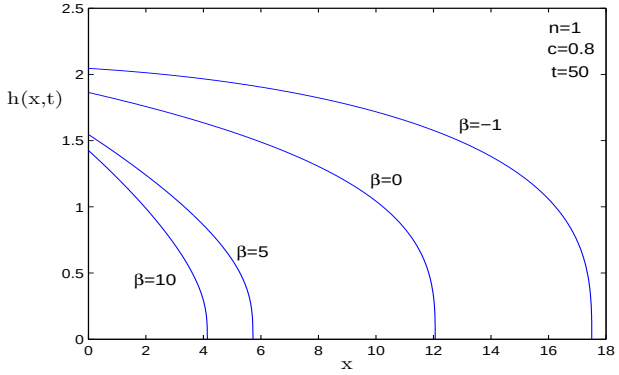

(iii)

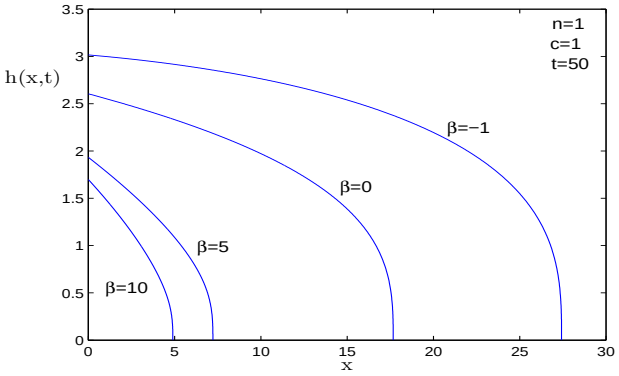

Figure 5.5.3: Numerical solution of the fracture half-width $h(x,t)$ plotted against x at time t=50 for a Newtonian fluid with $n = 1$ when (i) pressure at the fracture entry is constant $(c = 0.5)$, (ii) rate of fluid injection at the fracture entry is constant $(c = 0.8)$ and (iii) speed of propagation of the fracture is constant $(c = 1)$. The leak-off parameter β = -1, 0, 5 and 10. Time is scaled by T defined in (4.2.28) which is the same in (i), (ii) and (iii).

(i)

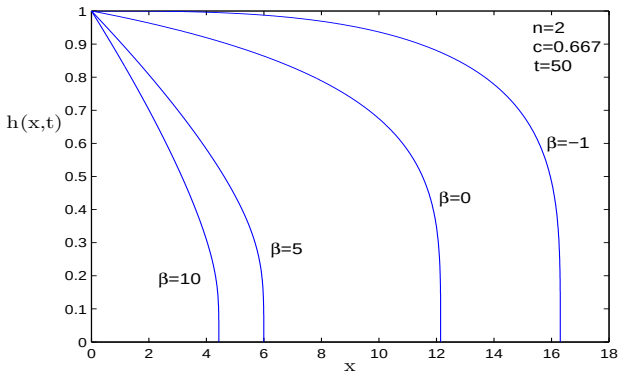

(ii)

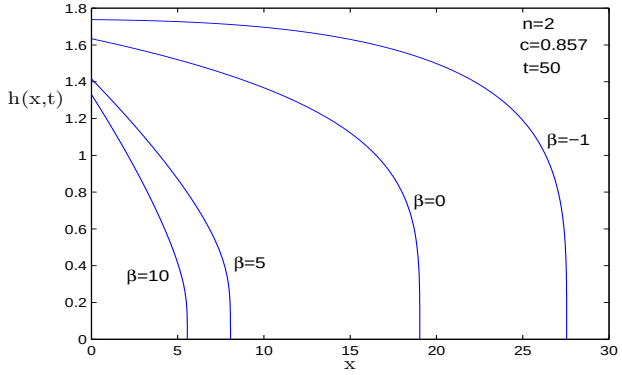

(iii)

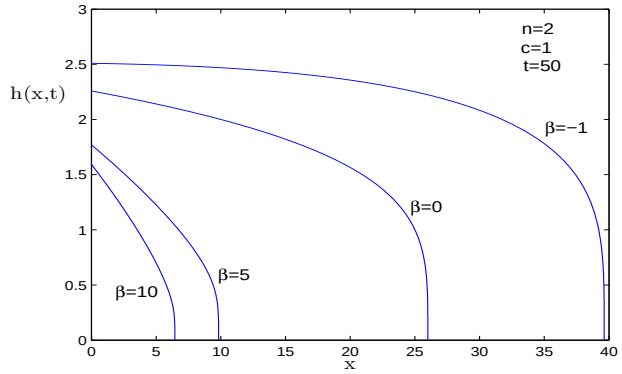

Figure 5.5.4: Numerical solution of the fracture half-width $h(x,t)$ plotted against x at time t=50 for a shear thickening fluid with $n = 2$ when (i) pressure at the fracture entry is constant $(c = 0.667)$, (ii) rate of fluid injection at the fracture entry is constant $(c = 0.857)$ and (iii) speed of propagation of the fracture is constant $(c = 1)$. The leak-off parameter β = -1, 0, 5 and 10. Time is scaled by T defined in (4.2.28) which is the same in (i), (ii) and (iii).

5.6 Width-averaged fluid velocity

The variation of the width-averaged fluid velocity, $\bar{v}_x(x,t)$, along a permeable fracture, $0 \leq x \leq L(t)$, or equivalently, $0 \leq u \leq 1$, is now investigated. From (5.2.19),

$$\bar{v}_x(x,t) = \left(-\frac{\partial h}{\partial x}\right)^{\frac{1}{n}} h^{\frac{n+1}{n}}. \tag{5.6.1}$$

But using (5.3.29) for $h(x,t)$ and (5.3.28) for $L(t)$, it can be verified that

$$\bar{v}_x(x,t) = F(u)^{\frac{n+1}{n}} \left(-\frac{dF}{du}\right)^{\frac{1}{n}} \frac{dL}{dt}, \quad 0 \leq u \leq 1. \tag{5.6.2}$$

Equation (5.6.2) has the same form as equation (4.6.18) but depends on β through the solution of the ordinary differential equation (5.4.3) for $F(u)$. The velocity ratio

$$\frac{\bar{v}_x(x,t)}{dL/dt} = F(u)^{\frac{n+1}{n}} \left(-\frac{dF}{du}\right)^{\frac{1}{n}} \tag{5.6.3}$$

does not depend explicitly on time, t. It depends on the dimensionless spatial variable u and through $F(u)$ on the power law index, n, leak-off parameter β and the working condition c.

When the rate of fluid injection into the fracture is zero, the exact solution for $F(u)$ is given by (5.4.12) and

$$F(u)^{\frac{n+1}{n}} \left(-\frac{dF}{du}\right)^{\frac{1}{n}} = u. \tag{5.6.4}$$

Therefore

$$\bar{v}_x(x,t) = u\frac{dL}{dt}, \qquad 0 \leq u \leq 1. \tag{5.6.5}$$

At the entry to the fracture, the average fluid velocity vanishes and therefore the fluid injection rate at the entry also vanishes. For the second exact solution, $F(u)$ is given by (5.4.21) and

$$F(u)^{\frac{n+1}{n}} \left(-\frac{dF}{du}\right)^{\frac{1}{n}} = 1. \tag{5.6.6}$$

Hence,

$$\bar{v}_x(x,t) = \frac{dL}{dt}, \qquad 0 \leq u \leq 1. \tag{5.6.7}$$

The average fluid velocity equals the speed of propagation of the fracture tip at each position u along the fracture. This is the physical condition which characterises the second exact solution which is defined by (5.4.22).

In each of the graphs in Figure 5.6.1, the velocity ratio along the fracture, given in equation (5.6.3) is plotted for a fracturing fluid with power-law index n and leak-off parameter β, but different working conditions c. For the cases considered, n= 0.5, 1 and 2. In Figure 5.6.1, the ordering of the curves according to working conditions at the fracture entry, is the same for shear thinning, Newtonian and shear thickening fluids. For working conditions (iv) to (vi) the average fluid velocity decreases along the fracture due to fluid leak-off. The average fluid velocity injected at the fracture entry must be greater than the speed of propagation of the fracture, $\frac{dL}{dt}$. For working conditions (i) and (ii) when there is either no fluid injection at the fracture entry or the total volume of the fracture remains constant, the average fluid velocity increases to $\frac{dL}{dt}$ along the fracture. The average fluid velocity $\bar{v}_x$ increases to $\frac{dL}{dt}$, even although there is fluid leak-off along the fracture, due to the decrease in the width along the fracture. For working conditions (iii) the decrease in the average velocity along the fracture due to leak-off is exactly balanced by the increase due to the decrease in the width along the fracture. The average fluid velocity therefore remains constant along the fracture and equals $\frac{dL}{dt}$. In Figure 5.6.2, the behaviour of $v_x/\frac{dL}{dt}$ when $\beta = -0.1$ is plotted along the fracture. The curves are bounded above by the exact solution (5.6.4) and below by the exact solution (5.6.6). Since $\beta = -0.1$, there is fluid inflow at the fluid-rock interface and when coupled with the inflow at the fracture entry the ratio $\bar{v}_x/\frac{dL}{dt}$ increases for working conditions (i) to (iii). For the working condition (iv) the increase in the average velocity due to the decrease in width of the fracture and due to fluid inflow at the fracture entry and at the interface combine such that the ratio $\bar{v}_x/\frac{dL}{dt}$ remains constant along the fracture.

(I)

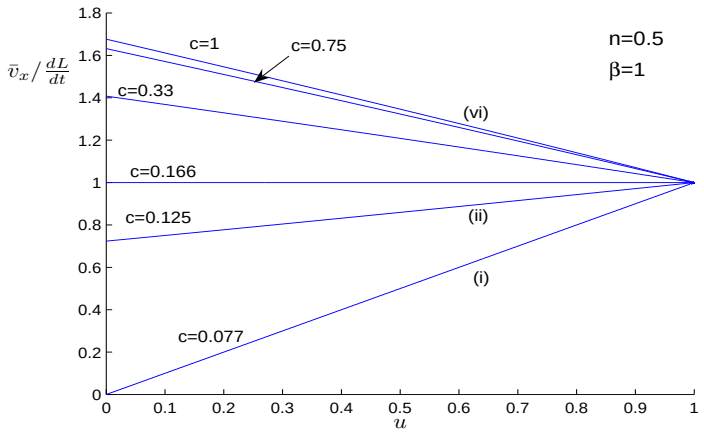

(II)

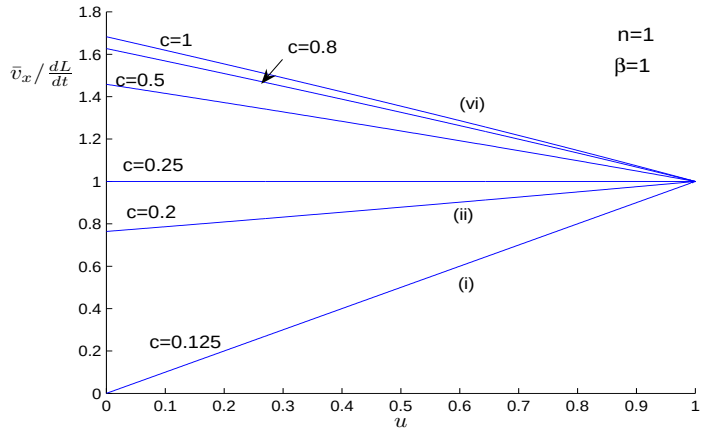

(III)

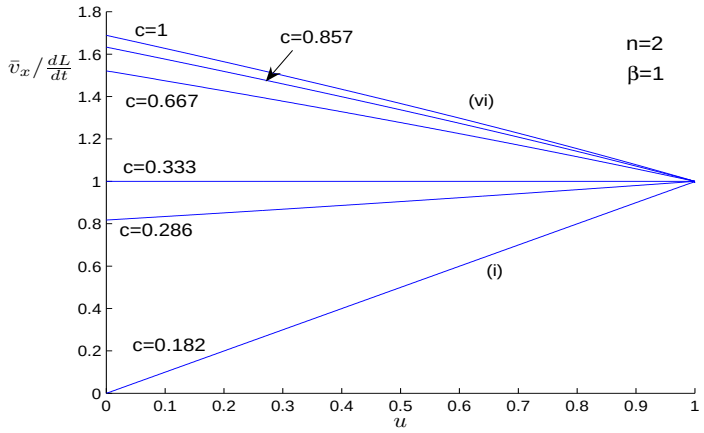

Figure 5.6.1: Velocity ratio $\bar{v}_x/\frac{dL}{dt}$ plotted against $u = x/L(t)$ for $n = 0.5, 1, 2$ and for a range of working conditions at the fracture entry: (i) zero fluid injection rate at fracture entry, (ii) total volume of the fracture is constant, (iii) average fluid velocity is constant along the fracture and equals the propagation speed of the fracture, (iv) constant pressure at fracture entry, (v) constant rate of fluid injection at entry , (vi) speed of propagation of the fracture is constant.

(I)

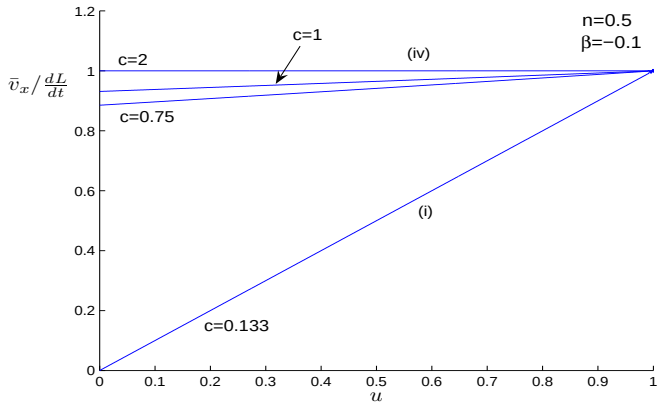

(II)

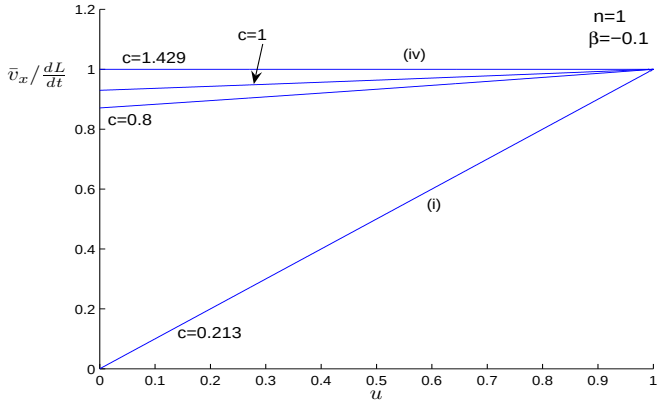

(III)

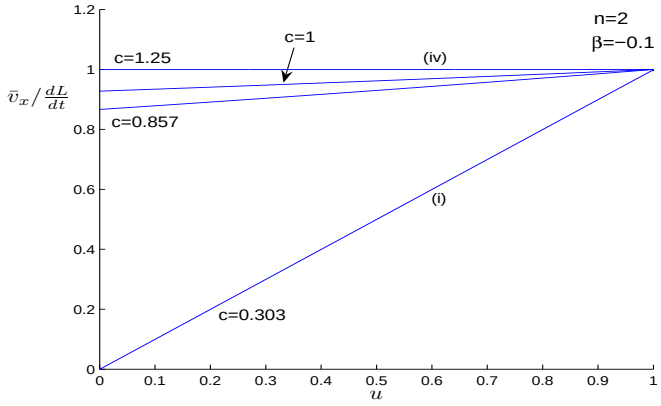

Figure 5.6.2: Velocity ratio $\bar{v}_x/\frac{dL}{dt}$ plotted against $u = x/L(t)$ for $n = 0.5, 1, 2$ and for a range of working conditions at the fracture entry: (i) zero fluid injection rate at fracture entry/pressure constant at fracture entry, (ii) rate of fluid injection is constant, (iii) speed of propagation of the fracture is constant (iv) average fluid velocity is constant along the fracture and equals the propagation speed of the fracture.

5.7 Approximate analytical solution

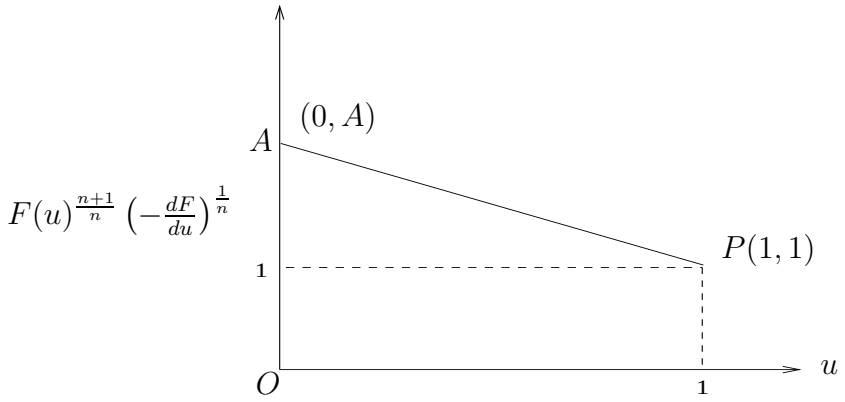

Figure 5.7.1: The straight line joining the points $(0, A)$ and $(1, 1)$ which approximates the curve joining the points.

The curves for the two cases leading to exact analytical solutions are straight lines in Figures 5.6.1 and 5.6.2. The other curves shown are approximately straight lines and will be approximated by a straight line equation. In Figure 5.7.1 the gradient of the line joining the points $(0, A)$ and $(1, 1)$ is $(1 - A)$. When $\beta = 1$, $n = 0.5$ and the pressure at the fracture entry is constant, $A = 1.4079$ and $(1 - A) = -0.4079$. The gradient of the numerical curve varies from -0.391 to -0.426 with a maximum departure from $1 - A$ of 4.46%. We approximate the curve joining the points $(0, A)$ and $(1, 1)$ by a straight line of the form

$$F(u)^{\frac{n+1}{n}} \left(-\frac{dF(u)}{du}\right)^{\frac{1}{n}} = -(A-1)u + A. \tag{5.7.1}$$

The solution of (5.7.1) subject to the boundary condition $F(1) = 0$ yields

$$F(u) = \left[\frac{n+2}{(n+1)(A-1)}\right]^{\frac{1}{n+2}} \left[\left[A - (A-1)u\right]^{n+1} - 1\right]^{\frac{1}{n+2}}. \tag{5.7.2}$$

The exact analytical solutions for $F(u)$ when $A = 0$ and $A = 1$ are known and given by (5.4.12) and (5.4.21). In (5.7.2), we will consider $A > 1$ for $F(u) \in \mathbb{R}$. For $A < 1$, (5.7.2) will be rewritten in the form in equation (4.7.2). For a specific value of the power-law exponent n, working condition c and leak-off parameter β, the numerical value of A can be used. However, in order to obtain a general expression for A which is approximately valid for a range of values

of n, c and β, consider the boundary condition (5.4.5) given as

$$F(0)^{\frac{2n+1}{n}}\left(-\frac{dF(0)}{du}\right)^{\frac{1}{n}}=\left[\frac{n}{n+2}\left(\frac{2n+3}{n}-\frac{1}{c}\right)+\beta\right]\int_0^1 F(u)\,\mathrm{d}u. \tag{5.7.3}$$

With (5.7.2) substituted into (5.7.3), the left hand side of (5.7.3) gives

$$F(0)^{\frac{2n+1}{n}}\left(-\frac{dF}{du}(0)\right)^{\frac{1}{n}}=A\left(\frac{(n+2)}{(n+1)(A-1)}\right)^{\frac{1}{n+2}}\left[A^{n+1}-1\right]^{\frac{1}{n+2}}. \tag{5.7.4}$$

By expanding in powers of $\frac{u(A-1)}{A}$ the integral on the right hand side becomes

$$\begin{aligned}\int_0^1 F(u)\,\mathrm{d}u&=\left[\frac{n+2}{(n+1)\,(A-1)}\right]^{\frac{1}{n+2}}\int_0^1\left[[A-(A-1)u]^{n+1}-1\right]^{\frac{1}{n+2}}\,\mathrm{d}u\\&=\left[\frac{n+2}{(n+1)\,(A-1)}\right]^{\frac{1}{n+2}}\int_0^1\Bigg[A^{n+1}\left(1-(n+1)\frac{u(A-1)}{A}\right.\\&\left.+\frac{(n+1)n}{2!}\left(\frac{u(A-1)}{A}\right)^2-\frac{(n+1)n(n-1)}{3!}\left(\frac{u(A-1)}{A}\right)^3+\ldots\ldots\right)-1\Bigg]^{\frac{1}{n+2}}\,\mathrm{d}u.\end{aligned} \tag{5.7.5}$$

For working conditions of interest, the range of values of A depends on the leak-off parameter β and n. For $1<A<2$, we retain only first order terms in $\frac{u(A-1)}{A}$ and we make the approximation

$$\left[[A-(A-1)u]^{n+1}-1\right]^{\frac{1}{n+2}}\simeq\left[(A^{n+1}-1)-(n+1)A^n(A-1)u\right]^{\frac{1}{n+2}} \tag{5.7.6}$$

and therefore (5.7.5) becomes

$$\begin{aligned}\int_0^1 F(u)\,\mathrm{d}u&=\left[\frac{n+2}{(n+1)\,(A-1)}\right]^{\frac{1}{n+2}}\left(A^{n+1}-1\right)^{\frac{1}{n+2}}\int_0^1\left[1-\frac{(n+1)A^n(A-1)}{A^{n+1}-1}u\right]^{\frac{1}{n+2}}\,\mathrm{d}u\\&=\left[\frac{n+2}{(n+1)\,(A-1)}\right]^{\frac{1}{n+2}}\left(\frac{n+2}{n+3}\right)\left[\frac{(A^{n+1}-1)^{\frac{n+3}{n+2}}}{(n+1)A^n(A-1)}\right]\left[1-\left(1-\frac{(n+1)A^n(A-1)}{A^{n+1}-1}\right)^{\frac{n+3}{n+2}}\right].\end{aligned} \tag{5.7.7}$$

We assume that the values of A in the range considered, $1<A<2$, are close to $A=1$ and we therefore make the approximation

$$\lim_{A\to 1}\frac{A^n(A-1)}{A^{n+1}-1}=\frac{1}{n+1}. \tag{5.7.8}$$

Equation (5.7.7) becomes approximately

$$\int_0^1 F(u)\,\mathrm{d}u = \left(\frac{n+2}{n+3}\right)\left[\frac{n+2}{(n+1)(A-1)}\right]^{\frac{1}{n+2}}\left[A^{n+1}-1\right]^{\frac{1}{n+2}}. \tag{5.7.9}$$

The boundary condition (5.7.3) yields, using (5.7.4) and (5.7.9), an approximate value for A given as

$$A = \frac{n}{n+3}\left(\frac{2n+3}{n}-\frac{1}{c}\right)+\left(\frac{n+2}{n+3}\right)\beta. \tag{5.7.10}$$

Although (5.7.10) was derived for $1 < A < 2$ it also applies for $0 < A < 1$.

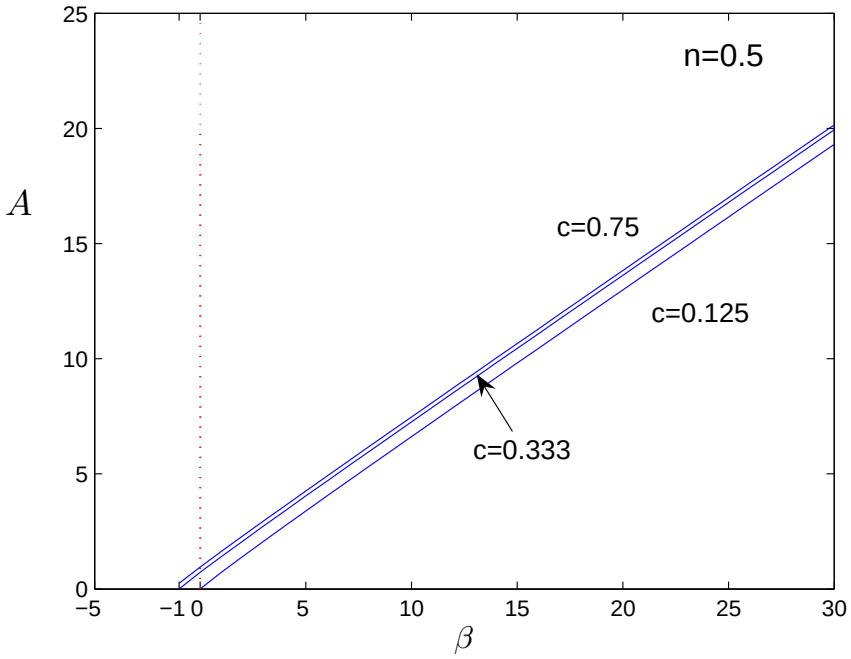

Figure 5.7.2: Velocity ratio at fracture entry, A, plotted against β for a range of working conditions: (i) Total volume of the fracture is constant $(c = 0.125)$, (ii) pressure at the fracture entry is constant $(c = 0.333)$ and (iii) constant rate of fluid injection at the entry $(c = 0.75)$.

In (5.7.10) the approximate expression for the velocity ratio at the entry, A, is obtained as a linear function of the leak-off parameter, β. In a graph of A against β, the slope of the graph is $\frac{n+2}{n+3}$ and the intercept on the A-axis is $\frac{n}{(n+3)}\left(\frac{(2n+3)}{n}-\frac{1}{c}\right)$. Putting $\beta = 0$ in (5.7.10), equation (4.7.10) for the approximate expression for A when there is no fluid leak-off is recovered. In Figure 5.7.2, an investigation of the numerical relationship between A and β for the three operating conditions considered shows that A varies almost linearly with β. In Figure 5.7.3

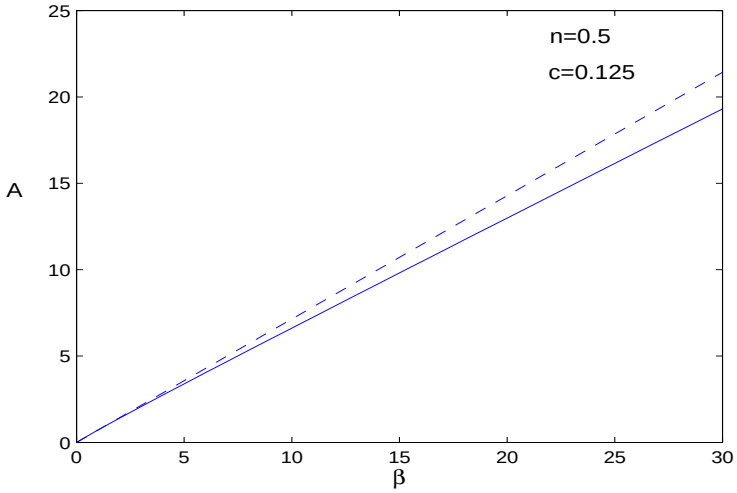

Figure 5.7.3: Velocity ratio at fracture entry, A, plotted against β when the total volume of fracture is constant: The numerical solution is (——) and the approximate solution (5.7.10) is (- - - - -).

the case in which the total volume of the fracture is constant is considered. It is seen that the approximate solution for A deviates from the numerical solution and that the deviation increases as β increases. Since the slope, $\frac{n+2}{n+3}$, is an increasing function of n, the deviation also increases with increase in n. The approximate expression for A given by (5.7.10) is therefore most accurate for small values of β satisfying

$$\frac{n}{n+2}\left(\frac{1}{c}-\frac{2n+3}{n}\right)<\beta<\frac{n}{n+2}\left(\frac{1}{c}+\frac{3}{n}\right), \tag{5.7.11}$$

for which $0<A<2$, for any working condition c and power-law index n.

Finally we now check that (5.7.2) and (5.7.10) approximately satisfy the differential equation (5.4.3). Substituting (5.7.2) into (5.4.3), and after simplifying we find that (5.7.2) is a solution of the differential equation provided

$$A=\frac{n}{(2n+3)-(n+1)\lambda(n,A)}\left[\frac{2n+3}{n}-\frac{1}{c}+\frac{(n+2)}{n}\beta\right], \tag{5.7.12}$$

where

$$\lambda(u;A)=\frac{[A-(A-1)\,u]^n-1}{[A-(A-1)\,u]^{n+1}-1}. \tag{5.7.13}$$

By using the approximation

$$\lim_{A\to 1}\lambda(u;A)=\frac{n}{n+1}, \tag{5.7.14}$$

it is readily verified that (5.7.12) agrees with (5.7.10).

In Figures 5.7.4 and 5.7.5 a comparison is made of the approximate and numerical solutions for $h(x,t)$ for two modes of working conditions. When the pressure at the fracture entry is constant, then c and A given by (5.7.10), are

$$c = \frac{n}{n+1}, \quad A = \left(\frac{n+2}{n+3}\right)(1+\beta)\,. \tag{5.7.15}$$

The approximate solution, using (5.3.29), is

$$h(x,t) = \frac{F(u)}{F(0)}, \tag{5.7.16}$$

where from (5.7.2)

$$F(u) = \left[\frac{(n+3)(n+2)}{(n+1)\left((n+2)\beta-1\right)}\right]^{\frac{1}{n+2}} \left[\left(\frac{(n+2)(1+\beta)}{(n+3)}\right)^{n+1}\left(1-\frac{\left((n+2)\beta-1\right)u}{(\beta+1)(n+2)}\right)^{n+1}-1\right]^{\frac{1}{n+2}} \tag{5.7.17}$$

and from (5.3.28)

$$x = uL(t) = u\left[1+\frac{(n+1)}{nF(0)^{\frac{n+2}{n}}}t\right]^{\frac{n}{n+1}}, \qquad 0 \le u \le 1. \tag{5.7.18}$$

When the rate of fluid injection into the fracture is constant c and A, given by (5.7.10), are:

$$c = \frac{2(n+1)}{2n+3}, \quad A = \left(\frac{n+2}{n+3}\right)\left[\frac{2n+3}{2(n+1)}+\beta\right]. \tag{5.7.19}$$

The approximate solution, using (5.3.29), is

$$h(x,t) = \left[1+\frac{(2n+3)}{2(n+1)F(0)^{\frac{n+2}{n}}}\,t\right]^{\frac{1}{2n+3}}\frac{F(u)}{F(0)}, \tag{5.7.20}$$

where from (5.7.2)

$$F(u) = \left[\frac{(n+3)}{(n+1)(\beta-\frac{n}{2(n+1)(n+2)})}\right]^{\frac{1}{n+2}}\left[\left(\left(\frac{n+2}{n+3}\right)\left(\frac{2n+3}{2(n+1)}+\beta\right)\right)^{n+1}\right.$$
$$\left.\left[1+\left(\frac{n}{(n+2)\left((2n+3)+2\beta(n+1)\right)}-\frac{2(n+1)}{\left((2n+3)+2\beta(n+1)\right)}\beta\right)u\right]^{n+1}-1\right]^{\frac{1}{n+2}}. \tag{5.7.21}$$

(i)

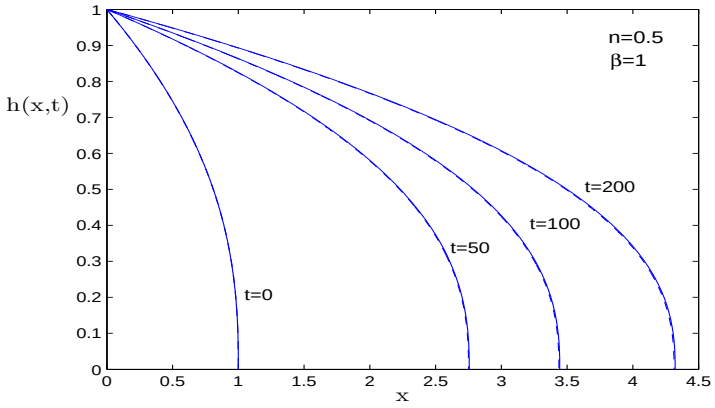

(ii)

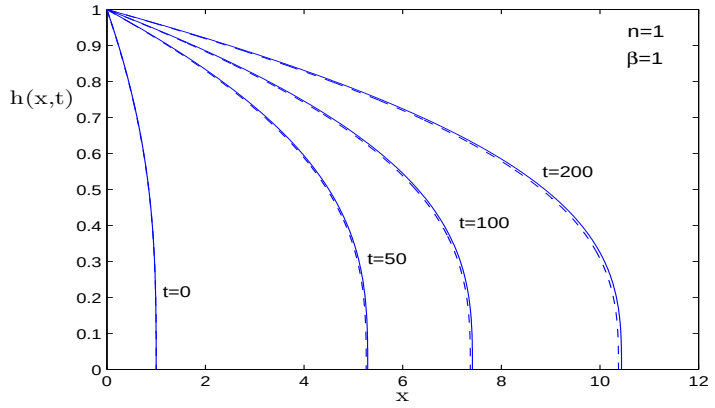

(iii)

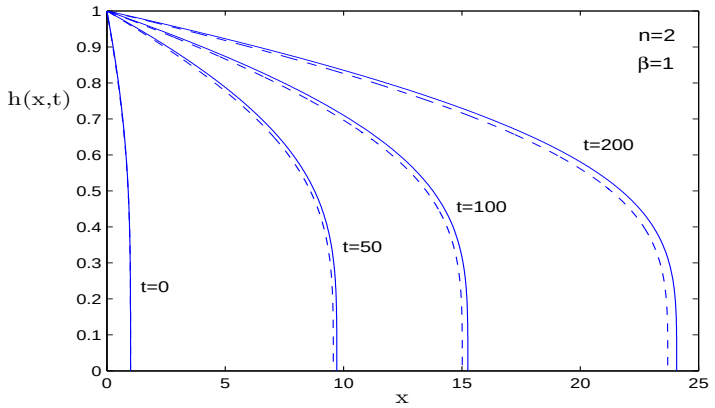

Figure 5.7.4: Comparison of the approximate solution (- - - - -) with the numerical solution (——) for $h(x,t)$ when pressure is constant at the fracture entry for $\beta = 1$ and $n = 0.5$, $n = 1$ and $n = 2$.

(i)

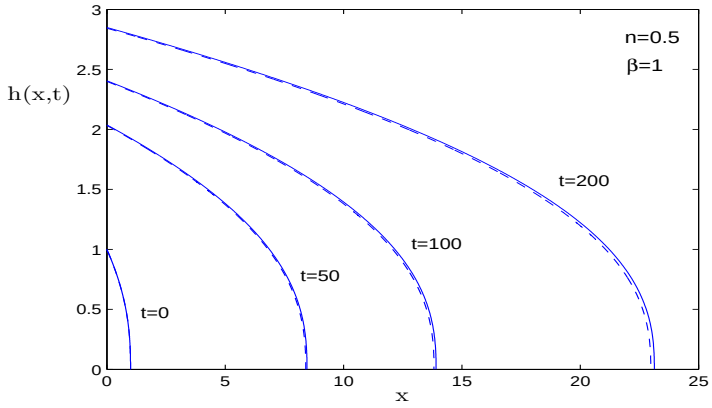

(ii)

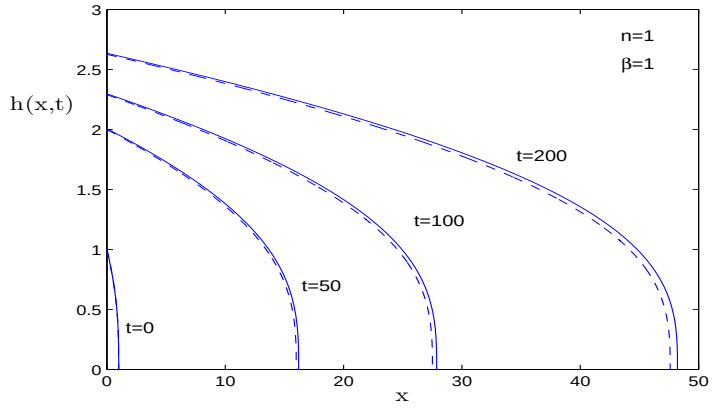

(iii)

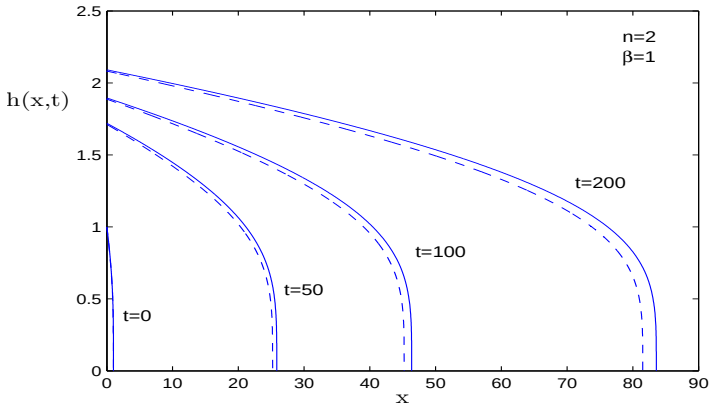

Figure 5.7.5: Comparison of the approximate solution (- - - - -) with the numerical solution (——) for $h(x,t)$ when the rate of fluid injection is constant at the fracture entry for $\beta = 1$ and $n = 0.5$, $n = 1$ and $n = 2$.

and from (5.3.28)

$$x = uL(t) = u\left[1 + \frac{(2n+3)}{2(n+1)F(0)^{\frac{n+2}{n}}}\, t\right]^{\frac{2(n+1)}{2n+3}}, \qquad 0 \leq u \leq 1. \tag{5.7.22}$$

The approximate solution slightly underestimates the width and length of the fracture, unlike in Figures 4.7.3 and 4.7.4 for no leak-off ($\beta = 0$) where the approximate solution slightly overestimated the width and length of the fracture. The graphs show that the approximate solution is more accurate for shear thinning fluids than for shear thickening fluids. In Figures 5.7.2 and 5.7.3 we see that A increases linearly with β and since the assumption was made that $0 < A < 2$ the approximate solution will be applicable for small values of β which satisfy the inequality (5.7.11).

In general the approximate solution is a useful approximation to $h(x,t)$ for shear thinning, Newtonian and shear thickening fluids over a large range of time and for small values of the leak-off parameter β.

5.8 Conclusions

In this chapter, we have considered a two-dimensional pre-existing fracture propagating in a permeable rock when fracturing fluid of power-law rheology, under high pressure, is injected into the fracture. As with Chapter 4, the governing equations for the flow of the non-Newtonian fluid in the fracture are the continuity and momentum balance equations, simplified with the aid of lubrication theory and PKN theory. Lubrication theory holds provided the ratio of the fracture half-width to the fracture length is sufficiently small. The distinguishing feature in Chapter 5 is that the interface between the fluid in the fracture and the rock mass is permeable and fluid leaks off into the surrounding rock mass with velocity $v_l(x,t)$. The leak-off condition was incorporated into the mathematical model through the interface boundary condition. With the aid of the relevant boundary conditions, a diffusion equation with a sink term, which describes the evolution of the half-width of the fracture, was derived.

In order to solve the diffusion equation, Lie symmetry analysis was first used to obtain the Lie point symmetries admitted by the nonlinear partial differential equation, with the sink term, $v_l(x,t)$, taken to be an arbitrary function of the spatial co-ordinate x and time coordinate

t. The nonlinear partial differential equation was reduced to a nonlinear second order ordinary differential equation by considering a linear combination of the admitted Lie point symmetries. The leak-off velocity, taken arbitrary during the symmetry analysis, had to satisfy a first order linear partial differential equation for the diffusion equation to admit Lie point symmetries. The leak-off velocity was therefore determined from a symmetry requirement

As with Chapter 4, the boundary value problem was solved by first transforming it into a pair of initial value problems, which together with the application of asymptotic results at the fracture tip gave good numerical solutions.

An approximate analytical solution was derived for small values of the leak-off parameter β. It was found that when there is leak-off at the fluid-rock interface, the approximate solution always underestimates the width and the length of the fracture. It was found that the approximate solution was more accurate for shear thinning fluids than for shear thickening fluids. It may be a useful approximation for small values of n close to $n = 0$. This is the region in which numerical methods for shear thinning fluids sometimes break down.

Chapter 6

Conservation laws

6.1 Introduction

This chapter investigates the existence of conservation laws for the problem of a pre-existing fracture which evolves by being driven by a non-Newtonian fluid in both permeable and impermeable rock.

Conservation laws play an important role in the study of differential equations arising in many physical processes, where physical quantities such as energy, mass and momentum are conserved. A general approach for obtaining conservation laws is given by Noether's theorem[48]. However, in order to use Noether's theorem, a knowledge of a Lagrangian formulation corresponding to the differential equation is required. This brings in a limitation to the applicability of Noether's theorem since there are many differential equations which do not admit a Lagrangian, for example, the partial differential equations derived for the evolution of the fracture half-width in this thesis. There are, however, several methods for obtaining conservation laws which do not need the formulation of a Lagrangian. These approaches are discussed with examples by R. Naz et al. [51]

In Sections 6.2, 6.3 and 6.4, we will consider three approaches to deriving conservation laws which are the direct method, the characteristic method and the partial Noether approach. Section 6.5 deals with conserved quantities for fluid flow in a fracture. Finally, we will establish a connection between conserved vectors for the partial differential equation describing

the evolution of the fracture half-width and the corresponding Lie point symmetry associated with these conserved vectors. This approach is due to Kara and Mahomed[52] and can be used to obtain group invariant solutions corresponding to conserved vectors. We will focus on the diffusion equation with the sink term $v_l(t,x)$ obtained from modelling the non-Newtonian fluid driven fracture in permeable rock, given by

$$\frac{\partial h}{\partial t}+\frac{\partial}{\partial x}\left(h^{\frac{2n+1}{n}}\left(-\frac{\partial h}{\partial x}\right)^{\frac{1}{n}}\right)+v_l(t,x)=0. \tag{6.1.1}$$

When $v_l(t,x)=0$, equation (6.1.1) reduces to (4.2.22) for a non-Newtonian fluid driven fracture in impermeable rock.

The equation

$$D_1T^1+D_2T^2=0 \tag{6.1.2}$$

is a conservation law for the differential equation (6.1.1) if it is satisfied for all solutions $h(t,x)$ of (6.1.1). In (6.1.2) the quantities $T^i(t,x,h,h_x,h_t,\ldots)$, where $i=1$ and 2, are the components of the conserved vector $T=(T^1,T^2)$ and D_1 and D_2 are the operators of total differentiation defined by

$$D_1=D_t=\frac{\partial}{\partial t}+h_t\frac{\partial}{\partial h}+h_{tt}\frac{\partial}{\partial h_t}+h_{xt}\frac{\partial}{\partial h_x}+\ldots, \tag{6.1.3}$$

$$D_2=D_x=\frac{\partial}{\partial x}+h_x\frac{\partial}{\partial h}+h_{xx}\frac{\partial}{\partial h_x}+h_{tx}\frac{\partial}{\partial h_t}+\ldots. \tag{6.1.4}$$

There are two forms for the elementary conserved vector and the elementary conservation law. Equation (6.1.1) can be written in the form of a conservation law as

$$\frac{\partial h}{\partial t}+\frac{\partial}{\partial x}\left[h^{\frac{2n+1}{n}}\left(-\frac{\partial h}{\partial x}\right)^{\frac{1}{n}}+\int_0^x v_l(t,\chi)\mathrm{d}\chi\right]=0. \tag{6.1.5}$$

By replacing the partial derivative operators on the left hand side of (6.1.5) with the total derivative operators (6.1.3) and (6.1.4) and treating t, x, h and its higher derivatives as independent variables, we obtain

$$\begin{aligned}D_t\left(h\right)+D_x\left(h^{\frac{2n+1}{n}}\left(-\frac{\partial h}{\partial x}\right)^{\frac{1}{n}}+\int_0^x v_l(t,\chi)\mathrm{d}\chi\right)&\\ =h_t-\frac{(2n+1)}{n}h^{\frac{n+1}{n}}\left(-h_x\right)^{\frac{n+1}{n}}-\frac{1}{n}h^{\frac{2n+1}{n}}\left(-h_x\right)^{\frac{1-n}{n}}h_{xx}+v_l(t,x).&\end{aligned} \tag{6.1.6}$$

Substituting the expression for h_t in (6.1.1) into (6.1.6), we obtain

$$D_t\left(h\right)+D_x\left(h^{\frac{2n+1}{n}}\left(-h_x\right)^{\frac{1}{n}}+\int_0^x v_l(t,\chi)\mathrm{d}\chi\right)=0. \tag{6.1.7}$$

The components

$$T^1 = h, \tag{6.1.8}$$

$$T^2 = h^{\frac{2n+1}{n}}\left(-h_x\right)^{\frac{1}{n}}+\int_0^x v_l(t,\chi)\mathrm{d}\chi, \tag{6.1.9}$$

are the components of the elementary conserved vector of the first kind and (6.1.7) is the elementary conservation law of the first kind.

Equation (6.1.1) can also be written in the form

$$\frac{\partial}{\partial t}\left[h+\int_0^t v_l(\tau,x)\mathrm{d}\tau\right]+\frac{\partial}{\partial x}\left[h^{\frac{2n+1}{n}}\left(-\frac{\partial h}{\partial x}\right)^{\frac{1}{n}}\right]=0 \tag{6.1.10}$$

which can be expressed as

$$D_t\left[h+\int_0^t v_l(\tau,x)\mathrm{d}\tau\right]+D_x\left[h^{\frac{2n+1}{n}}\left(-\frac{\partial h}{\partial x}\right)^{\frac{1}{n}}\right]=0. \tag{6.1.11}$$

The components

$$T^1 = h+\int_0^t v_l(\tau,x)\mathrm{d}\tau, \tag{6.1.12}$$

$$T^2 = h^{\frac{2n+1}{n}}\left(-\frac{\partial h}{\partial x}\right)^{\frac{1}{n}}, \tag{6.1.13}$$

are the components of the elementary conserved vector of the second kind and (6.1.11) is the elementary conservation law of the second kind. When $v_l=0$ the elementary conserved vector for a non-Newtonian fluid-driven fracture in impermeable rock is recovered from both the first and second kind conserved vectors:

$$T^1=h,\quad T^2=h^{\frac{2n+1}{n}}\left(-h_x\right)^{\frac{1}{n}}. \tag{6.1.14}$$

6.2 Direct method

The direct method uses (6.1.2), subject to (6.1.1) being satisfied, yielding a determining equation for the conserved vectors. We will look for conserved vectors of the form $T^i(t,x,h,h_x)$,

$i = 1, 2$, which satisfy the determining equation

$$D_t T^1 + D_x T^2 \Big|_{(6.1.1)} = 0. \tag{6.2.1}$$

Using (6.1.3) and (6.1.4) and by substituting h_t with its expression in (6.1.1), (6.2.1) becomes

$$\frac{\partial T^1}{\partial t} + \frac{1}{n} h^{\frac{2n+1}{n}} (-h_x)^{\frac{1-n}{n}} h_{xx} \frac{\partial T^1}{\partial h} + \frac{(2n+1)}{n} h^{\frac{n+1}{n}} (-h_x)^{\frac{n+1}{n}} \frac{\partial T^1}{\partial h} - v_l(t,x) \frac{\partial T^1}{\partial h} + h_{tx} \frac{\partial T^1}{\partial h_x} + \frac{\partial T^2}{\partial x} + h_x \frac{\partial T^2}{\partial h} + h_{xx} \frac{\partial T^2}{\partial h_x} = 0. \tag{6.2.2}$$

Since T^1 and T^2 are independent of h_{tx} and h_{xx}, (6.2.2) is separated with respect to h_{tx} and h_{xx} to give

$$h_{xx}: \quad \frac{\partial T^2}{\partial h_x} + \frac{1}{n} h^{\frac{2n+1}{n}} (-h_x)^{\frac{1-n}{n}} \frac{\partial T^1}{\partial h} = 0, \tag{6.2.3}$$

$$h_{tx}: \quad \frac{\partial T^1}{\partial h_x} = 0, \tag{6.2.4}$$

and the remaining expression in equation (6.2.2) is

$$\frac{\partial T^1}{\partial t} + \frac{(2n+1)}{n} h^{\frac{n+1}{n}} (-h_x)^{\frac{n+1}{n}} \frac{\partial T^1}{\partial h} - v_l(t,x) \frac{\partial T^1}{\partial h} + \frac{\partial T^2}{\partial x} + h_x \frac{\partial T^2}{\partial h} = 0. \tag{6.2.5}$$

From (6.2.4), $T^1 = T^1(t, x, h)$ and therefore (6.2.3) is integrated with respect to h_x to obtain

$$T^2 = h^{\frac{2n+1}{n}} (-h_x)^{\frac{1}{n}} \frac{\partial T^1}{\partial h} + A(t, x, h), \tag{6.2.6}$$

where $A(t, x, h)$ is an arbitrary function. Substituting (6.2.6) into (6.2.5) yields

$$\frac{\partial T^1}{\partial t} - v_l(t,x) \frac{\partial T^1}{\partial h} + h^{\frac{2n+1}{n}} (-h_x)^{\frac{1}{n}} \frac{\partial^2 T^1}{\partial x \partial h} + \frac{\partial A}{\partial x}(t,x,h) - h^{\frac{2n+1}{n}} (-h_x)^{\frac{n+1}{n}} \frac{\partial^2 T^1}{\partial h^2} + h_x \frac{\partial A}{\partial h}(t,x,h) = 0. \tag{6.2.7}$$

Equation (6.2.7) can be separated according to powers of h_x. However, some powers of h_x are the same for certain values of n. For example, when $n = 1$, $h_x^{\frac{1}{n}}$ and h_x have the same powers and their coefficients should be grouped together. It is therefore necessary to look for conserved vectors for two different cases, the first of which is when the fluid is Newtonian, with $n = 1$, and the second case is for general n, $n \neq 1$, for which the fluid is non-Newtonian.

6.2.1 Case $n = 1$

Equation (6.2.7) is separated thus

$$h_x^2 : \quad \frac{\partial^2 T^1}{\partial h^2} = 0, \tag{6.2.8}$$

$$h_x : \quad \frac{\partial A}{\partial h} - h^3 \frac{\partial^2 T^1}{\partial x \partial h} = 0, \tag{6.2.9}$$

$$\text{Remainder} : \quad \frac{\partial T^1}{\partial t} - v_l(t,x)\frac{\partial T^1}{\partial h} + \frac{\partial A}{\partial x} = 0. \tag{6.2.10}$$

Integrating (6.2.8) twice gives

$$T^1 = B(t,x)h + C(t,x). \tag{6.2.11}$$

Using (6.2.11), (6.2.9) is integrated with respect to h to obtain

$$A(t,x,h) = \frac{1}{4}h^4 \frac{\partial B}{\partial x}(t,x) + D(t,x). \tag{6.2.12}$$

In (6.2.11) and (6.2.12), $B(t,x)$, $C(t,x)$ and $D(t,x)$ are as yet undetermined. Substituting (6.2.11) and (6.2.12) into (6.2.10) and then separating according to powers of h yields

$$h^4 \quad : \frac{\partial^2 B}{\partial x^2} = 0, \tag{6.2.13}$$

$$h \quad : \frac{\partial B}{\partial t} = 0, \tag{6.2.14}$$

$$\text{remainder} \quad : \frac{\partial C}{\partial t} - v_l(t,x)B(t,x) + \frac{\partial D}{\partial x} = 0. \tag{6.2.15}$$

From (6.2.13) and (6.2.14), we have

$$B(x) = c_1 x + c_2, \tag{6.2.16}$$

where c_1 and c_2 are constants. Using (6.2.16), equation (6.2.15) becomes

$$\frac{\partial C}{\partial t}(t,x) - (c_1 x + c_2)v_l(t,x) + \frac{\partial D}{\partial x}(t,x) = 0. \tag{6.2.17}$$

From (6.2.11) and (6.2.16),

$$T^1(t,x,h) = (c_1 x + c_2)h + C(t,x), \tag{6.2.18}$$

and from (6.2.6), (6.2.12) and (6.2.16),

$$T^2(t,x,h,h_x) = -(c_1x + c_2)h^3h_x + \frac{c_1}{4}h^4 + D(t,x). \tag{6.2.19}$$

There are two ways of proceeding which lead to the two elementary conserved vectors found in Section 6.1. We can use (6.2.17) to replace either $C(t,x)$ or $D(t,x)$ in (6.2.18) and (6.2.19).

Consider first replacing $D(t,x)$. Integrating (6.2.17) with respect to χ from 0 to x gives

$$D(t,x) = D(t,0) - \frac{\partial E}{\partial t}(t,x) + c_1\int_0^x xv_l(t,\chi)\,\mathrm{d}\chi + c_2\int_0^x v_l(t,\chi)\,\mathrm{d}\chi, \tag{6.2.20}$$

where

$$E(t,x) = \int_0^x C(t,\chi)\,\mathrm{d}\chi, \quad \frac{\partial E}{\partial x} = C(t,x). \tag{6.2.21}$$

Then (6.2.18) and (6.2.19) become

$$T^1(t,x,h) = (c_1x + c_2)h + T^1_*, \tag{6.2.22}$$

$$T^2(t,x,h,h_x) = -(c_1x + c_2)h^3h_x + \frac{c_1}{4}h^4 + c_1\int_0^x \chi v_l(t,\chi)\,\mathrm{d}\chi + c_2\int_0^x v_l(t,\chi)\,\mathrm{d}\chi + T^2_*, \tag{6.2.23}$$

where

$$T^1_* = C(t,x), \quad T^2_* = D(t,0) - \frac{\partial E}{\partial t}(t,x). \tag{6.2.24}$$

Now, it is readily verified that

$$D_tT^1_* + D_xT^2_* \equiv 0 \tag{6.2.25}$$

without imposing (6.1.1). Thus T^1_* and T^2_* are the components of a trivial conserved vector and can be set equal to zero. By putting c_1 and c_2 equal to zero in turn we obtain from (6.2.22) and (6.2.23) the following two conserved vectors for a Newtonian fluid-driven fracture in permeable rock:

$$T^1 = h, \qquad T^2 = -h^3h_x + \int_0^x v_l(t,\chi)\,\mathrm{d}\chi, \tag{6.2.26}$$

$$T^1 = xh, \qquad T^2 = -xh^3h_x + \frac{1}{4}h^4 + \int_0^x \chi v_l(t,\chi)\,\mathrm{d}\chi. \tag{6.2.27}$$

Equation (6.2.26) is the elementary conserved vector of the first kind.

We next replace $C(t,x)$. Integrating (6.2.17) with respect to τ from 0 to t gives

$$C(t,x) = C(0,x) - \frac{\partial F}{\partial x}(t,x) + (c_1 x + c_2)\int_0^t v_l(\tau,x)\,\mathrm{d}\tau, \tag{6.2.28}$$

where

$$F(t,x) = \int_0^t D(\tau,x)\,\mathrm{d}\tau, \quad \frac{\partial F}{\partial t} = D(t,x). \tag{6.2.29}$$

Then (6.2.18) and (6.2.19) become

$$T^1(t,x,h) = (c_1 x + c_2)h + (c_1 x + c_2)\int_0^t v_l(\tau,x)\,\mathrm{d}\tau + T^1_*, \tag{6.2.30}$$

$$T^2(t,x,h,h_x) = -(c_1 x + c_2)h^3 h_x + \frac{c_1}{4}h^4 + T^2_* \tag{6.2.31}$$

where

$$T^1_* = C(0,x) - \frac{\partial F}{\partial x}(t,x), \quad T^2_* = D(t,x) \tag{6.2.32}$$

But it is readily verified that (6.2.25) is identically satisfied without imposing (6.1.1) and therefore T^1_* and T^2_* are the components of a trivial conserved vector. Equations (6.2.30) and (6.2.31) give the following two conserved vectors for a Newtonian fluid-driven fracture in permeable rock:

$$T^1 = h + \int_0^t v_l(\tau,x)\,\mathrm{d}\tau, \quad T^2 = -h^3 h_x, \tag{6.2.33}$$

$$T^1 = xh + x\int_0^t v_l(\tau,x)\,\mathrm{d}\tau, \quad T^2 = -xh^3 h_x + \frac{1}{4}h^4 \tag{6.2.34}$$

Equation (6.2.33) is the elementary conserved vector of the second kind.

6.2.2 General case $n > 0$, $n \neq 1$

Equation (6.2.7) is separated by powers of h_x as follows

$$h_x^{\frac{n+1}{n}} \quad : \frac{\partial^2 T^1}{\partial h^2} = 0, \tag{6.2.35}$$

$$h_x^{\frac{1}{n}} \quad : \frac{\partial^2 T^1}{\partial x \partial h} = 0, \tag{6.2.36}$$

$$h_x \quad : \frac{\partial A}{\partial h} = 0, \tag{6.2.37}$$

$$\text{remainder} \quad : \frac{\partial T^1}{\partial t} - v_l\frac{\partial T^1}{\partial h} + \frac{\partial A}{\partial x} = 0. \tag{6.2.38}$$

From (6.2.35) and (6.2.36),

$$T^1 = B(t)h + C(t,x), \tag{6.2.39}$$

where $B(t)$ and $C(t,x)$ are arbitrary functions. From (6.2.37), $A = A(t,x)$ and by substituting (6.2.38) into (6.2.39), we obtain

$$h\frac{dB}{dt} + \frac{\partial C}{\partial t} - v_l B(t) + \frac{\partial A}{\partial x} = 0, \tag{6.2.40}$$

from which we have by separating in powers of h,

$$B(t) = c_1, \qquad c_1 = \text{constant} \tag{6.2.41}$$

and

$$\frac{\partial C}{\partial t}(t,x) - c_1 v_l(t,x) + \frac{\partial A}{\partial x}(t,x) = 0. \tag{6.2.42}$$

From (6.2.6) and (6.2.39), the conserved vector components are

$$T^1 = c_1 h + C(t,x), \tag{6.2.43}$$

$$T^2 = c_1 h^{\frac{2n+1}{n}} (-h_x)^{\frac{1}{n}} + A(t,x). \tag{6.2.44}$$

Equation (6.2.42) corresponds to (6.2.17) for a Newtonian fluid. Again, there are two ways of proceeding. We can use (6.2.42) to replace either $C(t,x)$ or $A(t,x)$ in (6.2.43) and (6.2.44).

We first replace $A(t,x)$. Integrating (6.2.42) with respect to $\chi$from 0 to x gives

$$A(t,x) = A(t,0) - \frac{\partial E(t,x)}{\partial t} + c_1 \int_0^x v_l(t,\chi)\,\mathrm{d}\chi, \tag{6.2.45}$$

where

$$E(t,x) = \int_0^x C(t,\chi)\,\mathrm{d}\chi, \quad \frac{\partial E}{\partial x} = C(t,x). \tag{6.2.46}$$

Equations (6.2.43) and (6.2.44) become

$$T^1 = c_1 h + T^1_*, \tag{6.2.47}$$

$$T^2 = c_1 h^{\frac{2n+1}{n}} (-h_x)^{\frac{1}{n}} + c_1 \int_0^x v_l(t,\chi)\,\mathrm{d}\chi + T^2_*, \tag{6.2.48}$$

where

$$T^1_* = C(t,x), \quad T^2_* = A(t,0) - \frac{\partial E}{\partial t}(t,x). \tag{6.2.49}$$

It is easily shown that T_*^1 and T_*^2 satisfy (6.2.25) identically without (6.1.1) being imposed and are therefore the components of a trivial conserved vector. We therefore set T_*^1 and T_*^2 to zero. We obtain only one conserved vector

$$T^1 = h, \qquad T^2 = h^{\frac{2n+1}{n}} (-h_x)^{\frac{1}{n}} + \int_0^x v_l(t,\chi)\,\mathrm{d}\chi, \tag{6.2.50}$$

which is the elementary conserved vector of the first kind.

We next replace $C(t,x)$. Integrating (6.2.42) with respect to τ from 0 to t gives

$$C(t,x) = C(0,x) + c_1 \int_0^t v_l(\tau,x)\,\mathrm{d}\tau - \frac{\partial F}{\partial x}(t,x), \tag{6.2.51}$$

where

$$F(t,x) = \int_0^t A(\tau,x)\,\mathrm{d}\tau, \quad \frac{\partial F}{\partial t} = A(t,x). \tag{6.2.52}$$

The components (6.2.43) and (6.2.44) become

$$T^1 = c_1 h + c_1 \int_0^t v_l(\tau,x)\,\mathrm{d}\tau + T_*^1, \tag{6.2.53}$$

$$T^2 = c_1 h^{\frac{2n+1}{n}} (-h_x)^{\frac{1}{n}} + T_*^2, \tag{6.2.54}$$

where

$$T_*^1 = C(0,x) - \frac{\partial F}{\partial x}(t,x),, \tag{6.2.55}$$

$$T_*^2 = A(t,x). \tag{6.2.56}$$

The components (6.2.55) and (6.2.56) satisfy the conservation equation (6.2.25) identically and therefore form a trivial conserved vector and are set equal to zero. We again obtain only one conserved vector

$$T^1 = h + \int_0^t v_l(\tau,x)\,\mathrm{d}\tau, \quad T^2 = h^{\frac{2n+1}{n}} (-h_x)^{\frac{1}{n}} \tag{6.2.57}$$

which is the elementary conserved vector of the second kind.

The conserved vectors which we have found for the partial differential equation (6.1.1) are summarised in Table 6.2.1. The leak-off velocity $v_l(t,x)$ occurs in either T^1 or T^2. It does not occur in both components T^1 and T^2 in the same conserved vector. For a Newtonian fluid with leak-off, we found a second conserved vector that does not occur in a non-Newtonian fluid. The results reduce to those of Chapter 4 when $v_l(t,x) = 0$.

n	Conserved vector
1	$T^1 = h, \quad T^2 = -h^3 h_x + \int_0^x v_l(t,\chi)\,\mathrm{d}\chi$ $T^1 = xh\,, \quad T^2 = -xh^3 h_x + \frac{1}{4}h^4 + \int_0^x \chi v_l(t,\chi)\,\mathrm{d}\chi$
1	$T^1 = h + \int_0^t v_l(\tau,x)\,\mathrm{d}\tau, \quad T^2 = -h^3 h_x$ $T^1 = xh + x\int_0^t v_l(\tau,x)\,\mathrm{d}\tau, \quad T^2 - xh^3 h_x + \frac{1}{4}h^4$
$n > 0$ $n \neq 1$	$T^1 = h, \quad T^2 = h^{\frac{2n+1}{n}}(-h_x)^{\frac{1}{n}} + \int_0^x v_l(t,\chi)\mathrm{d}\chi$
$n > 0$ $n \neq 1$	$T^1 = h + \int_0^t v_l(\tau,x)\,\mathrm{d}\tau, \quad T^2 = h^{\frac{2n+1}{n}}(-h_x)^{\frac{1}{n}}$

Table 6.2.1: Conserved vector for the partial differential equation (6.1.1)

6.3 Conservation law via the multiplier approach

Here, we will look for conserved vectors with components T^i, $i = 1, 2$ whose dependence on $x, t, h, h_x, h_t, \ldots$ is unspecified aprori.

A multiplier Λ for the partial differential equation (6.1.1) has the property that

$$\Lambda\left[\frac{\partial h}{\partial t} + \frac{\partial}{\partial x}\left(h^{\frac{2n+1}{n}}\left(-\frac{\partial h}{\partial x}\right)^{\frac{1}{n}}\right) + v_l(t,x)\right] = D_t T^1 + D_x T^2, \tag{6.3.1}$$

for all function $h(t,x)$ where D_x and D_y are as given in (6.1.3) and (6.1.4). The right hand side of (6.3.1) is a divergence expression.

Consider now a multiplier of the form $\Lambda(t,x,h,h_t,h_x)$. The multiplier has the determining equation given by

$$E_h\left[\Lambda(t,x,h,h_t,h_x)\left(h_t - \frac{1}{n}h^{\frac{2n+1}{n}}(-h_x)^{\frac{1-n}{n}}h_{xx} - \frac{(2n+1)}{n}h^{\frac{n+1}{n}}(-h_x)^{\frac{n+1}{n}} + v_l\right)\right] = 0, \tag{6.3.2}$$

where

$$E_h = \frac{\delta}{\delta h} = \frac{\partial}{\partial h} - D_x\frac{\partial}{\partial h_x} - D_t\frac{\partial}{\partial h_t} + D_x^2\frac{\partial}{\partial h_{xx}} + D_x D_y\frac{\partial}{\partial h_{xt}} + D_t^2\frac{\partial}{\partial h_{tt}} - \ldots \tag{6.3.3}$$

is the standard Euler operator which annihilates the divergence on the right hand side of (6.3.1). Expanding (6.3.2), we have

$$\left[h_t - \frac{1}{n}h^{\frac{2n+1}{n}}(-h_x)^{\frac{1-n}{n}}h_{xx} - \frac{(2n+1)}{n}h^{\frac{n+1}{n}}(-h_x)^{\frac{n+1}{n}} + v_l\right]\Lambda_h + \Lambda\left[-\frac{(2n+1)}{n^2}(-h_x)^{\frac{1-n}{n}}h_{xx}h^{\frac{n+1}{n}}\right.$$
$$\left.-\frac{(2n+1)(n+1)}{n^2}(-h_x)^{\frac{n+1}{n}}h^{\frac{1}{n}}\right] - \left[h_t - \frac{1}{n}h^{\frac{2n+1}{n}}(-h_x)^{\frac{1-n}{n}}h_{xx} - \frac{(2n+1)}{n}h^{\frac{n+1}{n}}(-h_x)^{\frac{n+1}{n}} + v_l\right]D_x(\Lambda_{h_x})$$
$$-\Lambda_{h_x}D_x\left[h_t - \frac{1}{n}h^{\frac{2n+1}{n}}(-h_x)^{\frac{1-n}{n}}h_{xx} - \frac{(2n+1)}{n}h^{\frac{n+1}{n}}(-h_x)^{\frac{n+1}{n}} + v_l\right] - \left[\frac{(1-n)}{n^2}h^{\frac{2n+1}{n}}(-h_x)^{\frac{1-2n}{n}}h_{xx}\right.$$
$$\left.+\frac{(2n+1)(n+1)}{n^2}h^{\frac{n+1}{n}}(-h_x)^{\frac{1}{n}}\right]D_x(\Lambda) - \Lambda D_x\left[\frac{(1-n)}{n^2}h^{\frac{2n+1}{n}}(-h_x)^{\frac{1-2n}{n}}h_{xx}\right.$$
$$\left.+\frac{(2n+1)(n+1)}{n^2}h^{\frac{n+1}{n}}(-h_x)^{\frac{1}{n}}\right] - \left[h_t - \frac{1}{n}h^{\frac{2n+1}{n}}(-h_x)^{\frac{1-n}{n}}h_{xx} - \frac{(2n+1)}{n}h^{\frac{n+1}{n}}(-h_x)^{\frac{n+1}{n}} + v_l\right]$$
$$\times D_t(\Lambda_{h_t}) - \Lambda_{h_t}D_t\left[h_t - \frac{1}{n}h^{\frac{2n+1}{n}}(-h_x)^{\frac{1-n}{n}}h_{xx} - \frac{(2n+1)}{n}h^{\frac{n+1}{n}}(-h_x)^{\frac{n+1}{n}} + v_l\right] - D_t(\Lambda)$$
$$+D_x^2\left[\Lambda\left(-\frac{1}{n}h^{\frac{2n+1}{n}}(-h_x)^{\frac{1-n}{n}}\right)\right] = 0. \tag{6.3.4}$$

Since (6.3.4) must be satisfied for any function $h(t,x)$, the sum of the coefficients of like derivatives of $h(t,x)$ in (6.3.4) must vanish. We will now discuss the Newtonian case $n=1$ for the reason stated in Section 6.2.

6.3.1 Case $n = 1$

Equation (6.3.4) reduces to

$$\left[h_t - h^3h_{xx} - 3h^2h_x^2 + v_l\right]\Lambda_h + \Lambda\left[-3h^2h_{xx} - 6hh_x^2\right] - \left[h_t - h^3h_{xx} - 3h^2h_x^2 + v_l\right]$$
$$\times D_x(\Lambda_{h_x}) - \Lambda_{h_x}D_x\left[h_t - h^3h_{xx} - 3h^2h_x^2 + v_l\right] + 6h^2h_xD_x(\Lambda)$$
$$+\Lambda D_x\left[6h^2h_x\right] - \left[h_t - h^3h_{xx} - 3h^2h_x^2 + v_l\right]D_t(\Lambda_{h_t}) - \Lambda_{h_t}D_t\left[h_t - h^3h_{xx} - 3h^2h_x^2 + v_l\right]$$
$$-D_t(\Lambda) + D_x^2(-h^3\Lambda) = 0. \tag{6.3.5}$$

The coefficients of the highest order derivative terms, h_{xxx} and h_{xxt}, cancel out to give zero and from (6.3.5) the coefficients of $h_{tt}h_t$, h_{tt}, h_{xt}, h_{xx} and the terms independent of derivatives

of h yield

$$h_{tt}h_t: \qquad \Lambda_{h_th_t} = 0, \tag{6.3.6}$$

$$h_{tt}: \qquad \Lambda_{h_t} = 0, \tag{6.3.7}$$

$$h_{xt}: \qquad \Lambda_{h_x} = 0, \tag{6.3.8}$$

$$h_{xx}: \qquad \Lambda_h = 0, \tag{6.3.9}$$

$$\begin{matrix}\text{terms independent of} \\ \text{derivatives of } h\end{matrix}: \qquad \Lambda_t + \Lambda_{xx}h^3 = 0. \tag{6.3.10}$$

From (6.3.6) to (6.3.9), we obtain

$$\Lambda = \Lambda(t, x), \tag{6.3.11}$$

and therefore from (6.3.10), we have, separating by powers of h,

$$h^3: \qquad \Lambda_{xx} = 0, \tag{6.3.12}$$

$$1: \qquad \Lambda_t = 0. \tag{6.3.13}$$

Equation (6.3.13) yields $\Lambda = \Lambda(x)$ and integrating (6.3.12) gives

$$\Lambda = c_1x + c_2, \tag{6.3.14}$$

where c_1 and c_2 are constants. The multiplier is independent of the leak-off velocity $v_l(t, x)$.

As with the direct method there are two ways of proceeding. Firstly, equation (6.3.1) with $n = 1$ and (6.3.14) give, by doing elementary manipulations,

$$\begin{aligned}&(c_1x + c_2)\left[h_t - h^3h_{xx} - 3h^2h_x^2 + v_l\right] = D_t\left[c_1xh + c_2h\right] \\ &+ D_x\left[c_1\left(-xh^3h_x + \frac{1}{4}h^4 + \int_0^x \chi v_l(t, \chi)\,\mathrm{d}\chi\right) + c_2\left(-h^3h_x + \int_0^x v_l(t, \chi)\mathrm{d}\chi\right)\right]\end{aligned} \tag{6.3.15}$$

for all functions $h(t, x)$. Thus, when $h(t, x)$ is a solution of the diffusion equation (6.1.1) with $n = 1$,

$$D_t\left[c_1xh + c_2h\right] + D_x\left[c_1\left(-xh^3h_x + \frac{1}{4}h^4 + \int_0^x \chi v_l(t, \chi)\,\mathrm{d}\chi\right) + c_2\left(-h^3h_x + \int_0^x v_l(t, \chi)\mathrm{d}\chi\right)\right] = 0. \tag{6.3.16}$$

By putting c_1 and c_2 equal to zero in turn, we obtain again the two conserved vectors of the first kind, (6.2.26) and (6.2.27).

Secondly, equation (6.3.1) with $n = 1$ and (6.3.14) may be written in the form

$$(c_1x + c_2)\left[h_t - h^3h_{xx} - 3h^2h_x^2 + v_l\right] = D_t\left[c_1\left(xh + x\int_0^t v_l(\tau, x)\,\mathrm{d}\tau\right)\right.$$
$$\left. + c_2\left(h + \int_0^t v_l(\tau, x)\,\mathrm{d}\tau\right)\right] + D_x\left[c_1\left(-xh^3h_x + \frac{1}{4}h^4\right) + c_2\left(-h^3h_x\right)\right] \quad (6.3.17)$$

for all functions $h(t, x)$. Thus when $h(t, x)$ is a solution of the diffusion equation (6.1.1) with $n = 1$,

$$D_t\left[c_1\left(xh + x\int_0^t v_l(\tau, x)\,\mathrm{d}\tau\right) + c_2\left(h + \int_0^t v_l(\tau, x)\,\mathrm{d}\tau\right)\right]$$
$$+ D_x\left[c_1\left(-xh^3h_x + \frac{1}{4}h^4\right) + c_2\left(-h^3h_x\right)\right] = 0 \quad (6.3.18)$$

By putting c_1 and c_2 equal to zero in turn we obtain the two conserved vectors of the second kind, (6.2.33) and (6.2.34).

6.3.2 General case $n > 0$, $n \neq 1$

Equating to zero the coefficients of $h_{xx}h_x^{\frac{1-2n}{n}}$, $h_{xx}h_x^{\frac{1}{n}}$, $h_{tt}h_t$, h_{tt}, $h_{xx}h_x^{\frac{1-n}{n}}$ and the remaining terms in (6.3.4) which are independent of derivatives of h and simplifying, we have

$$h_{xx}h_x^{\frac{1-2n}{n}}: \quad \Lambda_x = 0, \quad (6.3.19)$$

$$h_{xx}h_x^{\frac{1}{n}}: \quad \Lambda_{h_x} = 0, \quad (6.3.20)$$

$$h_{tt}h_t: \quad \Lambda_{h_th_t} = 0, \quad (6.3.21)$$

$$h_{tt}: \quad \Lambda_{h_t} = 0, \quad (6.3.22)$$

$$h_{xx}h_x^{\frac{1-n}{n}}: \quad \Lambda_h = 0, \quad (6.3.23)$$

$$\text{remainder}: \quad \Lambda_t = 0. \quad (6.3.24)$$

From (6.3.19) to (6.3.24), we obtain

$$\Lambda = c. \quad (6.3.25)$$

There are two ways of proceeding. Firstly, from (6.3.1) and (6.3.25),

$$c\left[h_t - \frac{1}{n}h^{\frac{2n+1}{n}}\left(-h_x\right)^{\frac{1-n}{n}}h_{xx} - \frac{(2n+1)}{n}h^{\frac{n+1}{n}}\left(-h_x\right)^{\frac{n+1}{n}} + v_l\right]$$
$$= D_t\left[ch\right] + D_x\left[c\left(h^{\frac{2n+1}{n}}\left(-h_x\right)^{\frac{1}{n}} + \int_0^x v_l(t,\chi)\,\mathrm{d}\chi\right)\right] \quad (6.3.26)$$

for all functions $h(t,x)$. When $h(t,x)$ is a solution of the diffusion equation (6.1.1), it follows that

$$D_t\left[ch\right] + D_x\left[c\left(h^{\frac{2n+1}{n}}\left(-h_x\right)^{\frac{1}{n}} + \int_0^x v_l(t,\chi)\,\mathrm{d}\chi\right)\right] = 0. \quad (6.3.27)$$

By letting $c = 1$, we obtain the elementary conserved vector of the first kind, $T = (T^1, T^2)$, where

$$T^1 = h, \quad T^2 = h^{\frac{2n+1}{n}}\left(-h_x\right)^{\frac{1}{n}} + \int_0^x v_l(t,\chi)\,\mathrm{d}\chi. \quad (6.3.28)$$

Secondly, we also obtain from (6.3.1) and (6.3.25)

$$c\left[h_t - \frac{1}{n}h^{\frac{2n+1}{n}}\left(-h_x\right)^{\frac{1-n}{n}}h_{xx} - \frac{(2n+1)}{n}h^{\frac{n+1}{n}}\left(-h_x\right)^{\frac{n+1}{n}} + v_l\right]$$
$$= D_t\left[c\left(h + \int_0^t v_l(\tau,x)\,\mathrm{d}\tau\right)\right] + D_x\left[c\left(h^{\frac{2n+1}{n}}\left(-h_x\right)^{\frac{1}{n}}\right)\right] \quad (6.3.29)$$

for all functions $h(t,x)$. When $h(t,x)$ is a solution of (6.1.1), then

$$D_t\left[c\left(h + \int_0^t v_l(\tau,x)\,\mathrm{d}\tau\right)\right] + D_x\left[c\left(h^{\frac{2n+1}{n}}\left(-h_x\right)^{\frac{1}{n}}\right)\right] = 0. \quad (6.3.30)$$

Setting $c = 1$ we obtain the elementary conserved vector of the second kind with components

$$T^1 = h + \int_0^t v_l(\tau,x)\,\mathrm{d}\tau, \quad T^2 = h^{\frac{2n+1}{n}}\left(-h_x\right)^{\frac{1}{n}}. \quad (6.3.31)$$

The results obtained using the multiplier method starting with a multiplier of the form $\Lambda(t,x,h,h_t,h_x)$ agree with those obtained by the direct method starting with components of the form $T^1(t,x,h,h_x)$ and $T^2(t,x,h,h_x)$. The results are presented in Table 6.2.1.

6.4 Partial Lagrangian method

A Lagrangian for (6.1.1) does not exist since we cannot find a function $L(t,x,h,h_t,h_x)$ such that

$$\frac{\delta L}{\delta h} = \frac{\partial h}{\partial t} + \frac{\partial}{\partial x}\left(h^{\frac{2n+1}{n}}\left(-\frac{\partial h}{\partial x}\right)^{\frac{1}{n}}\right) + v_l(t,x), \quad (6.4.1)$$

where $\frac{\delta}{\delta h}$ is the Euler operator defined by (6.3.3). However, we can derive a partial Lagrangian for equation (6.1.1). Using the partial Lagrangian, conservation laws are obtained via the partial Noether approach [51].

Now, suppose the second order partial differential equation (6.1.1), $E(t, x, h, h_t, h_x, , h_{xx}) = 0$, can be written as

$$E = E^0 + E^1 = 0. \tag{6.4.2}$$

A function $L(t, x, h, h_t, h_x)$ is called a partial Lagrangian of equation (6.4.2) if (6.4.2) can be expressed as $\frac{\delta L}{\delta h} = fE^1$ for some non-zero function f, provided $E^1 \neq 0$.

Equation (6.1.1) when expanded is

$$\frac{\partial h}{\partial t} - \frac{(2n+1)}{n} h^{\frac{n+1}{n}} \left(-\frac{\partial h}{\partial x}\right)^{\frac{n+1}{n}} - \frac{1}{n} h^{\frac{2n+1}{n}} \left(-\frac{\partial h}{\partial x}\right)^{\frac{1-n}{n}} \frac{\partial^2 h}{\partial x^2} + v_l(t, x) = 0. \tag{6.4.3}$$

The separation of E in the form (6.4.2) is not unique. A separation of (6.4.3) for which we can find a simple partial Lagrangian is

$$E^0 = -\frac{(2n+1)}{n(n+1)} h^{\frac{n+1}{n}} (-h_x)^{\frac{n+1}{n}} - \frac{1}{n} h^{\frac{2n+1}{n}} (-h_x)^{\frac{1-n}{n}} h_{xx}, \tag{6.4.4}$$

$$E^1 = h_t + v_l(t, x) - \left(\frac{2n+1}{n+1}\right) h^{\frac{n+1}{n}} (-h_x)^{\frac{n+1}{n}}, \tag{6.4.5}$$

where E^1 depends in a simple way on h_t. Consider

$$L = \left(\frac{n}{n+1}\right) h^{\frac{2n+1}{n}} (-h_x)^{\frac{n+1}{n}} - v_l(t, x). \tag{6.4.6}$$

It follows from the definition (6.3.3) of the Euler operator and using the partial differential equation (6.4.3) to eliminate h_{xx} that

$$\frac{\delta L}{\delta h} = \left(\frac{2n+1}{n+1}\right) h^{\frac{n+1}{n}} (-h_x)^{\frac{n+1}{n}} - h_t - v_l(t, x) = fE^1, \tag{6.4.7}$$

where $f = -1$. It follows that L defined by (6.4.6) is a partial Lagrangian for the partial differential equation (6.4.3).

The partial Noether symmetry determining equation is

$$XL + L\left[D_t\xi^1 + D_x\xi^2\right] = D_tB^1 + D_xB^2 + \left(\eta - \xi^1 h_t - \xi^2 h_x\right) \frac{\delta L}{\delta h}, \tag{6.4.8}$$

where

$$X = \xi^1 \frac{\partial}{\partial t} + \xi^2 \frac{\partial}{\partial x} + \eta \frac{\partial}{\partial h} + \zeta_1 \frac{\partial}{\partial h_t} + \zeta_2 \frac{\partial}{\partial h_x} + \ldots \tag{6.4.9}$$

is the Lie-Backlund operator and ζ_i, $i = 1, 2$, are defined as

$$\zeta_i = D_i(\eta) - h_j D_i(\xi^j). \tag{6.4.10}$$

We will require $\zeta_2 = \zeta_x$ which when expanded is

$$\zeta_2 = \frac{\partial \eta}{\partial x} + \left(\frac{\partial \eta}{\partial h} - \frac{\partial \xi^2}{\partial x}\right) h_x - \frac{\partial \xi^1}{\partial x} h_t - \frac{\partial \xi^2}{\partial h} h_x^2 - \frac{\partial \xi^1}{\partial h} h_x h_t. \tag{6.4.11}$$

The functions B^1 and B^2 are gauge functions. In the partial Lagrangian approach the Euler operator is usually denoted by $\frac{\delta}{\delta h}$ while in the multiplier method it is denoted by E_h.

We consider gauge functions of the form $B^i = B^i(t, x, h)$, $i = 1, 2$. When expanded (6.4.8) becomes

$$\begin{aligned}
&-\xi^1 \frac{\partial v_l}{\partial t} - \xi^2 \frac{\partial v_l}{\partial x} + \left(\frac{2n+1}{n+1}\right) \eta h^{\frac{n+1}{n}} (-h_x)^{\frac{n+1}{n}} - h^{\frac{2n+1}{n}} (-h_x)^{\frac{1}{n}} \eta_x + h^{\frac{2n+1}{n}} (-h_x)^{\frac{n+1}{n}} \eta_h \\
&+h^{\frac{2n+1}{n}} (-h_x)^{\frac{1}{n}} h_t \xi_x^1 - h^{\frac{2n+1}{n}} (-h_x)^{\frac{n+1}{n}} h_t \xi_h^1 - h^{\frac{2n+1}{n}} (-h_x)^{\frac{n+1}{n}} \xi_x^2 + h^{\frac{2n+1}{n}} (-h_x)^{\frac{2n+1}{n}} \xi_h^2 \\
&+\left(\frac{n}{n+1}\right) h^{\frac{2n+1}{n}} (-h_x)^{\frac{n+1}{n}} \xi_t^1 + \left(\frac{n}{n+1}\right) h^{\frac{2n+1}{n}} (-h_x)^{\frac{n+1}{n}} h_t \xi_h^1 + \left(\frac{n}{n+1}\right) h^{\frac{2n+1}{n}} (-h_x)^{\frac{n+1}{n}} \xi_x^2 \\
&-\left(\frac{n}{n+1}\right) h^{\frac{2n+1}{n}} (-h_x)^{\frac{2n+1}{n}} \xi_h^2 - v_l \xi_t^1 - v_l h_t \xi_h^1 - v_l \xi_x^2 - v_l h_x \xi_h^2 = B_t^1 + h_t B_h^1 + B_x^2 \\
&+h_x B_h^2 - h_t \eta + \left(\frac{2n+1}{n+1}\right) h^{\frac{n+1}{n}} (-h_x)^{\frac{n+1}{n}} \eta - \eta v_l + h_t^2 \xi^1 - \left(\frac{2n+1}{n+1}\right) h^{\frac{n+1}{n}} (-h_x)^{\frac{n+1}{n}} h_t \xi^1 \\
&+h_t v_l \xi^1 + h_x h_t \xi^2 + \left(\frac{2n+1}{n+1}\right) h^{\frac{n+1}{n}} (-h_x)^{\frac{2n+1}{n}} \xi^2 + h_x v_l \xi^2.
\end{aligned} \tag{6.4.12}$$

We separate equation (6.4.12) by powers and products of the derivatives of $h(t, x)$. Two general results can be derived before we have to consider the cases $n = 1$ and $n > 0$, $n \neq 1$, separately. Consider first the coefficient of h_t^2.

$$h_t^2 : \quad \xi^1 = 0, \quad n > 0. \tag{6.4.13}$$

Put $\xi^1 = 0$ in (6.4.12) and then consider the coefficient of $h_x h_t$.

$$h_x h_t : \quad \xi^2 = 0, \quad n > 0. \tag{6.4.14}$$

The determining equation (6.4.12) reduces for all $n > 0$ to

$$-\frac{\partial \eta}{\partial x} h^{\frac{2n+1}{n}} (-h_x)^{\frac{1}{n}} + \frac{\partial \eta}{\partial h} h^{\frac{2n+1}{n}} (-h_x)^{\frac{1}{n}+1} = \frac{\partial B^1}{\partial t} + h_t \frac{\partial B^1}{\partial h} + \frac{\partial B^2}{\partial x} + h_x \frac{\partial B^2}{\partial h} - \eta h_t - \eta v_l(t, x). \tag{6.4.15}$$

The case $n = 1$ must now be treated separately from the general case $n > 0$, $n \neq 1$, because $h_x^{\frac{1}{n}}$ and h_x have the same power when $n = 1$.

6.4.1 Case $n = 1$

When $n = 1$, equation (6.4.15) reduces to

$$\frac{\partial \eta}{\partial x} h^3 h_x + \frac{\partial \eta}{\partial h} h^3 h_x^2 = \frac{\partial B^1}{\partial t} + h_t \frac{\partial B^1}{\partial h} + \frac{\partial B^2}{\partial x} + h_x \frac{\partial B^2}{\partial h} - \eta h_t - \eta v_l(t, x). \tag{6.4.16}$$

Separate (6.4.16) by partial derivatives of h.

$$h_x^2 : \quad \eta_h = 0, \tag{6.4.17}$$

$$h_x : \quad h^3 \eta_x - B_h^2 = 0, \tag{6.4.18}$$

$$h_t : \quad B_h^1 - \eta = 0, \tag{6.4.19}$$

$$\text{remainder} : \quad B_t^1 + B_x^2 - \eta v_l = 0. \tag{6.4.20}$$

From (6.4.17), $\eta = \eta(t, x)$ and the expressions for B^1 and B^2 are obtained by integrating (6.4.19) and (6.4.18) with respect to h to obtain

$$B^1 = \eta h + C(t, x), \tag{6.4.21}$$

$$B^2 = \frac{h^4}{4} \eta_x + D(t, x), \tag{6.4.22}$$

where $C(t, x)$ and $D(t, x)$ are arbitrary functions. Substituting (6.4.21) and (6.4.22) into (6.4.20) yields

$$h\eta_t + \frac{\partial C}{\partial t} + \frac{h^4}{4} \eta_{xx} + \frac{\partial D}{\partial x} - \eta v_l(t, x) = 0. \tag{6.4.23}$$

It now remains to separate (6.4.23) by powers of h which gives

$$h^4 : \quad \frac{\partial^2 \eta}{\partial x^2} = 0, \tag{6.4.24}$$

$$h : \quad \frac{\partial \eta}{\partial t} = 0, \tag{6.4.25}$$

$$\text{remainder} : \quad \frac{\partial C}{\partial t}(t, x) - \eta(t, x) v_l(t, x) + \frac{\partial D}{\partial x}(t, x) = 0. \tag{6.4.26}$$

Thus from (6.4.24) and (6.4.25)

$$\eta = c_1 x + c_2 \tag{6.4.27}$$

and (6.4.21), (6.4.22) and (6.4.26) become

$$B^1(t,x,h) = (c_1 x + c_2)\, h + C(t,x), \tag{6.4.28}$$

$$B^2(t,x,h) = c_1 \frac{h^4}{4} + D(t,x), \tag{6.4.29}$$

$$\frac{\partial C}{\partial t}(t,x) - (c_1 x + c_2) v_l(t,x) + \frac{\partial D}{\partial x}(t,x) = 0. \tag{6.4.30}$$

Since $\xi^1 = 0$ and $\xi^2 = 0$ and η is given by (6.4.27), the partial Noether symmetry is

$$X = (c_1 x + c_2) \frac{\partial}{\partial h}. \tag{6.4.31}$$

The partial Noether conserved vectors are

$$T^1 = B^1 - \xi^1 L - \left[\eta - \xi^1 h_t - \xi^2 h_x\right] \frac{\partial L}{\partial h_t}, \tag{6.4.32}$$

$$T^2 = B^2 - \xi^2 L - \left[\eta - \xi^1 h_t - \xi^2 h_x\right] \frac{\partial L}{\partial h_x}, \tag{6.4.33}$$

which yield the conserved vectors

$$T^1 = [c_1 x + c_2]\, h + C(t,x), \tag{6.4.34}$$

$$T^2 = -\left[c_1 x + c_2\right] h^3 h_x + c_1 \frac{h^4}{4} + D(t,x). \tag{6.4.35}$$

Equations (6.4.34), (6.4.35) for T^1 and T^2 and (6.4.30) relating $C(t,x)$ and $D(t,x)$ to $v_l(t,x)$ are exactly the same as (6.2.18), (6.2.19) and (6.2.17) of the direct method. We therefore obtain again the conserved vectors listed in Table 6.2.1 for $n = 1$.

6.4.2 General case $n > 0$, $n \neq 1$

We return to (6.4.15) and separate by the partial derivatives of h for $n \neq 1$:

$$(-h_x)^{1+\frac{1}{n}}: \qquad \eta_h = 0, \tag{6.4.36}$$

$$(-h_x)^{\frac{1}{n}}: \qquad \eta_x = 0, \tag{6.4.37}$$

$$h_x: \qquad B_h^2 = 0, \tag{6.4.38}$$

$$h_t: \qquad B_h^1 - \eta = 0, \tag{6.4.39}$$

$$\text{remainder}: \qquad B_t^1 + B_x^2 - \eta v_l(t,x) = 0. \tag{6.4.40}$$

From (6.4.36) and (6.4.37), $\eta = \eta(t)$ and from (6.4.38), B^2 is of the form

$$B^2 = A(t,x). \tag{6.4.41}$$

From (6.4.39),

$$B^1(t,x,h) = \eta(t)h + C(t,x). \tag{6.4.42}$$

Substituting (6.4.41) and (6.4.42) into (6.4.40) gives

$$h\frac{d\eta(t)}{dt} + \frac{\partial C}{\partial t}(t,x) + \frac{\partial A}{\partial x}(t,x) - \eta(t)v_l(t,x) = 0. \tag{6.4.43}$$

We separate (6.4.43) according to powers of h:

$$h: \qquad \frac{d\eta(t)}{dt} = 0, \tag{6.4.44}$$

$$\text{remainder}: \qquad \frac{\partial C}{\partial t}(t,x) - \eta(t)v_l(t,x) + \frac{\partial A}{\partial x}(t,x) = 0. \tag{6.4.45}$$

Thus from (6.4.44),

$$\eta(t) = c_1, \tag{6.4.46}$$

where c_1 is a constant. Equations (6.4.42) and (6.4.45) become

$$B^1(t,x,h) = c_1 h + C(t,x), \tag{6.4.47}$$

$$\frac{\partial C}{\partial t}(t,x) - c_1 v_l(t,x) + \frac{\partial A}{\partial x}(t,x) = 0. \tag{6.4.48}$$

Since $\xi^1 = 0$ and $\xi^2 = 0$ and $\eta = c_1$, the partial Noether symmetry is

$$X = c_1 \frac{\partial}{\partial h} \tag{6.4.49}$$

The partial Noether conserved vector is given by (6.4.32) and (6.4.33) which yields

$$T^1 = c_1 h + C(t, x), \tag{6.4.50}$$

$$T^2 = c_1 h^{\frac{2n+1}{n}} (-h_x)^{\frac{1}{n}} + A(t, x). \tag{6.4.51}$$

Equations (6.4.50) and (6.4.51) for the components T^1 and T^2 and (6.4.48) for $C(t, x)$ and $A(t, x)$ in terms of $v_l(t, x)$ are exactly the same as (6.2.43), (6.2.44) and (6.2.42) in the direct method. We therefore derive again the conserved vectors given in Table 6.2.1 for $n > 0$, $n \neq 1$.

The results obtained using the partial Lagrangian with gauge functions of the form $B^i = B^i(t, x, h)$ agree with the results obtained using the multiplier method with multipliers of the form $\Lambda(t, x, h, h_t, h_x)$ and with those obtained by the direct method starting with components of the form $T^i(t, x, h, h_x)$.

When the interface between the fluid and the rock is impermeable, v_l vanishes. Therefore, setting $v_l = 0$ yields conserved vectors for a fluid-driven fracture in impermeable rock. We have seen that for the general case $n > 0$, $n \neq 1$, which describes a non-Newtonian fluid driven fracture, we obtain only the elementary conserved vectors, unlike in the case of a Newtonian fluid for which $n = 1$ where the elementary conserved vectors and a second conserved vector of the first and second kind are obtained. This underscores a significant difference between Newtonian and non-Newtonian fluid-driven fractures. A conserved vector is lost when the fracturing fluid is non-Newtonian. The conserved vectors obtained for both the Newtonian and non-Newtonian fluid-driven fractures are non-local conserved vectors, because of the integral term $\int_0^x v_l(t, \chi) \mathrm{d}\chi$.

The conservation laws derived will now be used, first to investigate the conserved quantities and balance laws for non-Newtonian fluid driven fracture, and second, to derive the Lie point symmetries associated with the conserved vectors.

6.5 Balance law for fluid-driven fracture

The balance law derived in Chapters 4 and 5, solely from the physics of the fluid-driven fracture will be re-derived in this section from the integration of a conservation law subject to the relevant boundary conditions. We note that the conservation laws in Sections 6.2, 6.3 and 6.4 are derived from the partial differential equation governing the fluid-driven fracture process. These conservation laws apply to any physical problem described by the partial differential equation. However, conserved quantities and balance laws are derived from conservation laws and boundary conditions.

The conserved vectors (T^1, T^2) which have been derived depend on $h(t, x)$ and can therefore be expressed in terms of the independent variables t and x. Thus

$$D_t T^1 + D_x T^2 = \frac{\partial T^1(t,x)}{\partial t} + \frac{\partial T^2(t,x)}{\partial x}, \tag{6.5.1}$$

where on the right hand side, T^1 and T^2 are regarded as functions of t and x only. For a conserved vector the left-hand side of (6.5.1) vanishes for solutions of the partial differential equation and we have

$$\frac{\partial T^1(t,x)}{\partial t} + \frac{\partial T^2(t,x)}{\partial x} = 0. \tag{6.5.2}$$

The balance law will first be derived from the elementary conserved vector of the first kind with components given by

$$T^1 = h, \quad T^2 = h^{\frac{2n+1}{n}} (-h_x)^{\frac{1}{n}} + \int_0^x v_l(t,\chi)\,\mathrm{d}\chi. \tag{6.5.3}$$

Substitute (6.5.3) into (6.5.2) and integrating from $x = 0$ to $x = L(t)$ keeping t fixed during the integration, we have

$$\int_0^{L(t)} \frac{\partial h}{\partial t}(t,x)\,\mathrm{d}x + \int_0^{L(t)} \frac{\partial}{\partial x}\left(h^{\frac{2n+1}{n}} (-h_x)^{\frac{1}{n}} + \int_0^x v_l(t,\chi)\,\mathrm{d}\chi \right) \mathrm{d}x = 0. \tag{6.5.4}$$

Using the formula for differentiation under the integral sign [45], with boundary condition

$$h(t, L(t)) = 0, \tag{6.5.5}$$

equation (6.5.4) becomes after integration

$$\frac{d}{dt}\int_0^{L(t)} h(t,x)\,\mathrm{d}x + \left[h^{\frac{2n+1}{n}} (-h_x)^{\frac{1}{n}} + \int_0^x v_l(t,\chi)\,\mathrm{d}\chi \right]_0^{L(t)} = 0. \tag{6.5.6}$$

Now the total volume of the fracture is

$$V(t) = 2\int_0^{L(t)} h(t,x)\mathrm{d}x \tag{6.5.7}$$

and from (5.2.19)

$$h\bar{v}_x(t,x) = h^{\frac{2n+1}{n}}\left(-h_x\right)^{\frac{1}{n}} = \frac{1}{2}Q_1(t,x), \tag{6.5.8}$$

where $Q_1(t,x)$ is the flux of fluid along the fracture. Therefore (6.5.6) becomes

$$\frac{1}{2}\frac{dV}{dt} + h(t,L(t))\bar{v}_x(t,L(t)) - h(t,0)\bar{v}_x(t,0) + \int_0^{L(t)} v_l(t,x)\,\mathrm{d}x = 0. \tag{6.5.9}$$

At the tip of the fracture, the flux of fluid vanishes and therefore

$$Q_1(t,L(t)) = 2h(t,L(t))\bar{v}_x(t,L(t)) = 0. \tag{6.5.10}$$

Equation (6.5.9) becomes

$$\frac{dV}{dt} = 2h(t,0)\bar{v}_x(t,0) - 2\int_0^{L(t)} v_l(t,x)\,\mathrm{d}x, \tag{6.5.11}$$

which states that the rate of change of the volume of the fracture with respect to time equals the rate of fluid inflow at the fracture entry minus the rate of fluid leak-off at the interface between the fluid and the rock mass. Equation (6.5.11) is the balance law which was derived in equation (5.2.28).

The elementary conservation law of the first kind, integrated with respect to x from $x = 0$ to $x = L(t)$ and simplified subject to the boundary conditions, (6.5.5) and (6.5.10), therefore corresponds to the balance law for fluid volume.

We now show that the elementary conserved vector of the second kind,

$$T^1 = h + \int_0^t v_l(\tau,x)\,\mathrm{d}\tau, \qquad T^2 = h^{\frac{2n+1}{n}}\left(-h_x\right)^{\frac{1}{n}}, \tag{6.5.12}$$

also gives the balance law for fluid volume, (6.5.11). Substituting (6.5.12) into (6.5.2) gives

$$\frac{\partial}{\partial t}\left(h + \int_0^t v_l(\tau,x)\,\mathrm{d}\tau\right) + \frac{\partial}{\partial x}\left[h^{\frac{2n+1}{n}}\left(-h_x\right)^{\frac{1}{n}}\right] = 0. \tag{6.5.13}$$

But

$$\frac{\partial}{\partial t}\left(\int_0^t v_l(\tau,x)\,\mathrm{d}\tau\right) = v_l(t,x) \tag{6.5.14}$$

and integrating (6.5.13) with respect to x from $x = 0$ to $x = L(t)$ we obtain

$$\int_0^{L(t)} \frac{\partial h}{\partial t}(t,x)\,\mathrm{d}x + \int_0^{L(t)} v_l(t,x)\,\mathrm{d}x + \left[h^{\frac{2n+1}{n}}\,(-h_x)^{\frac{1}{n}}\right]_0^{L(t)} = 0. \tag{6.5.15}$$

Proceeding as before and using the boundary conditions (6.5.5) and (6.5.10), we have

$$\int_0^{L(t)} \frac{\partial h}{\partial t}(t,x)\,\mathrm{d}x = \frac{1}{2}\frac{dV}{dt} \tag{6.5.16}$$

and

$$\left[h^{\frac{2n+1}{n}}\,(-h_x)^{\frac{1}{n}}\right]_0^{L(t)} = -h(t,0)\bar{v}_x(t,0). \tag{6.5.17}$$

Equation (6.5.15) becomes

$$\frac{dV}{dt} = 2h(t,0)\bar{v}_x(t,0) - 2\int_0^{L(t)} v_l(t,x)\,\mathrm{d}x, \tag{6.5.18}$$

which is the same balance law, (6.5.11), derived using the elementary conserved vector of the first kind.

For the Newtonian fluid-driven fracture, two conserved vectors were derived. The first corresponds to (6.5.3) with $n = 1$ and the second is

$$T^1 = xh, \quad T^2 = -xh^3h_x + \frac{1}{4}h^4 + \int_0^x \chi v_l(t,\chi)\,\mathrm{d}\chi. \tag{6.5.19}$$

A balance law will now be derived for this conserved vector. We substitute (6.5.19) into (6.5.2) and integrate with respect to x from $x = 0$ to $x = L(t)$ to obtain

$$\int_0^{L(t)} \frac{\partial (xh)}{\partial t}\,\mathrm{d}x + \int_0^{L(t)} \frac{\partial}{\partial x}\left(-xh^3h_x + \frac{1}{4}h^4 + \int_0^x \chi v_l(t,\chi)\,\mathrm{d}\chi\right)\mathrm{d}x = 0. \tag{6.5.20}$$

Now, using Leibnitz theorem for differentiation under the integral sign[45] and the boundary condition (6.5.5), we have

$$\int_0^{L(t)} \frac{\partial (xh)}{\partial t}\,\mathrm{d}x = \frac{d}{dt}\int_0^{L(t)} xh(t,x)\,\mathrm{d}x. \tag{6.5.21}$$

Also, using (6.5.8) and the boundary condition (6.5.10) that the fluid flux at the fracture tip is zero, we obtain

$$\int_0^{L(t)} \frac{\partial}{\partial x}\left[-xh^3h_x\right]\,\mathrm{d}x = 0 \tag{6.5.22}$$

and again by the boundary condition (6.5.5), that

$$\int_0^{L(t)} \frac{\partial}{\partial x}h^4(t,x)\,\mathrm{d}x = -h^4(t,0). \tag{6.5.23}$$

Hence (6.5.20) becomes

$$\frac{d}{dt}\int_0^{L(t)} xh\,\mathrm{d}x + \int_0^{L(t)} xv_l\,\mathrm{d}x = \frac{1}{4}h^4(t,0). \tag{6.5.24}$$

The physical significance of this balance law for a Newtonian fluid-driven fracture is not immediately clear.

6.6 Relation between Lie point symmetries and the conservation laws

In this section we investigate the relation between the Lie point symmetries of the partial differential equation (6.1.1) and the conservation laws for the partial differential equation.

We first state a theorem due to Kara and Mahomed [53]. The theorem is quite general but it is stated specifically for the partial differential equation (6.1.1).

Theorem 6.6.1. *If X is a Lie point symmetry of the partial differential equation* (6.1.1) *and* $T = (T^1, T^2)$ *is a conserved vector for* (6.1.1)*, then*

$$T^i_* = X(T^i) + T^i D_k(\xi^k) - T^k D_k(\xi^i), \quad i = 1, 2 \tag{6.6.1}$$

are the components of a conserved vector for (6.1.1)*, that is,*

$$D_1 T^1_* + D_2 T^2_*\Big|_{PDE} = 0. \tag{6.6.2}$$

In (6.6.1)*,* X *is prolongated to as many orders as required when* T *depends on derivatives of* h *and there is summation over the values 1 and 2 of the repeated index* k*.*

Theorem 6.6.1 gives a way of generating new conserved vectors for the partial differential equation (6.1.1) from the Lie point symmetries of (6.1.1) and the conserved vectors already found. The generated conserved vectors may be trivial since T^* may be a linear combination of known conserved vectors or a trivial conserved vector for which the conservation law is identically satisfied or it may be zero.

The Lie point symmetry X of (6.1.1) is said to be *associated* with the conserved vector $T = (T^1, T^2)$ of the partial differential equation (6.1.1) if [52, 53]

$$T^i_* = X(T^i) + T^i D_k(\xi^k) - T^k D_k(\xi^i) = 0, \quad i = 1, 2. \tag{6.6.3}$$

Equation (6.6.3) consists of the two components

$$T^1_* = X(T^1) + T^1 D_2(\xi^2) - T^2 D_2(\xi^1), \tag{6.6.4}$$

$$T^2_* = X(T^2) + T^2 D_1(\xi^1) - T^1 D_1(\xi^2). \tag{6.6.5}$$

We will first investigate using Theorem (6.6.1) if new conserved vectors can be generated from the conserved vectors for the partial differential equation (6.1.1) listed in Table 6.2.1. We will use the linear combination of Lie point symmetries of (6.1.1) derived in Appendix A:

$$X = (c_1 + c_2 t)\frac{\partial}{\partial t} + (c_4 + c_3 x)\frac{\partial}{\partial x} + \left[\left(\frac{n+1}{n+2}\right)c_3 - \frac{n}{(n+2)}c_2\right] h\frac{\partial}{\partial h}, \tag{6.6.6}$$

which exists provided

$$(c_1 + c_2 t)\frac{\partial v_l}{\partial t} + (c_4 + c_3 x)\frac{\partial v_l}{\partial x} = \left(\frac{n+1}{n+2}\right)(c_3 - 2c_2)\, v_l. \tag{6.6.7}$$

Because the conserved vectors in Table 6.2.1 depend on h_x, we will require the first prolongation coefficient ζ_x of the Lie point symmetry (6.6.6) which is

$$\begin{aligned}\zeta_x = \frac{\partial \eta}{\partial x} + \left(\frac{\partial \eta}{\partial h} - \frac{\partial \xi^2}{\partial x}\right)h_x - \frac{\partial \xi^1}{\partial x}h_t - \frac{\partial \xi^2}{\partial h}h_x^2 - \frac{\partial \xi^1}{\partial h}h_t h_x \\ = -\left[\frac{c_3}{(n+2)} + \frac{n}{(n+2)}c_2\right]h_x.\end{aligned} \tag{6.6.8}$$

We will then determine the conditions on the constants c_1, c_2, c_3 and c_4 for the Lie point symmetry (6.6.6) to be associated with the conserved vectors of the partial differential equation (6.1.1).

Consider first the elementary conserved vector of the first kind

$$T^1 = h, \qquad T^2 = h^{\frac{2n+1}{n}}(-h_x)^{\frac{1}{n}} + \int_0^x v_l(t,\chi)\,\mathrm{d}\chi. \tag{6.6.9}$$

It is readily shown that

$$T^1_* = \left[\left(\frac{2n+3}{n+2}\right)c_3 - \frac{n}{(n+2)}c_2\right]T^1. \tag{6.6.10}$$

Also,

$$\begin{aligned}T^2_* = (c_1 + c_2 t)\int_0^x \frac{\partial v_l}{\partial t}(t,\chi)\,\mathrm{d}\chi + (c_4 + c_3 x)v_l(t,x) + c_2\int_0^x v_l(t,\chi)\,\mathrm{d}\chi \\ + \left[\left(\frac{2n+3}{n+2}\right)c_3 - \frac{n}{(n+2)}c_2\right]h^{\frac{2n+1}{n}}(-h_x)^{\frac{1}{n}}.\end{aligned} \tag{6.6.11}$$

But integrating (6.6.7) with respect to χ from $\chi = 0$ to $\chi = x$ gives

$$(c_1 + c_2 t) \int_0^x \frac{\partial v_l}{\partial t}(t, \chi)\, \mathrm{d}\chi + (c_4 + c_3 x)\, v_l(t, x)$$
$$= c_4 v_l(t, 0) + \left[\left(\frac{2n+3}{n+2} \right) c_3 - 2 \left(\frac{n+1}{n+2} \right) c_2 \right] \int_0^x v_l(t, \chi)\, \mathrm{d}\chi. \quad (6.6.12)$$

Substituting (6.6.12) into (6.6.11), we obtain

$$T_*^2 = \left[\left(\frac{2n+3}{n+2} \right) c_3 - \frac{n}{(n+2)} c_2 \right] T^2 + c_4 v_l(t, 0). \quad (6.6.13)$$

We can express (6.6.10) and (6.6.13) in vector form as

$$T_{(1)}^* = \left[\left(\frac{2n+3}{n+2} \right) c_3 - \frac{n}{(n+2)} c_2 \right] T_{(1)} + c_4 P_{(0)}, \quad (6.6.14)$$

where

$$T_{(1)} = \left[h,\ \ h^{\frac{2n+1}{n}} (-h_x)^{\frac{1}{n}} + \int_0^x v_l(t, \chi)\, \mathrm{d}\chi \right], \quad (6.6.15)$$

$$P_{(0)} = [0,\ \ v_l(t, 0)]. \quad (6.6.16)$$

The vector $P_{(0)}$ is a trivial conserved vector because

$$D_1 P_{(0)}^1 + D_2 P_{(0)}^2 \equiv 0. \quad (6.6.17)$$

Thus $T_{(1)}^*$ is not a new conserved vector. The Lie point symmetry associated with the conserved vector $T_{(1)}$ satisfies

$$\frac{c_3}{c_2} = \frac{n}{2n+3}, \quad c_4 = 0. \quad (6.6.18)$$

The Lie point symmetry associated with the elementary conserved vector of the first kind $T_{(1)}$ is therefore

$$X = \left(\frac{c_1}{c_2} + t \right) \frac{\partial}{\partial t} + \frac{n}{(2n+3)} x \frac{\partial}{\partial x} - \frac{n}{(2n+3)} h \frac{\partial}{\partial h}. \quad (6.6.19)$$

From (5.3.27), the Lie point symmetry (6.6.19) generates the solution for a fracture with constant volume. The flux of fluid into the fracture at the entry equals the leak-off flux at the fluid/rock interface.

We will denote the conserved vector of the second kind by S. Consider the elementary conserved vector of the second kind

$$S^1 = h + \int_0^t v_l(\tau, x)\, \mathrm{d}\tau, \qquad S^2 = h^{\frac{2n+1}{n}} (-h_x)^{\frac{1}{n}}. \quad (6.6.20)$$

Now,

$$S_*^1 = (c_1 + c_2 t)\, v_l(t,x) + (c_4 + c_3 x) \int_0^t \frac{\partial v_l}{\partial x}(\tau, x)\, \mathrm{d}\tau + \left[\left(\frac{n+1}{n+2} \right) c_3 - \frac{n}{(n+2)} c_2 \right] h + c_3 \left(h + \int_0^t v_l(\tau, x)\, \mathrm{d}\tau \right). \quad (6.6.21)$$

But integrating (6.6.7) with respect to τ from $\tau = 0$ to $\tau = t$ gives

$$(c_1 + c_2 t)\, v_l(t,x) + (c_4 + c_3 x) \int_0^t \frac{\partial v_l}{\partial x}(\tau, x)\, \mathrm{d}\tau = c_1 v_l(0,x) + \left[\left(\frac{n+1}{n+2} \right) c_3 - \frac{n}{(n+2)} c_2 \right] \int_0^t v_l(\tau, x)\, \mathrm{d}\tau. \quad (6.6.22)$$

Substituting (6.6.22) into (6.6.21) gives

$$S_*^1 = \left[\left(\frac{2n+3}{n+2} \right) c_3 - \frac{n}{(n+2)} c_2 \right] S^1 + c_1 v_l(0,x). \quad (6.6.23)$$

Also it is readily shown that

$$S_*^2 = \left[\left(\frac{2n+3}{n+2} \right) c_3 - \frac{n}{(n+2)} c_2 \right] S^2. \quad (6.6.24)$$

Expressed in vector form, (6.6.23) and (6.6.24) are

$$S_{(1)}^* = \left[\left(\frac{2n+3}{n+2} \right) c_3 - \frac{n}{(n+2)} c_2 \right] S_{(1)} + c_1 Q_{(0)}, \quad (6.6.25)$$

where

$$S_{(1)} = \left[h + \int_0^t v_l(\tau, x)\, \mathrm{d}\tau,\ \ h^{\frac{2n+1}{n}} \left(-h_x \right)^{\frac{1}{n}} \right], \quad (6.6.26)$$

$$Q_{(0)} = \left[v_l(0,x),\ \ 0 \right]. \quad (6.6.27)$$

The vector $Q_{(0)}$ is a trivial conserved vector. The vector $S_{(1)}^*$ is not a new conserved vector. The Lie point symmetry which is associated with $S_{(1)}$ satisfies

$$\frac{c_3}{c_2} = \frac{n}{2n+3}, \quad c_1 = 0. \quad (6.6.28)$$

The Lie point symmetry associated with the elementary conserved vector of the second kind $S_{(1)}$ is therefore

$$X = t \frac{\partial}{\partial t} + \left(\frac{c_4}{c_2} + \frac{n}{(2n+3)} x \right) \frac{\partial}{\partial x} - \frac{n}{(2n+3)} h \frac{\partial}{\partial h} \quad (6.6.29)$$

From (5.3.27) the volume of the fracture generated by (6.6.29) remains constant. The elementary conserved vectors of the first and second kind are both associated with Lie point symmetries which generate the solution for a fracture with constant volume.

Consider now the special case $n = 1$ for which second conserved vectors of the first and second kind exist. Consider the conserved vector of the first kind

$$T^1 = xh, \qquad T^2 = -xh^3 h_x + \frac{h^4}{4} + \int_0^x \chi v_l(t,\chi)\,\mathrm{d}\chi \tag{6.6.30}$$

It is readily shown that

$$T^1_* = c_4 h + \frac{1}{3}\left(8c_3 - c_2\right) T^1 \tag{6.6.31}$$

and that

$$\begin{aligned} T^2_* = (c_1 + c_2 t)\int_0^x \chi \frac{\partial v_l}{\partial t}(t,\chi)\,\mathrm{d}\chi + (c_4 + c_3 x)\, x v_l(t,x) + c_4\left(-h^3 h_x\right) \\ + \frac{1}{3}(8c_3 - c_2)\left(-xh^3 h_x\right) + \frac{1}{3}(8c_3 - c_2)\frac{h^4}{4} + c_2\int_0^x \chi v_l(t,\chi)\,\mathrm{d}\chi. \end{aligned} \tag{6.6.32}$$

Now, multiplying (6.6.7) by χ and integrating with respect to χ from $\chi = 0$ to $\chi = x$ gives

$$\begin{aligned} (c_1 + c_2 t)\int_0^x \chi \frac{\partial v_l}{\partial t}(t,\chi)\,\mathrm{d}\chi + (c_4 + c_3 x)\, x v_l(t,x) \\ = c_4\int_0^x v_l(t,\chi)\,\mathrm{d}\chi + \frac{1}{3}(8c_3 - 4c_2)\int_0^x \chi v_l(t,\chi)\,\mathrm{d}\chi. \end{aligned} \tag{6.6.33}$$

Substituting (6.6.33) into (6.6.32) we obtain

$$T^2_* = c_4\left[-h^3 h_x + \int_0^x v_l(t,\chi)\,\mathrm{d}\chi\right] + \frac{1}{3}(8c_3 - c_2)\left[-xh^3 h_x + \frac{h^4}{4} + \int_0^x \chi v_l(t,\chi)\,\mathrm{d}\chi\right]. \tag{6.6.34}$$

Equations (6.6.31) and (6.6.34) when expressed in vector form are

$$T^*_{(2)} = c_4 T_{(1)} + \frac{1}{3}(8c_3 - c_2) T_{(2)} \tag{6.6.35}$$

where $T_{(1)}$ is given by (6.6.15) with $n = 1$ and

$$T_{(2)} = \left[xh,\ -xh^3 h_x + \frac{h^4}{4} + \int_0^x \chi v_l(t,\chi)\,\mathrm{d}\chi\right]. \tag{6.6.36}$$

Thus $T^*_{(2)}$ is a linear combination of the conserved vectors of the first kind, $T_{(1)}$ and $T_{(2)}$, and is therefore not a new conserved vector. The Lie point symmetry associated with $T_{(2)}$ satisfies

$$c_4 = 0, \quad \frac{c_3}{c_2} = \frac{1}{8} \tag{6.6.37}$$

and is

$$X = \left(\frac{c_1}{c_2} + t\right)\frac{\partial}{\partial t} + \frac{1}{8}x\frac{\partial}{\partial x} - \frac{1}{4}h\frac{\partial}{\partial h}. \tag{6.6.38}$$

When $n = 1$, it follows from (5.3.27) that the Lie point symmetry which generates the solution for a fracture with constant volume satisfies $c_3/c_2 = 1/5$. When $c_3/c_2 = 1/8$ the total volume of the fracture per unit width, $V(t)$, decreases with time and this value of c_3/c_2 could describe a fracture with fluid extraction at the fracture entry and/or leak-off at the fluid-rock interface. When there is no leak-off, $c_3/c_2 = 1/8$ is the limiting value for a solution with fluid extraction at the fracture entry to exist [15]. The conserved vector $T_{(2)}$ may be related to the limiting solution for existence.

Finally, consider the second conserved vector of the second kind when $n = 1$,

$$S^1 = xh + x\int_0^t v_l(\tau, x)\,\mathrm{d}\tau, \quad S^2 = -xh^3h_x + \frac{h^4}{4}. \tag{6.6.39}$$

Now,

$$S^1_* = (c_1 + c_2t)xv_l(t,x) + (c_4 + c_3x)x\int_0^t \frac{\partial v_l}{\partial x}(\tau, x)\,\mathrm{d}\tau + c_4\left(h + \int_0^t v_l(\tau, x)\,\mathrm{d}\tau\right) + \frac{1}{3}\left(8c_3 - c_2\right)xh + 2c_3x\int_0^t v_l(\tau, x)\,\mathrm{d}\tau. \tag{6.6.40}$$

But by multiplying (6.6.7) by x, integrating with respect to τ from $\tau = 0$ to $\tau = t$ and also integrating by parts we obtain

$$(c_1 + c_2t)xv_l(t,x) + (c_4 + c_3x)x\int_0^t \frac{\partial v_l}{\partial x}(\tau, x)\,\mathrm{d}\tau = c_1xv_l(0,x) + \frac{1}{3}\left(2c_3 - c_2\right)x\int_0^t v_l(\tau, x)\,\mathrm{d}\tau. \tag{6.6.41}$$

Substituting (6.6.41) into (6.6.40) gives

$$S^1_* = c_1xv_l(0,x) + c_4\left[h + \int_0^t v_l(\tau, x)\,\mathrm{d}\tau\right] + \frac{1}{3}\left(8c_3 - c_2\right)\left[xh + x\int_0^t v_l(\tau, x)\,\mathrm{d}\tau\right]. \tag{6.6.42}$$

Also it is readily shown that

$$S^2_* = c_4\left[-h^3h_x\right] + \frac{1}{3}\left(8c_3 - c_2\right)\left[\frac{h^4}{4} - xh^3h_x\right]. \tag{6.6.43}$$

Equations (6.6.42) and (6.6.43) can be expressed in vector form as

$$S^*_{(2)} = c_4S_{(1)} + \frac{1}{3}\left(8c_3 - c_2\right)S_{(2)} + c_1R_{(0)}, \tag{6.6.44}$$

where $S_{(1)}$ is given by (6.6.26) with $n = 1$ and

$$S_{(2)} = \left[xh + x\int_0^t v_l(\tau, x)\,\mathrm{d}\tau,\ -xh^3 h_x + \frac{h^4}{4} \right], \tag{6.6.45}$$

$$R_{(0)} = \left[xv_l(0, x),\ 0 \right]. \tag{6.6.46}$$

The vector $R_{(0)}$ is a trivial conserved vector. We see that $S^*_{(2)}$ is not a new conserved vector because it is a linear combination of the two conserved vectors of the second kind, $S_{(1)}$ and $S_{(2)}$, and the trivial conserved vector $R_{(0)}$. The Lie point symmetry associated with $S_{(2)}$ satisfies

$$c_4 = 0, \quad \frac{c_3}{c_2} = \frac{1}{8}, \quad c_1 = 0 \tag{6.6.47}$$

and is

$$X = t\frac{\partial}{\partial t} + \frac{1}{8}x\frac{\partial}{\partial x} - \frac{1}{4}h\frac{\partial}{\partial h}. \tag{6.6.48}$$

The second conserved vectors of the first and second kind when $n = 1$ are associated with the Lie point symmetry with $c_3/c_2 = 1/8$.

The results are summarised in Table 6.6.1. When there is no leak-off the conserved vector for a Newtonian fluid with $n = 1$ was derived by Anthonyrajah [54].

Table 6.6.1: Generation of conserved vectors from known conserved vectors

$n > 0$	$T^*_{(1)} = \left[\left(\frac{2n+3}{n+2}\right) c_3 - \frac{n}{(n+2)} c_2 \right] T_{(1)} + c_4 P_{(0)}$
$n > 0$	$S^*_{(1)} = \left[\left(\frac{2n+3}{n+2}\right) c_3 - \frac{n}{(n+2)} c_2 \right] S_{(1)} + c_1 Q_{(0)}$
$n = 1$	$T^*_{(2)} = \frac{1}{3}\left[8c_3 - c_2\right] T_{(2)} + c_4 T_{(1)}$
$n = 1$	$S^*_{(2)} = \frac{1}{3}\left[8c_3 - c_2\right] S_{(2)} + c_4 S_{(1)} + c_1 R_{(0)}$
	Notation: Conserved vectors
$n > 0$	$T_{(1)} = \left[h,\ h^{\frac{2n+1}{n}} \left(-h_x\right)^{\frac{1}{n}} + \int_0^x v_l(t, \chi)\,\mathrm{d}\chi \right]$

$n > 0$	$S_{(1)} = \left[h + \int_0^t v_l(\tau, x)\,\mathrm{d}\tau,\ h^{\frac{2n+1}{n}}\left(-h_x\right)^{\frac{1}{n}}\right]$
$n = 1$	$T_{(2)} = \left[xh, -xh^3h_x + \frac{h^4}{4} + \int_0^x \chi v_l(t, \chi)\,\mathrm{d}\chi\right]$
$n = 1$	$S_{(2)} = \left[xh + x\int_0^t v_l(\tau, x)\,\mathrm{d}\tau,\ -xh^3h_x + \frac{h^4}{4}\right]$
	Notation: Trivial conserved vectors
	$P_{(0)} = [0, v_l(t, 0)],\quad Q_{(0)} = [v_l(0, x), 0],\quad R_{(0)} = [xv_l(0, x), 0].$

6.7 Conclusions

A new feature of conservation laws for a hydraulic fracture with leak-off is the existence of conservation laws of two kinds. This occurs in the elementary conservation law and also in the second conservation law when $n = 1$. In the conserved vector of the first kind, the component containing the leak-off velocity is the flux component while in the conserved vector of the second kind, it is the density component.

The conservation laws of the first and second kind are closely related. If trivial conserved vectors are not included they are associated with the same Lie point symmetry. The elementary conservation laws of the first and second kind lead to the same balance law for fluid volume.

We were not able to generate new conserved vectors from known conserved vectors. For the elementary conserved vectors of the first and second kind, the calculation gave a linear combination of the known elementary conserved vector and a trivial conserved vector while for the second conserved vector when $n = 1$, it gave a linear combination of the elementary conserved vector and the second conserved vector.

The conservation laws corresponding to the elementary conserved vector of the first and

second kind gave an alternative method for deriving the balance law for fluid volume. Insight into the physical significance of the conservation laws was obtained by determining the Lie point symmetry associated with the corresponding conserved vector. The Lie point symmetry associated with the elementary conserved vectors of the first and second kind generate the solution for a fluid fracture with constant volume. The Lie point symmetry associated with the second conserved vector when $n = 1$ describes a fracture that evolves with decreasing total volume and may be related to the limit of existence of solution for the extraction of a Newtonian fluid from the fracture.

Chapter 7

Conclusions

The aim of this thesis was to study the propagation of a two-dimensional PKN fracture model which evolves as a result of the injection, under high pressure, of a non-Newtonian fracturing fluid of power-law rheology into the fracture.

The two main assumptions made in the modelling were the PKN approximation and the lubrication approximation. The PKN approximation, that the fluid pressure is linearly related to the half-width of the fracture, closed the system of equations and determined the characteristic fluid velocity along the fracture. It may be applicable in an outer region away from the fracture tip [46]. It is the simplest assumption that could be made but the results obtained may suggest investigations to make with more robust elasticity models. The lubrication approximation lead to the simplification of the momentum balance equation describing fluid flow in the fracture. It also demonstrated the importance of formulating the theory in terms of the fluid velocity averaged across the fracture. The mathematical model resulted in a nonlinear diffusion equation which showed that nonlinear diffusion is the physical mechanism for the growth of the hydraulic fracture.

Pre-existing fractures play a key role in the success of hydraulic fracturing as a means of fracturing rock in the mining and petroleum industries. We have shown in this work that invariant solutions can be derived for a power-law fluid-driven pre-existing fracture in both permeable and impermeable rock by the adoption of the PKN elasticity hypothesis, lubrication theory and by using the Lie point symmetries of the resulting nonlinear diffusion equation. It was found that the Lie point symmetries which generate the solutions are not s-

caling symmetries and this is because the initial length of the fracture was non-zero. Methods used to derive similarity solutions for hydraulic fractures evolving from a point source, such as the scaling transformations described by Dresner [50] cannot be used for a fracture with initial non-zero length. The leak-off velocity was not prescribed a priori in the mathematical model. It was determined by insisting that the nonlinear diffusion equation admits Lie point symmetries. The Lie symmetry analysis transformed the nonlinear diffusion equation to a second order differential equation which admits one symmetry generator, which is insufficient to completely integrate the second order differential equation in general. When there is leak-off the boundary value problem obtained is expressed in terms of two dependent variables F and G which describe the half-width and leak-off velocity, respectively. In order to close the system of equations some assumption has to be made concerning $G(u)$. We have assumed that $G(u) = \beta F(u)$. By the PKN approximation the half-width is proportional to the fluid pressure and the assumption $G(u) = \beta F(u)$ therefore implies that the leak-off velocity is proportional to the fluid pressure. This is a physically reasonable assumption. Other relations can be specified, for example, $G \propto \frac{dF}{du}$, which also leads to exact analytical solutions for special cases. The proportionality constant plays a key role in understanding flow conditions at the fluid-rock interface.

For a hydraulic fracture in both impermeable and permeable rock we were able to derive two exact analytical solutions. The case when there is leak-off helped to clarify their physical significance. The first analytical solution describes the evolution of a hydraulic fracture with no fluid injection at the fracture entry. When there is no leak-off the total volume of the fracture remains constant but it does not remain constant when there is leak-off. The characteristic property of the solution is therefore not conservation of volume of the fracture but no fluid input at the fracture entry. The second analytical solution describes the evolution of a hydraulic fracture in which the average fluid velocity is constant along the fracture and therefore equal to the velocity of propagation of the fracture tip. When there is no leak-off the velocity of propagation of the fracture is constant but this is not the case when there is leak-off and it is therefore not the characteristic property of the fracture.

It was found that in the numerical solution the reformulation of the boundary value problem as a pair of initial value problems was easier to solve than the original boundary value

problem. The analytical asymptotic solution at the fracture tip played an important part in imposing the boundary condition at the fracture tip. Comparison with the analytical solutions showed that the numerical results were valid for a large range of values of n and β covering shear thinning, Newtonian and shear thickening fluids. Comparison of the approximate analytical solutions with the numerical solution in turn showed that the approximate analytical solutions were a good approximation.

Comparatively few results have been reported in the literature on the velocity of the fluid in a hydraulic fracture. We investigated the streamlines of the fluid flow in the fracture. The patterns of flow in the fracture were as expected, but the result for a fracture with no leak-off that the fluid velocity at the fracture tip exceeds the tip velocity was unexpected. The difficulty was resolved by considering the mean fluid velocity averaged over the width of the fracture. For a fracture with no leak-off this averaged fluid velocity at the fracture tip equalled the velocity of the tip as required by the physics. When there is fluid leak-off we found that the average fluid velocity at the tip also equals to the velocity of the tip. It can be concluded that in a thin fracture the mean velocity is more physically significant than the actual velocity and is the velocity to work with. For the two analytical solutions the averaged velocity varied linearly along the fracture. It was a surprise that it varied approximately linearly for the numerical solutions for the other working conditions. When there is fluid input at the fracture entry and there is no leak-off, the average fluid velocity increased along the fracture to the velocity of the tip because the cross-sectional area of the fracture decreased along the fracture. When there is leak-off the average fluid velocity decreased along the fracture to the tip velocity due to the fluid leak-off along the fracture.

The approximate analytical solutions were derived by considering the ratio of the average fluid velocity to the speed of propagation of the fracture tip along the fracture. They were based on the observation that this ratio varies approximately linearly along the length of the fracture. This applies for a hydraulic fracture in both impermeable and permeable rock and leads to an approximate first order differential equation for the half-width function $F(u)$. The approximate analytical solutions compared well with the numerical solutions even for a shear thinning fluid with small values of n close to zero. It may be a useful analytical approximation especially for a shear thinning fluid which can sometimes introduce numerical difficulties.

A new feature of the conservation laws for the nonlinear diffusion equation of a hydraulic fracture with leak-off is the existence of conservation laws of the first and second kind depending in which component of the conserved vector the leak-off term is included. However, the conservation laws of the first and second kind are related in the sense that they are associated with the same Lie point symmetry if trivial conserved vectors are not included. The elementary conserved vectors of the first and second kind generated the same balance law for fluid volume. The second conservation law which was found for a Newtonian fluid fracture did not exist for a non-Newtonian fluid fracture. Anthonyrajah [54] found, when considering a turbulent fluid fracture, that the second conservation law for the laminar Newtonian fracture did not exist for a turbulent fluid fracture. We investigated the possibility of obtaining new conserved vectors from the known conserved vectors and found that no new conserved vectors can be obtained from the known conserved vectors.

The fluid leak-off did not remove the singularity at the fracture tip. The lubrication approximation breaks down in the region close to the fracture tip. A difference between a hydraulic fracture with leak-off and one with no leak-off is that when there is leak-off the fluid velocity averaged across the fracture decreases along the fracture to the tip velocity while for no leak-off the averaged fluid velocity increases to the tip velocity along the fracture. For both leak-off and no leak-off the averaged fluid velocity along the fracture is approximately linear. We have also seen that leak-off helped to determined the defining physical characteristic of the exact analytical solutions.

We found that the behaviour of the solutions for shear thinning, Newtonian and shear thickening fluids were qualitatively very similar. The ordering of the curves in the figures in general did not depend on whether $0 < n < 1$, $n = 1$ or $n > 1$. There were quantitative differences in the solution for shear thinning, Newtonian and shear thickening fluids. The characteristic time depends on n and on the properties of the fluid as well as on the properties of the surrounding rock mass. To investigate the quantitative differences the values of the parameters would have to be given.

The study gave an insight into understanding how fractures evolve under varying operating conditions of interest, when driven by the injection, under high pressure, of a power-law fluid. In our study, we have considered the PKN elasticity theory and only fluid injection into the

fracture at the entry which is the most important case in hydraulic fracturing. What we would like to consider in the future is a more physically realistic elasticity model such as the Cauchy principal value expression for the stress, fluid extraction at the fracture entry and other non-Newtonian constitutive models for fracturing fluids.

APPENDIX A

Derivation of the Lie point symmetries of the nonlinear diffusion equation for fluid-driven fracture in permeable rock

In this section we will show in full the derivation of the Lie point symmetries of the nonlinear diffusion equation

$$\frac{\partial h}{\partial t} + \frac{\partial}{\partial x}\left(h^{\frac{2n+1}{n}}\left(-\frac{\partial h}{\partial x}\right)^{\frac{1}{n}}\right) + v_l(x,t) = 0. \tag{A.1}$$

The nonlinear diffusion equation (A.1) describes the evolution of the fracture half-width during hydraulic fracturing by a non-Newtonian fluid in permeable rock. Since the rock is permeable, fluid leaks off into the surrounding rock formation. The leak-off velocity relative to the fluid/rock interface is $v_l(t,x)$.

Equation (A.1) is rewritten as

$$F(t,x,h,h_t,h_x,h_{xx}) = 0, \tag{A.2}$$

where

$$F = h_t - \frac{1}{n}h^{\frac{2n+1}{n}}(-h_x)^{\frac{1-n}{n}}h_{xx} - \frac{(2n+1)}{n}h^{\frac{n+1}{n}}(-h_x)^{\frac{n+1}{n}} + v_l. \tag{A.3}$$

The Lie point symmetry generator

$$X = \xi^1(t,x,h)\frac{\partial}{\partial t} + \xi^2(t,x,h)\frac{\partial}{\partial x} + \eta(t,x,h)\frac{\partial}{\partial h} \tag{A.4}$$

of equation (A.1) is derived by solving the determining equation

$$X^{[2]}F\Big|_{F=0} = 0 \tag{A.5}$$

for the unknown functions $\xi^1(t,x,h)$, $\xi^2(t,x,h)$ and $\eta(t,x,h)$, where $X^{[2]}$, the second prolongation of X, is given by

$$X^{[2]} = X + \zeta_1 \frac{\partial}{\partial h_t} + \zeta_2 \frac{\partial}{\partial h_x} + \zeta_{11} \frac{\partial}{\partial h_{tt}} + \zeta_{12} \frac{\partial}{\partial h_{tx}} + \zeta_{22} \frac{\partial}{\partial h_{xx}} \tag{A.6}$$

and ζ_i and ζ_{ij} are defined by

$$\zeta_i = D_i(\eta) - h_k D_i(\xi^k), \qquad i = 1,2, \tag{A.7}$$

$$\zeta_{ij} = D_j(\zeta_i) - h_{ik} D_j(\xi^k), \qquad i,j = 1,2, \tag{A.8}$$

with summation over the repeated index k from 1 to 2. The total derivatives with respect to the independent variables t and x are given by

$$D_1 = D_t = \frac{\partial}{\partial t} + h_t \frac{\partial}{\partial h} + h_{tt} \frac{\partial}{\partial h_t} + h_{xt} \frac{\partial}{\partial h_x} + \ldots \,, \tag{A.9}$$

$$D_2 = D_x = \frac{\partial}{\partial x} + h_x \frac{\partial}{\partial h} + h_{tx} \frac{\partial}{\partial h_t} + h_{xx} \frac{\partial}{\partial h_x} + \ldots . \tag{A.10}$$

The leak-off velocity $v_l(x,t)$ is to be treated as an arbitrary function of the independent variables t and x.

The determining equation (A.5) yields

$$\begin{aligned} &\xi^1 \frac{\partial v_l}{\partial t} + \xi^2 \frac{\partial v_l}{\partial x} + \eta \left(-\frac{(2n+1)}{n^2} (-h_x)^{\frac{1-n}{n}} h_{xx} h^{\frac{n+1}{n}} - \frac{(2n+1)(n+1)}{n^2} (-h_x)^{\frac{n+1}{n}} h^{\frac{1}{n}} \right) \\ &+ \zeta_1 + \zeta_2 \left(\frac{(1-n)}{n^2} h^{\frac{2n+1}{n}} h_{xx} (-h_x)^{\frac{1-2n}{n}} + \frac{(2n+1)(n+1)}{n^2} h^{\frac{n+1}{n}} (-h_x)^{\frac{1}{n}} \right) \\ &+ \zeta_{22} \left(-\frac{1}{n} h^{\frac{2n+1}{n}} (-h_x)^{\frac{1-n}{n}} \right) \Bigg|_{F=0} = 0. \end{aligned} \tag{A.11}$$

We now calculate the expressions for ζ_1, ζ_2, and ζ_{22} according to equations (A.7) and (A.8):

$$\zeta_1 = D_t(\eta) - h_t D_t(\xi^1) - h_x D_t(\xi^2), \tag{A.12}$$

$$\zeta_2 = D_x(\eta) - h_t D_x(\xi^1) - h_x D_x(\xi^2), \tag{A.13}$$

$$\zeta_{22} = D_x(\zeta_2) - h_{xt} D_x(\xi^1) - h_{xx} D_x(\xi^2). \tag{A.14}$$

Expanding equations (A.12), (A.13) and (A.14) using (A.9) and (A.10), we obtain

$$\zeta_1 = \eta_t + h_t\eta_h - h_t\left(\xi_t^1 + h_t\xi_h^1\right) - h_x\left(\xi_t^2 + h_t\xi_h^2\right), \tag{A.15}$$

$$\zeta_2 = \eta_x + h_x\eta_h - h_t\left(\xi_x^1 + h_x\xi_h^1\right) - h_x\left(\xi_x^2 + h_x\xi_h^2\right), \tag{A.16}$$

$$\begin{aligned}\zeta_{22} = {} & \eta_{xx} + 2h_x\eta_{xh} + h_x^2\eta_{hh} + h_{xx}\eta_h - h_t\xi_{xx}^1 - 2h_xh_t\xi_{xh}^1 - h_th_x^2\xi_{hh}^1 - h_th_{xx}\xi_h^1 \\ & -2h_{xt}\xi_x^1 - 2h_xh_{xt}\xi_h^1 - 2h_{xx}\xi_x^2 - 3h_xh_{xx}\xi_h^2 - h_x\xi_{xx}^2 - 2h_x^2\xi_{xh}^2 - h_x^3\xi_{hh}^2.\end{aligned} \tag{A.17}$$

The expressions for ζ_1, ζ_2 and ζ_{22} are substituted into the determining equation (A.11) to obtain

$$\begin{aligned}& \xi^1\frac{\partial v_l}{\partial t} + \xi^2\frac{\partial v_l}{\partial x} + \eta\left(-\frac{(2n+1)}{n^2}(-h_x)^{\frac{1-n}{n}}h_{xx}h^{\frac{n+1}{n}} - \frac{(2n+1)(n+1)}{n^2}(-h_x)^{\frac{n+1}{n}}h^{\frac{1}{n}}\right) \\ & +\eta_t + h_t\eta_h - h_t\left(\xi_t^1 + h_t\xi_h^1\right) - h_x\left(\xi_t^2 + h_t\xi_h^2\right) + \big(\eta_x + h_x\eta_h - h_x\xi_x^2 - h_x^2\xi_h^2 \\ & -h_t\xi_x^1 - h_xh_t\xi_h^1\big)\left(\frac{(1-n)}{n^2}h^{\frac{2n+1}{n}}(-h_x)^{\frac{1-2n}{n}}h_{xx} + \frac{(2n+1)(n+1)}{n^2}h^{\frac{n+1}{n}}(-h_x)^{\frac{1}{n}}\right) \\ & + \big(\eta_{xx} + 2h_x\eta_{xh} + h_x^2\eta_{hh} + h_{xx}\eta_h - h_t\xi_{xx}^1 - 2h_xh_t\xi_{xh}^1 - h_th_x^2\xi_{hh}^1 \\ & -h_th_{xx}\xi_h^1 - 2h_{xt}\xi_x^1 - 2h_xh_{xt}\xi_h^1 - 2h_{xx}\xi_x^2 - 3h_xh_{xx}\xi_h^2 - h_x\xi_{xx}^2 - 2h_x^2\xi_{xh}^2 \\ & -h_x^3\xi_{hh}^2\big)\left(-\frac{1}{n}h^{\frac{2n+1}{n}}(-h_x)^{\frac{1-n}{n}}\right)\Bigg|_{h_t=\frac{1}{n}h^{\frac{2n+1}{n}}(-h_x)^{\frac{1-n}{n}}h_{xx}+\frac{2n+1}{n}h^{\frac{n+1}{n}}(-h_x)^{\frac{n+1}{n}}-v_l} = 0.\end{aligned} \tag{A.18}$$

We now expand equation (A.18), replacing h_t by its expression in (A.1). This gives the deter-

mining equation for the unknown functions $\xi^1(t,x,h)$, $\xi^2(t,x,h)$ and $\eta(t,x,h)$:

$$
\begin{aligned}
&\xi^1\frac{\partial v_l}{\partial t}+\xi^2\frac{\partial v_l}{\partial x}-\frac{(2n+1)}{n^2}(-h_x)^{\frac{1-n}{n}}h_{xx}h^{\frac{n+1}{n}}\eta-\frac{(2n+1)(n+1)}{n^2}(-h_x)^{\frac{n+1}{n}}h^{\frac{1}{n}}\eta\\
&+\eta_t+\frac{1}{n}h^{\frac{2n+1}{n}}(-h_x)^{\frac{1-n}{n}}h_{xx}\eta_h+\frac{(2n+1)}{n}h^{\frac{n+1}{n}}(-h_x)^{\frac{n+1}{n}}\eta_h-v_l\eta_h+(-h_x)\xi_t^2\\
&+\frac{1}{n}h^{\frac{2n+1}{n}}(-h_x)^{\frac{1}{n}}h_{xx}\xi_h^2+\frac{(2n+1)}{n}h^{\frac{n+1}{n}}(-h_x)^{\frac{2n+1}{n}}\xi_h^2-(-h_x)v_l\xi_h^2-\frac{1}{n}h^{\frac{2n+1}{n}}(-h_x)^{\frac{1-n}{n}}h_{xx}\xi_t^1\\
&-\frac{(2n+1)}{n}h^{\frac{n+1}{n}}(-h_x)^{\frac{n+1}{n}}\xi_t^1+v_l\xi_t^1-\frac{1}{n^2}h^{\frac{4n+2}{n}}(-h_x)^{\frac{2-2n}{n}}h_{xx}^2\xi_h^1-\frac{(4n+2)}{n^2}h^{\frac{3n+2}{n}}(-h_x)^{\frac{2}{n}}h_{xx}\xi_h^1\\
&+\frac{2}{n}h^{\frac{2n+1}{n}}(-h_x)^{\frac{1-n}{n}}h_{xx}v_l\xi_h^1-\frac{(2n+1)^2}{n^2}h^{\frac{2n+2}{n}}(-h_x)^{\frac{2n+2}{n}}\xi_h^1+\frac{(4n+2)}{n}h^{\frac{n+1}{n}}(-h_x)^{\frac{n+1}{n}}v_l\xi_h^1-v_l^2\xi_h^1\\
&+\frac{(1-n)}{n^2}h^{\frac{2n+1}{n}}(-h_x)^{\frac{1-2n}{n}}h_{xx}\eta_x+\frac{(2n+1)(n+1)}{n^2}h^{\frac{n+1}{n}}(-h_x)^{\frac{1}{n}}\eta_x-\frac{(1-n)}{n^2}h^{\frac{2n+1}{n}}(-h_x)^{\frac{1-n}{n}}h_{xx}\eta_h\\
&-\frac{(2n+1)(n+1)}{n^2}h^{\frac{n+1}{n}}(-h_x)^{\frac{n+1}{n}}\eta_h+\frac{(1-n)}{n^2}h^{\frac{2n+1}{n}}(-h_x)^{\frac{1-n}{n}}h_{xx}\xi_x^2+\frac{(2n+1)(n+1)}{n^2}h^{\frac{n+1}{n}}\\
&\times(-h_x)^{\frac{n+1}{n}}\xi_x^2-\frac{(1-n)}{n^2}h^{\frac{2n+1}{n}}(-h_x)^{\frac{1}{n}}h_{xx}\xi_h^2-\frac{(2n+1)(n+1)}{n^2}h^{\frac{n+1}{n}}(-h_x)^{\frac{1+2n}{n}}\xi_h^2\\
&-\frac{(1-n)}{n^3}h^{\frac{4n+2}{n}}(-h_x)^{\frac{2-3n}{n}}h_{xx}^2\xi_x^1-\frac{(2n+1)(1-n)}{n^3}h^{\frac{3n+2}{n}}(-h_x)^{\frac{2-n}{n}}h_{xx}\xi_x^1+\frac{1-n}{n^2}h^{\frac{2n+1}{n}}\\
&\times(-h_x)^{\frac{1-2n}{n}}h_{xx}v_l\xi_x^1-\frac{(2n+1)(n+1)}{n^3}h^{\frac{3n+2}{n}}(-h_x)^{\frac{2-n}{n}}h_{xx}\xi_x^1-\frac{(2n+1)^2(n+1)}{n^3}h^{\frac{2n+2}{n}}(-h_x)^{\frac{n+2}{n}}\xi_x^1\\
&+\frac{(2n+1)(n+1)}{n^2}h^{\frac{n+1}{n}}(-h_x)^{\frac{1}{n}}\xi_x^1v_l+\frac{1-n}{n^3}h^{\frac{4n+2}{n}}(-h_x)^{\frac{2-2n}{n}}h_{xx}^2\xi_h^1+\frac{(2n+1)(1-n)}{n^3}h^{\frac{3n+2}{n}}\\
&\times(-h_x)^{\frac{2}{n}}h_{xx}\xi_h^1-\frac{1-n}{n^2}h^{\frac{2n+1}{n}}(-h_x)^{\frac{1-n}{n}}h_{xx}\xi_h^1v_l+\frac{(2n+1)(n+1)}{n^3}h^{\frac{3n+2}{n}}(-h_x)^{\frac{2}{n}}h_{xx}\xi_h^1\\
&+\frac{(2n+1)^2(n+1)}{n^3}h^{\frac{2n+2}{n}}(-h_x)^{\frac{2n+2}{n}}\xi_h^1-\frac{(2n+1)(n+1)}{n^2}h^{\frac{n+1}{n}}(-h_x)^{\frac{n+1}{n}}\xi_h^1v_l\\
&-\frac{1}{n}h^{\frac{2n+1}{n}}(-h_x)^{\frac{1-n}{n}}\eta_{xx}+\frac{2}{n}h^{\frac{2n+1}{n}}(-h_x)^{\frac{1}{n}}\eta_{xh}-\frac{1}{n}h^{\frac{2n+1}{n}}(-h_x)^{\frac{1-n}{n}}h_{xx}\eta_h-\frac{1}{n}h^{\frac{2n+1}{n}}(-h_x)^{\frac{1+n}{n}}\eta_{hh}\\
&-\frac{1}{n}h^{\frac{2n+1}{n}}(-h_x)^{\frac{1}{n}}\xi_{xx}^2+\frac{2}{n}h^{\frac{2n+1}{n}}(-h_x)^{\frac{n+1}{n}}\xi_{xh}^2-\frac{3}{n}h^{\frac{2n+1}{n}}(-h_x)^{\frac{1}{n}}h_{xx}\xi_h^2-\frac{1}{n}h^{\frac{2n+1}{n}}(-h_x)^{\frac{2n+1}{n}}\xi_{hh}^2\\
&+\frac{2}{n}h^{\frac{2n+1}{n}}(-h_x)^{\frac{1-n}{n}}h_{xx}\xi_x^2+\frac{1}{n^2}h^{\frac{4n+2}{n}}(-h_x)^{\frac{2-2n}{n}}h_{xx}\xi_{xx}^1+\frac{2n+1}{n^2}h^{\frac{3n+2}{n}}(-h_x)^{\frac{2}{n}}\xi_{xx}^1\\
&-\frac{1}{n}h^{\frac{2n+1}{n}}(-h_x)^{\frac{1-n}{n}}\xi_{xx}^1v_l-\frac{2}{n^2}h^{\frac{4n+2}{n}}(-h_x)^{\frac{2-n}{n}}h_{xx}\xi_{xh}^1-\frac{4n+2}{n^2}h^{\frac{3n+2}{n}}(-h_x)^{\frac{n+2}{n}}\xi_{xh}^1\\
&+\frac{2}{n}h^{\frac{2n+1}{n}}(-h_x)^{\frac{1}{n}}\xi_{xh}^1v_l+\frac{1}{n^2}h^{\frac{4n+2}{n}}(-h_x)^{\frac{2-2n}{n}}h_{xx}^2\xi_h^1+\frac{2n+1}{n^2}h^{\frac{3n+2}{n}}(-h_x)^{\frac{2}{n}}h_{xx}\xi_h^1\\
&-\frac{1}{n}h^{\frac{2n+1}{n}}(-h_x)^{\frac{1-n}{n}}h_{xx}\xi_h^1v_l+\frac{1}{n^2}h^{\frac{4n+2}{n}}(-h_x)^{\frac{2}{n}}h_{xx}\xi_{hh}^1+\frac{2n+1}{n^2}h^{\frac{3n+2}{n}}(-h_x)^{\frac{2n+2}{n}}\xi_{hh}^1\\
&-\frac{1}{n}h^{\frac{2n+1}{n}}(-h_x)^{\frac{n+1}{n}}\xi_{hh}^1v_l+\frac{2}{n}h^{\frac{2n+1}{n}}(-h_x)^{\frac{1-n}{n}}h_{xt}\xi_x^1-\frac{2}{n}h^{\frac{2n+1}{n}}(-h_x)^{\frac{1}{n}}h_{xt}\xi_h^1=0.
\end{aligned}
\tag{A.19}
$$

Since the functions to be determined do not depend on the derivatives of h, equation (A.19) is separated according to powers and products of the partial derivatives of h. One then equates the sum of the coefficients of the partial derivatives of h to zero. In this manner, (A.19)

decomposes into an overdetermined system of equations in which there are more equations than unknown variables. The case $n = 1$ is a special case because when $n = 1$, the pairs of derivatives

$$-h_x \text{ and } (-h_x)^{\frac{1}{n}}, \quad 1 \text{ and } (-h_x)^{\frac{1-n}{n}}, \quad (-h_x)^{\frac{2}{n}} \text{ and } (-h_x)^{\frac{n+1}{n}}, \quad (-h_x)^{\frac{2-n}{n}} h_{xx} \text{ and } (-h_x)^{\frac{1}{n}} h_{xx}$$

have the same powers and must be treated together. The Lie point symmetry and the condition on $v_l(t, x)$ for $n = 1$ were derived by Fareo and Mason [15]. Here we will therefore consider only the general case $n \neq 1$.

General case $n > 0$, $n \neq 1$

Equating the coefficients of the partial derivatives of h to zero yields

$$(-h_x)^{\frac{1}{n}} h_{xt} : \ \xi_h^1 = 0, \tag{A.20}$$

$$(-h_x)^{\frac{1-n}{n}} h_{xt} : \ \xi_x^1 = 0, \tag{A.21}$$

$$(-h_x)^{\frac{2}{n}} : \ \xi_{xx}^1 = 0, \tag{A.22}$$

$$(-h_x)^{\frac{2-2n}{n}} h_{xx} : \ \xi_{xx}^1 = 0, \tag{A.23}$$

$$(-h_x)^{\frac{2-3n}{n}} h_{xx}^2 : \ \xi_x^1 = 0, \tag{A.24}$$

$$(-h_x)^{\frac{n+2}{n}} : \ \frac{(2n+1)^2(n+1)}{n^3} h^{\frac{2n+2}{n}} \xi_x^1 - \frac{4n+2}{n^2} h^{\frac{3n+2}{n}} \xi_{xh}^1 = 0, \tag{A.25}$$

$$\begin{aligned}(-h_x)^{\frac{2-n}{n}} h_{xx} : \ & -\frac{(1-n)(2n+1)}{n^3} h^{\frac{3n+2}{n}} \xi_x^1 - \frac{(2n+1)(n+1)}{n^3} h^{\frac{3n+2}{n}} \xi_x^1 \\ & + \frac{2}{n^2} h^{\frac{4n+2}{n}} \xi_{xh}^1 = 0,\end{aligned} \tag{A.26}$$

$$(-h_x)^{\frac{1-n}{n}} : \ \frac{1}{n} h^{\frac{2n+1}{n}} \eta_{xx} + \frac{1}{n} h^{\frac{2n+1}{n}} v_l \xi_{xx}^1 = 0, \tag{A.27}$$

$$(-h_x)^{\frac{1-2n}{n}} h_{xx} : \ \frac{1-n}{n^2} h^{\frac{2n+1}{n}} \eta_x + \frac{1-n}{n^2} h^{\frac{2n+1}{n}} v_l \xi_x^1 = 0, \tag{A.28}$$

$$\begin{aligned}(-h_x)^{\frac{2n+2}{n}} : \ & -\frac{(2n+1)^2}{n^2} h^{\frac{2n+2}{n}} \xi_h^1 + \frac{(2n+1)^2(n+1)}{n^3} h^{\frac{2n+2}{n}} \xi_h^1 \\ & - \frac{2n+1}{n^2} h^{\frac{3n+2}{n}} \xi_{hh}^1 = 0,\end{aligned} \tag{A.29}$$

$$(-h_x) : \ -\xi_t^2 + v_l \xi_h^2 = 0, \tag{A.30}$$

$$(-h_x)^{\frac{1}{n}} h_{xx} : \ \frac{1}{n} h^{\frac{2n+1}{n}} \xi_h^2 - \frac{1-n}{n^2} h^{\frac{2n+1}{n}} \xi_h^2 - \frac{3}{n} h^{\frac{2n+1}{n}} \xi_h^2 = 0, \tag{A.31}$$

$$(-h_x)^{\frac{2n+1}{n}}: \ -\frac{2n+1}{n}h^{\frac{n+1}{n}}\xi_h^2+\frac{(2n+1)(n+1)}{n^2}h^{\frac{n+1}{n}}\xi_h^2-\frac{1}{n}h^{\frac{2n+1}{n}}\xi_{hh}^2=0, \tag{A.32}$$

$$(-h_x)^{\frac{2-2n}{n}}h_{xx}^2: \ -\frac{1}{n^2}h^{\frac{4n+2}{n}}\xi_h^1-\frac{n-1}{n^3}h^{\frac{4n+2}{n}}\xi_h^1+\frac{1}{n^2}h^{\frac{4n+2}{n}}\xi_h^1=0, \tag{A.33}$$

$$\begin{aligned}(-h_x)^{\frac{2}{n}}h_{xx}: \ & \frac{4n+2}{n^2}h^{\frac{3n+2}{n}}\xi_h^1-\frac{(1-n)(2n+1)}{n^3}h^{\frac{3n+2}{n}}\xi_h^1-\frac{(2n+1)(n+1)}{n^3}h^{\frac{3n+2}{n}}\xi_h^1\\ & -\frac{2n+1}{n^2}h^{\frac{3n+2}{n}}\xi_h^1+\frac{1}{n^2}h^{\frac{4n+2}{n}}\xi_{hh}^1=0,\end{aligned} \tag{A.34}$$

$$1: \ \xi^1\frac{\partial v_l}{\partial t}+\xi^2\frac{\partial v_l}{\partial x}+\eta_t-v_l\eta_h+v_l\xi_t^1-v_l^2\xi_h^1=0, \tag{A.35}$$

$$\begin{aligned}(-h_x)^{\frac{1-n}{n}}h_{xx}: \ & \frac{2n+1}{n^2}h^{\frac{n+1}{n}}\eta-\frac{1}{n}h^{\frac{2n+1}{n}}\eta_h+\frac{1}{n}h^{\frac{2n+1}{n}}\xi_t^1-\frac{2}{n}h^{\frac{2n+1}{n}}v_l\xi_h^1\\ & +\frac{1-n}{n^2}h^{\frac{2n+1}{n}}\eta_h-\frac{1-n}{n^2}h^{\frac{2n+1}{n}}\xi_x^2+\frac{1-n}{n^2}h^{\frac{2n+1}{n}}v_l\xi_h^1+\frac{1}{n}h^{\frac{2n+1}{n}}\eta_h\\ & -\frac{2}{n}h^{\frac{2n+1}{n}}\xi_x^2+\frac{1}{n}h^{\frac{2n+1}{n}}v_l\xi_h^1=0,\end{aligned} \tag{A.36}$$

$$\begin{aligned}(-h_x)^{\frac{n+1}{n}}: \ & -\frac{(2n+1)(n+1)}{n^2}h^{\frac{1}{n}}\eta+\frac{2n+1}{n}h^{\frac{n+1}{n}}\eta_h-\frac{2n+1}{n}h^{\frac{n+1}{n}}\xi_t^1\\ & +\frac{4n+2}{n}h^{\frac{n+1}{n}}v_l\xi_h^1-\frac{(2n+1)(n+1)}{n^2}h^{\frac{n+1}{n}}\eta_h+\frac{(2n+1)(n+1)}{n^2}h^{\frac{n+1}{n}}\xi_x^2\\ & -\frac{(2n+1)(n+1)}{n^2}h^{\frac{n+1}{n}}v_l\xi_h^1+\frac{1}{n}h^{\frac{2n+1}{n}}\eta_{hh}-\frac{2}{n}h^{\frac{2n+1}{n}}\xi_{xh}^2\\ & +\frac{1}{n}h^{\frac{2n+1}{n}}v_l\xi_{hh}^1=0,\end{aligned} \tag{A.37}$$

$$\begin{aligned}(-h_x)^{\frac{1}{n}}: \ & -\frac{(2n+1)(n+1)}{n^2}h^{\frac{n+1}{n}}\eta_x-\frac{(2n+1)(n+1)}{n^2}h^{\frac{n+1}{n}}v_l\xi_x^1+\frac{2}{n}h^{\frac{2n+1}{n}}\eta_{xh}\\ & -\frac{1}{n}h^{\frac{2n+1}{n}}\xi_{xx}^2+\frac{2}{n}h^{\frac{2n+1}{n}}v_l\xi_{xh}^1=0.\end{aligned} \tag{A.38}$$

From (A.20) to (A.24), we have

$$\xi^1=\xi^1(t). \tag{A.39}$$

Since $n\neq 1$, equation (A.28) reduces to

$$\eta_x=0, \tag{A.40}$$

which implies that

$$\eta=\eta(t,h). \tag{A.41}$$

From (A.30) and (A.31),

$$\xi^2 = \xi^2(x). \tag{A.42}$$

Equation (A.20) to (A.38) therefore reduce to

$$1: \ \xi^1 \frac{\partial v_l}{\partial t} + \xi^2 \frac{\partial v_l}{\partial x} + \eta_t - v_l \eta_h + v_l \xi_t^1 = 0, \tag{A.43}$$

$$\begin{aligned}(-h_x)^{\frac{1-n}{n}} h_{xx}: \ & \frac{2n+1}{n^2} h^{\frac{n+1}{n}} \eta - \frac{1}{n} h^{\frac{2n+1}{n}} \eta_h + \frac{1}{n} h^{\frac{2n+1}{n}} \xi_t^1 \\ & + \frac{1-n}{n^2} h^{\frac{2n+1}{n}} \eta_h - \frac{1-n}{n^2} h^{\frac{2n+1}{n}} \xi_x^2 + \frac{1}{n} h^{\frac{2n+1}{n}} \eta_h - \frac{2}{n} h^{\frac{2n+1}{n}} \xi_x^2 = 0, \end{aligned} \tag{A.44}$$

$$\begin{aligned}(-h_x)^{\frac{n+1}{n}}: \ & -\frac{(2n+1)(n+1)}{n^2} h^{\frac{1}{n}} \eta + \frac{2n+1}{n} h^{\frac{n+1}{n}} \eta_h - \frac{2n+1}{n} h^{\frac{n+1}{n}} \xi_t^1 + \frac{1}{n} h^{\frac{2n+1}{n}} \eta_{hh} \\ & - \frac{(2n+1)(n+1)}{n^2} h^{\frac{n+1}{n}} \eta_h + \frac{(2n+1)(n+1)}{n^2} h^{\frac{n+1}{n}} \xi_x^2 = 0. \end{aligned} \tag{A.45}$$

Simplifying (A.44) and (A.45) gives

$$-(2n+1)\eta - nh\xi_t^1 + (n-1)h\eta_h + (n+1)h\xi_x^2 = 0 \tag{A.46}$$

and

$$-(2n+1)(n+1)\eta - (2n+1)h\eta_h - n(2n+1)h\xi_t^1 + (2n+1)(n+1)h\xi_x^2 + nh^2\eta_{hh} = 0, \tag{A.47}$$

respectively. Differentiating (A.46) with respect to x and then with respect to h, we obtain

$$\xi_{xx}^2 = 0 \tag{A.48}$$

and

$$-(n+2)\eta_h - n\xi_t^1 + (n-1)h\eta_{hh} + (n+1)\xi_x^2 = 0. \tag{A.49}$$

From (A.48), we have

$$\xi^2 = c_4 + c_3 x. \tag{A.50}$$

Differentiating (A.49) again with respect to h and rearranging gives the third order ordinary differential equation

$$(n-1)h\eta_{hhh} - 3\eta_{hh} = 0, \tag{A.51}$$

the solution of which is

$$\eta = A(t)h^{\frac{2n+1}{n-1}} + B(t)h + C(t). \tag{A.52}$$

Substitute (A.52) into (A.47) to obtain

$$\begin{aligned}&(2n+1)(n+1)A(t)h^{\frac{2n+1}{n-1}}+(2n+1)(n+1)B(t)h+(2n+1)(n+1)C(t)\\&-\frac{(2n+1)^2}{n-1}A(t)h^{\frac{2n+1}{n-1}}-(2n+1)B(t)h-n(2n+1)\xi_t^1h\\&+(2n+1)(n+1)h\xi_x^2+\frac{n(n+2)(2n+1)}{(n-1)^2}A(t)h^{\frac{2n+1}{n-1}}=0.\end{aligned}\tag{A.53}$$

Separate according to the powers of h to obtain since $n>0$,

$$h^{\frac{2n+1}{n-1}}:\ (n+1)A(t)-\frac{(2n+1)}{n-1}A(t)+\frac{n(n+2)}{(n-1)^2}A(t)=0,\tag{A.54}$$

$$h:\ -(n+1)B(t)-B(t)-n\xi_t^1+(n+1)\xi_x^2=0,\tag{A.55}$$

$$h^0:\ C(t)=0.\tag{A.56}$$

Equations (A.54) and (A.55) give

$$\left(n^3-2n^2+2n+2\right)A(t)=0,\tag{A.57}$$

$$-(n+2)B(t)-n\xi_t^1+(n+1)\xi_x^2=0.\tag{A.58}$$

Since the roots of the cubic equation

$$n^3-2n^2+2n+2=0$$

are

$$n=-0.5747,\quad n=1.2874+1.35i,\quad n=1.2874-1.35i$$

and we are considering $n>0$, $n\in\mathbb{R}$, it follows that

$$A(t)=0.\tag{A.59}$$

Differentiate (A.58) with respect to t to obtain

$$(n+2)\frac{dB(t)}{dt}+n\xi_{tt}^1=0.\tag{A.60}$$

Using (A.56) and (A.57), it follows that

$$\eta=B(t)h.\tag{A.61}$$

Substitute (A.61) into (A.43) to obtain

$$\xi^1 \frac{\partial v_l}{\partial t} + \xi^2 \frac{\partial v_l}{\partial x} + \frac{dB(t)}{dt} h - v_l B(t) + v_l \xi_t^1 = 0. \tag{A.62}$$

Separate (A.62) according to powers of h:

$$h^0 : \ \xi^1 \frac{\partial v_l}{\partial t} + \xi^2 \frac{\partial v_l}{\partial x} - v_l B(t) + v_l \xi_t^1 = 0, \tag{A.63}$$

$$h : \ \frac{dB(t)}{dt} = 0. \tag{A.64}$$

Using (A.64), equation (A.60) reduces to

$$\xi_{tt}^1 = 0 \tag{A.65}$$

and we have

$$\xi^1 = c_2 t + c_1. \tag{A.66}$$

Using (A.50) and (A.66), (A.58) becomes

$$B = \frac{1}{n+2} \left((n+1)c_3 - nc_2 \right). \tag{A.67}$$

Hence

$$\eta = \frac{1}{n+2} \left((n+1)c_3 - nc_2 \right) h. \tag{A.68}$$

When (A.66) and (A.67) are substituted into (A.63), we obtain

$$(c_1 + c_2 t) \frac{\partial v_l}{\partial t} + (c_4 + c_3 x) \frac{\partial v_l}{\partial x} = \left(\frac{n+1}{n+2} \right) (c_3 - 2c_2) \, v_l. \tag{A.69}$$

The Lie point symmetry generator is therefore of the form

$$\begin{aligned} X &= (c_1 + c_2 t) \frac{\partial}{\partial t} + (c_4 + c_3 x) \frac{\partial}{\partial x} + \frac{1}{n+2} \left((n+1)c_3 - nc_2 \right) h \frac{\partial}{\partial h} \\ &= c_1 X_1 + c_2 X_2 + c_3 X_3 + c_4 X_4, \end{aligned} \tag{A.70}$$

where

$$X_1 = \frac{\partial}{\partial t}, \tag{A.71}$$

$$X_2 = t \frac{\partial}{\partial t} - \frac{n}{n+2} h \frac{\partial}{\partial h}, \tag{A.72}$$

$$X_3 = x \frac{\partial}{\partial x} + \frac{n+1}{n+2} h \frac{\partial}{\partial h}, \tag{A.73}$$

$$X_4 = \frac{\partial}{\partial x}, \tag{A.74}$$

provided that the leak-off velocity $v_l(x,t)$ satisfies the first order linear partial differential equation (A.69).

Special case $n = 1$

Although the case $n = 1$ must be treated separately the final result derived by Fareo and Mason [15] for the Lie point symmetry X and for the partial differential equation for $v_l(t,x)$ is obtained by putting $n = 1$ in (A.70) and (A.69). The Lie point symmetry (A.70) and the partial differential equation for $v_l(t,x)$ in (A.69) are therefore valid for all $n > 0$.

APPENDIX B

Derivation of the Lie point symmetry of a nonlinear second order ordinary differential equation

We derive the Lie point symmetry of the second order nonlinear ordinary differential equation

$$\frac{d}{du}\left[F(u)^{\frac{2n+1}{n}}\left(-\frac{dF}{du}\right)^{\frac{1}{n}}\right]+A\frac{d}{du}\left(uF\right)+BF(u)=0, \tag{B.1}$$

where A and B are constants. We will first consider $n>0$, $n\neq 1$ and $n\neq 1/2$ and then show that the Lie point symmetry derived holds true when $n=1$ and $n=1/2$. The Lie point symmetry of (B.1) for $n=1$ was derived by Fareo [44].

Equation (B.1) can be written in the form

$$H(u,F,F_u,F_{uu})=0, \tag{B.2}$$

where

$$H=-\frac{1}{n}F^{\frac{2n+1}{n}}\left(-\frac{dF}{du}\right)^{\frac{1-n}{n}}\frac{d^2F}{du^2}-\left(\frac{2n+1}{n}\right)\left(-F\frac{dF}{du}\right)^{\frac{n+1}{n}}+Au\frac{dF}{du}+\left(A+B\right)F. \tag{B.3}$$

The Lie point symmetry generator,

$$X=\xi(u,F)\frac{\partial}{\partial u}+\eta(u,F)\frac{\partial}{\partial F} \tag{B.4}$$

of equation (B.1) is derived by solving the determining equation

$$X^{[2]}H\Big|_{H=0}=0, \tag{B.5}$$

for the unknowns $\xi(u,F)$ and $\eta(u,F)$ where $X^{[2]}$, the second prolongation of X, is

$$X^{[2]} = X + \zeta_1(u,F,F_u)\frac{\partial}{\partial F_u} + \zeta_2(u,F,F_u,F_{uu})\frac{\partial}{\partial F_{uu}}, \tag{B.6}$$

with

$$\zeta_1 = D(\eta) - F_u D(\xi), \tag{B.7}$$

$$\zeta_2 = D(\zeta_1) - F_{uu} D(\xi) \tag{B.8}$$

and

$$D = \frac{d}{du} + F_u\frac{d}{dF} + F_{uu}\frac{d}{dF_u} + \cdots . \tag{B.9}$$

The expanded form of ζ_1 and ζ_2 is

$$\zeta_1 = \eta_u + F_u\left(\eta_F - \xi_u\right) - F_u^2\xi_F, \tag{B.10}$$

$$\begin{aligned}\zeta_2 &= \eta_{uu} + 2\eta_{uF}F_u + \eta_{FF}F_u^2 + \eta_F F_{uu} - \xi_{uu}F_u \\ &\quad -2F_u^2\xi_{uF} - F_u^3\xi_{FF} - 2\xi_u F_{uu} - 3\xi_F F_u F_{uu}.\end{aligned} \tag{B.11}$$

The determining equation (B.5) becomes

$$\begin{aligned}&\xi\left(AF_u\right) + \eta\left(-\frac{2n+1}{n^2}F^{\frac{n+1}{n}}\left(-F_u\right)^{\frac{1-n}{n}}F_{uu} - \frac{(n+1)(2n+1)}{n^2}\left(-F_u\right)^{\frac{n+1}{n}}F^{\frac{1}{n}} + A + B\right) \\ &\quad + \zeta_1\left(Au + \frac{(n+1)(2n+1)}{n^2}F^{\frac{n+1}{n}}\left(-F_u\right)^{\frac{1}{n}} + \frac{1-n}{n^2}F^{\frac{2n+1}{n}}\left(-F_u\right)^{\frac{1-2n}{n}}F_{uu}\right) \\ &\quad + \zeta_2\left(-\frac{1}{n}F^{\frac{2n+1}{n}}\left(-F_u\right)^{\frac{1-n}{n}}\right)\Bigg|_{H=0} = 0.\end{aligned} \tag{B.12}$$

We now substitute the expressions (B.10) and (B.11) for ζ_1 and ζ_2 into (B.12) to obtain the determining equation

$$\begin{aligned}&\xi AF_u - \frac{(2n+1)}{n^2}\left(-F_u\right)^{\frac{1-n}{n}}F^{\frac{n+1}{n}}F_{uu}\eta - \frac{(n+1)(2n+1)}{n^2}F^{\frac{1}{n}}\left(-F_u\right)^{\frac{n+1}{n}}\eta + (A+B)\eta + Au\eta_u \\ &+\frac{(n+1)(2n+1)}{n^2}F^{\frac{n+1}{n}}\left(-F_u\right)^{\frac{1}{n}}\eta_u + \frac{(1-n)}{n^2}F^{\frac{2n+1}{n}}\left(-F_u\right)^{\frac{1-2n}{n}}F_{uu}\eta_u + AuF_u\eta_F \\ &-\frac{(n+1)(2n+1)}{n^2}F^{\frac{n+1}{n}}\left(-F_u\right)^{\frac{n+1}{n}}\eta_F - \frac{(1-n)}{n^2}F^{\frac{2n+1}{n}}\left(-F_u\right)^{\frac{1-n}{n}}F_{uu}\eta_F - AuF_u\xi_u \\ &+\frac{(n+1)(2n+1)}{n^2}F^{\frac{n+1}{n}}\left(-F_u\right)^{\frac{n+1}{n}}\xi_u + \frac{(1-n)}{n^2}F^{\frac{2n+1}{n}}\left(-F_u\right)^{\frac{1-n}{n}}F_{uu}\xi_u - AuF_u^2\xi_F \\ &-\frac{(n+1)(2n+1)}{n^2}F^{\frac{n+1}{n}}\left(-F_u\right)^{\frac{2n+1}{n}}\xi_F - \frac{(1-n)}{n^2}F^{\frac{2n+1}{n}}\left(-F_u\right)^{\frac{1}{n}}F_{uu}\xi_F - \frac{1}{n}F^{\frac{2n+1}{n}}\left(-F_u\right)^{\frac{1-n}{n}}\eta_{uu}\end{aligned}$$

$$+\frac{2}{n}F^{\frac{2n+1}{n}}\left(-F_u\right)^{\frac{1}{n}}\eta_{uF}-\frac{1}{n}F^{\frac{2n+1}{n}}\left(-F_u\right)^{\frac{1+n}{n}}\eta_{FF}-\frac{1}{n}F^{\frac{2n+1}{n}}\left(-F_u\right)^{\frac{1-n}{n}}F_{uu}\eta_F-\frac{1}{n}F^{\frac{2n+1}{n}}\left(-F_u\right)^{\frac{1}{n}}\xi_{uu}$$
$$+\frac{2}{n}F^{\frac{2n+1}{n}}\left(-F_u\right)^{\frac{n+1}{n}}\xi_{uF}-\frac{1}{n}F^{\frac{2n+1}{n}}\left(-F_u\right)^{\frac{2n+1}{n}}\xi_{FF}+\frac{2}{n}F^{\frac{2n+1}{n}}\left(-F_u\right)^{\frac{1-n}{n}}F_{uu}\xi_u$$
$$\left.-\frac{3}{n}F^{\frac{2n+1}{n}}\left(-F_u\right)^{\frac{1}{n}}F_{uu}\xi_F\right|_{H=0}=0. \tag{B.13}$$

We will impose the condition $H=0$ on (B.13) by using equation (B.3) for H which is

$$F_{uu}=-(2n+1)F^{-1}F_u^2-nAuF^{-\frac{2n+1}{n}}\left(-F_u\right)^{\frac{2n-1}{n}}+n(A+B)F^{-\frac{n+1}{n}}\left(-F_u\right)^{\frac{n-1}{n}}. \tag{B.14}$$

By replacing F_{uu} in (B.13) by (B.14), the determining equation becomes

$$\xi AF_u-\frac{(2n+1)^2}{n^2}F^{\frac{1}{n}}\left(-F_u\right)^{\frac{n+1}{n}}\eta-\frac{(2n+1)}{n}AuF^{-1}F_u\eta-(A+B)\frac{(2n+1)}{n}\eta-\frac{(n+1)(2n+1)}{n^2}F^{\frac{1}{n}}$$
$$\times\left(-F_u\right)^{\frac{n+1}{n}}\eta+(A+B)\eta+Au\eta_u+\frac{(n+1)(2n+1)}{n^2}F^{\frac{n+1}{n}}\left(-F_u\right)^{\frac{1}{n}}\eta_u-\frac{(1-n)(2n+1)}{n^2}F^{\frac{n+1}{n}}\left(-F_u\right)^{\frac{1}{n}}\eta_u$$
$$-\frac{(1-n)}{n}Au\eta_u+(A+B)\frac{(1-n)}{n}\left(-F_u\right)^{-1}F\eta_u+AuF_u\eta_F-\frac{(n+1)(2n+1)}{n^2}F^{\frac{n+1}{n}}\left(-F_u\right)^{\frac{n+1}{n}}\eta_F$$
$$+\frac{(1-n)(2n+1)}{n^2}F^{\frac{n+1}{n}}\left(-F_u\right)^{\frac{n+1}{n}}\eta_F-\frac{(1-n)}{n}AuF_u\eta_F-(A+B)\frac{(1-n)}{n}F\eta_F-AuF_u\xi_u$$
$$+\frac{(n+1)(2n+1)}{n^2}F^{\frac{n+1}{n}}\left(-F_u\right)^{\frac{n+1}{n}}\xi_u-\frac{(1-n)(2n+1)}{n^2}F^{\frac{n+1}{n}}\left(-F_u\right)^{\frac{n+1}{n}}\xi_u+\frac{(1-n)}{n}AuF_u\xi_u$$
$$+(A+B)\frac{(1-n)}{n}F\xi_u-AuF_u^2\xi_F-\frac{(n+1)(2n+1)}{n^2}F^{\frac{n+1}{n}}\left(-F_u\right)^{\frac{2n+1}{n}}\xi_F+\frac{(1-n)(2n+1)}{n^2}F^{\frac{n+1}{n}}$$
$$\times\left(-F_u\right)^{\frac{2n+1}{n}}\xi_F+\frac{(1-n)}{n}AuF_u^2\xi_F+\frac{(A+B)(1-n)}{n}FF_u\xi_F-\frac{1}{n}F^{\frac{2n+1}{n}}\left(-F_u\right)^{\frac{1-n}{n}}\eta_{uu}+\frac{2}{n}F^{\frac{2n+1}{n}}$$
$$\times\left(-F_u\right)^{\frac{1}{n}}\eta_{uF}-\frac{1}{n}F^{\frac{2n+1}{n}}\left(-F_u\right)^{\frac{n+1}{n}}\eta_{FF}+\frac{(2n+1)}{n}F^{\frac{n+1}{n}}\left(-F_u\right)^{\frac{n+1}{n}}\eta_F-AuF_u\eta_F-(A+B)F\eta_F$$
$$-\frac{1}{n}F^{\frac{2n+1}{n}}\left(-F_u\right)^{\frac{1}{n}}\xi_{uu}-\frac{2}{n}F^{\frac{2n+1}{n}}\left(-F_u\right)^{\frac{n+1}{n}}\xi_{uF}-\frac{1}{n}F^{\frac{2n+1}{n}}\left(-F_u\right)^{\frac{2n+1}{n}}\xi_{FF}-\frac{4n+2}{n}F^{\frac{n+1}{n}}$$
$$\times\left(-F_u\right)^{\frac{n+1}{n}}\xi_u+2AuF_u\xi_u+2(A+B)F\xi_u+\frac{(6n+3)}{n}F^{\frac{n+1}{n}}\left(-F_u\right)^{\frac{2n+1}{n}}\xi_F+3AuF_u^2\xi_F$$
$$+3(A+B)FF_u\xi_F=0. \tag{B.15}$$

Since ξ and η are independent of the derivative F_u, (B.15) can be separated according to the coefficients of powers of the derivative F_u. Equation (B.15) holds provided each of these coefficients vanishes.

However, the cases $n=1$ and $n=1/2$ need to be considered separately. When $n=1$, $F_u^{\frac{n+1}{n}}$, $F_u^{\frac{1}{n}}$ and $F_u^{\frac{1-n}{n}}$ become F_u^2, F_u and 1, and since there are terms with derivatives F_u^2, F_u

and 1 in (B.15) their coefficients have to be grouped together. Also, when $n = 1/2$, $F_u^{\frac{1}{n}}$ and $F_u^{\frac{1-n}{n}}$ become F_u^2 and F_u and their respective coefficients have to be grouped together as well.

Assuming $A \neq 0$, $A \neq -B$, $n \neq 1$ and $n \neq 1/2$, we have

$$F_u^{-1}: \quad \eta_u = 0, \tag{B.16}$$

$$F_u^2: \quad \xi_F = 0, \tag{B.17}$$

$$F_u^{\frac{1-n}{n}}: \quad \eta_{uu} = 0, \tag{B.18}$$

$$F_u^{\frac{2n+1}{n}}: \quad (2n+1)\xi_F - F\xi_{FF} = 0, \tag{B.19}$$

$$F_u^{\frac{1}{n}}: \quad 2n(2n+1)\eta_u + 2nF\eta_{uF} - nF\xi_{uu} = 0, \tag{B.20}$$

$$F_u: \quad AuF\xi_u - (1-n)AuF\eta_F + nA\xi F - (2n+1)Au\eta = 0, \tag{B.21}$$

$$1: \frac{(n+1)(A+B)}{n}\eta - \frac{(2n-1)}{n}Au\eta_u + \frac{(A+B)}{n}F\eta_F - \frac{(A+B)(n+1)}{n}F\xi_u = 0, \tag{B.22}$$

$$F_u^{\frac{n+1}{n}}: \quad (2n+1)\eta - (2n+1)F\eta_F - F^2\eta_{FF} + 2F^2\xi_{uF} = 0. \tag{B.23}$$

When $A = -B$, the term in F_u^{-1} vanishes in (B.15) and by separating (B.15) according to the coefficients of powers of the derivative F_u, the overdetermined system (B.17) to (B.23) is obtained, with $(A+B) = 0$ in (B.22). Equation (B.22) for the case $A + B = 0$ yields, since $n \neq 1/2$, $\eta_u = 0$. Therefore, when $A \neq 0$, the cases $A + B = 0$ and $A + B \neq 0$ in (B.15) give the same results.

From (B.16) and (B.17),

$$\eta = \eta(F) \tag{B.24}$$

and

$$\xi = \xi(u). \tag{B.25}$$

Equation (B.20) reduces to

$$\xi_{uu} = 0, \tag{B.26}$$

which on integration gives

$$\xi = c_1 u + c_2. \tag{B.27}$$

From (B.21), since $A \neq 0$, we have

$$c_1 uF + (n-1)uF\eta_F + n\left(c_1 u + c_2\right)F - (2n+1)u\eta = 0. \tag{B.28}$$

Since η does not depend on u, we set the coefficients of the powers of u to zero:

$$u^0 : c_2 = 0, \tag{B.29}$$

$$u^1 : Fc_1 + (n-1)F\eta_F + nc_1 F - (2n+1)\eta = 0. \tag{B.30}$$

Hence, from (B.29), $c_2 = 0$, which implies

$$\xi = c_1 u. \tag{B.31}$$

From (B.30),

$$(1-n)\,F\eta_F + (2n+1)\,\eta = (n+1)\,c_1 F. \tag{B.32}$$

From (B.22),

$$\eta = -\frac{1}{n+1}F\eta_F + Fc_1. \tag{B.33}$$

Substituting (B.33) into (B.32) gives

$$\left(\frac{n+2}{n+1}\right)\frac{d\eta}{dF} = c_1, \tag{B.34}$$

which on integration yields

$$\eta = \left(\frac{n+1}{n+2}\right)c_1 F + K, \tag{B.35}$$

where K is a constant. Finally, substituting (B.35) into (B.23), we obtain $K = 0$. Hence

$$\eta = \left(\frac{n+1}{n+2}\right)c_1 F \quad \text{and} \quad \xi = c_1 u \tag{B.36}$$

and therefore

$$X = \frac{c_1}{n+2}\left((n+2)\,u\frac{\partial}{\partial u} + (n+1)\,F\frac{\partial}{\partial F}\right). \tag{B.37}$$

We have shown that if $A \neq 0$, for any $B \in \mathbb{R}$ and for all $n > 0$, except $n = 1$ and $n = 1/2$, the Lie point symmetry generator admitted by (B.1) is

$$X = (n+2)\,u\frac{\partial}{\partial u} + (n+1)\,F\frac{\partial}{\partial F}. \tag{B.38}$$

Special case $n=\frac{1}{2}$

When $n = 1/2$, equation (B.15) is separated according to the coefficients of powers of the derivative F_u to obtain equations (B.16), (B.19), (B.22) and (B.23) with $n = \frac{1}{2}$ which become

$$F_u^{-1}: \ \eta_u = 0, \tag{B.39}$$

$$F_u^4: \ 2\xi_F - F\xi_{FF} = 0, \tag{B.40}$$

$$1: \ 3(A+B)\eta + 2(A+B)F\eta_F - 3(A+B)F\xi_u = 0, \tag{B.41}$$

$$F_u^3: \ 2\eta - 2F\eta_F - F^2\eta_{FF} + 2F^2\xi_{uF} = 0 \tag{B.42}$$

and

$$F_u^2: \ 3Au\xi_F + 8F^3\eta_u + 4F^4\eta_{uF} - 2F^4\xi_{uu} = 0, \tag{B.43}$$

$$F_u: \ \frac{1}{2}AF\xi - 2Au\eta + 2(A+B)F^2\xi_F - \frac{1}{2}AuF\eta_F + AuF\xi_u + F^5\xi_{uu} = 0. \tag{B.44}$$

Differentiating (B.41) with respect to u, and using (B.39), we obtain, since $A + B \neq 0$,

$$\xi_{uu} = 0. \tag{B.45}$$

From (B.39),

$$\eta = \eta(F), \tag{B.46}$$

and from (B.43), using (B.39) and (B.45), and since $A \neq 0$,

$$\xi = \xi(u). \tag{B.47}$$

Integrating (B.45) therefore yields

$$\xi = c_1u + c_2 \tag{B.48}$$

and (B.42) reduces to

$$F^2\eta_{FF} + 2F\eta_F - 2\eta = 0, \tag{B.49}$$

which is solved to obtain

$$\eta = k_1F + k_2F^{-2}. \tag{B.50}$$

When (B.48) and (B.50) are substituted into (B.44), and after separating with respect to powers of F, we obtain

$$A\left[\left(3c_1 - 5k_1\right)u + c_2\right] = 0, \tag{B.51}$$

$$Ak_2u = 0. \tag{B.52}$$

For $A \neq 0$, $k_2 = 0$ in (B.52) and setting the coefficients of powers of u to zero in (B.51) yields $k_1 = \frac{3}{5}c_1$ and $c_2 = 0$. Therefore

$$\xi = c_1u \tag{B.53}$$

and

$$\eta = \frac{3}{5}c_1F. \tag{B.54}$$

Equations (B.53) and (B.54) agree with (B.36) when $n = 1/2$. Therefore for $n = \frac{1}{2}$, the Lie point symmetry of (B.1) is given by (B.38) with $n = \frac{1}{2}$.

The case $n = 1$ also has to be treated separately. Fareo [44] found that for $n = 1$ the Lie point symmetry of (B.1) is (B.38) with $n = 1$. The Lie point symmetry of (B.1) is therefore given by (B.38) for all $n > 0$.

References

[1] D.A. Spence and D.L. Turcotte. Magma-driven propagation of cracks. *J. Geophysical Research*, 90:575–580, 1985.

[2] S. Khristianovic and Y. Zheltov. Formation of vertical fractures by means of highly viscous fluids. In *4th World Petroleum Congress*, pages 579–586, Rome, 1955.

[3] G.I. Barenblatt. On the formation of horizontal cracks in hydraulic fracture of an oil-bearing stratum. *Prikladnaya Matematica*, 20:475–486, 1956.

[4] T. Perkins and L. Kern. Widths of hydraulic fractures. *Journal of Petroleum Technology*, 222:937–949, 1961.

[5] J. Geertsma and F. de Klerk. A rapid method of predicting width and extent of hydraulic induced fractures. *Journal of Petroleum Technology*, 246:1571–1581, 1969.

[6] R. Nordgren. Propagation of vertical hydraulic fractures. *Journal of Petroleum Technology*, 253:306–314, 1972.

[7] D.A. Spence and P.W. Sharp. Self similar solution for elasto-hydrodynamic cavity flow. *Proc. R. Soc. London, Ser. A*, 400:289–313, 1985.

[8] J.R. Lister. Buoyancy driven fluid fracture: the effects of material toughness and of low-viscosity precursors. *J. Fluid Mechanics*, 210:263–280, 1990.

[9] J. Geertsma and R. Haafkens. A comparison of the theories for predicting width and extent of vertical hydraulically induced fractures. *ASME Journal of Energy Research*, 101:8–19, 1979.

[10] J.I. Adachi and E. Detournay. Self-similar solutions of a plane strain fracture driven by a power-law fluid. *International Journal for Numerical and Analytical Methods in Geomechanics*, 26:579–604, 2002.

[11] R.J. Clifton and A.S. Abou-Sated. On the computation of the three-dimensional geometry of hydraulic fractures. In *Proceedings of the SPE Symposium on Low Permeability Gas Reservoirs*, pages 307–313, Denver, Richardson TX, 1979. Society of Petroleum Engineers.

[12] R.J. Clifton. Three-dimensional fracture-propagation models. In J.L. Gidley, S.A. Holditch, D.E. Nierode, and R.W. Veatch, editors, *Recent Advances in Hydraulic Fracturing-SPE Monographs*, volume 12, pages 95–108. Society of Petroleum Engineers, 1989.

[13] A. Peirce and E. Detournay. An implicit level set method for modelling hydraulically driven fractures. *Computer Methods in Applied Mechanics and Engineering*, 197:2858–2885, 2008.

[14] A.D. Fitt, D.P. Mason, and E.A. Moss. Group invariant solution for a pre-existing fluid-driven fracture in impermeable rock. *Zeitschrift fur Angewandte Mathematik und Physik (ZAMP)*, 58:1049–1067, 2007.

[15] A.G. Fareo and D.P. Mason. Group invariant solutions for a pre-existing fluid driven fracture in permeable rock. *Journal of Nonlinear Analysis: Real World Applications*, 12:767–779, 2011.

[16] K Ben-Naceur. Modelling of hydraulic fractures. In M.J. Economides and K.G. Nolte, editors, *Reservoir Stimulation (2nd edn)*. Prentice-Hall, Englewood Cliffs, NJ, 1989.

[17] J.R. Cameron and R.K. Prud'homme. Fracturing-fluid flow behaviour. In J.L. Gidley, S.A. Holditch, D.E. Nierode, and R.W. Veatch, editors, *Recent Advances in Hydraulic Fracturing-SPE Monographs*, pages 177–209. Society of Petroleum Engineers, Richardson, 1989.

[18] D.J. Acheson. *Elementary Fluid Dynamics*. Clarendon Press, Oxford, 1990.

[19] R.B. Bird, R.C. Armstrong, and O. Hassager. *Dynamics of Polymeric Fluids*. John Wiley and Sons, Inc, New York, 1987.

[20] D.H. Everett. *Basic Principles of Colloid Science*. Royal Society of Chemistry, Burlington House, Piccadilly, London, 1988.

[21] R.P. Chhabra and J.F. Richardson. *Non-Newtonian Flow and Applied Rheology*. Butterworth-Heinemann, Oxford, 2008.

[22] D.I. Garagash. Transient solution for a plane-strain fracture driven by a shear-thinning, power-law fluid. *Int. J. Numer. Anal. Meth. Geomech*, 30:1439–1475, 2006.

[23] P.J. Carreau, D. Dekee, and R.P. Chhabra. *Rheology of Polymeric Systems*. Hanser, Munich, 1997.

[24] M.M. Cross. Rheology of non-Newtonian fluids: a new flow equation for pseudoplastic systems. *J Colloid Sci*, 20:417–437, 1965.

[25] P.J. Carreau. *Trans. Soc. Rheol*, 16:99–127, 1972.

[26] N.P. Cheremisinoff, editor. *Rheology and Non-Newtonian Flows*, volume 7 of *Encyclopedia of Fluid Mechanics*. Gulf publishing co, Houston, Texas, USA, 1988.

[27] T.G. Myers. Application of non-Newtonian models to thin-film flow. *Phys. Rev. E*, 72(066302), 2005.

[28] S. Matsuhisa and R.B. Bird. Analytical and numerical solutions for laminar flow of the non-Newtonian Ellis fluid. *AICHE J.*, 11:588–595, 1965.

[29] R.H. Perry and D.W. Green. *Perry's Chemical Engineers' handbook*. McGraw-Hill, 7th edition, 1997.

[30] H.A. Barnes. The yield stress- a review or $\pi\alpha\nu\tau\alpha\ \rho\epsilon\iota$ - everything flows? *J. Non-Newtonian Fluid Mech*, 81:133–178, 1999.

[31] H.A. Barnes and K. Walters. The yield stress myth? *Rheol Acta*, 24:323–326, 1985.

[32] H.A. Barnes. Thixotropy- a review. *J. Non-Newtonian Fluid Mech*, 70:1–33, 1997.

[33] A. Mujumdar, A.N. Beris, and A.B. Metzner. Transient phenomena in thixotropic systems. *J. Non-Newtonian Fluid Mech*, 102:157–178, 2002.

[34] G. Böhme. *Non-Newtonian Fluid Mechanics*, volume 31 of *North-Holland series in Applied Mathematics and Mechanics*. North- Holland, 1987.

[35] J.E. Dunn and J.R. Rajagopal. Fluids of differential type: Critical review and thermodynamic analysis. *Int. J. Eng. Sci*, 33:689–729, 1995.

[36] G.W. Bluman and J.D. Cole. The general similarity solution of the heat equation. *J. Math. Mech*, 18:1025–1042, 1969.

[37] M.S. Klamkin. On the transformation of a class of boundary value problems into initial value problems for ordinary differential equations. *SIAM Review*, 4:43–47, 1962.

[38] T.Y. Na. Transforming boundary conditions into initial conditions for ordinary differential equations. *SIAM Rev*, 10:85–87, 1968.

[39] T.Y. Na. Further extensions on transforming from boundary value to initial value problems. *SIAM Rev*, 10:85–87, 1968.

[40] M.S. Klamkin. Transformation of boundary value problems into initial value problems. *J. Math. Anal. Applic*, 32:308–330, 1970.

[41] T.Y. Na. *Computational Methods in Engineering Boundary Value Problems*, volume 145 of *Mathematics in Science and Engineering*. Academic Press, inc, New York, 1979.

[42] N.H. Ibragimov and R.L. Anderson. One-parameter transformation groups. In N.H. Ibragimov, editor, *CRC Handbook of Lie Group Analysis of Differential Equations*, volume 1:Symmetries, Exact Solutions and Conservation Laws, pages 7–14. CRC Press, Boca Raton, 1994.

[43] D.A. Mendelsohn. A review of hydraulic fracture modelling - Part I: General concepts, 2D models and motivation for 3D modelling. *ASME J. Energy Res. Tech*, 106:369–376, 1984.

[44] A.G. Fareo. Group invariant solutions for a pre-existing fluid-driven fracture in permeable rock. Master's thesis, University of the Witwatersrand, Johannesburg, South Africa, 2008.

[45] R.P. Gillespie. *Integration*. Oliver and Boyd, Edinburgh, 1959, pages 113-115.

[46] J.I. Adachi and A.P. Pierce. Asymptotic analysis of an elasticity equation for a finger-like hydraulic fracture. *Journal of Elasticity*, 90:43–69, 2008.

[47] A. Kovalyshen and E. Detournay. A reexamination of the classical PKN model of hydraulic fracture. *Transp Porous Med*, 81:317–339, 2010.

[48] N.H. Ibragimov. *Elementary Lie Group Analysis and Ordinary Differential Equations*. John Wiley and Sons, Chichester, 1999.

[49] J.M. Acton, H.E. Huppert, and M.G. Worster. Two-dimensional viscous gravity currents flowing over a deep porous medium. *J. Fluid Mech.*, 440:359–380, 2001.

[50] L. Dresner. *Similarity Solutions of Nonlinear Partial Differential Equations*. Pitman, Boston, 1983.

[51] R. Naz, F.M. Mahomed, and D.P. Mason. Comparison of different approaches to conservation laws for some partial differential equations in fluid mechanics. *Applied Mathematics and Computations*, 205:212–230, 2008.

[52] A.H. Kara and F.M. Mahomed. Relationship between symmetries and conservation laws. *Int. J Theor Phys*, 39:23–40, 2000.

[53] A.H. Kara and F.M. Mahomed. A basis of conservation laws for partial differential equations. *J Nonlinear Mathematical Physics*, 9:60–72, 2002.

[54] M. Anthonyrajah. Turbulent flow in channels and fractures: conservation laws and Lie group analysis. Master's thesis, University of the Witwatersrand, Johannesburg, South Africa, 2011.